Engineering Mutations into the Mouse NR2B Gene of the NMDA Receptor

Emese Gabriella Kicsi

PhD

The University of Edinburgh

2006

channel (Ascher and Nowak, 1988), these findings suggest that the M2 re-entrant loop constitutes to the ion channel lining the pore of the receptor.

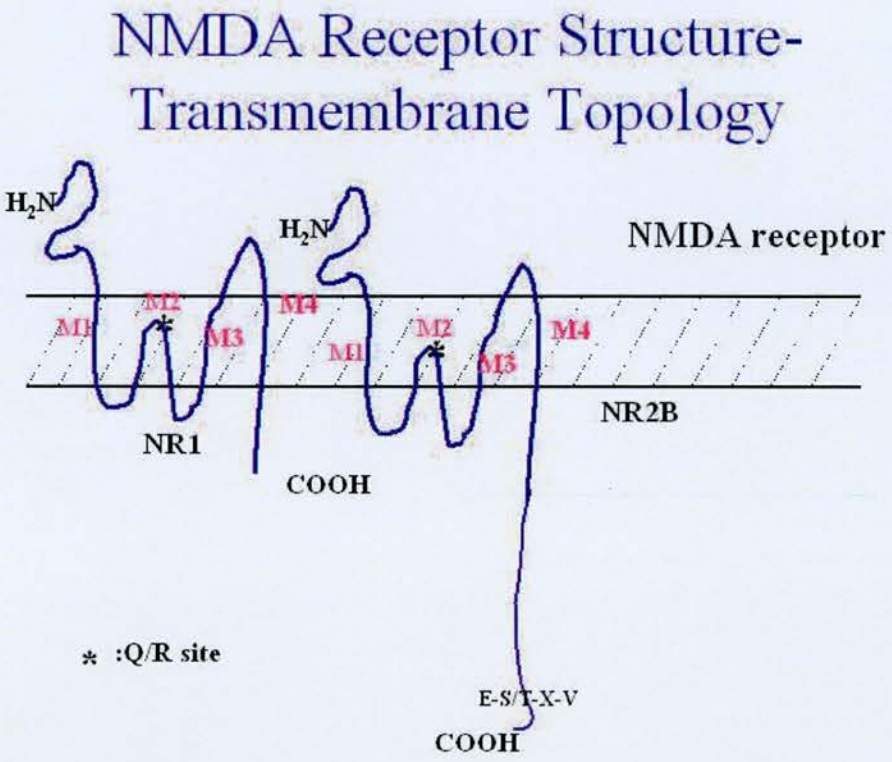

Figure 1. NMDA Receptor Structure and Transmembrane Topology.
The structure resembles that of the nicotinic acetylcholine receptor, but it has three transmembrane loops and M2 is a cytoplasm facing re-entrant loop. The N-terminus is extracellular while the C-terminus is intracellular.

The phosphorylation domain of the receptor is the C-terminus of the different subunits found intracellularly. The C-terminus of NR1 is phosphorylated in primary cultures and in transfected HEK 293 cells (Tingley et al., 1993). The NR2 subunits are directly phosphorylated on the C-terminus by protein kinases for example PKC (Figure 4, Table 3). Protein kinases and their sites of phosphorylation on the various subunits will be discussed in detail in section 1C and 1F. Another important feature of the C-termini of the different subunits is that they bind to cytoskeletal proteins and neurofilaments regulating synaptic localization of the receptor. The C1 exon of the NR1 N-terminus binds alpha actinin (Wyszynszki et al., 1997). This interaction is antagonized by calcium calmodulin (Ca^{2+}/CaM). Alpha actinin also selectively binds

Declaration

I hereby confirm that the thesis submitted was composed by myself based on the results of my own work. I declare that if any procedures were done by other members of the laboratory or by collaborating groups or if any material was provided by a collaborating laboratory it is clearly stated so in the manuscript.

I further confirm that this work has not been submitted for any other degree or professional qualification except for the PhD degree at The University of Edinburgh.

15th September 2006
Edinburgh

Acknowledgement

I hereby would like to take the opportunity to say thank you to all those people who made any kind of contribution to my work by supervising me, advising me, working with me in the day-to-day laboratory life and those who supported me as part of my personal life.

I would like to thank Prof Seth G N Grant, my supervisor, for giving me the opportunity to do my PhD in such a well-known, top laboratory and for all the positive encouragement he has given me during the years. I thank Noboru H Komiyama for acquainting me with a new exciting field of research, showing me all the techniques of gene manipulation and advising me. I greatly appreciate the support and suggestions that I have received from both Dr David J A Wyllie and Dr Andrew Smith, my second supervisor and advisors in my PhD committee. I am grateful to all members of my laboratory, all the people supporting my work in the tissue culture and the animal house both in the Centre for Genome Research and the Centre for Neuroscience, especially Karen Porter, who I was lucky to work together with and Jane Robinson, our manager of the laboratory, who is also the one carrying out the blastocyst injections, the 'mother' of my mice. I am most grateful to Dr Susan Fleetwood-Walker and Dr Karl Peter Giese for the invaluable help they have given me in improving my thesis and finishing my PhD.

Finally let me thank my family, who have always been encouraging me and believed in me throughout, in my mother tongue:
Szeretettel köszönöm a sok bátorítást, bizalmat, hitet és segítséget amit szüleimtől, testvéreimtől, nagyszüleimtől kaptam éveken át, különösen a szakdolgozatom megírásának utolsó időszakában, a Magyarországon töltött munkával teli, boldog hónapok alatt.

" Quiero decirte que creía en tu palabra
Quiero explicarte que la vida era a tu lado
Que había puesto yo mis sueños en tus manos
Que sin dudar te seguiría
Sin preguntarte confiaría"

TABLE OF CONTENTS

Abbreviations

ACC	Anterior cingulate cortex
ACPD	1-amino-cyclopentane-1,3-dicarboxylic acid
AIDA	1-aminoindan-1,5-dicarboxylic acid
ALS	Amyotrophic lateral sclerosis
AMPA	α-amino-3-hydroxy-5-methyl-4-isoxazolepropionic acid
AP-4	2-amino 4 phosphobutyric acid
AP-5	2-amino 5-phosphonopentanoic acid
AP-7	2-amino 7-phosphonopentanoic acid
Arg (R)	Arginine
Asp (N)	Asparagine
C	Catalytic subunit
CaM	Calmodulin
CaMKII	Ca^{2+}-calmodulin-dependent protein kinase II
CaMKIV	Ca^{2+}-calmodulin-dependent protein kinase IV
cAMP	Cyclic adenosyl monophosphate
Cdk5	Cyclin-dependent kinase 5
CIPP	Channel-interacting PDZ protein
CREB	cAMP response element binding protein
DCG-IV	3-dicarboxy-cyclopropylglycine
DG	Dentate gyrus
DHPG	3,5-dihydroxyphenylglycine
DIV	Day in vitro
Dlg	Product of the Drosophila lethal(1)disclarge-1 tumor suppressor gene
E1	Embryonic day 1
EC_{50}	Efficient concentration for half-maximum response
EGLU	alpha-ethylglutamic acid
ERK	Extracellular signal-related kinase

EPSC	Excitatory postsynaptic current
ES cell	Embryonic stem cell
fMRI	Functional magnetic resonance imaging
Fyn	Human locus IDDM15 gene FYN
GABA	Gamma-Aminobutyric Acid
GKAP	Guanylate kinase-associated protein
Glu (Q)	Glutamine
GYKI 52466	1-(4-aminophenyl)-4-methyl-7,8-methylenedioxy-2,3 benzodiazepine hydrochloride
HA966	3-amino-1-hydroxypyrrolidin-2-one
5-HT	5-hyroxytryptamine
IC_{50}	Half maximal inhibitory concentration
Leu	Leucine
LTD	Long-term depression
LTP	Long term potentiation
LY 293558	2-tetrazole-ethyl-decahydroisoquinoline-3-carboxylic acid
LY 294486	2-tetrazole-methyl-oxymethyl-alpha-decahydroisoquinoline-3-carboxylic acid
LY 382884	6-(4-carboxyphenyl)-methyl-decahydroisoquinoline-3-carboxylic acid
Lys	Lysine
M2	Membrane domain
MAGUK	Membrane associated guanylate kinases
MAO	Monoaminooxidase
MAP-1A	Microtubule-associated protein-1A
MAP-2	Microtubule-associated protein-2
MAP4	Methylamino-phosphonium-butyric acid
MAPK	Mitogen-activated protein kinase
MCCG	2-methyl-2-carboxypropyl-glycine
MCPG	alpha-methyl-4-carboxyphenylglycine
MEK	MAP kinase kinase

mGluR	Metabotropic glutamate receptor
MK-801	Dizocilpine,(+)-10,11-dihydro-5-methyl-5H-Dibenzo[a,d]cyclohepten-5,10-imine, C16H15N
MNQX	5,7-dinitroquinoxaline-2,3-dione
MSOP	alpha-methylserine-O-phosphate
NBQX	6-nitro-7-sufamoyl-benzoquinoxaline-2,3-dione
N-CAM	Neural-cell adhesion molecule
NMDA	*N*-methyl-D-aspartate
nNOS	Neuronal nitric oxidase synthase
NO	Nitric oxide
P1	Postnatal day 1
PAC1	Pituitary adenylate cyclase activating polypeptide type I receptor
PACAP	Pituitary adenylate cyclase activating polypeptide
PCP	Phencyclidine
PCR	Polymerase chain reaction
PI3K	Phosphatidylinositol 3-kinase
PKA	Protein kinase A
PKC	Protein kinase C
PLA_2	Phospholipase A_2
PLC-γ	Phospholipase C-γ
PSD	Postsynaptic density
PSD-95	Postsynaptic density protein-95
R	Regulatory subunit
RSK	Ribosomal S6 kinase
SAP-97	Synapse associated protein 97
SAP-102	Synapse associated protein 102
Ser	Serine
SOD	Superoxide dismutase
SOP	serine-O-phosphate
S-SCAM	Synaptic SCAffolding Molecule
SynGAP	Synaptic Ras GTPase

Tet	Tetracycline
tetO	Tetracycline resistance operon
Thr	Threonine
Trk	Tyrosine receptor kinase
tTA	Transcriptional activator
Tyr	Tyrosine

Abstract

Engineering Mutations into the Mouse NR2B Gene of the NMDA Receptor

N-methyl-D-aspartate (NMDA) receptors are glutamate gated ion channels and essential for forms of synaptic plasticity, learning and memory formation. The developmental expression patterns of NMDA receptor subunits suggest that they are important in early postnatal life and therefore it is not surprising that mice lacking NR1 and NR2B subunits die shortly after birth. The C-terminal domain of NR2B subunits is not necessary for channel function, but binds proteins involved in signal transduction. Since mice expressing the C-terminal truncated form of the NR2B subunit also die at birth, this suggests the importance of the C-terminal domain in the signalling pathways.

The C-terminus of the NR2B subunit is 616 in length and the terminal valine residue is essential for binding the PDZ domains of postsynaptic density protein-95 (PSD-95). PSD-95 is essential for plasticity and learning and is an adaptor for other signalling proteins such as synaptic Ras GTPase (SynGAP) and neuronal nitric oxidase synthase (nNOS). Knockin mice were created, which lack the terminal valine residue of NR2B in order to disrupt the connection between the NR2B and the downstream signalling components. Although much is needed to be done to properly characterise this mutant, we made a very important step forward to understand how molecular interactions within the C-terminal domain of the NR2B subunit affect the function of the NMDA receptor by generating viable mutants.

I also created a mutation in the calcium- and calmodulin-dependent protein kinase II (CaMKII) binding site of NR2B, which eliminates a different signalling pathway, and finally, deleted the COOH-exon of the NR2B subunit and replaced it by that of the NR2A, which experiment shows the importance of the interactions via the NR2B cytoplasmic tail. The analysis of the mutant mice can provide precise insight into the function of NMDA receptor interacting proteins in synaptic plasticity, learning and memory formation.

Chapter 1: Introduction

1A General introduction to glutamate receptors

A brief history of synapses and the discovery of glutamate

Human kind's constant fascination with the perfection and imperfection of the brain has led to extensive research, through the trials and errors of which we uncover more and more details up till today.

A major milestone in the history of neuroscience was when Golgi developed the silver impregnation method and was able to visualize the individual units in the brain. Prior to that, the general belief was that the brain is a glandular organ and that the nerves are like the veins, carrying fluid to the periphery. With Golgi's method the cell body and its two types of processes, the dendrites and the axon could be shown, proving that the brain is a well-organised structure of distinct cells rather than a syncytium. The work of Golgi and later Ramón y Cajal in the 19th century led to the *neuron doctrine*, which stated that the brain is composed of individual signalling elements, the neurons and that they communicate via specialized points of interaction.

With the development of anatomy, neurophysiology and pharmacology more and more details of the function of the brain were available, that turned the interest towards behavioural studies. One of the most interesting theories of the late 19th century was that of Franz Joseph Gall. He believed that the cerebral cortex had 35 regions, each of which corresponded to certain mental functions and behaviours, in that way building up one's personality. He had regions for *hope*, *spirituality* as well as *destructiveness*, which corresponded to fairly large areas. In contrast areas for perception, such as visualising *colour* or for learning certain tasks, such as *language*, *calculation* or *order* were relatively small. He stated however, that by differential usage of certain areas, they increased in size differentially, resulting in protrusions, which could be visualized as bumps on the skull. Since then many different theories

have emerged, some opposing, some favouring his view, nevertheless the basic idea is correct, the brain is organised into different regions built up of individual neurons. These individual neurons are the signalling units of the brain and they are connected to each other in a precise order, communicate with each other via specialized points of interaction and certain groups of neurons in different brain regions mediate different functions of the brain and are involved in certain behavioural patterns.

The term synapse was introduced by Charles Sherrington used for those specialized points of interaction between neurons, that were histological described by Ramón y Cajal. During the 1920's, 1930's debate arose whether the means of transmission was electrical or chemical. The first molecule shown to be an example of the latter was acetylcholine, mediating synaptic transmission from the vagal nerve to the heart. In the 1950's with the improvement of physiological techniques both were shown to exist. The differences between the structure of the electrical and chemical synapses were visualized using the electron microscope. Electrical synapses can be found in nerve cells, smooth muscle and the heart. Transmission is ionic current mediated, it can be bi-directional and is rapid. The cytoplasm of the pre- and postsynaptic cells is connected via ion channels at the site of interaction, the gap junction. Their distance is only 3.5 nanometers. Chemical synapses are more common in the brain. Transmission is chemical messenger mediated, it is unidirectional and can be excitatory or inhibitory. At chemical synapses the neurons are separated by a cleft, which is 30-50 nanometers.

In the brain the predominant form of synaptic transmission is chemical. Information from the presynaptic neuron is transmitted onto the postsynaptic cell via chemical messengers, where a receptor is activated. The activated receptor then can directly gate an ion channel, activate the production of a second messenger. There are certain criteria that a second messenger has to meet in order to be called a transmitter. They have to be synthesized in the neuron and there is a specific mechanism, which removes them from the site of action. They have to be present in the presynaptic neurons and be released in amounts, which are sufficient to induce activation of the postsynaptic cell. Finally exogenous application of the transmitter has to exert the

same effects as the endogenous messenger. The first molecules recognised to meet these criteria were acetylcholine and norepinephrine described in the 1930's. Since then more have been identified and classified into two groups, small-molecule transmitters (acetylcholine, amines such as dopamine or norepinephrine or amino acids) and neuroactive peptides (certain hormones and peptides).

Glutamate, aspartate or homocysteine belong to the group of small-molecule transmitters and they can be found in the central nervous system in high concentrations. They are involved in excitatory synaptic transmission and activate the group of glutamate receptors. Glutamate seems to be the most important of these having been researched during the past sixty years. In the 1940's it was claimed that it could improve the condition of mentally impaired patients. In the 1950's it was shown that glutamate caused convulsions (Hayashi, 1952; Hayashi, 1954) and was proposed to be a central synaptic transmitter. Later it was proven to be an excitatory transmitter (Curtis et al., 1959). Since then various receptor subtypes have been discovered and characterised in detail, which are activated by glutamate. It activates cation-selective channels, thereby mediating fast excitatory neurotransmission. According to rough estimations 50% of all central nervous system synapses and about 90% of all excitatory synapses are mediated by glutamate. In the next section the different ionotropic receptors will be classified and characterised before discussing aspects of the *N*-methyl-D-aspartate receptor in great detail.

Ionotropic glutamate receptors

Glutamate receptors provide for synaptic plasticity, learning and memory. They mediate the toxicity of excess glutamate release from cells in pathological conditions like stroke. All known ionotropic glutamate receptors belong to the same gene family. They are categorized into three groups, high affinity α-amino-3-hydroxy-5-methyl-4-isoxazolepropionic acid (AMPA) or low affinity kainate receptors, high affinity kainate receptors and *N*-methyl-D-aspartate (NMDA) receptors (Wisden and Seeburg, 1993).

The high affinity AMPA or low affinity kainate receptor type of the ionotropic glutamate receptors is a ligand-gated ion channel localized postsynaptically. Its main agonists are L-glutamate and AMPA. It mediates fast excitatory synaptic transmission and contributes to LTP (Kakegawa et al., 2004; Kakegawa and Yuzaki, 2005; Sun et al., 2005; Oh et al., 2006) and LTD (Steinberg et al., 2004; Moult et al., 2006) in various brain regions.

Postsynaptic AMPA receptors are located to the plasma membrane or are internalized into intracellular pools thereby regulating synaptic strength (Carroll et al., 2001; Malinow and Malenka, 2002). Receptor internalization occurs during LTD via clathrin-mediated endocytosis upon which the receptors are stabilized by AMPA interacting proteins such as GRIP (Dong et al., 1999). Cell surface delivery of the receptors occurs during LTP (increased synaptic strength) by exocytosis as a result of NMDA receptor activation (Liao et al., 2001; Park et al., 2004).

AMPA receptors are heteromeric consisting of GluR1-4 or A-D subunits and have a tetrameric structure (Mansour et al., 2001; Brorson et al., 2004). They exist in two splice variants, flip and flop, which correspond to two different amino acid sequences preceding TM4 (Sommer et al., 1990). This sequence difference determines the distinct kinetic properties of the two splice variants (Sommer et al., 1990). The GluR-B subunit is present in nearly all AMPA receptors and it influences properties of the ion flow. In the second membrane domain (M2) a site referred to as Q/R site has been identified. The GluR-B pre-mRNA can be edited at this site (Higuchi et al., 1993; Puchalski et al., 1994). The unedited, glutamine-containing (Q607) form is Ca^{2+} permeable, the edited, arginine-containing (R607) is Ca^{2+} impermeable. Ca^{2+} permeability of the channel is increased, LTP is enhanced, and motor coordination is reduced in the GluR-B knock-out mutants (Jia et al., 1996; Gerlai et al., 1998). GluR-B, GluR-C and GluR–D subunits are also edited at the secondary R/G site influencing the channel kinetics (Lomeli et al., 1994).

High affinity kainate receptors are another type of ionotropic, ligand-gated receptor channels. The main agonist is L-glutamate, others are kainite and domoate

(Bleakman, 1999). AMPA and 4 methyl glutamate are GluR5- and GluR6-specific agonists respectively (Bleakman, 1999). Kainate receptors are localized both pre- and postsynaptically (Jaskolski et al., 2005). Postsynaptic receptors are stabilized by protein interactions with PDZ-containing molecules such as PSD-95, SAP-97 or SAP-102 (Garcia et al., 1998). Kainate receptors are involved in fast excitatory synaptic transmission and in nociception (Ruscheweyh and Sandkuhler et al., 2002). They induce NMDA receptor-independent mossy-fibre LTP (Bortolotto et al., 1999; Bortolotto et al., 2005) and their involvement was implicated in induction of LTD (Park et al., 2006).

The subunits are divided into two subgroups corresponding to two separate gene families, the high affinity KA-1 and KA-2, and the low affinity GluR-5, GluR-6 and GluR-7 subunits. The δ-1 and δ-2 subunits are most related to the first group, but do not function *in vitro* (orphans). The receptor is tetrameric in structure. GluR-5, GluR-6 and GluR-7 can, KA subunits cannot form functional homomeric receptors *in vitro* (Wisden and Seeburg, 1993). Homomeric GluR-5 receptors resemble native kainate receptors in dorsal root ganglia cells and can be gated by AMPA. Homomeric GluR-6 cannot be gated by AMPA. KA-2/GluR-6 heteromeric receptors are sensitive to AMPA (Herb et al., 1992; Wisden and Seeburg, 1993).

GluR-5 and GluR-6 subunits are edited at the Q/R site, which is located before the third transmembrane domain (Sommer et al., 1991). Ca^{2+} permeability is reduced in the edited form, which is more abundant in the adult animals. GluR-6 subunits can also be edited at two sites located to the first transmembrane domain (I/V editing at position 567 and Y/C editing at position 571), which also influences Ca^{2+} permeability (Kohler et al., 1993).

NMDA receptors are the third type of ligand gated-ion channels. L-glutamate and NMDA are agonists, glycine is coagonist (Wisden and Seeburg, 1993) (Table 1). They are localized postsynaptically interacting with PSD-95 via PDZ-domain interactions (Find in detail in section 1Band 1C.), but there is evidence of presynaptic presence as well (Liu et al., 1994; Bardoni et al., 2004).

NMDA receptors are heteromeric comprising of two NR1 and two NR2A, NR2B, NR2C or NR2D subunits *in vivo*, however many previous studies demonstrated different stoichiometry (Find in detail in section 1B.). This heteromeric structure is the most efficient assembly upon activation of which, the highest increase in current can be observed. The NR1 and NR2 subunits are only 18% homologous in their polypeptide sequence. In the second membrane domain (M2) an asparagine residue is present homologous to the Q/R site in AMPA receptors, which mediates Ca^{2+} permeability (Burnashev et al., 1992). The glycine binding site is located to the NR1 subunit extracellular 1 domain (Kuryatov et al., 1994), while the glutamate binding site is located to the NR2 subunits (Find in detail in section 1B.). The NR2 subunits bear a large (~600 amino acids compared to 50-100 in other ionotropic glutamate receptors) cytoplasmic tail via which they interact with downstream signalling molecules (Find in detail in section 1C.).

NMDA receptors are activated by NMDA and glutamate, but not activated by AMPA and kainite. They mediate excitatory synaptic transmission and are involved in some forms of learning and memory formation. They are important in excitotoxicity (overexcitation of neurons caused by excessive glutamate release resulting in cell-death) (Choi et al., 1988), numerous neurological and psychiatric conditions and neuropathic pain. The NMDA receptor is a "coincidence detector", for channel opening a simultaneous postsynaptic (depolarization removing the Mg^{2+} block) and presynaptic activity (glutamate release) is required. In the next sections the subunit composition, ion channel properties and signalling functions of the NMDA receptor will be described in greater detail.

1B NMDA receptor channel

Subunit characterization

The *N*-methyl-D-aspartate (NMDA) receptors are heteromeric ligand gated ion channels localized mostly to the postsynaptic site, but there is evidence of

presynaptic presence (Liu et al., 1994; Bardoni et al., 2004). NMDA receptors are derived from at least seven known genes. One encodes the NR1 subunit, the variability of which arises from alternative splicing, which results in eight different functional forms. Alternative splicing occurs via insertion or deletion of three exons, the N1 in the N-terminal and the C1 and C2 in the C-terminal domain (Hollmann et al., 1993). Other genes provide for the NR2 subunit diversity, encoding for NR2A-D forms. Recently NR3A-B subunits have also been reported (Sucher et al., 1995; Andersson et al., 2001; Nishi et al., 2001; Bendel et al., 2005).

The coassembly of the distinct NR1 splice variants with the particular NR2A-D subunits is required for functional NMDA receptors. The developmental (NR1 and NR2B embryonic and postnatal, NR2A and NR2C postnatal, NR2D embryonic expression) and regional distribution (NR1 all through the brain, NR2A forebrain and basal ganglia, NR2B forebrain, NR2C cerebellum, NR2D thalamus and subthalamus) of these subunits results in various receptor types (Monyer et al., 1992; Monyer et al., 1994; Standaert et al., 1996; Weiss et al., 1998), which have distinct electrophysiological and pharmacological properties. Modulation by zinc, inhibition by proton and stimulation by polyamines is attenuated by the presence of the N1 exon of the NR1 subunit (Hollmann et al., 1993; Durand et al., 1993). The C1 exon of the NR1 subunit mediates binding to alpha actinin (Wyszynszki et al., 1997) regulating synaptic localization. The C2 exon contains an "endoplasmatic reticulum signal" preventing cell surface delivery of homomeric NR1 subunits (Okabe et al., 1999; Scott et al., 2001).

The primary structure of the NMDA receptor subunits was proposed based on the cDNA sequence. The NR1 subunit was cloned from rat cDNA library by expression cloning (Moriyoshi et al., 1991), the NR2A-D subunits by PCR and cross hybridisation (Ikeda et al., 1992; Kutsuwada et al., 1992; Meguro et al., 1992; Monyer et al., 1992; Ishii et al., 1993). All subunits contain an extracellular N-terminal domain, four hydrophobic membrane domains (M1-4) and a C-terminal domain. The size of the different subunits varies with NR1 being the smallest consisting of 920 amino acids (103 kDa), then NR2C containing 1218 or 1220 amino

acids (133 or 134 kDa), NR2D containing 1296 amino acids (144 kDa), NR2A with 1445 amino acids (163 kDa) and NR2B with 1456 amino acids (163 kDa). The various NR2 subunits are very similar, showing considerable (40-50%) homology while there is only about 18% similarity between the NR1 and the NR2 subunits. However comparing the C-termini of the NR2 subunits, the homology is only about 30% suggesting that the functional differences arise from the variability of this domain.

The transmembrane topology (Figure 1) based on the cDNA sequence (Moriyoshi et al., 1991) suggested a similar structure to that of the nicotinic acethylcholine receptor. With the N-terminus being extracellular and having four hydrophobic, possibly transmembrane domains (M1-4), the C-terminus was thought to be extracellular as well. However phosphopeptide mapping revealed that the NR1 subunit is phosphorylated *in vivo* (Tingley et al., 1993) and interactions of the C-termini of the different NR2 subunits with various intracellular molecules were also described. Glycosylation sites of the N-terminal domain were identified as well (Hollmann et al., 1994). These findings suggested that a three transmembrane model theory is more accurate according to which there are four hydrophobic regions, but M2 is a cytoplasm facing re-entrant loop and only M1, 3 and 4 are transmembrane (Figure 1). The N-terminus is extracellular, while the C-terminus is intracellular. The region between M3 and M4 is extracellular as well (Sullivan et al., 1994). The various domains of the NMDA receptor subunits will be described next.

The channel pore domain is responsible for determining channel properties, ion flux, and permeability. In the M2 region of NR1 and NR2 subunits there is an asparagine residue, homologous to the Q/R site in AMPA receptors, which plays a role in the Ca^{2+} permeability of the channel. In the NR2B subunit it is in position 589. Mutation of this asparagine to glutamine removes the voltage dependent Mg^{2+} block and alters the permeability to divalent cations (Burnashev et al., 1992). Mutating a tryptophan residue (W607L) in the NR2 M2 region also abolished Mg^{2+} block (Williams et al., 1998) indicating the importance of other residues apart from the asparagines'. Since Mg^{2+} binds to a site in the ionophore that causes voltage-dependent block of the

channel (Ascher and Nowak, 1988), these findings suggest that the M2 re-entrant loop constitutes to the ion channel lining the pore of the receptor.

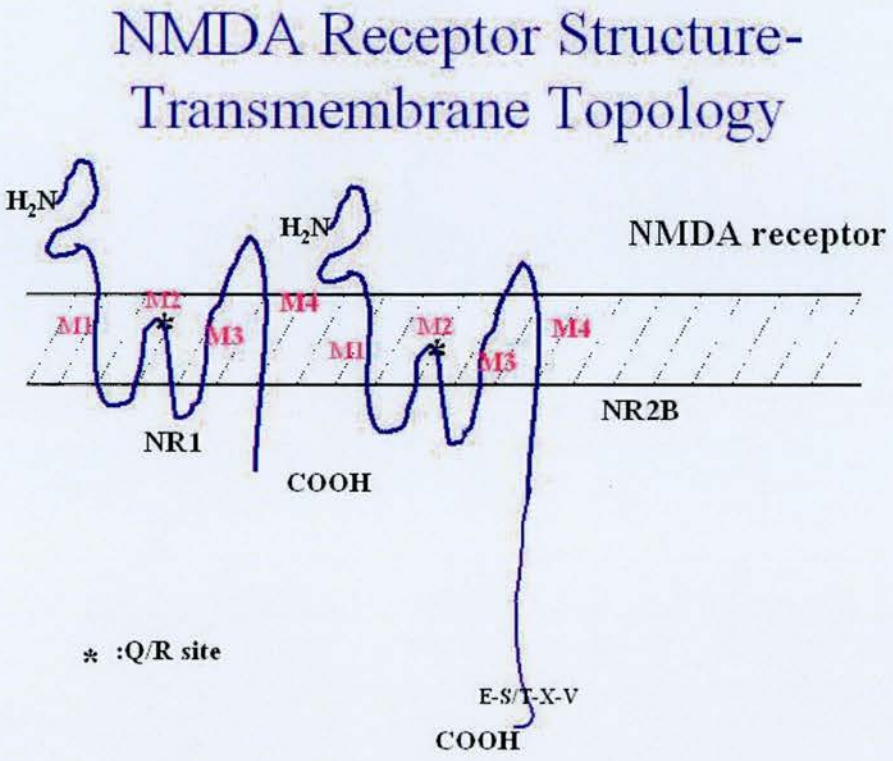

Figure 1. NMDA Receptor Structure and Transmembrane Topology.
The structure resembles that of the nicotinic acetylcholine receptor, but it has three transmembrane loops and M2 is a cytoplasm facing re-entrant loop. The N-terminus is extracellular while the C-terminus is intracellular.

The phosphorylation domain of the receptor is the C-terminus of the different subunits found intracellularly. The C-terminus of NR1 is phosphorylated in primary cultures and in transfected HEK 293 cells (Tingley et al., 1993). The NR2 subunits are directly phosphorylated on the C-terminus by protein kinases for example PKC (Figure 4, Table 3). Protein kinases and their sites of phosphorylation on the various subunits will be discussed in detail in section 1C and 1F. Another important feature of the C-termini of the different subunits is that they bind to cytoskeletal proteins and neurofilaments regulating synaptic localization of the receptor. The C1 exon of the NR1 N-terminus binds alpha actinin (Wyszynszki et al., 1997). This interaction is antagonized by calcium calmodulin (Ca^{2+}/CaM). Alpha actinin also selectively binds

NR2B amongst the NR2 subunit types (Wyszynszki et al., 1997). NR1 further interacts with calmodulin (CaM) via the C0 region (Krupp et al., 1999), neurofilaments and yotaio while NR2 subunits bind PSD-95, SAP-102 and chapsyn-110 (Bassand et al., 1999).

The allosteric modulation domain is located in the extracellular region found between the M3 and M4 transmembrane regions. Polyamines such as spermine and spermidine can inhibit the NMDA receptor response at high concentrations. At low concentrations however they potentiate NMDA function (channel opening) by increasing the channel's affinity to glycine or by increasing the channel's opening frequency with no change in affinity (Rock and MacDonald, 1992). Cysteine 726 and 780 in NR1 seems important in mediating the effects of certain molecules. The mutation of these residues eliminates potentiation by dithiothreitol, spermine and inhibition by proton (Sullivan et al., 1994). Other allosteric modulators are various redox reagents, ethanol or nitric oxide. Dithiothreitol mediated inhibition of NR1/NR2A channels is not dependent on alkylation (Kohr et al., 1994) while modulation of NR1/NR2B, NR1/NR2C and NR1/NR2D receptor activity by dithiothreitol is blocked by alkylation (Kohr et al., 1994). The effect of nitric oxide is either mediated by binding to the redox site or via direct channel block. It decreases the channel conductance in a voltage-dependent and open probability in a voltage-independent manner (Fagni et al., 1995).

Binding of both glutamate and glycine is required for full activation of the NMDA receptor (Johnson and Ascher, 1987). The key residues in the ligand binding domain were identified by site directed mutagenesis. In NR1 a glycine binding domain (phenylalanine-X-tyrosine) at around residue 370, the phenylalanine 448 in the amino-terminal and the extracellular region between M3 and M4 were found important (Kuryatov et al., 1994). The mutations of these sites affect the efficient concentration for half-maximum response (EC_{50}). The NR2 subunits do not bind glycine, but modulate interaction by changing the affinity of the receptor for glycine. NR1/NR2B receptors have a higher affinity while NR1/NR2A receptors have lower affinity (Honer et al., 1998).

While NR1 subunits are responsible for the glycine binding, the glutamate binding site is located to the NR2 subunits. The residues crucial for the interaction are located to the region N-terminal to the first transmembrane domain (S1) and the extracellular loop between the third and fourth transmembrane regions (S2) (Armstrong et al., 1998). Pharmacological effects of agonists and antagonists will be summarized separately in section 1B/Ion channel properties and pharmacology.

Subunit composition

The most commonly used method to determine the subunit composition of the various NMDA receptors in different brain regions is to solubilize them and then use immunoprecipitation or immunoaffinity purification using subunit specific anti-NMDA receptor antibody 1. Thereafter subunit colocalization is determined by immunoblotting with other high specificity anti-NMDA receptor subunit antibodies.

For normal receptor function NR1 subunits have to co-assemble with distinct NR2 subunits. Although NR1 homomeric channels are expressed in for example Xenopus oocytes (Yamazaki et al., 1992) and are responsive to glutamate and glycine or NMDA and glycine, the current responses are relatively small. In mature Purkinje cells, which only express NR1 and not NR2 subunits, there is no NMDA receptor activity observed at all (Perkel et al., 1990; Quinlan and Davies, 1985). As opposed to that the NR1/NR2 heteromeric channels found in other brain regions are highly active. It is the most efficient assembly upon activation of which, the highest increase in current can be observed. The responses evoked by glutamate and glycine are suppressed by 2-amino 5-phosphonopentanoic acid (AP-5), 7-chlorokynurenate, Mg^{2+} and dizocilpine (+)-10,11-dihydro-5-methyl-5H-dibenzo[a,d]cyclohepten-5,10-imine (MK-801) (Meguro et al., 1992; Monyer et al., 1992). Biochemical studies also support the heteromeric structure. Anti-NR1 subunit antibodies immunoprecipitate NR2A and NR2B subunits in rat cerebral cortex (Sheng et al., 1994), anti-NR2A precipitates NR2B and vice versa suggesting that part of the NR2A and NR2B subunits are present in the same complex in vivo.

NR1/NR2A containing receptors are present in the forebrain and cerebellum (Sheng et al., 1994; Chazot et al., 1997), NR1/NR2B containing receptors in the forebrain (Sheng et al., 1994; Chazot et al., 1997). NR1/NR2C association can be observed in the cerebellum (Sheng et al., 1994) and NR1/NR2D in the forebrain and the thalamus (Dunah et al., 1998). In forebrain (Luo et al., 1997) and in developing cerebellar granule cells (Didier et al., 1995) co-association of three different subunits NR1, NR2A and NR2B was shown. This receptor population accounts for only a minor part of the total receptor pool. Ternary complexes of NR1/NR2A/NR2D were found in forebrain, thalamus and spinal cord (Dunah et al., 1998).

The stoichiometry of NMDA receptors has always been debated. Evidence for both pentameric and tetrameric structures has been shown. The size of the chemically cross-linked NMDA receptor suggests pentameric structure (Brose et al., 1993). According to single channel current patterns some assume that the NMDA receptors contain three NR1 and two NR2 subunits (Premkumar et al., 1997) some suggest the association of two NR1 and two NR2 subunits (Laube et al., 1998). Other studies suggest that both the subunit composition and stoichiometry is variable depending on the brain region and developmental status. Co-transfection of FLAG and c-Myc tagged subunits into HEK293 cells suggests the existence of two NR1 and three NR2 subunit-containing receptors (Hawkins et al., 1999). A recent expression study with truncated subunits supported the tetrameric model (Schorge et al., 2003). Most of the evidence supports the two NR1 two NR2 assembly *in vivo*, which is the accepted model.

Diversity of NMDA receptors in different neuronal populations

NMDA receptors play an important role in brain development for example in corticogenesis, synaptogenesis or neural migration. The differences between the expression patterns of the different NMDA receptor genes during various developmental stages might account for these processes.

In different species there are only slight alterations between the NR2B gene and protein expressions *in vivo*. The expression patterns *in vitro* (for example in mouse

primary cultures) match that of the *in vivo* results. *In vivo*, from as early as embryonic day 14 (E14), NR2B expression is evident in the spinal cord and the hypothalamus (Monyer et al., 1994). By E17 the expression increases in the cerebral cortex, thalamus and spinal cord and at a lower level in the hippocampus and the hypothalamus. After birth and until postnatal day 7-12 (P7-12) the expression continues to increase mainly in the cerebral cortex and the hippocampus. By P21 the expression reaches adult level. The NR2A mRNA expression is undetectable until birth and then increases from P2 to P21 to adult level. It is abundant in the cortex and hippocampus (Wenzel et al., 1997). NR2C is expressed in the cerebellum, NR2D in the subcortical areas whereas NR1 is abundantly expressed throughout the brain from early stages of development.

In primary cultured cortical neurons prepared from E17 rat neocortex the expression levels of the different NMDA receptor subunits were low or undetectable. Expression of NR1 started to increase from day in vitro 1 to 21, NR2A expression increased from day in vitro 7 to 21 (Zhong et al., 1994). The level of NR2B increased from day in vitro (DIV) 1 to 7 and stayed the same until day in vitro 21 (Zhong et al., 1994).

Apart from neuronal localization, the NMDA receptor subunits can also be found in non-neuronal tissue like keratinocytes, osteoclasts, osteoblasts or developing rat heart (Seeber et al., 2000; Itzstein et al., 2001). The presence of different NMDA receptor subunits in osteoclasts and osteoblasts (Itzstein et al., 2001) suggests a role in bone cell formation. In developing rat heart it is specifically the NR2B subunit, which is expressed, NR1 or other NR2 subunits are not, nor are GluR2 or PSD-95. NR1 and NR2B subunits were observed in the cat retina using immunocytochemical experiments (Pourcho et al., 2001) and in the rat retina using immunofluorescence studies (Fletcher et al., 2000).

Subcellular localization at synapses

For determining the cellular and subcellular localization the most frequently used methods are again immunoblotting and in situ hybridisation. Others are

immunohistochemistry or electron microscopy. The presence of the various subunits in the different brain regions and cell types connects them to various functions, which will be described through a few examples.

In rhesus monkeys the NR2B mRNA is detected throughout the primary sensory cortex and area 5 and in area 4 with a peak level of expression (Munoz et al., 1999). This implicates their involvement in processing sensory and motor information. Connection to the limbic system is suggested by localization in the midline of the medial septal region in rats (Plant et al., 1997).

In rat vestibular periphery and in rat retina immunohistochemistry and electron microscopy was used to localize the various NMDA subunits. In the inner plexiform layer of the rat retina NR1/NR2A, NR1/NR2B and NR1/NR2A/NR2B receptor complexes colocalized with PSD-95, SAP-102 postsynaptically (Fletcher et al., 2000), while electron microscopical evidence was demonstrated showing presynaptic NR1C2 presence (Fletcher et al., 2000). In the rat vestibular periphery NR1, NR2A and NR2B subunits showed immunoreactivity in the type I vestibular hair cells and not in type II (Ishiyama et al., 2002).

In cultured hippocampal neurons NR2B mRNA was detected in the dendrites and the soma (Miyashiro et al., 1994). When hippocampal neurons were transfected with GFP-NR2A and GFP-NR2B clusters were observed at the dendritic shafts and spines (Luo et al., 2002). In cultured cortical neurons NR1/NR2B receptors were expressed in the cell bodies of the mature neurons (Hall and Soderling, 1997). In the rat striatum NR1/NR2A and NR1/NR2B receptor types were localized to the light membrane, synaptosomal membrane and intracellular compartments while the ternary NR1/NR2A/NR2B receptors were only found in the synaptosomal membrane (Dunah and Standaert, 2003). Considering the cell surface expression the greatest proportion of the NR2B subunits are found in the plasma membrane while almost half of the NR1 subunits contribute to an intracellular pool awaiting coassembly with the available NR2B subunits (Hall and Soderling, 1997).

The post-synaptic density (PSD) is an organized network of receptors, signalling molecules and scaffolding proteins located in the vicinity of the postsynaptic membrane, the function of which is to facilitate synaptic plasticity, protein phosphorylation, learning and memory formation. Immunoblotting of rat cortical and cerebellar tissue shows that NR2A and NR2B subunits are highly expressed at the PSD together with their binding partners, PSD-95 or chapsyn-110 (Al Hallaq et al., 2001). Synapse associated protein 102 (SAP-102) is located both at axonal sites and postsynaptically (El Husseini et al., 2000).

Ion channel properties and pharmacology

The subunits of the NMDA receptor form a channel permeable to cations. When in an activated state inward Ca^{2+} and Na^{+} flow can be observed, while K^{+} ions move outwards, which can be blocked in the presence of Mg^{2+} and Zn^{2+} (Nowak et al., 1984; Paoletti et al., 1997). For activation of the receptor it is important that the glutamate binding site is activated, the voltage-dependent Mg^{2+} blockade is lifted (upon depolarisation) and that the glycine activated co-agonist binding site is in an active state (Nowak et al., 1984; Johnson and Ascher, 1987). The main endogenous agonists of the glutamate binding sites are glutamate and aspartate, that of the glycine site is glycine. However the former can bind endogenous homocysteic acid or quinolinic acid activating the NMDA receptor (Lipton et al., 1997), the latter endogenous D-cycloserine (Baranano et al., 2001) or 3-amino-1-hydroxypirrolidin-2-one (HA966) (partial agonist) with high affinity.

Aside from the glutamate and glycine binding site there is an allosteric binding site on the N-terminus. It is activated by endogenous polyamines like spermidine, spermine or putrescine (Rock and MacDonald, 1992). These are physiological modulators of NMDA receptor function and were discussed previously in detail. The Mg^{2+} (Ascher and Nowak, 1988) and Zn^{2+} binding sites can be found inside of the channel. Another binding site in the same position is the phencyclidin (PCP) or MK-801 site, which are exposed only in open channel position and are named after their specific blockers (Table 1).

The voltage dependent Mg^{2+} block, which is stronger in NR1/NR2A and NR1/NR2B receptors than in NR1/NR2C and NR1/NR2D (Kuner and Schoepfer, 1996) is regulated by the Q/R site in the M2 region of the NR1 and NR2 subunits. In the NR2B subunit it is in position 589. Mutation of this asparagine to glutamine removes the voltage dependent Mg^{2+} block and alters the permeability to divalent cations (Burnashev et al., 1992). It also modulates the inhibition by argiotoxin and Joro toxin (Raditsch et al., 1993). Mutating the tryptophan residue (W607L) in the NR2 M2 region also abolished Mg^{2+} block (Williams et al., 1998).

Zn^{2+} mediates voltage-dependent and voltage-independent receptor blockade in a manner that is NMDA receptor subunit specific. The voltage-dependent inhibition is the same for NR1/NR2A and NR1/NR2B containing receptors, while the voltage-independent mechanism is characterized by high affinity inhibition (at lower Zn^{2+} concentrations) in the case of the NR1/NR2A receptors and a lower affinity inhibition (at higher Zn^{2+} concentration) in the NR1/NR2B receptors (Paoletti et al., 1997). The presence of the N1 exon of the NR1 subunit increases the half maximal inhibitory concentration (IC_{50}) for Zn^{2+} in the voltage-independent mechanism (Traynelis et al., 1998). The binding sites for Zn^{2+} can be found inside of the channel. Other binding sites in the intramembrane loop are for phencyclidine (PCP) and dizocilpine (MK-801) with the latter requiring extra sequence information in the M3 region (Ferrer-Montiel et al., 1995).

NMDA receptors frequently colocalize with AMPA or kainate receptors. Stimulation of the NMDA receptors results in slow depolarisation and increased Ca^{2+} influx, while stimulation of AMPA or kainite receptors results in fast depolarisation and the Ca^{2+} permeability stays low. The former is involved in the plasticity of the central nervous system while the latter is connected to fast synaptic transmission. The reason is that for the lift of the Mg^{2+} blockade of the NMDA receptor an intense depolarising stimulus is required, which happens for example during the prolonged excitation of the AMPA or kainite receptors (for example during long term potentiation). The NMDA receptors contribute to the process via the Ca^{2+} influx, the

protein kinase C (PKC) activation and the nitric oxide (NO) release. Through this process the NMDA receptor is involved in the formation of learning and memory.

Receptor family	**Ionotropic**			**Metabotropic**	
Receptor-type	**NMDA**	**AMPA**	**Kainate**	**Group I**	**Group II/III**
Signal transmission	Na^+ K^+ ↑ $Ca2^+$ ↑	Na^+ K^+ ↑		IP_3/DAG ↑	cAMP ↓
Agonist	NMDA aspartate	AMPA 5-fluorowillardiine	kainate domoate	ACPD 3,5-DHPG	DCG-IV*(II) ACPD (II) AP-4 (III) SOP (III)
Positive allosteric modulator	glycine (coagonist) d-cycloserine (PA) (+)HA966 (PA)				
Antagonist	AP-5 AP-7	NBQX	LY294486	MCPG AIDA 4CPG	MCPG MCCG (II) EGLU (II) MAP4 (III) MSOP (III)
Negative allosteric modulator	5,7-dichloro-kynurenic acid MNQX	GYKI52466			
Channel inhibitor	dizocilpine Mg^{2+} PCP ketamine	Intracellular: polyamines Extracellular: argiotoxin, Joro toxin	Intracellular: polyamines Extracellular: argiotoxin, Joro toxin		

Table 1. Glutamate receptor agonists. (Fürst K. Introduction to the pharmacology of positive psychotropic compounds. Pharmacology. 2001: 323-325.)
The agonists and modulators of the various glutamate receptors are summarized.
PA: parcial agonist; ACPD: 1-amino-cyclopentane-1,3-dicarboxylic acid; AIDA: 1-aminoindan-1,5-dicarboxylic acid; AP-4: 2-amino 4 phosphobutyric acid; AP-5: 2-amino 5-phosphopentanoic acid; AP-7: 2-amino 7- phosphopentanoic acid; DCG-IV: 3-dicarboxy-cyclopropylglycine; DHPG: 3,5-dihydroxyphenylglycine; EGLU: alpha-ethylglutamic acid; GYKI 52466: 1-(4-aminophenyl)-4-methyl-7,8-methylenedioxy-2,3 benzodiazepine hydrochloride; HA966: 3-amino-1-hydroxypyrrolidin-2-one; LY 293558: 2-tetrazole-ethyl-decahydroisoquinoline-3-carboxylic acid; LY 294486: 2-tetrazole-methyl-oxymethyl-alpha-decahydroisoquinoline-3-carboxylic acid; MAP4: methylamino-phosphonium-butyric acid; MCCG: 2-methyl-2-carboxypropyl-glycine; MCPG: alpha-methyl-4-carboxyphenylglycine; MNQX: 5,7-dinitroquinoxaline-2,3-dione; MSOP: alpha-methylserine-O-phosphate; NBQX: 6-nitro-7-sufamoyl-benzoquinoxaline-2,3-dione; SOP: serine-O-phosphate

If the intracellular Na^+ concentration increases due to constant depolarisation, overactivation of the receptor then the Ca^{2+} influx increases and it results in apoptotic

cell death. It can be observed in pathological conditions like ischaemia or hypoglycaemia. Apart from these NMDA receptor is involved in other acute neurodegenerative disorders such as stroke, mechanic head injuries and hypoxic conditions after convulsion or chronic diseases like Alzheimer's disease, Parkinson's disease, amyotrophic lateral sclerosis (ALS), Huntington-chorea and AIDS-dementia.

1C NMDA receptor signalling complex

NMDA receptor signalling complex composition

The NMDA receptor complex is a ~2000 kDa complex (Husi et al., 2000), consisting of at least 75 proteins, which are either directly interacting with different subunits of the receptor, or are indirectly linked via other molecules. These proteins can be categorised into five groups, which are cell adhesion molecules, adaptors, neurotransmitter receptors, signalling enzymes and cytoskeletal proteins (Husi and Grant, 2001). There is evidence for the importance of the C-terminal intracellular domain of the NR2 subunits in providing binding sites for downstream signalling molecules (Find in detail in section 1D and 1F.).

The direct binding partners can be categorised into two major groups (Figure 2, Table 2a, b and c). One is the group of membrane associated guanylate kinase (MAGUK) proteins. They all contain PDZ domains and via this domain they bind to the E-S/T-X-V motif located at the extreme C-termini of the NR2 subunits. A few of these proteins are PSD-95, chapsyn-110 or SAP 102. These further interact with neuronal nitric oxidase synthase (nNOS) (Holscher et al., 1997), fyn (Human locus IDDM15 gene FYN) (Grant et al., 1992) or synaptic Ras GTPase (SynGAP) (Chen et al., 1998), which is also a regulator of Ras.

The first MAGUK protein to be characterized was Dlg, the product of the Drosophila lethal(1)disclarge-1 tumor suppressor gene (Woods and Bryant, 1991) localized to the septate junction at the apical edge of polarized epithelial cells. Mammalian

members of the protein family were then cloned, amongst which are the neuronal proteins, PSD-95 (SAP-90), PSD-93 (Chapsyn-110), SAP-97 (hDLG) and SAP-102 (Cho et al., 1992; Muller et al., 1995; Muller et al., 1996; Brenman et al., 1996). PSD-95, PSD-93 (abundantly at the PSD) and SAP-102 can be found postsynaptically (Muller et al., 1996; Rao et al., 1998) while SAP-97 is presynaptic (Muller et al., 1995). The zonula occludens proteins (ZOP), ZO-1, ZO-2 and ZO-3 can be found in epithelial and endothelial intracellular junctions (Stevenson et al., 1986; Jesaitis and Goodenough, 1994; Haskins et al., 1998). ZO-1 can also be found in astrocytes, fibroblasts and myeloma cell lines.

The distinct localization and function of the MAGUK proteins might be accounted for by the differences in their N-terminal structure. All MAGUK proteins contain a guanylate kinase (GUK), a Src homology (SH3) and a PDZ domain. The N-terminal region is variable, due to the presence of an additional two PDZ domains or a CaMKII homology domain and alternative splicing. PSD-95 and PSD-93 contain cysteine residues in the N-terminal region, which are sites for post-translational palmitoylation (Brenman et al., 1996; Topinka and Bredt; 1998; El Husseini et al., 2000). SAP-102 also contains cysteines, but instead of being palmitoylated they bind to zinc (Muller et al., 1996; El Husseini et al., 2000). SAP-97 lacks N-terminal cysteines. In addition to that PSD-93 is alternatively spliced at the N-terminus yielding two major isoforms (α and β), which contain the cysteine residues at different positions (Brenman et al., 1996). Using mutants it was shown that the subcellular localization of MAGUKs and ion channel clustering at the plasma membrane (mediated by MAGUK interactions) is connected to palmitoylation (El Husseini et al., 2000). The PDZ domains bind voltage and ligand gated ion channels, the proline rich SH3 domains bind PXXP sequences (with evidence also for binding molecules without the PXXP motif) and the GUK domain interacts with GKAP proteins or the microtubule-associated protein-1A (MAP-1A) (Kim et al., 1996; Kim et al., 1997; Garner et al., 2000; Jia et al., 2005). These findings suggest that the MAGUKs are important in the assembly of macromolecular protein complexes and the interaction with GKAPs was shown to be connected to their recruitment to synaptic junctions (Thomas et al., 2000).

The PDZ domains of PSD-95 are responsible for its binding to NMDA receptors (second PDZ domain), Shaker-type K+ channels and cell adhesion molecules (Kim et al., 1995; Garner et al., 2000; Irie et al., 1997). PSD-95 enhances NMDA receptor clustering at the synaptic membrane, inhibits internalization mediated by NR2 subunits (Kim et al., 1996; Roche et al., 2001) and it regulates NMDA channel gating (increased channel opening probability and channel opening rate) and trafficking. The deletion of the PDZ binding domain of NR2A results in the blockade of PSD-95 induced increase in surface expression of the NMDA receptors and decrease in internalization (Lin et al., 2004). Overexpression of PSD-95 preferentially stabilizes NR1/NR2A receptor types at the synapses by facilitating synaptic insertion of NR2A subunits and decreasing NR2B expression (Losi et al., 2003).

The other group of molecules interacting with the NR2 C-termini is the non-MAGUK proteins, which bind to sites of the C-terminus other than the terminal E-S/T-X-V motif, and include for example Ca^{2+}-calmodulin-dependent protein kinase II (CaMKII), phospholipase C-γ (PLC-γ) and PI3-K. One signalling pathway connected to these is the mitogen-activated protein kinase (MAPK) pathway, connecting MAP kinase kinase (MEK), extracellular signal-related kinase (ERK) and ribosomal protein S6 kinase (Suzuki et al., 2001).

Ca^{2+}-calmodulin-dependent protein kinase II is a serine/threonine kinase encoded by four genes, with α and β predominantly found in the brain, yielding over 30 alternatively spliced isoforms. CaMKII monomers assemble into a holoenzyme possibly dodecamers, a dimer of two hexameric rings (Gaertner et al., 2004). Postsynaptic calcium influx results in the autophosphorylation of Thr 286 residue of CaMKIIα, which enables the molecule to remain activated even after dissociating from Ca^{2+}/CaM, its activator (Miller et al., 1988; Lou and Schulman, 1989). Further sites then become autophosphorylated in the Ca^{2+}/CaM binding domain of CaMKII blocking Ca^{2+}/CaM reassociation. Thr 286 autophosphorylated CaMKIIα is persistently active, translocates to the PSD and is necessary for NMDA dependent

LTP induction but only at certain synapses such as Schaffer commissural synapses in the CA1 region (Giese et al., 1998; Cooke et al., 2006). In medial perforant path-granule cell synapses LTP is connected to cyclic AMP-dependent signalling in Thr 286 autophosphorylation site mutant mice where CaMKII signalling is absent (Cooke et al., 2006).

CaMKII directly binds to subunits NR1 and NR2B of the NMDA receptor (Leonard et al., 1999). It demonstrates high affinity binding to the NR2B (induced by autophosphorylation of CaMKII), but not the NR2A C-terminus (Strack and Colbran, 1998). Residues 1290-1309 of the NR2B subunit are critical for the interaction. The key residues in this region were identified by site directed mutagenesis (Strack et al., 2000), which are Lysine (Lys) 1292, Leucine (Leu) 1298, Arginine (Arg) 1299, Arginine 1300, Glutamine (Glu) 1301 and Serine (Ser) 1303. Phosphorylation of Ser 1303 inhibits binding to CaMKII. For recruitment of CaMKII to the NMDA receptor residues 1260-1316 of NR2B are sufficient (Leonard et al., 1999).

Binding of CaMKII to NR2B can occur in two distinct ways. One is the enzyme-substrate binding via the catalytic (active) site of CaMKII resulting in the phosphorylation of NR2B Serine 1303, the other via the non-catalytic site of CaMKII, which results in the localization of CaMKII to the PSD (Leonard et al., 1999; Strack et al., 2000; Bayer et al., 2001; Bayer et al., 2006). CaMKII bound to NR2B in the non-catalytic mode can still bind to and phosphorylate other NR2B molecules at Serine 1303 (Bayer et al., 2001).

Both NR2A and NR2B bind to the SH2 domain of PLC-γ when phosphorylated on tyrosine residues (Gurd and Bissoon, 1997). Binding of PLC-γ triggers its phosphorylation by receptor- and also non-receptor tyrosine kinases and consequently its activation leading to the hydrolysis of phosphatidylinositol 4,5-bisphosphate yielding diacylglycerol and inositol 1,4,5-trisphosphate (Margolis et al., 1990; Vetter et al., 1991; Liao et al., 1992). This is an important step in many signalling pathways.

Calmodulin binds in the region of the C1 exon of the NR1 subunit in a calcium-dependent manner. Ca^{2+} entering through the NMDA receptor channel binds to calmodulin thereby activating it, which then binds to NR1 inactivating the NMDA receptor (Vyklicky, 1993). This high affinity interaction is weakened by PKC-mediated phosphorylation of NR1 on serine residues (Hisatsune et al., 1997) thereby preventing inactivation of NMDA receptor channels by Ca^{2+}. Inhibitors of calmodulin also block long-term potentiation and long-term depression in the hippocampal CA1 region (Malenka et al., 1989a).

NMDA receptors at excitatory postsynaptic membranes directly bind to or indirectly interact with cytoskeletal molecules thereby ensuring anchoring at the PSD. Alpha-actinin-2 (an actin cross-linking protein) binds to the C-terminus of NR1 and NR2B subunits (Wyszynski et al., 1997). F-actin depolymerization disperses alpha-actinin-2, which reduces NMDA receptor clustering at the synapses (Allison et al 1998). Another actin-binding protein, spectrin is interacting with NR1, NR2A and NR2B subunits. PKA, PKC mediated phosphorylation of NR1 and calcium/calmodulin antagonizes association of NR1 and spectrin, while phosphorylation of NR2B by Fyn and also calcium weakens the interaction between NR2B and spectrin (Wechsler and Teichberg, 1998). The interaction of spectrin with the plasma membrane is also regulated by calcium (Steiner et al., 1989). Another molecule, yotaio binds to the C1 region of the NR1 subunit (Lin et al., 1998).

Other molecules of the NMDA receptor signalling complex, such as nNOS, fyn or SynGAP, interact with MAGUKs thereby regulating receptor function. SynGAP interacts with PSD-95 and SAP-102 via PDZ interaction and it is a negative regulator of Ras thereby modulating synaptic plasticity (Chen et al., 1998; Kim et al., 1998). Phosphorylation by CaMKII inhibits SynGAP resulting in the inhibition of the inactivation of GTP-bound Ras and the activation of the MAP kinase pathway.

The molecules within the NMDA receptor signalling complex are organized in a well regulated network providing for synaptic plasticity, some forms of learning and

memory formation. The involvement of the NMDA receptor in these events will be discussed in the next chapters.

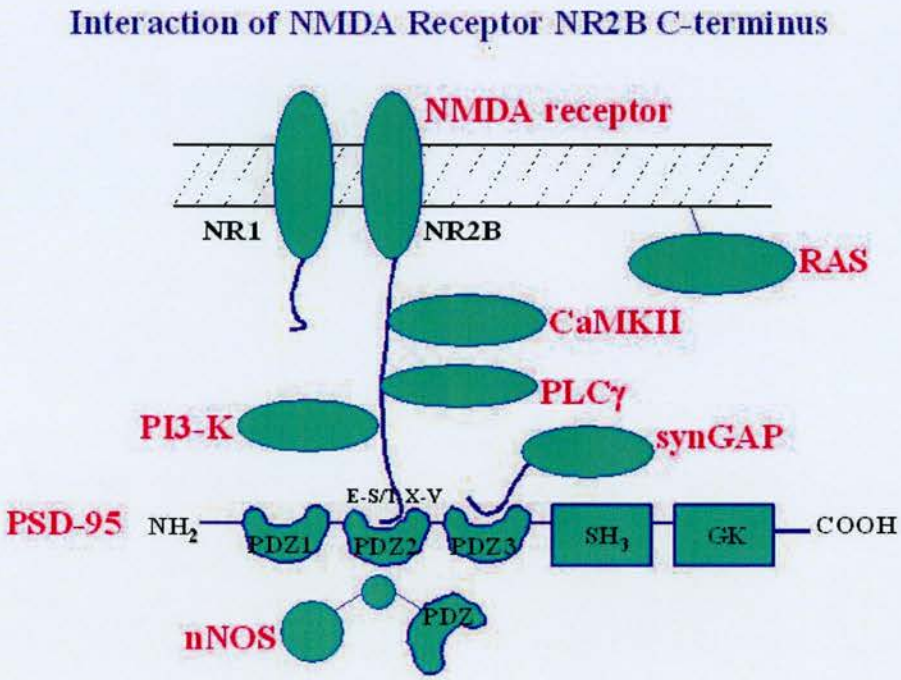

Figure 2. Interactions of the NMDA Receptor NR2B C-terminus.
The binding partners can be categorised into two major groups. The MAGUK proteins all contain PDZ domains via which they bind to the E-S/T-X-V motif located at the extreme C-termini of the NR2 subunits. A few of these proteins are PSD-95, chapsyn-110 or SAP 102. These further interact with nNOS (Holscher et al., 1997), fyn (Grant et al., 1992) or SynGAP (Chen et al., 1998). The non-MAGUK proteins, which bind to sites of the C-terminus other than the terminal E-S/T-X-V motif, include for example CaMKII, PLC-γ and PKC.

Role of phosphorylation in interactions and signalling

Phosphorylation of receptor ion channels is an important regulatory mechanism that may be underlying synaptic plasticity. The following findings give bases to that hypothesis. Phosphorylation of certain signalling molecules activates them, which enables them to bind to other molecules. Secondly, the agonist-induced responses of ionotropic glutamate receptors are generally potentiated after phosphorylation. Thirdly, certain kinases are required for LTP providing for learning and memory.

Two of these are protein kinase C (PKC) and CaMKII, which are involved in generation of long term potentiation (LTP) (Lovinger et al., 1987; Reymann et al., 1988; Malenka et al., 1989a; Malenka et al., 1989b; Malinow et al., 1989; Giese et al., 1998; Cooke et al., 2006). Others are src family tyrosine kinases (O'Dell et al., 1991), cAMP-dependent kinase (Frey et al., 1993; Cooke et al., 2006) and the mitogen-activated protein kinase (English et al., 1997).

NMDA Receptor NR1 Subunit Interactions

Interacting molecule	Site of interaction on NR2B	Reference
NR2A		Hawkins et al., 1999
NR2B		Hawkins et al., 1999
NR2C		Laurie et al., 1994
NR2D		Williams, 1995
NR3		Laurie et al., 1994
CaMKII		Leonard et al., 1999
CaM	AS 834-863 and 864-900	Krupp et al., 1999
Yotaio	AS 864-900	Lin et al., 1998
Spectrin	In the region AS 834-938	Wechsler et al., 1998
Tubulin		Van Rossum et al., 1999
α-actinin-2	AS 834-863	Krupp et al., 1999

Table 2a. NMDA Receptor NR1 Subunit Interactions.
The binding sites for the different molecules interacting with the NR1 C-terminus and the references are listed above.

Production of mutant mice was used to determine the function of certain domains of the NMDA receptor, uncovering the fact that the C-terminus of the NR2 subunit is the most important in synaptic plasticity via binding to downstream molecules (Figure 2, Table 2a, b and c), forming the initiating point of signalling cascades (Find in detail in sections 1D and 1F.). The NR2 subunit binds to the 1st and 2nd PDZ domains of PSD-95 through the E-S/T-X-V motif located at the extreme C-termini (Kornau et al., 1995; Tochio et al., 2000), which is connected to other downstream signalling molecules. Mice expressing C-terminal truncated forms of NR2A, NR2B and NR2C subunits were produced (Köhr and Seeburg, 1996; Sprengel et al., 1998).

No interference with the formation of gateable receptor channels was observed *in vitro* however mice expressing these truncated subunits manifested great phenotypic resemblance with mice lacking the respective subunits (Kutsuwada 1996), namely that mice lacking the NR2B C-terminus ($NR2B^{\Delta C}$) died perinatally (Sprengel et al., 1998). The channel function was normal, however the $NR2B^{\Delta C}$ protein level and NMDA receptor currents were reduced by about half in both the lethal homozygous and the surviving heterozygous mice as well. Immunostaining of cultured cerebral neurons showed a reduced number of NR2B immunofluorescent puncta demonstrating disrupted clustering and synaptic localization of the NMDA receptor channel (Mori 1998). This suggests that the cause of lethality is the lack of protein-protein interactions via the C-terminus, rather than the reduction in receptor currents.

NMDA Receptor NR2A Subunit Interactions

Interacting molecule	Site of interaction on NR2B	Reference
NR1		Hawkins et al., 1999
CaMKII	AS 1349-1458	Gardoni et al., 1998
PSD-95	E-S/T-X-V motif (AS 1459-1464)	Bassand et al., 1999
Chapsyn-110	E-S/T-X-V motif (AS 1459-1464)	Bassand et al., 1999
SAP-97 and 102	E-S/T-X-V motif (AS 1459-1464)	Bassand et al., 1999
PLC-γ	Y1325(SH2)	Gurd et al., 1997
Fyn	Y1325(SH2)	Takagi et al., 1999
Src	Y1325(SH2)	Takagi et al., 1999
Veli	E-S/T-X-V motif (AS 1459-1464)	Jo et al., 1999
Spectrin	In the region AS 838-1464	Wechsler et al., 1998
S-SCAM	E-S/T-X-V motif (with PDZ-5)	Hirao et al., 1998

Table 2b. NMDA Receptor NR2A Subunit Interactions.
The different molecules interacting with the C-terminus of the NR2A subunit, their binding sites and the references are listed above.

NMDA Receptor NR2B Subunit Interactions

Interacting molecule	Site of Interaction on NR2B	Reference
NR1		Hawkins et al., 1999
CaMKII	AS 1290-1309	Gardoni et al., 1998
PSD-95, Chapsyn-110, SAP-97 and 102	E-S/T-X-V motif (AS 1479-1482)	Bassand et al., 1999
PLC-γ	Y1122, 1252, 1336, 1472 (SH2)	Gurd et al., 1997
Fyn	Y1122, 1252, 1336, 1472 (SH2)	Takagi et al., 1999
Src	Y1122, 1252, 1336, 1472 (SH2)	Takagi et al., 1999
PI3-kinase	YAHM (AS 1336-1339)	Hisatsune et al., 1999
PTP1D	Y1122, 1252, 1336, 1472 (SH2)	Lin et al., 1999
CIPP	E-S/T-X-V motif (AS 1479-1482)	Kurschner et al., 1998
Veli	E-S/T-X-V motif (AS 1479-1482)	Jo et al., 1999
Spectrin	In the region AS 1086-1481	Wechsler et al., 1998
Tubulin	AS 1243-1376	Van Rossum et al., 1999
α-actinin-2	AS 1308-1440	Wyszynski et al., 1997
S-SCAM	E-S/T-X-V motif (with PDZ-5)	Hirao et al., 2000

Table 2c. NMDA Receptor NR2B Subunit Interactions.
The different molecules interacting with the C-terminus of the NR2B subunit form signalling cascades by further interacting with other proteins. The binding sites and references are listed above.

The same method was used for searching for different kinases that are involved in LTP generation, learning and memory formation (Find in detail in sections 1D and 1F.). Mutation in the src family tyrosine kinase or fyn reduces LTP and produces abnormal hippocampal morphology (Grant et al., 1992). Knockout of PKCγ (Abeliovich et al., 1993), αCaMKII subunit (Silva et al., 1992a) or protein kinase A (PKA) Rlβ and Cβ1 subunits (Brandon et al., 1995; Huang et al., 1995) also reduce LTP, impair synaptic plasticity. In the next chapters synaptic plasticity and the involvement of the NMDA receptor in signalling will be discussed in great detail.

1D Synaptic Plasticity

In determining behaviour, the process of learning and memory formation is extremely important. Memory can be categorised into two main groups, implicit or non-declarative and explicit or declarative memory, the former being required for simple associations or motor skills, which is not dependent on the temporal lobe but involves sensory, motor and associative pathways, the latter being a conscious recall of objects, which is dependent on the hippocampus, subiculum and entorhinal cortex. According to Hebb´s hypothesis (1949), "When an axon of cell A is near enough to excite cell B and repeatedly or persistently takes part in firing it, some growth process or metabolic change takes place in one or both cells, such that A's efficiency, as one of the cells firing B, is increased.", the condition that has to be met in order to strengthen a synapse is the co-activation of the two neurons connected. Strengthening of the synapse occurs when the use of the synapses is associated with the generation of action potentials in the postsynaptic neuron. This process was proposed to account for associative learning.

The first experiment that gave evidence that long lasting plasticity exists was carried out on the perforant path synapse with the dentate gyrus in the hippocampus (Bliss and Lømo, 1973). High frequency stimulation (5-100 Hz) in this system produced an increase in synaptic efficiency termed long-term potentiation (LTP). This form of synaptic plasticity was observed in the CA3 (Alger et al., 1976) and CA1 (Schwartzkroin et al., 1975) regions of the hippocampus. Evidence for a decrease in the synaptic efficiency termed long-term depression (LTD) induced by low frequency (1 Hz) stimulation was also found (Bear et al., 1996). Changes in synaptic strength were termed synaptic plasticity. These experiments were followed by many others, confirming the diversity of the different forms of LTP and LTD (See in detail in the next paragraphs.), however Hebb's postulate remained the basis for many theories investigating the processes underlying synaptic plasticity, learning and memory.

Aplysia and synaptic transmission

Synaptic plasticity and its connection to long-term memory formation in marine molluscs have been thoroughly studied as a simple, but good model of hippocampal learning in vertebrates. Associative learning (Find in detail in section 1E.) was examined in Hermissenda (Alkon, 1980), while nonassociative learning types such as habituation and sensitization were examined in Aplysia (Castellucci and Kandel, 1974; Frost et al., 1985). Habituation was connected to synaptic depression while sensitization was connected to synaptic facilitation.

In Aplysia sensitization and switch from short to long term memory and the underlying processes can be studied on the gill- and siphon-withdrawal reflex. Following a single noxious stimulus to the tail the mollusc acquires a short-term memory lasting minutes, which results in an enhanced gill- and siphon withdrawal reflex to tactile stimulation. Five or more stimuli result in a long-term memory lasting days or weeks. The proposed underlying mechanism is that the noxious stimulus activates facilitatory interneurons, which synapse on the sensory neurons and strengthen the connection between the sensory neurons and their target cells (Hawkins et al., 1981). This can be reconstituted in cell culture as well, where serotonine (5-HT) can be used as a noxious stimulus (Montarolo et al., 1986). A single application of 5-HT produces short-term changes in synaptic efficiency while five separate applications of 5-HT produce long-term changes (Montarolo et al., 1986; Glanzman et al., 1989).

Short-term facilitation requires covalent modifications of existing proteins and is not blocked by inhibitors of transcription and translation while long-term changes are connected to transcription, translation and growth of new synaptic connections (Bailey and Chen 1988; Bailey and Chen, 1989; Castellucci et al., 1989). Transition between short-term and long-term synaptic facilitation is CREB-mediated as showed in experiments using recombinant phospho-CREB1 and inhibitory transcription factor CREB2 (Bartsch et al., 1995; Casadio et al., 1999; Pittenger and Kandel, 2003). Many parallels have been pointed out between the long-term facilitation in

Aplysia and the hippocampal long-term LTP in mammals (Find in detail in the next paragraphs.) and their connection to long-term memory, such as its graded nature, the involvement of PKA and CREB or the requirement of the growth of new synaptic connections (Pittenger and Kandel, 2003).

Synaptic plasticity and the involvement of the NMDA receptor

LTP has been studied in great detail in the rodent hippocampus and neocortex. Three main subtypes have been identified and characterized, which are NMDA receptor-dependent LTP, AMPA receptor-dependent LTP and mossy fibre LTP. Two forms of LTD will also be discussed, namely the NMDA receptor-dependent and the metabotropic glutamate receptor-dependent forms. LTP also has stages like long-term facilitation in Aplysia, which are early-stage LTP (E-LTP) requiring αCaMKII and fyn and late-stage LTP (L-LTP) requiring PKA and protein synthesis (Bliss and Collinridge, 1993; Frey et al., 1993).

NMDA receptor-dependent LTP is triggered by high frequency tetani to a critical number of afferent fibres or by coincident postsynaptic depolarization (resulting in the relief from Mg^{2+} blockade) and presynaptic stimulation (glutamate release) allowing for Ca^{2+} and Na^{+} influx via the NMDA receptor. This Ca^{2+} influx was proposed to be the initiation factor in the induction of LTP (Lynch et al., 1993). The latter mechanism made the NMDA receptor a candidate for mediating Hebbian synaptic plasticity.

Downstream of the NMDA receptor there are two major Ca^{2+}-dependent signalling pathways identified. One is the CaMKII signalling, the other is the cAMP-dependent signalling. CaMKII(α) is the major component of the postsynaptic density, in fact it is one of the most abundant proteins in neurons, 1-2% of the total. It is a molecule linking the transient calcium signals connected to NMDA/AMPA activation to neuronal plasticity. It has been suggested as a molecular switch for long-term memory storage based on its property to autophosphorylate and self-activate and its ability to bind to NMDA thereby anchoring AMPA receptors at the PSD (Lisman and Zhabotinsky, 2001).

Upon NMDA receptor activation the intracellular Ca^{2+} concentration increases, which in turn activates CaMKII. It is autophosphorylated on threonine-286 (Thr-286), which allows persistent activation of the kinase (Miller et al., 1988; Lou and Schulman, 1989). Autophosphorylation of αCaMKII also induces its translocation to the PSD where it binds the NMDA receptor NR2A or NR2B subunit (Gardoni et al., 1998; Leonard et al., 1999; Strack et al., 2000; Bayer et al., 2001; Bayer et al., 2006) and is necessary for NMDA receptor-dependent LTP induction but only at certain synapses such as Schaffer commissural synapses in the CA1 region (Giese et al., 1998; Cooke et al., 2006). In medial perforant path-granule cell synapses LTP is connected to cyclic AMP-dependent signalling in Thr 286 autophosphorylation site mutant mice where CaMKII signalling is absent (Cooke et al., 2006).

Inhibition of CaMKII also blocks LTP in hippocampal CA1 region (Malinow et al., 1998). The deletion of αCaMKII impairs E-LTP in the CA1 neurons of the hippocampus and spatial learning (Silva et al., 1992a; Silva et al., 1992b). CaMKII is involved in AMPA receptor activation, too. GluR1 is CaMKII phosphorylated on serine-831 (Ser-831) and AMPA receptor delivery to the spine after LTP induction is CaMKII-dependent, which is the step needed for the transition of silent synapses to functional (Liao et al., 2001).

There is great evidence for the involvement of the cAMP-signalling cascade in the induction of protein synthesis-dependent changes important for the formation of LTP and long-term memory (Nguyen and Kandel., 1997). If the intracellular cAMP concentration increases, PKA activation occurs, which ultimately leads to activation of various transcription factors (such as CREB) and translation. It has been shown that induction of LTP results in PKA activation. Results of the Kandel group showed that cAMP/PKA have a role in the late-phase LTP. Delivery of one high-frequency train (100 Hz) induces LTP, which persists for 1-3 hours (Huang et al., 1994). This was inhibited by CaMKII blockers, but not by inhibitors of PKA. In contrast, the three high-frequency train-induced LTP persisted for up to 6-10 hours and was blocked by PKA inhibitors (Huang et al., 1994). There is a clear correlation between

changes in elevated intracellular cAMP concentration-induced PKA activation and induction of LTP. This is demonstrated in transgenic mice expressing R(AB), the inhibitory form of the regulatory subunit of PKA. In these mutants PKA activity and late-phase LTP was reduced in the CA1 region of the hippocampus and they exhibited spatial learning deficits (Abel et al., 1997). The cAMP/PKA system is also involved in other forms of plasticity, for example in the visual cortex contributing to ocular plasticity (Beaver et al., 2001).

The next step in this signalling cascade is the mitogen-activated kinase (MAPK). The MAPK/ERK cascade is essential in the signal transduction processes involved in LTP formation and certain forms of learning (Figure 3). The increase in cAMP concentration triggers the activation of ERK (Impey et al., 1998) and the nuclear translocation of MAPK (Martin et al., 1997). Activation of ERK and translocation of MAPK, which is required for at least some forms of L-LTP in the mammalian hippocampus can be mediated by cAMP stimulation of tyrosine receptor kinase (Trk) via the Ras/raf pathway or by induction of NMDA, AMPA or mGluR followed by subsequent activation of PI3-K, PKA, PKC or CaMKII (Martin et al., 1997; Patterson et al., 2001). The downstream substrates of ERK are signalling proteins like phospholipase A_2 (PLA_2); cytoskeletal proteins for example microtubule-associated protein-2 (MAP-2) or Tau; or nuclear proteins like CREB, c-fos or c-jun. The ultimate effects of ERK activation therefore are translation and transcription (Thomson et al., 1999). This requires ERK translocation to the nucleus (Boglari et al., 1998). If ERK is inhibited, the LTP in hippocampal CA1 region and in the dentate gyrus is suppressed (English and Sweatt, 1997; McGahon et al., 1999). Vice versa, the induction of LTP leads to phosphorylation of MAPK/ERK (English and Sweatt, 1997; McGahon et al., 1999). Activation of ERK is increased after contextual fear conditioning (Atkins et al., 1998).

Activation of CREB is induced by phosphorylation of MAPK/ERK. It is one of the most important transcription factors in memory formation and it has been associated with long-term memory (Silva et al., 1998).It is another molecule that has been implicated to act as a molecular switch (Chen et al., 2003; Mizuno and Giese, 2005)

for long-term memory (Find in further detail in sections 1D/Aplysia and 1E). Phosphorylation of CREB is increased in the hippocampus after contextual fear conditioning (Impey et al., 1998) and in hippocampus and the entorhinal cortex after training in the Morris water maze (Gooney et al., 2002). CREB activation is the essential step prior to gene transcription and protein synthesis and it is also involved in the induction of morphological changes such as generation of new dendritic spines (Murphy and Segal, 1997) proposed to underlie L-LTP and some forms of learning and memory formation. Mice with targeted disruption of CREB or expressing a repressor of CREB have disrupted late-phase LTP and hippocampus-dependent long-term memory (Bourtchuladze et al., 1994; Bozon et al., 2003). Mice expressing an inhibitor of an endogenous CREB repressor have enhanced L-LTP and long-term memory (Chen et al., 2003).

Phosphatidylinositol 3-kinase (PI3-kinase) is another molecule downstream of NMDA (Figure 3), which can activate MEK (Divecha and Irvine, 1995) triggering ERK phosphorylation. PI3-kinase inhibitors block LTP in both CA1 (Sanna et al., 2002) and the dentate gyrus (Kelly and Lynch, 2000). Inhibition of PI3-kinase also blocks LTP-triggered activation of ERK and cAMP response element binding protein (CREB) (Lin et al., 2001), which might be the reason for PI3-kinase inhibitor induced blockade of LTP and interference with long-term fear memory (Lin et al., 2001), which requires translation and transcription connected to ERK/CREB. The short-term memory however is intact.

AMPA receptor-dependent LTP

AMPA receptors contribute to fast excitatory synaptic transmission and have been postulated to be involved in expression of LTP (Figure 3). The GluR2 subunit modulates the calcium entry. If its expression is high for example in pyramidal cells of the hippocampus then the calcium permeability of the AMPA receptor is low. In GluR2 mutant mice the calcium permeability is higher and the LTP is enhanced (Jia et al., 1996). Evidence suggests that the primary requirement of LTP induction is the increased expression of AMPA receptors at the postsynaptic membrane. This is the base of the silent synapse theory, which suggests that certain synapses are not

functional (silent) because of the lack of AMPA receptors (Isaac et al., 1995). The different mutants are listed in section 1H.

A type of use-dependent LTP can be observed even in the presence of NMDA receptor blockers in the amygdala and the dorsal horn (Gu et al., 1996; Mahanty and Sah, 1998). This LTP is induced by Ca^{2+} permeable AMPA channels. The Ca^{2+} influx is maximal when presynaptic glutamate release coincides with postsynaptic hyperpolarization.

Mossy fibre LTP

Mossy fibre LTP is observed in the hippocampus, in mossy fibre synapses on CA3 pyramidal neurons (Harris and Cotman, 1986). This form of LTP does not require coincident pre- and postsynaptic activity and its expression is thought to be presynaptic. Initial experiments using ionotropic glutamate receptor blockers suggested that this form of LTP is independent of AMPA, NMDA and kainite receptors, dependent on Ca^{2+} entry into the presynaptic neuron via voltage-gated ion channels and cAMP signalling (Castillo et al., 1994; Weisskopf et al., 1994; Yeckel et al., 1999). In later experiments however the selective GluR5 subunit-containing kainite receptor antagonist 6-(4-carboxyphenyl)-methyl-decahydroisoquinoline-3-carboxylic acid (LY382884) completely blocked mossy fibre LTP (Bortolotto et al., 1999). Experiments with different kainite receptor knockout mice suggested the importance of the GluR6 subunit containing receptor in the mossy fibre LTP (Contractor et al., 2001).

Long term depression (LTD)

LTD is a long lasting decrease in synaptic strength. Different types of LTD have been characterized such as the NMDA receptor-dependent, AMPA receptor-dependent and metabotropic glutamate receptor (mGluR)-dependent forms (Bashir et al., 1993; Mulkey et al., 1994; O'Mara et al., 1995; Kobayashi et al., 1996; Levenes et al., 1998; Laezza et al., 1999; Morishita et al., 2005).

The standard protocol to induce LTD uses long trains of low-frequency (1 Hz) stimulation or mismatching of pre- and postsynaptic potentials (Dudek and Bear, 1992; Markram et al., 1997). In earlier experiments LTD was only induced (in the Schaffer-CA1 synapses) in neonatal or juvenile animals using this protocol and not in adults (Kemp et al., 2000). Novel types of protocols however managed to induce LTD in the hippocampus of the adult animals as well (Kemp et al., 2000; Chen et al., 2006). It was proposed that the 2 Hz tetanus-induced LTD is NMDA receptor-dependent and the 5 Hz tetanus-induced LTD is mGluR-dependent corresponding to different signalling mechanisms (Chen et al., 2006). LTD could also be produced in the anterior cingulate cortex (ACC) of the adult mouse (Toyoda et al., 2005).

NMDA receptor-dependent LTD was described in hippocampal CA1 region. It requires prolonged, low concentration Ca^{2+} influx and protein phosphatase activity (Mulkey et al., 1994; Cummings et al., 1996). Serine/threonine protein phosphatase 1 (PP1) was shown to contribute to NMDA receptor-dependent LTD induction (Mulkey et al., 1994).

The mGluR-dependent LTD type was observed in the CA1 area of the hippocampus, the dentate gyrus and at mossy fibre-CA3 synapses (Bashir et al., 1993; O'Mara et al., 1995; Kobayashi et al., 1996). It is blocked by mGluR antagonist (MCPG). The underlying mechanism was proposed to be the tyrosine dephosphorylation of AMPA receptors by protein tyrosine phosphatases upon which they are removed from the synapses (Moult et al., 2006; Huang and Hsu, 2006).

An unusual form of LTD can be observed in the hippocampal CA3 interneurons expressing Ca^{2+} permeable AMPA channels. Induction of this form of LTD requires activation of presynaptic mGluRs and postsynaptic Ca^{2+} influx through AMPA receptors (Laezza et al., 1999).

Cerebellar LTD at parallel fibre-Purkinje cell synapses is implicated in some forms of motor learning. It requires a cascade of Ca^{2+} influx, mGluR1 activation, PKCα activation and serine 880 phosphorylation of GluR2 subunit (Levenes et al., 1998;

Shin and Linden, 2005). Mossy fibre-deep cerebellar nuclear (DCN) synapses demonstrate non-NMDA receptor-dependent LTD, which requires mGluR activity (mGluR1) and protein translation (Zhang and Linden, 2006).

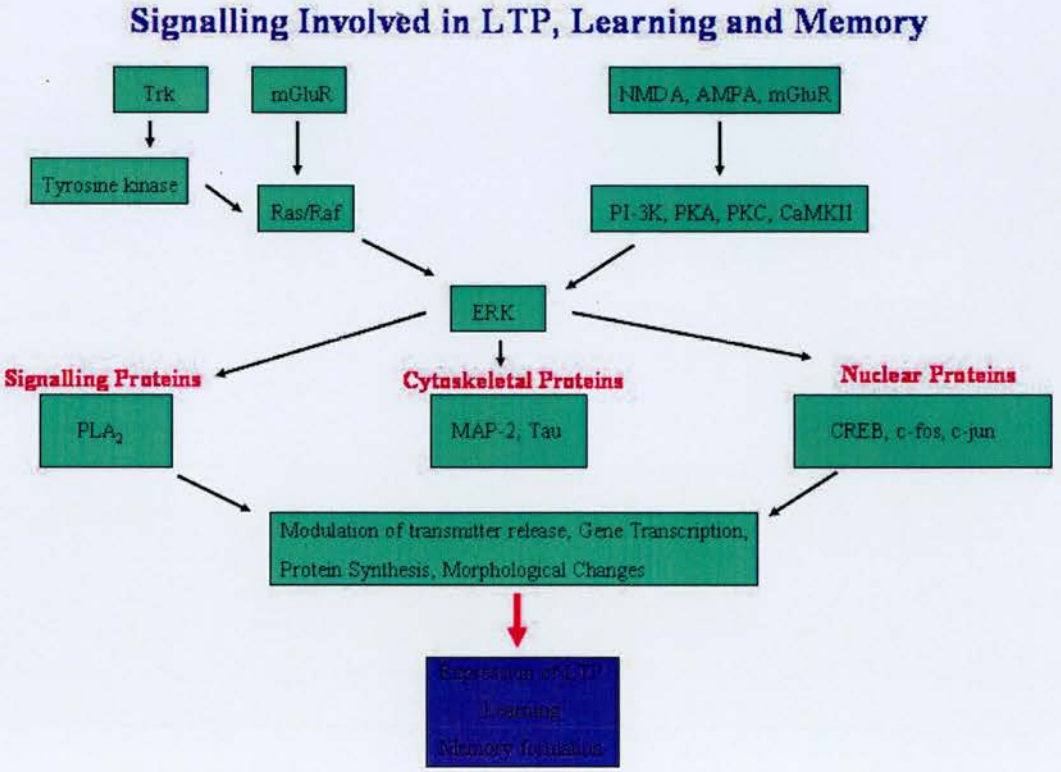

Figure 3. NMDA Receptor Signalling (Based on Lynch, 2004).
Various signalling cascades via ERK contribute to LTP, learning and memory formation. NMDA receptors interact with ERK via PI-3K, PKA, PKC or CaMKII.

1E Learning and Memory

The action of the brain includes relatively simple motor behaviours and elaborate affective and cognitive behaviours. Learning is the process of acquiring knowledge about the world that falls into the second category. Memory is the retention or storage of that knowledge. The study of learning and memory is central to understanding both normal and abnormal behaviour. Early studies of memory formation suggest that input to the brain is processed in a short-term memory store,

which has very limited capacity. If the information is converted into long-term memory, that process requires the synthesis of new proteins and the formation of new synaptic connections.

Associative and nonassociative learning

Psychologists study learning by exposing animals to information about the world like sensory experience. The use of two major procedures showed the existence of the first two distinct forms of learning types that had been thoroughly investigated, the nonassociative and the associative (Kandel et al., 1991; Milner et al., 1998). Nonassociative learning results when the animal is exposed to a single type of stimulus. During associative learning the animal learns the relationship of two stimuli. There are different subtypes of these learning forms as described below.

Examples for nonassociative learning are habituation or sensitization. Habituation is a decrease in behavioural response to a repeated, nonnoxious stimulus. Sensitization or pseudoconditioning means an increased response following an intense or noxious stimulus. Dishabituation is the process when an already habituated response is restored by a sensitising stimulus.

When studying associative learning different conditioning experiments were developed. Classical conditioning was introduced to science by Ivan Pavlov. The basic concept is to pair an unconditioned stimulus with a conditioned one. The conditioned stimulus produces no or weak responses. The unconditioned stimulus or reinforcement produces overt response termed unconditioned response without learning (for example salivation upon presentation of food). After the conditioned stimulus has been repeatedly followed by the unconditioned one the conditioned stimulus will elicit response termed conditioned response. It can be appetitive or defensive depending on weather the unconditioned response is rewarding or not. After repeated pairing of the two stimuli the conditioned stimulus will produce the response previously evoked by the unconditioned one. A widely used type of classical conditioning is the "rabbit eyeblink response" (Gormezano et al., 1962). It localized that particular type of memory to the cerebellum (Thompson and Krupa,

1994; Christian and Thompson, 2003). Recently the cerebellar interpositus nucleus was implicated in long-term memory storage of tasks learnt in classical conditioning (Christian and Thompson, 2005).

Operant conditioning was developed by Edward Thorndike. The animal learns the relationship of one reinforcing stimulus in connection with its own behaviour. An example of this type of conditioning is when a hungry animal is placed in a cage where if it presses a lever, it will be given food. The animal learns that a certain behaviour or response is rewarded and will repeat it.

During food-aversion conditioning animals learn to associate stimuli, which are relevant to their survival. It enables them to distinguish for example poisonous food from harmless. If a conditioned stimulus like a particular taste is followed by nausea caused by poison then a strong aversion will be produced to that flavour. It develops even if the nausea occurs several hours after the tasting. Food aversion is useful in the treatment of chronic alcoholism.

Storage of information, implicit and explicit memory

According to the storage and recall of information, long-term memory can be divided into two categories, implicit, non-declarative or reflexive memory and explicit or declarative memory (Kandel et al., 1991; Milner et al., 1998; Cooke and Bliss, 2006).

Implicit, non-declarative or reflexive memory is not dependent on comparison or evaluation and the formation and recall is non-conscious (Kandel et al., 1991; Milner et al., 1998; Cooke and Bliss, 2006). It develops over many trials. Examples of implicit memory are the learning of perceptual and motor skills or different rules such as grammar. Different brain areas are involved such as the cerebellum in motor learning (associative memory); amygdala in emotional responses, learnt fear (associative memory); the basal ganglia in operant conditioning; the neocortex in priming or the primary sensory pathways in habituation and sensitization (nonassociative memory) (Milner et al., 1998).

The cerebellum is connected to memories of motor acts. It was thought to be responsible for only the coordination of voluntary movements (such as posture, speech) at first. It was however found that the cerebellum is also responsible for learnt motor responses tested in for example conditioned eye-blink response (Thompson, 1990; Thach et al., 1992; Thompson and Krupa, 1994; Christian and Thompson, 2003). The underlying site is the mossy fibre-parallel fibre Purkinje cell synapse (Thompson et al., 1998).

The amygdala is involved in emotional memory, recognition of emotional expression in faces (Morris et al., 1996). Electric stimulation to the amygdala produces fear while damage to the amygdala produces tameness. Blocking noradrenaline receptors interferes with formation of emotional memory in humans suggesting a role for the cAMP pathway (Cahill et al., 1994). LTP was previously shown to be existing in synapses known to be responsible for fear conditioning. It is graded (early and late phase), in part dependent on NMDA receptor activation and is dependent on PKA and MAP kinase activity (Chapman et al., 1990; Huang and Kandel, 1998). Disruption of PKA also interferes with fear conditioning demonstrating that LTP might account for that type of memory (Schafe et al., 1999). Another group showed LTP underlying fear conditioning to be AMPA receptor-dependent in the inhibitory interneurons of the basolateral amygdala (Mahanty and Sah, 1998). The amygdala is also involved in the enhancement of declarative memory when there is an emotional implication (Adolphs et al., 1997).

For studying the neocortex-dependent implicit memory type a special task is used (Warrington and Weiskrantz, 1968). The patients are showed a list of words and pictures of objects together with novel objects and designs. When later shown a fragment of a word they tend to complete it to form a word previously studied rather than any other possible options. Severely amnesic patients have intact priming however they are unable to recognise the objects previously shown to them (Warrington and Weiskrantz, 1968; Tulving and Schacter, 1990).

Explicit, declarative or procedural memory is dependent on comparison or evaluation and means the conscious recall of things (Kandel et al., 1991; Milner et al., 1998; Cooke and Bliss, 2006). It encodes information about a specific event and also personal associations. It can be obtained in a single trial and is dependent on the medial temporal lobe and the hippocampus in particular. It can be subdivided into episodic memory, which is the recall of autobiographical information and semantic memory, which relates to non-autobiographical facts (Cooke and Bliss, 2006). The involvement of the medial temporal lobe is involved in spatial, semantic and recognition memory was shown in functional magnetic resonance imaging (fMRI) studies (Bartha et al., 2003; Rosenbaum et al., 2004; Kirwan and Stark, 2004). A well studied example of explicit memory is the spatial learning in mice, which will be discussed in the next paragraphs.

The case of patient HM served as an initial evidence for the necessity of the medial temporal lobe in declarative memory (Scoville and Milner, 1957; Penfield and Milner, 1958; Milner 1972). H.M. underwent bilateral medial temporal lobectomy at the age of 23 to control severe epileptic seizures. The dramatic result of the surgery was amnesia for events following the surgery however intact memory for events 19 months prior to the lobectomy and no apparent intellectual loss. In later observations it was noted that he could acquire new motor skills such as "mirror drawing task" learnt over a period of three days (Milner and Glickman, 1965; Milner et al., 1989), but couldn't recall new faces or places thus the hippocampus was implicated in formation of explicit, but not implicit memory.

In the hippocampus four major pathways can be easily detected, which are the perforant pathway, the Schaffer collateral pathway, the mossy fibre pathway and the commissural connections. Experiments with lesions or genetically modified mice suggest that the Schaffer collateral (CA3 synapses onto CA1 pyramidal cells) has a major role in the encoding and storage of spatial memory. Interfering with mossy fibre LTP doesn't affect spatial or contextual memory (Huang et al., 1995).

Spatial memory in rodents is often tested in the water maze. In the hidden platform task, the platform is submerged and the animal has to learn the location of the platform by learning the spatial cues in the environment (Morris et al., 1982). Once the training sessions are done during which the animal is supposed to learn the task, the platform is removed and the animals are assessed by checking how much time they spend in the quadrant of the previously submerged platform. The visible platform task is not dependent on the hippocampus and is used as a control.

The correlation between LTP and memory in the Schaffer collateral was shown in several experiments using pharmacological blockade or genetic modifications. Knocking out certain genes in a spatially and temporally controlled manner can give specific information in the underlying processes of memory formation. Knocking out the NR1 subunit of the NMDA receptor in the pyramidal cells of the CA1 region resulted in disrupted LTP in the Schaffer collateral pathway and the mice displayed deficits in spatial learning (Tsien et al., 1996b). Expressing a persistently active form of CaMKII interfered with LTP formation in the hippocampus and the mice were deficient in spatial learning and memory, however when the transgene was turned off, LTP and spatial learning were both restored (Mayford et al., 1996). In transgenic mice expressing R(AB), the inhibitory form of the regulatory subunit of PKA the PKA activity was reduced, late-phase LTP was reduced in the CA1 region of the hippocampus and they exhibited spatial learning deficits (Abel et al., 1997). Disruption of CREB results in deficits of the late-phase LTP and hippocampal-dependent spatial memory (Bourtchuladze et al., 1994).

In summary interference with E-LTP in the Schaffer collateral blocks L-LTP and produces deficits in both short and long-term memory while interfering with L-LTP results in impaired long-term memory however the short-term memory remains intact.

The hippocampus is also involved in contextual memory tested in contextual conditioning (Anagnostaras et al., 2001). The task involves learning the environment as a whole (a context) and associate it with a noxious stimulus such as mild foot

shock upon which the animal exhibits "freezing". Hippocampal contextual long-term memory has similar molecular requirements as spatial learning (Mizuno and Giese et al., 2005). CREB mutant mice that are impaired in spatial learning are also impaired in contextual memory (Bourtchuladze et al., 1994). The requirement for CREB activating kinases, which phosphorylate CREB at Serine 133 (Sun et al., 1996), for example CaMKIV, is similar (Kang et al., 2001). Dominant negative PKA mutants have impaired long-term memory in contextual conditioning and impaired spatial memory formation (Abel et al., 1997). Other molecules however have distinct roles in the two types of long-term memory formation such as the involvement of CaMKKβ (Ca2+ calmodulin kinase kinase phosphorylating CaMKIV) and Rap1 (Ras related small GTPase) in spatial memory and CaMKKα (Ca2+ calmodulin kinase kinase phosphorylating CaMKIV) and pituitary adenylate cyclase activating polypeptide (PACAP) type I receptor (PAC1) (G-protein coupled receptor) in contextual memory (Mizuno and Giese, 2005).

Molecular mechanism of the storage of the memory

Short-term memory lasts minutes to hours requiring only covalent modification of pre-existing molecules, while long-term memory requires synthesis of new proteins and growth of new synaptic connections (Bliss and Collinridge, 1993; Frey et al., 1993; Pittenger and Kandel, 2003). In parallel, LTP in Drosophila and mammals or long-term facilitation in Aplysia also has stages, which are early-stage LTP (E-LTP) requiring αCaMKII and fyn and late-stage LTP (L-LTP) requiring PKA, CREB and protein synthesis (Bliss and Collinridge, 1993; Frey et al., 1993; Yin et al., 1994). αCaMKII deficient mice display a partial loss of E-LTP in hippocampal CA1 neurons and impaired spatial memory (Silva et al., 1992a; Silva et al., 1992b). Expression of the dominant negative inhibitor of PKA in the hippocampus and the forebrain using αCaMKII promoter results in reduced hippocampal PKA activity, normal E-LTP and decreased L-LTP in the CA1 region in mice (Abel et al., 1997). In parallel, it also resulted in deficient spatial memory and long-term memory for contextual fear conditioning (Abel et al., 1997).

In the conversion of short-term to long-term memory thus cAMP, PKA and CREB is essential (Find in detail in section 1D.). The importance of CREB was shown in Aplysia, Drosophila and mice as well (Casadio et al., 1999; Yin et al., 1994; Bourtchuladze et al., 1994). Mice with targeted disruption of CREB or expressing a repressor of CREB have disrupted LTP and hippocampal-dependent long-term memory (Bourtchuladze et al., 1994; Bozon et al., 2003). Mice expressing an inhibitor of an endogenous CREB repressor have enhanced LTP and long-term memory (Chen et al., 2003).

1F Involvement of NMDA receptor signalling in learning and memory

Hippocampal function has been studied by pharmacological experiments using various receptor antagonists and by analysing genetically modified mice. Intrahippocampal injection of NMDA receptor antagonists is a more targeted approach to uncover the role of hippocampus specifically in learning and memory. Injection of AP-5 prevents spatial learning tested by Morris water maze, which shows that the NMDA receptor is essential for learning (Morris et al., 1986), however it is not required for recall of information (Morris et al., 1989). Normal hippocampal function and AMPA receptor activity is essential for the recall of the spatial information (Morris et al., 1990). Analysis of mutant mice also gave evidence for the importance of the NMDA receptor signalling in learning and memory (Find in detail in section 1H).

In the hippocampus both NR2A and NR2B subunit-dependent signalling is implicated in long-term synaptic plasticity (McHugh et al., 1996; Kohr et al., 2003). It has been suggested that the NR2A containing NMDA receptors are important in the induction of LTP while NR2B containing receptors are important for LTD in the hippocampus (Liu et al., 2004). Previous studies however using NR2B overexpressing mice with enhanced CA1 LTP and long-term memory suggested the contribution of NR2B subunits to hippocampal LTP and learning (Tang et al., 1999).

While the hippocampus is crucial for spatial memory formation, yet it does not store long-lasting memories, the anterior cingulate cortex (ACC) has been implicated in remote fear and spatial memory as well (Maviel et al., 2004; Frankland et al., 2004). Both NR2A and NR2B subunits were shown to be important for LTP induction in the ACC and the NR2B subunit was implicated in mediating contextual fear memory tested by assessing freezing behaviour (Zhao et al., 2005). The phosphorylation of the NMDA receptors, which is thought to be contributing to LTP (Lu et al., 1998), is decreased in the ACC compared to the hippocampus in both NR2A and NR2B containing NMDA receptors (Zhao et al., 2005). It was hypothesized that while in the hippocampus the differential phosphorylation of NR2A and NR2B subunits allows for them to participate in distinct forms of synaptic plasticity (LTP and LTD), in the ACC the lower basal phosphorylation of the particular subunits doesn't allow that (Zhao et al., 2005).

Regulation of NMDA receptors by phosphorylation

Generation of mice carrying mutations in the NMDA receptor phosphorylation sites or in the kinases, which phosphorylate the NMDA receptor is a very useful tool in uncovering the role of these molecules in synaptic plasticity, learning and memory formation. Below are a few examples of these kinases and the effect of various mutations on hippocampal function and learning ability.

The phosphorylation state of the NR2B subunit of the NMDA receptor is implicated in LTP in various brain areas. Prenatal ablation of CA1 neurons resulted in decreased CaMKII-dependent phosphorylation of NR2A and NR2B and impaired LTP (Caputi et al., 1999). After the induction of LTP in the CA1 region of mice it was specifically the Tyr 1472 residue, which was shown to be phosphorylated (Nakazawa et al., 2001). In H-Ras knockout mice in the hippocampus the phosphorylation of NR2A and NR2B subunits is increased, NMDA receptor-dependent synaptic responses are enhanced and LTP is enhanced (Manabe et al., 2000). LTP in the dentate gyrus is also correlated with the phosphorylation of the NR2B subunit (Rosenblum et al., 1996). Recently generation of Y1472F mutant mice implicated the NR2B Tyr 1472

phosphorylation in fear learning and synaptic plasticity of the amygdala (Nakazawa et al., 2006). The NMDA receptor-dependent CaMKII signalling was impaired, LTP was reduced in the amygdala and the amygdala-dependent fear learning was impaired in these mutants.

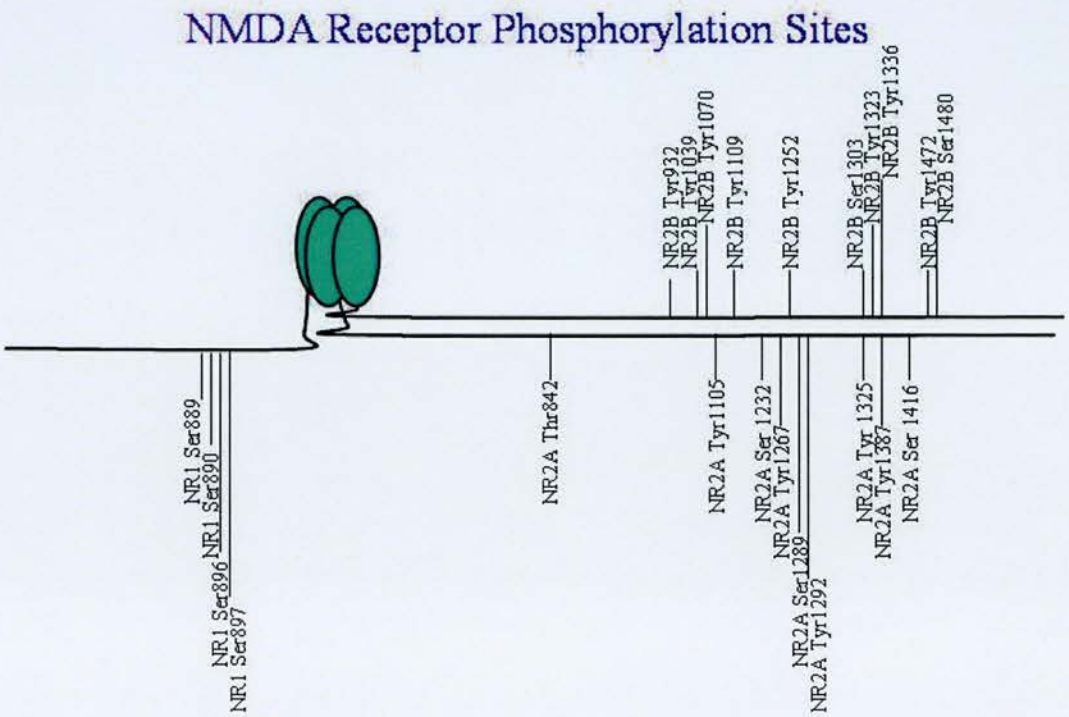

Figure 4. NMDA Receptor Phosphorylation Sites.
NMDA receptors are highly regulated by tyrosine and serine phosphorylation. Genetically modified mice carrying mutations in the NMDA receptor and the different kinases helped to uncover the details of the signalling cascades involved in learning and memory formation. The phosphorylation sites of the various subunits are displayed.

NMDA Receptor Phosphorylation Sites

	NR1		NR2A		NR2B	
	Site	**Reference**	**Site**	**Reference**	**Site**	**Reference**
Src			Tyr 1292 Tyr 1325 Tyr 1387	Yang et al., 2001	Tyr 1336 Tyr 1472	Cheung et al., 2001
PKA	Ser 897	Tingley et al., 1997	Thr 842	Woodward et al., 2002	+	
PKC	Ser 889 Ser 890 Ser 896	Tingley et al., 1997	Ser 1416	Gardoni et al., 2001	Ser 1303 Ser 1323	Liao et al., 2001
Fyn			Tyr 1105 Tyr 1267 Tyr 1387		Tyr 932 Tyr 1039 Tyr 1070 Tyr 1109 Tyr 1252 Tyr 1336 Tyr 1472	Nakazawa et al., 2001
CaMKII			Ser 1289	Gardoni et al., 1999	Ser 1303	Omkumar et al., 1996
Cdk5			Ser 1232	Li et al., 2001		
Pyk2			+	Liu et al., 2001		
Unknown					Ser 1480	Chung et al., 2001

Table 3. NMDA Receptor Phosphorylation sites.
Kinases involved in NMDA receptor signalling phosphorylate the particular receptor subunits on different serine and tyrosine residues.

Phospholipase C (PLC)-γ

The NMDA receptor is highly phosphorylated on serine and tyrosine residues, which potentiates receptor responses and induces transduction of intracellular signals. An early event in most signalling pathways is the generation of second messengers diacylglycerol and inositol 1,4,5-trisphosphate by hydrolysis of phosphatidylinositol 4,5-bisphosphate by PLC. For activation of PLC-γ its phosphorylation is essential, which occurs via its binding to phosphotyrosine residues of receptor tyrosine kinases. Both NR2A and NR2B subunits of the NMDA receptor bind to the SH2 domain of PLC-γ (Gurd and Bissoon, 1997) triggering various signalling pathways. Phosphorylation of PLC-γ is increased in transgenic mice overexpressing neurotrophin receptor trkB (Koponen et al., 2004). These mice display enhanced learning and memory in water maze and conditioned taste aversion tests, suggesting the importance of the particular signalling cascade.

Fyn

In the C-terminus of the NR2B subunit 25 tyrosine (Tyr) residues can be found. Seven out of twenty-five are phosphorylated in vitro (Nakazawa et al., 2000), confirmed by phosphopeptide mapping. Coexpression with Fyn in HEK 293 cells results in the phosphorylation of Tyr 1252, Tyr 1336 and Tyr 1472 (Figure 4, Table 3) with the latter being the major site of phosphorylation (Nakazawa et al., 2000). Tyrosine phosphorylation of NR2B by Fyn is responsible for binding of NR2B to phosphatidylinositol 3-kinase (PI3K). In Fyn deficient mice this binding is decreased (Hisatsune et al., 1999). Fyn knock out mice have disrupted hippocampal morphology and although the NMDA receptor contribution to excitatory postsynaptic current (EPSC) is normal, they display learning deficits (Grant et al., 1992).

Ca^{2+}-calmodulin-dependent protein kinase II (CaMKII)

CaMKII directly binds to subunits NR1 and NR2B of the NMDA receptor (Leonard et al., 1999) (Find in detail in section 1C.). Residues 1290-1309 of the NR2B subunit are critical for the interaction. The key residues in this region were identified by site directed mutagenesis (Strack et al., 2000), which are Lysine (Lys) 1292, Leucine (Leu) 1298, Arginine (Arg) 1299, Arg 1300, Glutamine (Glu) 1301 and Ser 1303. Phosphorylation of Ser 1303 inhibits binding to CaMKII. For recruitment of CaMKII to the NMDA receptor residues 1260-1316 of NR2B are sufficient (Leonard et al., 1999). The deletion of αCaMKII impairs E-LTP in the CA1 neurons of the hippocampus and spatial learning (Silva et al., 1992a; Silva et al., 1992b) (Find in further detail in section 1D and 1H.).

Protein kinase C (PKC)

Protein kinase C phosphorylates subunits NR1, NR2A and NR2B (Leonard and Hell, 1997; Sanchez-Perez et al., 2005) with NR2B being directly phosphorylated on residues Ser 1303 and Ser 1323 (Liao et al., 2001) (Figure 4, Table 3). PKC activation also induces tyrosine phosphorylation of NR2B (Grosshans and Browning,

2001). Mice lacking PKCγ exhibited impaired LTP but only mild learning deficits (Abeliovich et al., 1993).

Protein kinase A (PKA)

Protein kinase A similarly to PKC phosphorylates the NR1, NR2A and NR2B subunits of the NMDA receptor (Leonard and Hell, 1997) (Figure 4, Table 3). It has two regulatory (R) and two catalytic (C) subunits and is physically attached to the NMDA receptor via a scaffolding protein called yotiao (Lin et al., 1998), which directly binds to NR1. PKA Rlβ or Cβ1 mutant mice have impaired LTP, but normal learning (Brandon et al., 1995; Huang et al., 1995), which might be due to the fact that PKA activity was unaffected by the mutation.

Mitogen-activated protein kinase (MAPK) pathway

Apart from the pharmacological evidence, the phenotype of ERK1 and ERK2 knock out mice show the importance of the MAPK pathway in LTP formation, learning and memory and also viability (Find in detail in section 1D and 1E.). ERK1 has a modulatory function, while ERK2 is required for LTP induction (English et al., 1996). ERK1 knock out mice show some LTP reduction, but only using certain electrophysiological protocols (Mazzucchelli et al., 2002). Interestingly they display improved memory in the two-way avoidance test Mazzucchelli et al., 2002). ERK2 knock out mice are embryonically lethal (Adams et al., 2002).

1G Mouse genome manipulation

General gene targeting

A major milestone in the *in vitro* technology that enabled the production of mutant mice was the establishment of embryonic stem (ES) cell lines, derived from the inner cell mass of pre-implantation embryos (Evans et al., 1981; Martin et al., 1981). They maintain their pluripotency under the right culture conditions and using them, the *in vitro* manipulation of the endogenous gene locus can be achieved by homologous recombination. The targeting of endogenous loci by homologous recombination is a

rare event but the use of drug resistance cassettes increases efficiency significantly. The drug-resistant colonies can however have the targeting vector inserted correctly or incorrectly. For that reason the clones have to be checked by polymerase chain reaction (PCR) and Southern blotting to ensure the insertion of the targeting vector into the right locus. The cultured ES cells carrying the right mutation can be injected into blastocysts, forming chimaeras with exogenous ES cell contribution to all somatic tissues (Bradley et al., 1984). If the ES cells contribute to the germ line of the chimaera, the mutation can be transmitted resulting in mice carrying the mutated gene in all of their cells (Gossler et al., 1986; Robertson et al., 1986). By crossing these littermates we can obtain homozygosity.

Conditional gene targeting

In general gene targeting approaches different point mutations are produced or expression of various genes is abolished in an all or none manner. Knockout mice are useful to state the importance of a certain molecule in the signalling process of interest, but in a lot of cases the mutation itself is lethal therefore further physiological or biochemical analysis of the homozygous mice is not possible. For that reason the temporal and spatial control of gene expression is very important in these cases and is widely used for example in the studies of learning and memory formation. By producing conditional knockouts, it is possible to maintain viability and have a more thorough investigation of the function of a particular protein not only in specific brain regions, but also in different phases of memory, for example encoding versus retrieval.

In conditional gene inactivation techniques loxP or FRT sites as part of the targeting vector are inserted into specific loci by homologous recombination. These sites are short, 34 base pair recognition sequences for the bacteriophage recombinase Cre or the yeast recombinase Flp. In the absence of the particular recombinase the gene function is maintained, if it is present, recombination of two recognition sites in series excises the intervening DNA resulting in the loss of gene product. Using this method the expression of the gene in interest can be ablated in certain brain areas or

at certain developmental time points by either crossing the mice with Cre-expressing mice or by injecting the mice with Cre-expressing vectors, such as adenoviruses.

Different Cre-expressing mice have been produced by usage of tissue-specific promoters. Using the Thy-1 promoter restricts the expression to the brain (Kellendonk et al., 1999), while αCaMKII promoter-driven Cre restricts it to the forebrain (Tsien et al., 1996a). Different transgenic lines using the same promoter might however exhibit different expression patterns. A good example is the αCaMKII-driven Cre line T29-2 line. It exhibits particularly high expression in the CA1 region with little expression outside the hippocampus (Tsien et al., 1996a). It has been useful for the study of CA1 function in synaptic plasticity, learning and memory (Tsien et al., 1996a; Tsien et al., 1996b).

In addition, the Tet system (Find detailed description below.) can regulate Cre expression in a temporal fashion (St-Onge et al., 1996), however a Tet-driven Cre transgenic exhibiting suitably restricted brain expression has not yet been developed. To combine the advantages of the temporal and spatial control direct injection of Cre-expressing vectors can be used. One possibility is the usage of the adenoviral system. Systemic injection of Cre-expressing adenovirus resulted in a wide tissue distribution, although preference for certain organs was observed while expression was absent from the brain (Akagi 1997). If green fluorescent protein-expressing adenovirus is used for the injections (Harding et al., 1998) the specific brain regions can be accurately targeted at a chosen time point.

The tetracycline-controlled transcriptional activator (tTA) drives expression via the tetracycline (Tet) resistance operon (tetO), but in the presence of the tetracycline analogue, doxycycline, transcription is repressed (Gossen et al., 1992). Since doxycycline is stored in muscle and bone, tTA was mutated and a reverse tTA identified, in which doxycycline stimulates transcription (Gossen et al., 1995). This system was used in the production of transgenic mice expressing either a calcium-independent CaMKII or a calcineurin inhibitor peptide under the control of the tetO

promoter (Malleret et al., 2001). These animals exhibited phenotypes that were reversible.

1H Knockouts affecting synaptic plasticity and learning

NMDA receptor transgenic mice

As the central molecule in learning and memory formation, the NMDA receptor is the obvious target of gene manipulation when trying to determine signalling pathways involved in the underlying processes. To examine their functional roles all NMDA receptor subunits have been genetically modified. Most of the mice produced are global knockouts (the expression of the gene of interest is abolished throughout the brain), but conditional knockouts (the deletion of the expression of the gene of interest is located to specific brain areas) and knockins (for example over-expression models) have also been made.

Global NR1 knockouts have been produced by homologous recombination in embryonic stem cells. Normal expression of the NR1 subunit is essential to NMDA receptor function, somatosensory map formation and neonatal survival. In the case of one of the NR1 global knockouts (Forrest et al., 1994) the NR1 expression is lost throughout the brain and the NR2B expression is reduced. This mutation is lethal within a day of birth due to respiratory failure. A complete loss of NMDA-induced rise in intracellular calcium and a complete loss of whisker-related barrel formation can be observed (Forrest et al., 1994; Li et al., 1994). The condition can be rescued by ectopic expression of the NR1-1a splice variant and viability is dependent on the level of expression (Forrest et al., 1994; Li et al., 1994; Iwasato et al, 1997). Another global NR1 mutant has been produced by homologous recombination (Mohn et al, 1999) in which case the NR1 expression is reduced to about 5-10% of the normal level. These mice develop to normal size, but have abnormal sexual function, locomotor and behavioural deficits (Mohn et al, 1999).

When using a global knockout for studying spatial memory it is not possible to out rule that the deficits arise from the loss of gene product and its developmental consequences rather than the lack of hippocampal LTP. It is possible to overcome these problems if the gene deletion is restricted to a particular area of the brain such as the CA1 region of the hippocampus (Tsien et al., 1996a).

NR1 conditional knockouts have been created using cre-loxP recombination. The expression has been abolished in the hippocampal CA1, CA3 or the cortical region. When NR1 subunit expression is abolished in the CA1 region of the hippocampus, mice are viable and develop normally, but LTP and LTD cannot be induced in the CA1 neurons (Tsien et al., 1996b). However LTP can be induced in the dentate gyrus. The mice are deficient in spatial learning tasks as tried using the hidden platform in the Morris water maze test and they have a deficit in relational memory, however memory consolidation is unaffected (McHugh et al., 1996; Shimizu et al., 2000). The nonspatial learning abilities were measured using a slightly submerged platform in the water maze (Kolb et al., 1994) together with a large "landmark" cue. The animals could perform this task, which only relies on a simple association and is not hippocampus-dependent (Tsien et al., 1996b). These results show that NMDA synaptic plasticity in CA1 hippocampal neurons is important in acquisition and representation of spatial information. Plasticity in CA3 on the other hand is involved in associative memory. When the NR1 expression is abolished in the CA3 pyramidal cells in adult mice, NMDA dependent LTP in CA1-CA3 synapses is absent (Nakazawa et al., 2002). The spatial memory is normal tested by Morris water maze (Nakazawa et al., 2002), but there is a deficit in pattern completion after some cues are removed. Cortical NR1 knockouts are viable, but they develop slower than wild type littermates (Iwasato et al., 2000). NMDA receptor mediated synaptic plasticity is absent in the barrel cortex. In the barrel cortex there are no barrel boundaries formed, the cells are distributed uniformly (Iwasato et al., 2000). This shows that the NMDA receptor activity is required to form maps in the somatosensory cortex. The maps in the brain stem however are normal.

Point mutations in the NR1 gene have also been generated by homologous recombination in embryonic stem cells. Replacing asparagine (N) 598 by glutamine (Q) or arginine (R) alters the ion channel properties of the NMDA receptor (Single et al., 2000). The calcium permeability of the ion channel decreases and in the case of the second mutation the magnesium block is incomplete. Homozygous mice die within an hour of birth due to respiratory failure and lack of suckling response (Single et al., 2000). Heterozygous mice can survive up to weeks.

Global NR2 knockouts have also been produced by homologous recombination in embryonic stem cells. C-terminal deletion mutants and over-expression models are available. Since it is the NR2B subunit, which is expressed in embryonic stage and also in juvenile animals, this subunit is the most important in neonatal survival and somatosensory map formation. Therefore the most severe deficits and lethality can be observed in NR2B mutants (Find in detail below.).

The NR2A subunit is not expressed in the embryonic brain therefore the global NR2A knockout mice develop normally and have normal fertility. The neuroanatomy is normal, the somatosensory maps are intact, but there is a reduction of the NMDA receptor current and LTP at CA1 synapses (Sakimura et al., 1995). They show impaired spatial learning in the Morris water maze and deficits in associative learning (Sakimura et al., 1995). NR2A C-terminal deletion mice are viable and show similar LTP deficits as the global knockout mutants (Sprengel et al., 1998).

The NR2B subunit is essential for neonatal survival and somatosensory map formation as it is highly expressed in embryonic brain. The C-terminus of the NR2B receptor is important for correct synaptic targeting of the NMDA receptor (Mori et al., 1998) and for normal signal transduction. Global NR2B knockout mice have been produced by homologous recombination (Kutsuwada et al., 1996). Loss of barrel formation and lack of LTD in CA1 neurons can be observed (Kutsuwada et al., 1996). NR2B C-terminal deletion has similar effects as the global knockout, the barrel formation is disrupted in the brainstem, the number of NMDA receptors, which are synaptically localized is decreased (Sprengel et al., 1998; Mohrmann et al.,

2002). The homozygous mice die perinatally (Sprengel et al., 1998). In culture conditions the synaptic localization improves when the NR2A subunits are expressed (Mohrmann et al., 2002). NR2B knockin was created by pronuclear injection where the NR2B subunit is overexpressed in the forebrain (Tang et al., 1999). The neuroanatomy and development is normal, but LTP is enhanced in CA1 neurons resulting in improved ability to retain information, better long-term memory (Tang et al., 1999).

Two different NR2C knockout strains have been created, the first shows reduction in the EPSC component mediated by NMDA, the second shows higher EPSC peak amplitude, but shorter decay time (Ebralidze et al., 1996). Mice lacking both NR2A and NR2C subunits display motor coordination deficits (Kadotani et al., 1996). Deletion of the C-terminus impairs NMDA dependent LTP (Sprengel et al., 1998).

NR2D knockout mice grow normally (Ikeda et al., 1995), suggesting that the role of the subunit is compensated by NR2B. They display reduced locomotion and reduced sensitivity to stress (Miyamoto et al., 2002) measured in elevated maze or forced swimming tests. NR2D subunit overexpression results in impairement of CA1 LTD in juvenile mice and CA1 LTP in adult mice (Okabe et al., 1998). Overexpression also decreases the development of induced epileptic seizures, which suggests a role for NR2D in epilepsy (Bengson et al., 1999).

Mutations in other molecules of the NMDA receptor complex

The NMDA receptor complex (Husi et al., 2000) consists of numerous proteins directly interacting with different subunits of the receptor, and a lot more, which are indirectly linked via other molecules, forming different signalling pathways. The core is the NMDA receptor, but mutations in the other molecules of the complex can also generate useful data determining details of signalling pathways involved in learning and memory formation.

The fact that metabotropic glutamate receptor (mGluR) agonist ACPD enhances LTP (McGuinness et al., 1991) was evidence for the involvement of metabotropic

glutamate receptors in LTP formation and learning. Since mGluR inhibition didn't consistently block LTP in experiments of different groups (Anwyl et al., 1999), mutant mice were generated. The mGluR1 knockout mice are viable, have normal hippocampal anatomy (Aiba et al., 1994). They are however deficient in LTD, have reduced LTP and moderate impairment of associative learning (Aiba and Chen et al., 1994). LTP is absent at the mossy fiber-CA3 synapses in mGluR2 knockout mice (Yokoi et al., 1996). Enhanced LTP in CA1 was also reported (Jia et al., 2001), but conclusion on the changes in spatial learning couldn't be made since mGluR2 knockout mice exhibit reduced exploration. Mutant mice lacking mGluR5 exhibit impaired CA1 and dentate gyrus (DG) LTP, but normal CA3 LTP (Lu et al., 1997; Jia et al., 2001). They also exhibit impaired spatial learning (Lu et al., 1997; Jia et al., 2001). These findings suggest that some forms of learning are dependent on mGluR activation.

Mutation of some other receptors alters induction of LTP or has an effect on spatial learning. Serotonin receptor 5-HT(1A) knockout mice have normal CA1 LTP, but impaired spatial learning (Sarnyai et al., 2000). Serotonin receptor 5-HT(3C) knockout mice exhibit impaired DG LTP and spatial learning (Heisler et al., 1999). In TrkB knockout mice both CA1 LTP and spatial learning is impaired (Minichiello et al., 1999). CA1 LTP is normal, DG LTP is impaired in mu-opioid receptor knockout mice (Matthies et al., 2000) while nociceptin knockout mice exhibit enhanced LTP in CA1 and enhanced spatial learning (Noda et al., 2000).

Mutations of many signalling molecules have similar effects to that of the above receptors. Fyn knockout mice are viable, they develop normally, but LTP in hippocampal CA1 synapses is impaired and they exhibit impaired spatial learning tested in the Morris water maze (Grant et al., 1992). Long-term potentiation can be rescued by introduction of Fyn transgene (Kojima et al., 1997). Alpha-CaMKII knockout mice are also viable, have no obvious neuroanatomical abnormalities and have intact NMDA receptor function (Silva and Stevens et al., 1992). They however have impaired spatial learning and behavioural abnormalities, such as decreased fear response or increase in defensive aggression (Silva and Paylor et al., 1992; Stevens et

al., 1994). Impaired CA1 LTP was also shown in alpha-CaMKII knockout mice (Silva and Stevens et al., 1992; Hinds et al., 1998). Expression of CaMKII-Asp-286 impairs CA1 LTP and spatial memory, however contextual memory remains normal (Bach et al., 1995). PKCγ knockout mice have reduced LTP in hippocampal CA1 synapses (Abeliovitch et al., 1993) and impaired spatial learning (Abeliovitch et al., 1993). Knocking out SynGAP or expressing inhibitory PKA regulatory subunit (eg. R(AB) mice) impairs both CA1 LTP and spatial learning (Abel et al., 1997; Komiyama et al., 2002).

Some structural proteins, presynaptic molecules have also been mutated triggering changes in LTP or spatial memory. Neural-cell adhesion molecule (N-CAM) knockout mice have normal LTP, but impaired spatial learning (Bliss et al., 2000). Thy-1 knockout mice are viable, show impairment in DG LTP, but normal spatial learning (Nosten-Bertrand, 1996). Overexpression of presynaptic protein GAP43 enhances LTP in the dentate gyrus and enhances spatial learning (Routtenberg et al., 2000). Abolishing somatostatin (type2) expression leaves the LTP normal, but again spatial learning is enhanced (Dutar et al., 2002).

In some of the above examples the changes in hippocampal LTP coincide with the changes in spatial learning, in others the correlation is not coincident. These differences contribute to the debate whether LTP and spatial learning is based on the same cellular mechanism, if LTP is a model for some forms of learning. Some studies showed that saturating LTP impairs spatial learning (Castro et al., 1989), some others failed to find correlation. Reasons for LTP not blocking learning might be that LTP was induced in the wrong pathway or to a lesser extent than required (Bliss et al., 1993). On the other hand evidences for sharing the same cellular mechanism are that they both are accompanied by glutamate release, PKC or ERK activation; they both are inhibited by AP-5 (Morris et al., 1986); and both LTP and spatial learning is decreased in aged or stressed rats (Rapp et al., 1987). The findings of this study, outlined below, might contribute with useful facts to this ongoing debate.

1I Experimental Objectives

Analysis of different mouse mutants has been a successful approach in examining the functions of different genes and gene products. It is possible to introduce point mutations, to delete certain sequences or whole genes. The effects of these mutations can be analysed *in vitro* using embryonic stem (ES) cells and *in vivo* by generating the mutant mice by injecting the ES cells carrying the mutation back into the host blastocyst. The evolution of different gene targeting techniques and the increasing amount of data available enables laboratories to use this type of analysis in all fields of research.

The aim of this project is to acquire basic knowledge on the molecular mechanisms of NMDA ion channel and receptor function, learning and memory by producing mice carrying different mutations in the C-terminus of the NR2B subunit of the NMDA receptor, which is believed to be involved in different signalling pathways as a part of a multi-component signalling complex. Its binding partners can be categorised into two major groups. One is the MAGUK proteins, which all contain PDZ domains via which they bind to the E-S/T-X-V motif located at the extreme C-termini of the NR2 subunits. A few of these proteins are PSD-95, chapsyn-110 or SAP 102. These further interact with nNOS (Holscher et al., 1997), fyn (Grant et al., 1992) or SynGAP (Chen et al., 1998). The other group is the non-MAGUK proteins, which bind to sites of the C-terminus other than the terminal E-S/T-X-V motif and include for example CaMKII, PLC-γ and PKC.

I introduced three different mutations into the C-terminus of the NR2B subunit of the NMDA receptor. One is designed to ablate the interactions with the PDZ domain containing molecules by deleting the terminal valine from the E-S/T-X-V motif of the NR2B C-terminus (NR2B DelValine mutation). The other is designed to prevent the interaction between the NR2B subunit and CaMKII by modifying key residues in the binding site (NR2B CaMKII mutation). The third, when deleting the COOH-exon

of the NR2B subunit and replacing it by that of the NR2A (NR2A/NR2B SWAP mutation), reveals the functional differences between the NR2A and NR2B subunits and the importance of the interactions via the NR2B cytoplasmic tail.

In further sections abbreviations will be used for various mutations generated and different mutant mice already available, which were used for breeding purposes. In the case of the NR2B DelValine mutation the ES cell clones will be named DelVal and their respective number (eg. DelVal 8-8). The chimaera with which we achieved germline transmission will be called DelVal 8-8 chimaera coming from the name of the ES cell line it originated from. In the NR2B CaMKII mutation the ES cell clones will be referred to as CaMKII and their respective number (eg. CaMKII 1-6) while in the case of the NR2A/NR2B SWAP mutation, NR2A and their respective number (eg. NR2A 2-20). Mice expressing C-terminal truncated forms of NR2A or NR2B subunits (Sprengel et al., 1998) will be referred to as $NR2A^{\Delta C}$ and $NR2B^{\Delta C}$ respectively.

Chapter 2: Materials and Methods

2A Techniques related to manipulation of DNA

Vector preparation, subcloning

Small-scale plasmid purification was achieved using Promega's Wizard Plus Minipreps DNA Purification System. One colony was inoculated into 3 ml of LB media, incubated overnight at 37 °C providing appropriate aeration by shaking at 225 rpm. The saturated culture was spun at 10000 g in a picofuge for 2 minutes and the resulting pellet was resuspended in 200 µl Cell Resuspension Solution (50 mM Tris-HCl pH 7.5, 10 mM EDTA, 100 µg/ml Rnase A). 200 µl Cell Lysis Solution (0.2 M NaOH, 1% SDS) was added followed by 200 µl Neutralization Solution (1.32 M potassium acetate pH 4.8). The tube was spun at 14000 rpm for 5 minutes and the DNA containing supernatant was transferred into a new tube and mixed with 1 ml of DNA Purification Resin. The mixture was filtered through a Minicolumn and washed with 2 ml Column Wash Solution (80 mM potassium acetate, 8.3 mM Tris-HCl pH 7.5, 40 µM EDTA, 55% ethanol). 50 µl TE (10mM Tris-Cl pH 8.0, 1 mM EDTA) buffer was added to the Minicolumn and the plasmid DNA was eluted by spinning at 14000 rpm for 30 seconds. The DNA was stored at –20 °C.

Large-scale plasmid purification was achieved using Qiagen's Plasmid Midi Kit. A few colonies were inoculated into 50 ml of LB media, incubated overnight at 37 °C providing appropriate aeration by shaking at 225 rpm. The saturated culture was spun in a Falcon tube at 3000 rpm for 15 minutes at 4 °C. The pellet was resuspended in 4 ml buffer P1 (50 mM Tris-HCl pH 8.0, 10 mM EDTA, 100 µg/ml Rnase A) and the solution was transferred into a Falcon 2059 tube. 4 ml buffer P2 (0.2 M NaOH, 1% SDS) was added followed by 4 ml buffer P3 (3.0 M potassium acetate pH 5.5). A midiprep column was washed with 10 ml buffer QBT (750 mM NaCl, 50 mM MOPS pH 7.0, 15% isopropanol, 0.15% triton X-100), then the solution was added and the column was washed with 10 ml buffer QC (1 M NaCl, 50 mM MOPS pH 7.0, 15%

isopropanol) twice. The DNA was eluted with 5 ml buffer QF (1.25 M NaCl, 50 mM Tris-HCl pH 8.5, 15% isopropanol), mixed with 3.5 ml isopropanol and spun at 8000 rpm for 30 minutes at 4 °C. The pellet was washed with 2 ml 70% ethanol, spun at 8000 rpm for 10 minutes at 4 °C, air-dried and resuspended in 0.5 ml TE (10 mM Tris-Cl pH 8.0, 1 mM EDTA) buffer. The DNA was stored at –20 °C.

Restriction digestion of DNA

Digests were performed at 10 unit restriction enzyme per μg DNA, in reactions of 50-100 μg/ml DNA using 1x restriction enzyme buffer for 1-2 hours at the recommended temperature. After digestion the DNA fragment of interest was separated from other fragments by electrophoresis on a 0.8 - 2% agarose gel and recovered from the gel. When the digestion was used for vector linearization approximately 200 ng digest was run alongside uncut DNA on a gel to check digestion. The linearised vector was purified by phenol: chloroform extraction and ethanol precipitation. When used for ligations with phosphorylated insert, the vector was dephosphorylated before purification to prevent self-ligation.

Dephosphorylation of vector DNA

Dephosphorylation of the vector 5' end was performed to prevent self-ligation of vector digested with only one restriction enzyme. Directly following vector restriction digestion, 3 units of calf intestinal alkaline phosphatase per μg vector DNA was added (CIAP, Boehringer Mannheim). After incubating for one hour at 37 °C, extra 0.5 units CIAP per μg vector DNA was added, followed by 15 minutes incubation at 55 °C. The entire reaction was run on a 1% agarose gel to separate the vector backbone from the stuffer fragment before recovering the dephosphorylated vector from the gel, using the phenol: chloroform extraction method. CIAP-treated DNA requires phenol: chloroform extractions twice (Stratagene Catalogue) to separate the CIAP as it binds strongly to the DNA.

Phenol: chloroform: isoamyl alcohol extraction of DNA

After estimating the volume of the DNA solution an equal volume of phenol: chloroform: isoamyl alcohol solution (25:24:1) was added. The mixture was vortexed

or if purifying genomic DNA inverted 6 times to minimize shearing and spun at 14000 *g* for 3 minutes. The aqueous top phase was transferred into a new tube and to the phenol phase equivalent volume of TE (0.1 mM EDTA, 10 mM Tris-HCl pH 8) was added. After vortexing and spinning again the aqueous layer was transferred to the new tube to ensure maximum DNA recovery. The DNA was then ethanol precipitated.

Ethanol precipitation of DNA

After estimating the volume of the DNA solution 3 M Potassium Acetate (pH 5.2) was added to a final concentration of 0.3 M followed by two volumes -20 °C ethanol. The mixed solution was incubated in the -70 °C freezer or snap frozen in liquid nitrogen to allow DNA precipitation for 15-20 min. DNA was recovered by spinning at 4 °C for 10 minutes at 14000 g (10,500 rpm SS-35). After removing the supernatant the tube was filled half way with ice cold 70% ethanol and spun at 14000 *g* for 2 minutes at 4 °C (10500rpm SS-35). The resulting pellet was air-dried at room temperature and dissolved in TE. After phenol: chloroform: IAA DNA extraction and ethanol precipitation, DNA recovery should be above 80%.

Recovery of DNA from agarose gels (phenol method)

The desired DNA band was excised from the gel using a sterile blade. After estimating the volume of the gel piece it was doubled with TE buffer then melted at 65 °C for 5-10 minutes. Equal volume of Tris-buffered phenol was added and after mixing the tube was spun for 3 minutes at 10-12000 rpm. The aqueous phase was transferred to a new tube and the phenol extraction step was repeated. 0.1 volume of 4 M lithium chloride was added to the aqueous solution and after the formation of a white precipitate the tube was placed on ice for two minutes, spun for 3 minutes at 10-12000 rpm. 1 µl of carrier (glycogen) and 2.5 volumes of cold ethanol were added to the aqueous phase, which was transferred to a new tube. The sample was snap frozen in liquid nitrogen to precipitate and spun as previously at 10-12000 rpm for 10 minutes. The pellet was washed with 1 ml 70% ethanol, air-dried and resuspended in 10-20 µl of TE buffer.

Recovery of DNA from agarose gels using BIO101 Geneclean Spin Kit

When smaller amount of DNA was available and when working with smaller DNA fragments BIO101's Geneclean Spin Kit was used for recovering the desired fragments from agarose gel. The standard protocol described in the kit was used. The elution was achieved by adding 11 µl TE buffer to the Spin Filter and spinning for 30 seconds at 10-12000 rpm. This step was repeated twice for increasing DNA yield.

Ligation of insert and vector

The vector and the insert was ligated in reactions containing 50 ng or 100 ng vector with a varying insert to vector ratios of 1:1 to 5:1. The control reactions were to assay for re-ligation of the digested vector (no insert DNA control), to monitor ligation reagents for contaminants (no DNA control), to check for contaminating plasmids (competent cells only) and to monitor for background level (no ligase). The ligation reactions were set up containing 3 units of T4 DNA ligase (Promega) in 1x ligase buffer. The tubes were incubated on ice overnight and competent *E. coli* cells were transformed with the ligation mixture next day.

Preparation of chemical competent cells

The DH5α cells were spread onto a bacterial plate from glycerol stock-solution kept at –20 °C and the plate was incubated overnight at 37 °C. A few colonies were inoculated into a 50 ml LB media-containing beaker next day and incubated overnight at 37 °C providing appropriate aeration by shaking at 225 rpm. The following day the saturated culture was diluted 100X into 10 ml of fresh LB media and incubated at 37 °C while shaking at 225 rpm until the optical density reached 0.6-0.7. After incubating on ice for 5 minutes the culture was spun at 3000 rpm for 15 minutes in the cold room. The pellet was then dissolved in 1 ml 10 mM $CaCl_2$ solution by shaking then diluted to 10 ml. After incubating on ice for 1 hour the culture was spun again at 3000 rpm for 15 minutes in the cold room. The pellet was resuspended in a final volume of 1 ml 10 mM $CaCl_2$ solution. 100 µl cell suspension was used per transformation.

Transformation of chemical competent cells

5 µl of DNA ligation mixture was added to a 100 µl aliquot of competent cells. The tubes were incubated on ice for 20 minutes followed by a 1-minute heat shock at 42 °C to allow DNA uptake by the cells. After 5 more minutes of incubation on ice 900 µl of SOC medium (1.5 mL SOB base; 7.5 µl 2M $MgCl_2$; 30 µl 1M glucose) was added to the cells. The tubes were shaken at 225 rpm, 37 °C for 45 minutes to allow expression of the ampicillin resistance gene. For vector stock transformations 50-100 µl of the culture was spread onto L-agar plates containing the appropriate antibiotics. For ligation reactions the cells were pelleted by spinning at 3000 rpm for 2 minutes, resuspended in 100-200 µl of the supernatant and plated out using 100 µl stock.

Preparation of electro competent cells

The DH5α cells were spread onto a bacterial plate from glycerol stock-solution kept at –20 °C and the plate was incubated overnight at 37 °C. A few colonies were inoculated into a 50 ml LB media-containing beaker next day and incubated overnight at 37 °C providing appropriate aeration by shaking at 225 rpm. The following day the saturated culture was diluted 100X by adding 2,5 ml solution to 250 ml of fresh LB media and incubated at 37 °C while shaking at 225 rpm until the optical density reached 0.6-0.7. After incubating on ice for 30 minutes the culture was poured into 4 Falcon tubes, each containing 45 ml and spun at 3000 rpm for 15 minutes in the cold room. The supernatant was decanted and the rest of the culture solution was added and the tube was spun again. The pellet was then dissolved in 45 ml 10% glycerol spun at 3000 rpm for 5 minutes in cold room. This step was repeated twice and the pellet was resuspended into a final volume of 150 µl. The contents of the four tubes were merged and the solution was aliquoted into 0.5 ml eppendorf tubes (40 µl each). The tubes were snap frozen in liquid nitrogen and stored at –80 °C.

Transformation of electro competent cells

An aliquot of electro competent cells was thawed on ice and 5µl of DNA ligation mixture was added. The cell-DNA mixture was transferred into a prechilled Gene

Pulser (BioRad) cuvette and was electroporated at 25 μF, 200 Ω, 2,5 kV. After electroporation 900μl of SOC medium (1.5 mL SOB base [2% tryptone, 0.5% yeast extract, 10 mM NaCl]; 7.5 μl 2 M $MgCl_2$; 30 μl 1 M glucose) was added to the cells. The rest of the procedure was the same when using chemical competent cells.

Sequencing reaction for automated sequencer

PCR reactions were carried out on Omnigene (Hybaid) or Mastercycler gradient (Eppendorf) PCR machines. The dNTPs were supplied by Roche.

The reaction mixture was prepared in a total volume of 10 μl containing 0.5 μg DNA template, 1 μl of 3.2 pmol/μl primer, 4 μl Big Dye Terminator Ready Reaction Mix and dH_2O up to 10 μl. A drop of mineral oil was added to the tube and the sequencing reaction (96 °C 30 seconds, 50 °C 15 seconds, 60 °C 4 minutes repeated 25 times) was run. After the program finished, 10 μl dH_20 was added to the reaction mixture to increase the volume and the whole solution was removed from under the mineral oil and transferred into a new tube. 2 μl 3 M sodium acetate pH 4.6 and 50 μl 95% ethanol was added to the tube and incubated on ice for 15 minutes. The solution was spun at 14000 rpm for 20 minutes increasing the speed gradually. The pellet was washed with 120 μl 70% ethanol, air-dried and resuspended in 4 μl ABI loading buffer (deionised formamide and 25 mM EDTA pH 8.0 containing 50 mg/ml Blue dextran in a ratio of 5:1 formamide to EDTA/Blue dextran). The samples were sequenced in ABI PRISM 310 Genetic Analyzer.

Analysis of embryonic stem cell derived genomic DNA

Southern Blotting

Preparation of filter

Genomic DNA was digested with the appropriate high concentration enzyme overnight. A small amount of extra enzyme was added the next day and the samples were further incubated for 6-8 hours to ensure complete digestion. The samples were run on an agarose gel containing no ethidium bromide at 12-18 V overnight. The gel was stained and photographed as normal then immersed in 0.2 N HCl for 10 minutes, in 0.5 M NaOH; 1.5 M NaCl for 45min followed by 30 minute incubation in 1 M

Tris-Cl pH 7.4; 1.5 M NaCl. Between each step the gel was rinsed with dH_2O. The gel was then placed on a gel tank turned upside down, which was previously covered with a layer of dH_2O and Saran wrap in a way that no air bubbles were present. A piece of nitrocellulose (Hybond^{TM}-N) was cut to the same dimensions as the gel and was given an orientation marker. The nitrocellulose was carefully placed onto the gel followed by 3 mm Whatman filter paper cut to the same dimensions as the gel. Finally a stack of Kleenex paper was placed on top enough that it stood at 10-15 cm of height. A gel tray and a small weight was placed on he top of the stack and the filter was left that way overnight at room temperature. Next day the sheets of paper were removed with forceps and the DNA was crosslinked to the filter using UV.

Prehybridisation

The hybridisation tube was pre-warmed to 65 °C. The prehybridisation solution (27 ml of 6X SSC and 0.5% SDS, 3 ml of 50X Denhardts (BSA, Ficoll, PVP), 300 µl of Salmon Testes DNA previously fragmented by boiling at 100 °C for 5 minutes and placing it on ice for 2 minutes) was prepared and poured into the hybridisation tube. The filter was soaked in 20X SSC for 5 seconds and placed into the hybridisation tube with the DNA facing to the inside of the tube. The tube was then rotated at 65 °C for 4 hours.

Probing the filter

The DNA probe to be labelled was diluted to a concentration of 2.5-25 ng/45 µl in TE buffer, denatured by heating to 95-100 °C for 5 minutes in water bath and placed on ice for 5 minutes. The DNA then was added to the reaction tube of Rediprime^{TM} II, random prime labelling system (Amersham Pharmacia), mixed with 5 µl Redivue [^{32}P] dCTP and mix and incubated at 37 °C for 10 minutes. 5 µl 0.2 M EDTA was added to stop the reaction and the reaction mixture was added to a ProbeQuant G-50 Microcolumn, spun at 3000 rpm for 1 minute. The labelled DNA was denatured by heating to 95-100 °C for 5 minutes in water bath then placed on ice for 5 minutes.

The freshly prepared probe was added to the hybridisation solution and the filter was then incubated at 65 °C overnight.

Washing the filter

The hybridisation solution was discarded from the tube and the filter was rinsed with 65 °C wash buffer 1 (2X SSC, 0.5% SDS). After rinsing twice 30 ml wash buffer 1 was added and the hybridisation tube was rotated at 65 °C for 10 minutes. The additional steps were using 30 ml wash buffer 1 for another 10 minutes, 30 ml wash buffer 2 (1X SSC, 0.25% SDS) for 15 minutes and 30 ml wash with buffer 3 (0.5X SSC, 0.1% SDS) for 15 minutes if the background was still high. The filter then was wrapped in Saran wrap while still damp, placed into a cassette. Kodak X-ray film was placed over the filter in the dark room and the cassette was left at –80 °C to expose. The film was developed 3-5 days later.

Genotyping

Preparation of high molecular weight (HMW) DNA from mouse tails

Mice were earmarked at three weeks of age and half an inch of tail was cut and placed into 750 µl of tail buffer (50 mM Tris pH 8.0, 1 mM EDTA, 1 mM NaCl, 1% SDS). After adding 30 µl of 10 mg/ml Proteinase K the tail was incubated in a rotator at 55 °C overnight. Next day 20 µl of 30 mg/ml RNAse A was added and the tube was incubated in water bath at 37 °C for 1 hour. 500 µl of phenol was then added and the tail was rotated overnight at 4 °C. Next day the tube was spun at 14000 rpm for 5 minutes, the aqueous top layer and interphase was transferred into a new tube. 500 µl of phenol: chloroform: isoamyl alcohol solution (25:24:1) was added and rotating for 4 hours at 4 °C the tube was spun at 14000 rpm for 5 minutes. The aqueous top layer was transferred into a new tube and the previous cleaning step was repeated using 500 µl of chloroform: isoamyl alcohol solution (24:1). 1 ml of isopropanyl alcohol was added to the final aqueous top layer and upon gentle mixing the precipitation of fibrous HMW DNA could be observed. The DNA was spooled

with a yellow tip, dipped briefly into 70% ethanol then placed into 100 µl of TE (pH 7.4). The DNA was allowed to resuspend overnight at 4 °C.

NR2A$^{\Delta C}$ genotyping

The mastermix (5 µl 10X buffer, 5 µl DMSO, 1 µl 10mM dNTP's, 1 µl 40 µM primer Rsp10, 1 µl 40 µM primer Rsp 26, 34.75 µl dH_2O, 0.25 µl Qiagen Hot Star Taq added last after 2.5 minute UV irradiation of the mastermix) was prepared and 48 µl was dispensed per tube. 2 µl of tail DNA solution was added to each sample and the samples were run on Hybaid PCR machine (15 minutes at 95 °C then 40 cycles of 30 seconds at 94 °C, 1 minute at 57 °C, 3 minutes at 72 °C).

NR2B$^{\Delta C}$ genotyping

The mastermix (5 µl 10X buffer, 1 µl 10mM dNTP's, 1 µl 40 µM primer NR2B-1, 1 µl 40 µM primer NR2B-3, 39.75 µl dH_2O, 0.25 µl Qiagen Hot Star Taq added last after 2.5 minute UV irradiation of the mastermix) was prepared and 48 µl was dispensed per tube. 2 µl of tail DNA solution was added to each sample and the samples were run on Hybaid PCR machine (15 minutes at 95 °C then 35 cycles of 20 seconds at 94 °C, 30 seconds at 55 °C, 1 minute at 72 °C then a final 10 minutes at 72 °C). The homozygous band is 1311 bp, the WT band is 136 bp.

NR2B DelValine genotyping

Reaction using Qiagen Hot Star Taq

The mastermix (5 µl 10X buffer, 1 µl 10mM dNTP's, 1 µl 40 µM primer 1, 1 µl 40 µM primer 2, 39.75 µl dH_2O, 0.25 µl Qiagen Hot Star Taq added last after 2.5 minute UV irradiation of the mastermix) was prepared and 48 µl was dispensed per tube. 2 µl of tail DNA solution was added to each sample and the samples were run on Hybaid PCR machine (15 minutes at 95 °C then 35 cycles of 20 seconds at 94 °C, 30 seconds at 65 °C, 2 minute at 72 °C then a final 10 minutes at 72 °C). For the analysis different combinations of primers A (NR2B 5910), B (pLox 413), C (pLox

1540) and D (NR2B 6456) and primers A' (SWAP NR2A 3924), B' (pLox 91), C' (pLox 1603) and D' (NR2B 8035) were used explained in the figure below.

Reaction using Long Range PCR

25 µl of mastermix A (20 µl dH_2O, 0.6 µl 25mM dNTP's, 2 µl 20 µM primer NR2B 5910, 2 µl 20 µM primer NR2B 6456 per tube), 19 µl of mastermix B (16 µl dH_2O, 5 µl buffer 1), 2 µl of dH_2O and 2 µl tail DNA was combined and mixed. Samples were run on Eppendorf PCR machine. After 30 seconds at 93 °C the reaction was paused and incubated at 93 °C for 15 minutes (hot start) and 1 µl expand enzyme (Roche) was added to each sample. The reaction was then restarted (10 cycles of 10 seconds at 93 °C, 30 seconds at 60 °C, 2 minutes at 65 °C then 20 cycles of 10 seconds at 93 °C, 30 seconds at 60 °C, 2 minutes at 65 °C with 20 seconds of increment followed by 7 minutes incubation at 68 °C).

Analysis of results

The offsprings were first genotyped using three different combinations of primers A (NR2B 5910), B (pLox 413), C (pLox 1540) and D (NR2B 6456) with *Qiagen Hot Star Taq*. The reaction with *Long Range PCR* used primers NR2B 5910 and NR2B 6456. Depending on the primers and the reaction used different sizes of bands or none were amplified. Comparing the results of the different reactions (Find in detail in the table below.) the genotype could be specified.

In wild type mice AXB and CXD combination didn't result in amplification because of the lack of the neo cassette while the AXD combination gave a 546 base pair band (~0.5 kB). In the heterozygous offsprings a 642 base pair band was amplified in the AXB combination, a 546 base pair band in the AXD combination (~0.5 kB) and an extra 2346 base pair band using *Long Range PCR.* In homozygous mice (further described) we got a 642 base pair band in the AXB and a 734 base pair band in the CXD combination (~0.5 kB). The AXD combination produced a 2.3 kB homozygous

band, but only using *Long Range PCR* since the Taq polymerase can't amplify that size fragment.

Another set of primers was designed to get a larger band that is easier to visualize, which were primers A' (SWAP NR2A 3924), B' (pLox 91), C' (pLox 1603) and D' (NR2B 8035). By using the *Qiagen Hot Star Taq* system and primer combination A'XB' a ~2.3 kB band was obtained in heterozygous and homozygous mice and no band in wild type mice. By using the *Qiagen Hot Star Taq* system and the primer combination C'XD' a ~2 kB band was obtained in heterozygous and homozygous mice and no band in wild type mice.

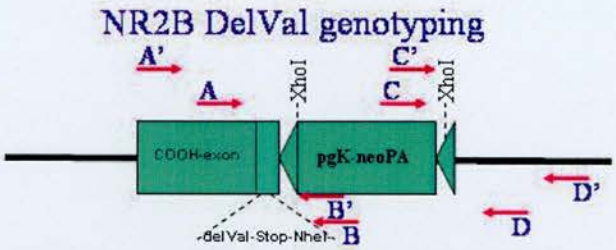

Genotype / Primers and PCR reaction	Wild Type	Heterozygous	Homozygous
A X B Taq polymerase	NO AMPLIFICATION	~ 0.5 KB BAND AMPLIFIED	~ 0.5 KB BAND AMPLIFIED
A' X B' Taq polymerase	NO AMPLIFICATION	~ 2.3 KB BAND AMPLIFIED	~ 2.3 KB BAND AMPLIFIED
C X D Taq polymerase	NO AMPLIFICATION	~ 0.5 KB BAND AMPLIFIED	~ 0.5 KB BAND AMPLIFIED
C' X D' Taq polymerase	NO AMPLIFICATION	~ 2.0 KB BAND AMPLIFIED	~ 2.0 KB BAND AMPLIFIED
A X D Taq polymerase	~ 0.5 KB wt BAND AMPLIFIED	~ 0.5 KB wt BAND AMPLIFIED	NO AMPLIFICATION
A X D Long Template PCR	~ 0.5 KB wt BAND AMPLIFIED	~ 0.5 KB wt AND 2.3 KB homo BAND AMPLIFIED	~ 2.3 KB homo BAND AMPLIFIED

2B Tissue culture of embryonic stem cells

The main supplier of the tissue culture is Iwaki from Bibby Sterilin. Other suppliers used are Falcon, Corning and Nunc.

The 25, 75 and 150 cm^2flasks; 6, 12, 24 and 96 well plates; and the 100 mm dishes were provided by Iwaki. The 4 and 48 well plates, the 1 ml cryotubes were provided by Nunc. The 30 ml universals and the 30, 60 and 100 mm petri dishes were purchased from Bibby Sterilin. The 15 and 150 ml tubes, the 60 mm dishes were provided by Corning. The electroporation cuvette was purchased from Biorad.

Media preparation

All media was prepared in the Class II cabinets using sterile technique. For 440 ml (1 bottle) media 380 ml of 1X GMEM, 4 ml of non-essential amino acids, 8 ml of glutamine: sodium pyruvate mixture, 400 µl of mercaptoethanol and 40 ml of foetal calf serum (FCS) was mixed. Once the media was prepared a TESTER was set up (5ml of media should be added to the 5ml tester) and incubated overnight to ensure sterility. For ES cells 1ul of leukemia inhibitory factor (LIF) / ml of media was added to get a final concentration of 1000 units LIF/ ml media.

Thawing embryonic stem cells

E14TG2a cells were kept in liquid nitrogen storage in individual vials. When thawing the cells, 9.5 ml of prewarmed media was placed into a universal. The frozen cells were retrieved from the liquid nitrogen and thawed as quickly as possible by placing them in the 37 ^{o}C water bath or by holding the vial in bare hand. The cells then were transferred into the warm media to dilute out the DMSO in which the cells had been frozen. The cells were then spun at 1000 rpm for 5 minutes, resuspended in an adequate amount of prewarmed media and transferred to an appropriate flask followed by gassing with a CO_2/air mixture (5%/95%). The cells were then placed in the tissue culture incubator at 37 ^{o}C and 5% CO_2.

Passaging embryonic stem cells

The cell culture grown to 80-90% confluence was washed with PBS twice after removing the media by aspirator. Appropriate volume of trypsin was added (1ml for small flask, 0.5 ml for 1 well of a 6 well plate or 4 drops of trypsin for 1 well of a 24 well plate) and the culture was placed into the incubator for approximately for 4 minutes. The flask was then tapped gently to dissociate the cells and placed back into

the incubator for 1 minute. 4 ml of media was added for 1ml of trypsin to stop the action of the trypsin, the cells were then transferred to a universal and spun for 5 minutes at 1200 rpm. The resuspended cells (in 5 ml media) were counted using a haemocytometer and 10^6 cells were added to a 25 cm^2 gelatinised flask. The number of cells added to larger flasks was adjusted accordingly. The flask was gassed with 5%CO_2/95% air mixture and returned to the incubator.

Freezing embryonic stem cells

10% DMSO in culture media was used as freezing solution prepared by adding 2 ml of DMSO to 18 ml of media to provide a stock solution.

The cells were trypsinised as normal, but at the end of the procedure they were resuspended in an appropriate volume of freezing solution instead of media. 0.5 ml cell suspension was placed into each cryotube and stored in the –80 °C freezer overnight, then transferred to the cellbank the following day.

Embryonic stem cell electroporation

150 μg of vector was linearised with NotI, precipitated, washed with 70% ethanol and resuspended in 100 μl PBS the night before electroporation. E14TG2a cells were grown up from frozen stock to yield about 5×10^7 cells, trypsinised and resuspended in a final volume of PBS that gave about $1X10^8$ cells/600 μl. Using a plugged pipette the cells were added to the electroporation cuvette followed by the 100 μl DNA solution. The cuvette was placed in the gene pulsar and the cells were electroporated at 0.8 kV, 3 μF. (Time constant should be 0.1 s.) The mixture was then incubated in the cuvette at room temperature for 10 minutes. After incubation the cells were added to 20 ml warm media and plated in 10 cm tissue culture dishes at densities of 5×10^6, 10^6, 5×10^5 and 10^5 cells per plate. G418 (200 μg/ml) was added one day after electroporation and selection was continued for 10 days.

A large number of colonies were picked 10-12 days after electroporation and grown up in 24 well plates. The confluent wells were split to generate one plate to freeze for later expansion of cell line and a duplicate plate from which DNA was extracted for analysis by Southern blotting.

Picking colonies

Two drops of trypsin or media was added to alternate rows of 96 well plates. Well-separated colonies were chosen and marked on the underside of the plate. The plate was washed with PBS twice then 5 ml PBS was added. A p200 Gilson pipette set to 50 µl was used to pick up the colony by scraping it off the plate and drawing it into the pipette tip. The colony was placed into the prepared 96 well plate and was dissociated. The solution containing the cells was then transferred into 1 well of a 24 well plate and 1.5 ml of media was added.

Extraction of genomic DNA from embryonic stem cells in culture

The extraction buffer contains 0.1 M EDTA, 0.2 M NaCl, 0.05 M Tris-HCl pH 8, 0.5% SDS and 50 µg/ml DNase-free RNase.

For large scale extraction 10^8 cells were grown up as a monolayer and the cells were recovered by trypsinisation. Trypsin was quenched with media and transferred to a 50 ml Falcon tube. The tube was centrifuged at 500 g for 10 minutes and the cell pellet resuspended in 20 ml Extraction Buffer. Proteinase K was added to achieve 100 µg/ml concentration and gently mixed. The tube was incubated in the water bath for 3 hours, gently inverting the tube every 20 minutes. The solution should be reasonably clear and viscous at the end of the incubation. The solution then was transferred to a large beaker and 20 ml of pre-equilibrated phenol: chloroform: IAA (first check pH = 8) was added. The beaker was then gently swirled by hand for 10-15 minutes to mix the two phases. After transferring the mixture to a 50 ml plastic tube it was centrifuged at 1500 g for 10 minutes at room temperature to separate the phases. The aqueous phase was removed into a new tube using a 5 ml disposable pipette tip, which had the end cut off. The aqueous phase was dialysed against 1000 volume of TE.

For small scale extraction from a 24 well plate 500 µl of extraction buffer/well was used and extraction was performed overnight at 37 °C as normal. 500 µl phenol then 500 µl phenol: chloroform: IAA was used for cleaning of DNA. The genomic DNA

was then used in the resulting form or the procedure used previously was followed and the DNA was resuspended in 100 µl TE buffer.

2C Animals

All animals were housed and treated in accordance with the animals (scientific procedures) act 1986. Animals were housed in a 12:12 hour light dark cycle with food and water provided *ad libitum*. Wild type littermate controls were used with the mutants.

Targeted gene replacement in mice

Embryonic stem cells (E14TG2a) isolated from the light coloured 129 P2/Ola Hsd mouse strain were targeted to carry the mutations specified before in one chromosome. These cells were then injected into blastocyst-stage embryos coming from superovulated and mated C57Bl/6 mice where upon survival they assimilated into the inner cell mass and participated in the formation of the chimaeric mice (mice containing cells from two different strains). The microinjections were carried out by Jane Robinson, our chief technician.

The *agouti* gene produces brown fur colour even if present in one copy in the cells therefore the chimaeras are easy to select from amongst the offsprings. Chimaeric males were mated back first to MF1 females (white), which was general procedure at the Centre for Genome Research, to obtain big litters and confirm germline transmission, which was indicated by silver fur colour and identified by analysis of their DNA. The chimaeras were then crossed with C57Bl/6 (black) females in which case germline transmission was indicated by agouti pups (black pups indicated no transmission) followed by mating with 129 P2/Ola Hsd females (beige), in which case all pups are beige and genotyping is needed to check germline transmission. The heterozygous offsprings from these test crosses were then intercrossed to produce homozygous mice containing the desired mutation in both chromosomes.

2D Materials

Antibiotics

Ampicillin	Sigma
Penicillin/Streptomycin (P/S)-solution	Gibco
G418 sulphate	Gibco

Bacterial strains

DH5α

E.coli XL1-Blue

Embryonic stem cell lines

E14TG2a ES cells

General and tissue culture reagents

Agarose	Sigma
Agar	Sigma
BSA	Gibco
B27 supplement	Gibco
Dimethylformamide (DMF)	Sigma
Dimethyl sulfoxide (DMSO)	Sigma
Dulbecco´s MEM Nut Mix F-12 (DMEM/F12)	Gibco
Ethylenediamine-tetraacetic acid (EDTA)	Sigma/BDH
Ethidium bromide	Sigma
Expand long template PCR system	Roche
Foetal calf serum (FCS)	Gibco
Formaldehyde	Fluka
Formamide	Sigma
Glasgow´s Modified Eagle Medium (GMEM)	Gibco
Gelatin	Sigma

L-Glutamine	Gibco
Laminin	Sigma
LB capsules	BIO 101
Lysozyme	Sigma
ß-Mercaptoethanol	Gibco
Neurobasal medium	Gibco
Non-essential Amino Acids	Gibco
PBS sol/tablets	Gibco/Oxoid
Phenol	Sigma
Phenol: Chloroform	Fisher
Poly-D-lysine (PDL)	Sigma
RNase	Sigma
Sodium pyruvate	Gibco
Taq DNA polymerase	Promega
Tris-hydroxymethyl-aminomethane (Tris Base)	Sigma
Triton X-100	BDH
Trypsin	Gibco

Nucleotides and Nucleic acids

Desoxyribonucleotides (dNTPs)	Invitrogen
DNA size marker: 1kb ladder, 100bp ladder	Invitrogen

Chapter 3: Results

3A Introduction

Production of mutant mice has been used to determine the function of certain domains of the NMDA receptor uncovering the fact that the C-terminus of the NR2 subunit is the most important in synaptic plasticity via binding to downstream molecules, forming the initiating point of signalling cascades. The binding partners can be categorised into two major groups (Figure 2, Table 2a, b and c). One is the group of MAGUK proteins. They all contain PDZ domains and via this domain they bind to the E-S/T-X-V motif located at the extreme C-termini of the NR2 subunits. A few of these proteins are PSD-95, chapsyn-110 or SAP 102. These further interact with nNOS (Holscher et al., 1997), fyn (Grant et al., 1992) or SynGAP (Chen et al., 1998), which is also a regulator of Ras. The other group is the non-MAGUK proteins, which bind to sites of the C-terminus other than the terminal E-S/T-X-V motif, and include for example CaMKII, PLC-γ and PI3-K.

I introduced three different mutations into the C-terminus of the NR2B subunit of the NMDA receptor. One is designed to ablate the interactions with the PDZ domain containing molecules by deleting the terminal valine from the E-S/T-X-V motif (NR2B DelValine mutation) of the NR2B C-terminus (Figure 9). The second is designed to prevent the interaction between the NR2B subunit and CaMKII (NR2B CaMKII mutation) by modifying key residues in the binding site (Figure 41). The third is to exchange the COOH exon of the NR2B subunit with that of NR2A (NR2A/NR2B SWAP mutation) (Figure 48).

All mutants were generated using conventional gene targeting technology. The mutation was introduced and the neo selection cassette was inserted. Unlike in conditional systems, in this case the spatial and temporal control over gene expression is not possible.

3B NR2B DelValine Mutation

Introduction

According to the time expression of the different subunits NR1 and NR2B play an important role in brain development and therefore it is not surprising that mice lacking these subunits die shortly after birth (Forrest et al., 1994; Li et al., 1994; Kutsuwada 1996). Mice without postnatally expressed NR2A and NR2C subunits are viable (Sakimura et al., 1995; Ebralidze et al., 1996).

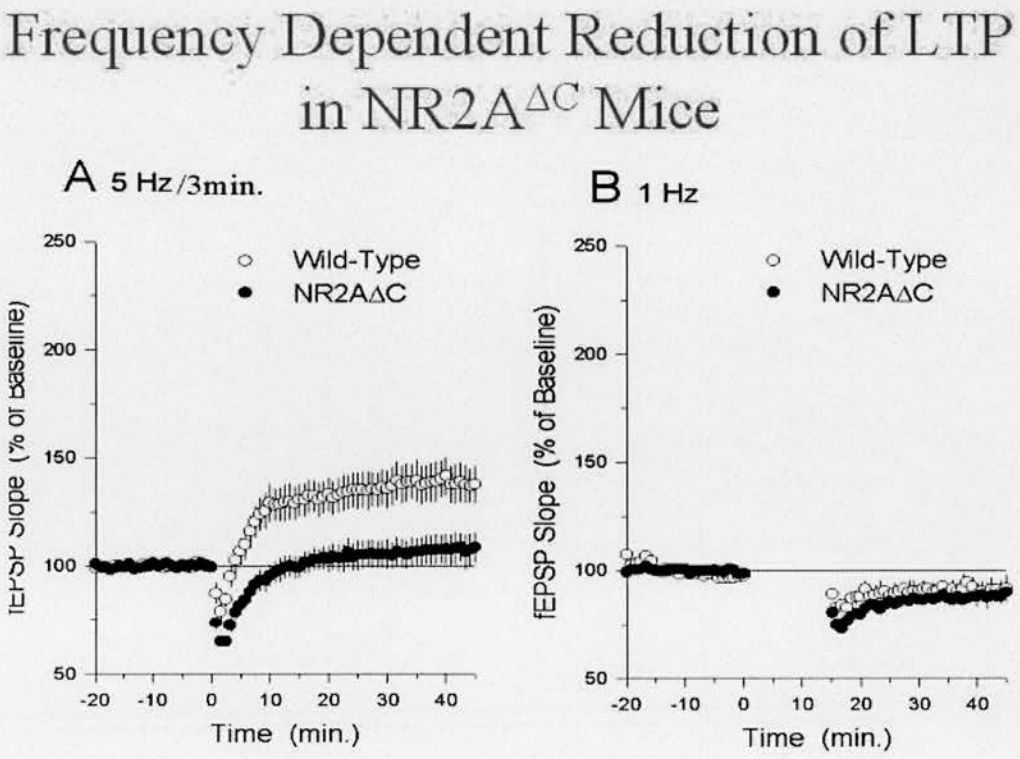

Figure 5. Electrophysiological data of NR2A$^{\Delta C}$ mice.
LTP of mutant mice is reduced compared to wild type using the 5 Hz/3 min protocol. The data was produced by collaborator Dr Thomas J O'Dell.

The intracellular C-terminal domains of the NMDA receptors appear to be involved in different signalling pathways by coupling to proteins such as PSD-95, chapsyn-110 or other proteins in the membrane-associated guanylate kinase family. Mice expressing C-terminal truncated forms of NR2A, NR2B and NR2C subunits have been produced (Köhr and Seeburg, 1996; Sprengel et al., 1998). No interference with the formation of gateable receptor channels have been observed *in vitro* however

mice expressing these truncated subunits manifested great phenotypic resemblance with mice lacking the respective subunits (Kutsuwada 1996), namely that mice lacking the NR2B C-terminus ($NR2B^{\Delta C}$) died perinatally (Sprengel et al., 1998).

The analysis of various mouse mutants helps to determine the underlying mechanisms of learning and memory formation. Experiments comparing the LTP data are only possible if the mice are viable. In the case of $NR2A^{\Delta C}$ mice frequency dependent reduction of LTP can be observed (Figure 5). Since $NR2B^{\Delta C}$ mice are not viable a different strain had to be produced in which the interaction between the NR2B subunit and downstream molecules was inhibited, but the viability was preserved. It is the E-S/T-X-V motif of the C-terminus, which binds to PSD-95 therefore I deleted the terminal valine codon present at the very end of the C-terminal tail of the NR2B subunit (NR2B DelValine) to prevent the interaction between these two molecules.

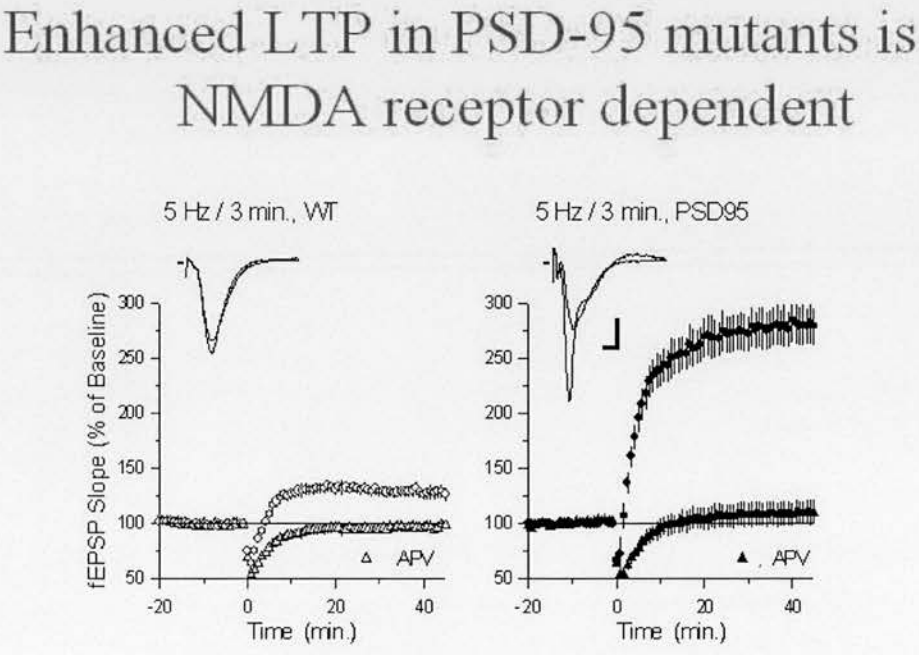

Figure 6. Electrophysiological data of PSD-95 mutant mice.
The enhanced LTP of the mutant mice is abolished by the NMDA receptor antagonist AP-5. The data was produced by collaborator Dr Thomas J O'Dell.

In PSD-95 mutant mice enhanced LTP can be observed (Figure 6). This is NMDA-receptor dependent since treatment with AP-5 brings LTP to baseline. In the case of the NR2B DelValine mice, the changes in the LTP features due to interrupted interaction between NR2B and PSD-95 could be observed, which was not possible to do in $NR2B^{\Delta C}$ mice.

In the next section I will describe the construction of the DelValine targeting vector in detail to provide an insight into basic DNA manipulation techniques. Further sections will only contain the details of the most important targeting steps.

Vector construction

The vectors and subclones used (Figure 57) were provided by collaborator Dr Rolf Sprengel. From the plasmid pNR2B-2.6 the NdeI-EcoRI fragment was subcloned into pRK172 vector (Figure 8, Figure 7 Step 1). This vector consists of 2558 base pairs and contains an NdeI site at position 2392 and an EcoRI site at position 2415. Both pNR2B-2.6 containing the desired fragment and pRK172 were restriction digested by NdeI and EcoRI as described in the methods. The resulting fragments were purified, ligated, the DNA mixture was then electroporated into DH5α cells, which were plated and grown on ampicillin containing bacterial plates. From the resulting colonies six individual ones were picked and tested for correct subcloning by digesting with NdeI and EcoRI. In the case of the correct clones an 872 base pair band (NdeI-EcoRI fragment inserted) and the backbone of the vector (~2.5 kB) was visualized. The smaller band was identical to that cut out from the original vector pNR2B-2.6. All six colonies were tested positive (Figure 8).

The new vector, pRK172-NdeI-EcoRI was used as a template for site directed mutagenesis to delete the valine from the end of the COOH exon of NR2B using Stratagene Quick Change™ Site-directed Mutagenesis Kit. At the same time an XhoI and an NheI site was created to use later for checking homologous recombination (Figure 9, Figure 7 Step 2).

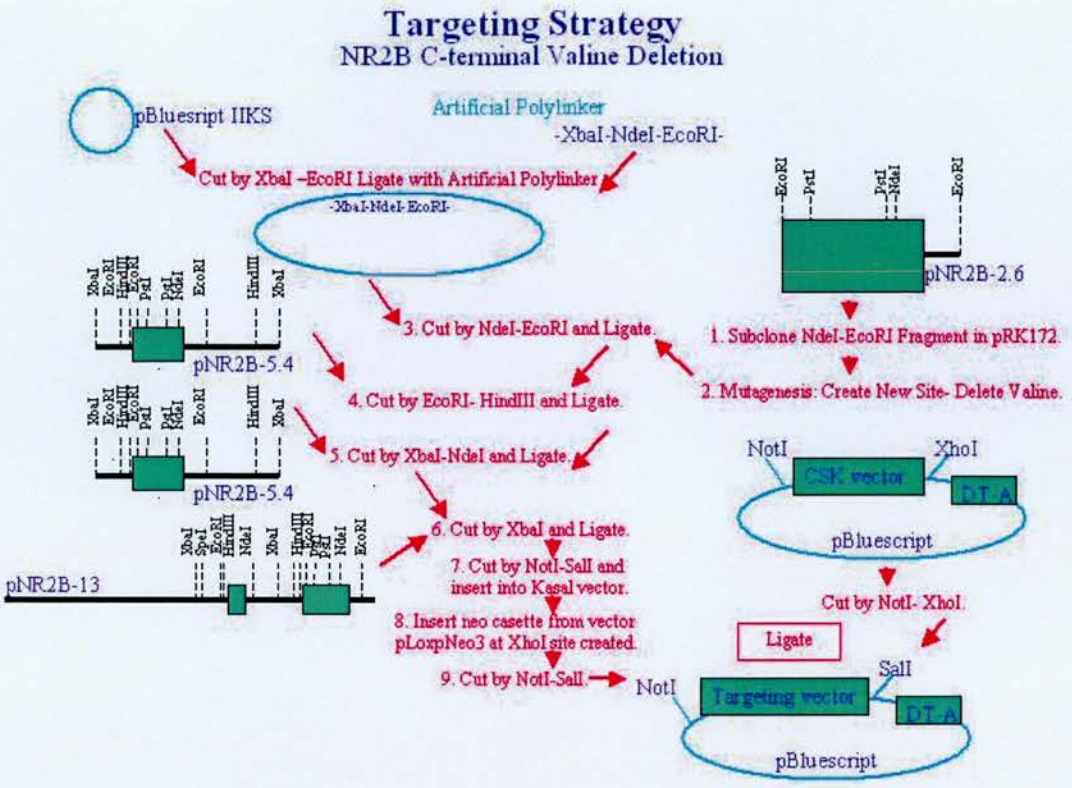

Figure 7. Targeting strategy of NR2B Valine deletion vector.
Fragments from the plasmids pNR2B-5.4 and pNR2B-13 were inserted into pBlueScript KSII containing the artificial polylinker to produce the targeting vector. The vectors and subclones used were provided by collaborator Dr Rolf Sprengel.

18 colonies were picked from the bacterial plates for further testing. Prescreening of correct mutagenesis was done by XhoI restriction digestion. XhoI digest linearised the circular plasmid DNA of the correct clones. By digesting with XbaI and XhoI the correct band of 472 bases was obtained (and the backbone ~3 kB) in the cases of the four subclones 14, 16, 17 and 18. The parental subclone was only linearised by XbaI (~3.5 kB), which is present in the original vector pRK172 (Figure 10). All four subclones were found correct by restriction digestion and 16, 17, 18 were checked by sequencing. The sequencing primers used were DelVal 1 to 4 and DelVal I to VI (Find sequence information in the appendix.). Only pBlue-DelVal 16 and 17 were containing the correct sequence. Subclone pBlue-DelVal 17 was used for further cloning reactions.

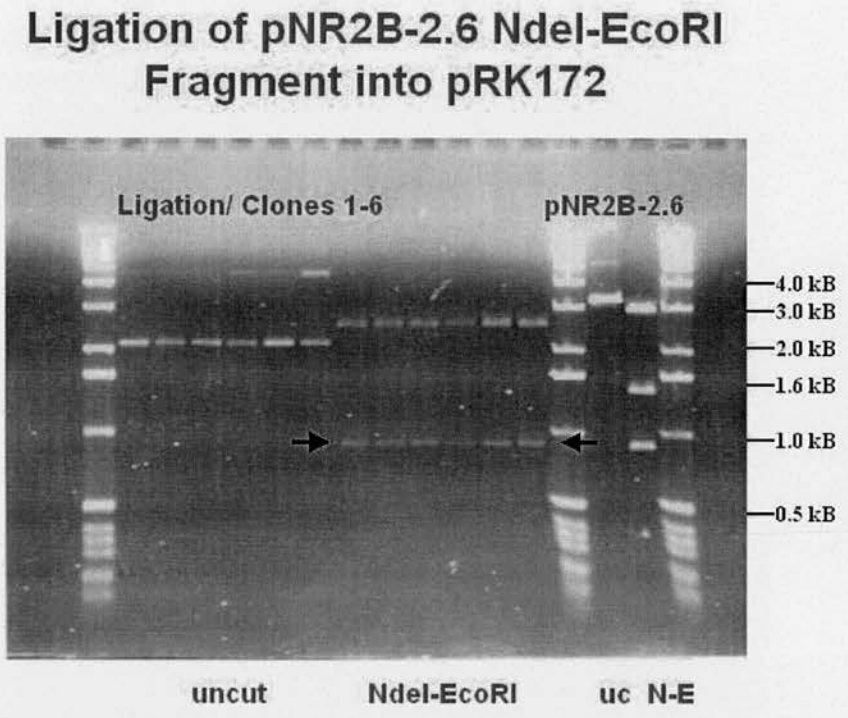

Figure 8. Ligation of pNR2B-2.6 NdeI-EcoRI fragment into pRK172.
NdeI-EcoRI fragments from pNR2B-2.6 clone and pRK172 vector were isolated. The gel picture shows the result of the ligation of the two fragments. Correct subcloning was tested by NdeI-EcoRI restriction digestion of the colonies picked after ligation and also the original pNR2B-2.6 clone. The resulting bands, about 800 bases, are the same in both cases.

A new plasmid was generated from pBlueScript KSII by inserting an artificial polylinker -XbaI-NdeI-EcoRI-. This was done to enable us to insert various fragments from the plasmids pNR2B-5.4 and pNR2B-13 (Figure 7) to produce the final targeting vector.

First the NdeI-EcoRI fragment carrying the mutation was inserted into the modified pBlueScript KSII (Figure 7 Step 3, Figure 11). From the bacterial plate 12 colonies were picked and were prescreened by NdeI-EcoRI digest. Using this digest I obtained the 472 base pair fragment containing the mutation that was inserted. Two of them were further screened with XhoI, EcoRI and NdeI digest (Figure 11) and both clones were found correct. The parental clone pRK172-DelValMut was also digested with the same enzymes. On the gel photo the size difference between the

two vectors (pRK172-2558 base pairs, pBlueIIKS-2961 base pairs) can be seen (Figure 11).

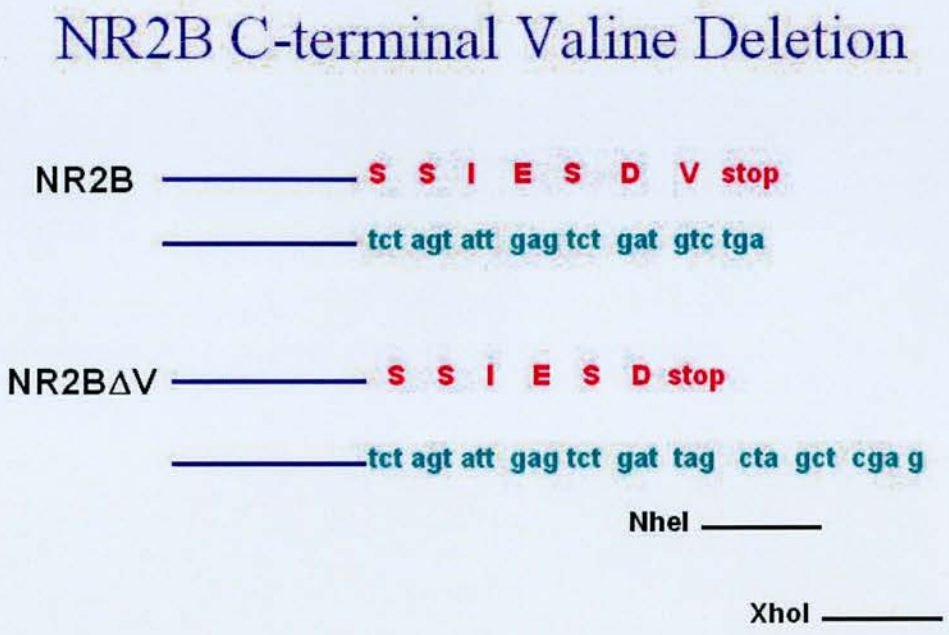

Figure 9. NR2B C-terminal valine deletion.
Stratagene Quick Change™ Site-directed Mutagenesis Kit was used to delete the terminal valine codon. The primers used were DelValMut 1 and 2.

In the next step the EcoRI-HindIII fragment was inserted 3' (Figure 7 Step 4, Figure 12). Six clones were picked from the bacterial plate, grown and the resulting DNA was digested by HindIII-EcoRI along with the parental clone. A 1325 base pair fragment can be visualized (insert) in all six clones and the size difference between the uncut vectors (parental clone-3833 base pairs, clones 1 to 6-5158 base pairs) can also be seen on the gel picture. All six clones were found positive.

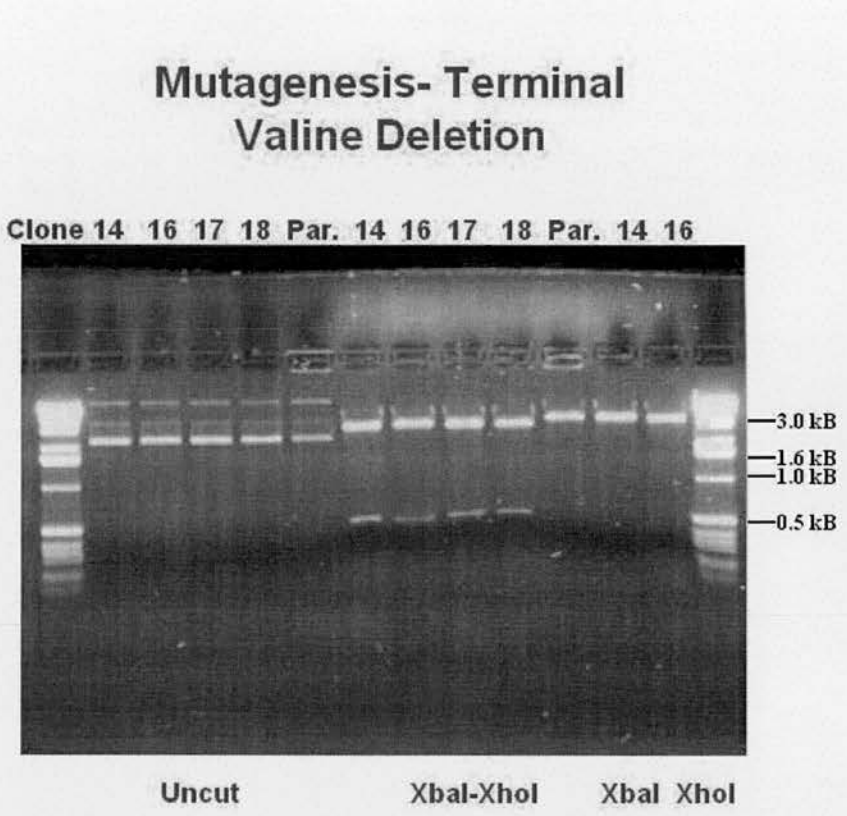

Figure 10. NR2B C-terminal valine deletion- Screening for correct mutagenesis.
On the figure the parental subclone (Par.) and clones 14, 16, 17 and 18 are presented. By digesting with XbaI and XhoI correct bands of about 500 bases were obtained in the cases of the four subclones while the parental subclone was only linearised by XbaI which is present in pRK172. The last two lanes on the right show single digestions of two colonies by XbaI and XhoI resulting in linearization.

In the next step the XbaI-NdeI fragment (Figure 7 Step 5, Figure 13) was inserted 5'. On the bacterial plates only twelve colonies grew as a result of lower transformation efficiency due to a larger plasmid being transformed. All 12 colonies were grown up and the resulting DNA was digested with NdeI-XbaI to check correct insertion. Clones 1, 2, 4, 6, 7, 8, 9, 10 and 11 were found correct in which cases I could visualize the 2443 base pair NdeI-XbaI fragment and the backbone of the vector, which was equal in size as the only visible band of the incorrect clones (No insertion occurred, the size is equal to that of the linearised parental vector, 5158 base pairs.).

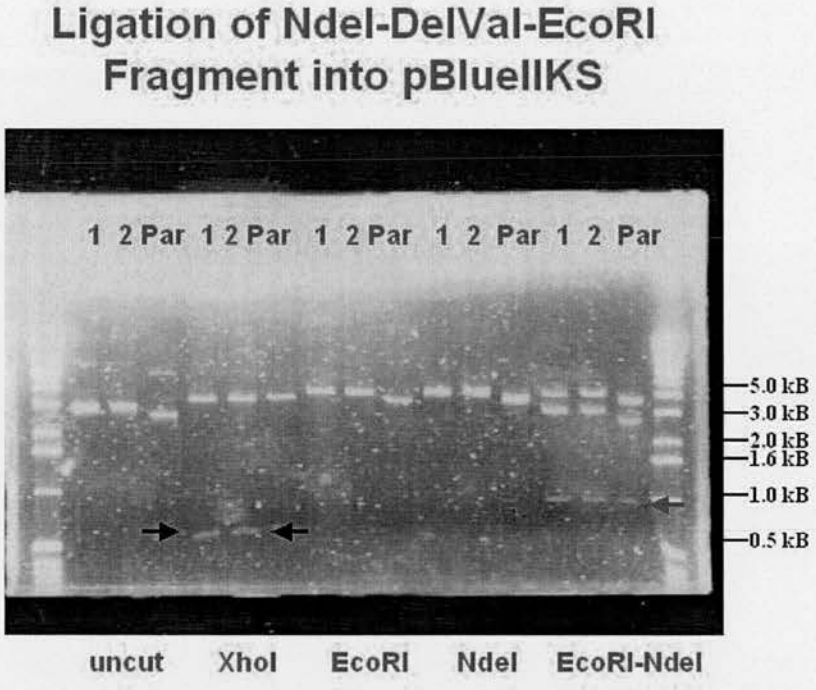

Figure 11. Ligation of NdeI-DelVal-EcoRI fragment.
On the figure the parental subclone (Par.) and clones 1 and 2 are presented. By digesting clones 1 and 2 with XhoI I could visualize a band of about 500 bases (XhoI site is present in pBluelIKS and in the mutation site) indicated by the black arrows. The parental clone only contains one XhoI site in the mutation site therefore the vector is only linearised.
When digesting with EcoRI or NdeI all clones are linearised and the size difference resulting from the different vectors (pRK172-2558 base pairs, pBluIIKS-2961 base pairs) can be seen.
When digesting with EcoRI-NdeI, the 872 base pair inserted fragment was dropped (indicated by the blue arrows), which is the same size in the two clones and the parental subclone. Again the size difference can be seen in the backbone of the vector. The top bands correspond to linearised plasmid DNA (incomplete double digest) where the size difference can also be visualized.

The XbaI-XbaI (Figure 7 Step 6, Figure 14) fragment was then inserted 5'. From the resulting 7 colonies 4 were grown up and screened with XbaI, NdeI and HindIII digest. The XbaI digest clarified that the fragment was inserted only in clones 1, 2 and 3 where the 2993 base pair fragment could be seen on the gel picture. The other two digests clarified whether the orientation of the fragment was correct. In the case of the NdeI digest I could see a 3295 base pair NdeI-NdeI band if the orientation was correct (clone 1) and a 4584 base pair NdeI-NdeI band if the orientation was

incorrect (clone 2 and 3). The HindIII digest resulted in a 3030 and a 3769 base pair HindIII-HindIII fragment in the correct orientation, while in the case of the incorrect orientation a 1705 base pair and a 3769 base pair HindIII-HindIII fragment was visualized.

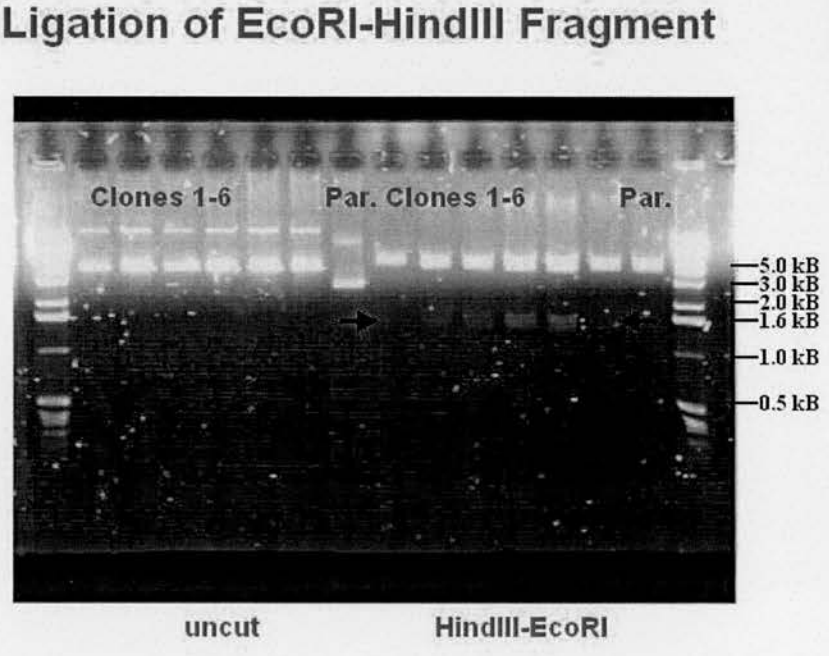

Figure 12. Ligation of EcoRI-HindIII fragment.
The parental clone and clones 1 to 6 are shown on the figure. The size difference between the uncut vectors is apparent. The HindIII-EcoRI digest excises the 1325 base pair inserted fragment in all 6 clones (In the case of clone 1 and 6 it is not clearly visible on the photo.) while the backbone of the vector is the same size as the linear parental clone confirming that all 6 clones are correct.

The NotI-SalI fragment was then excised and inserted into Kasal vector (Modified pUC8 vector in which the KasI-PvuII fragment was replaced by a 59 base pair polylinker sequence, obtained from Noboru H Komiyama.) to ablete the XhoI site present in the polylinker of pBlueIIKS (Figure 7 Step 7, Figure 15). The resulting

vector contained only one XhoI site into which the XhoI-neo-XhoI sequence could be inserted.

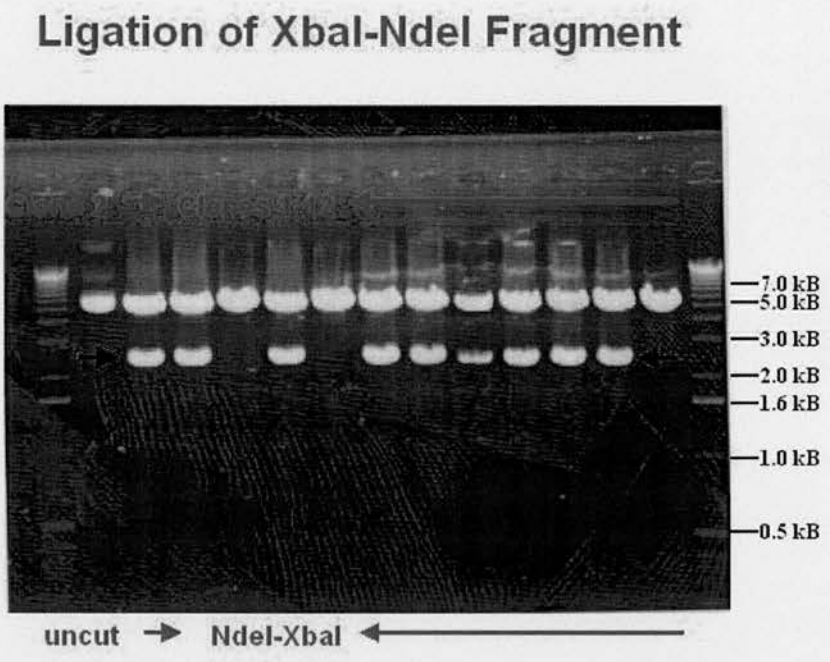

Figure 13. Ligation of XbaI-NdeI fragment.
Undigested vector DNA from clone 2 was run alongside the NdeI-XbaI digested DNA of clones 1 to 12. In the correct clones (1, 2, 4, 6, 7, 8, 9, 10 and 11) a 2443 base pair fragment could be visualized. In the incorrect clones only one band of ~ 5100 base pairs could be seen showing a lack of insertion.

Three colonies were picked from the bacterial plates and the DNA was checked using XhoI and NotI-SalI digest. XhoI digest linearised the correct clones giving a 9975 base pair band. When digesting with NotI-SalI the resulting smaller band was the same size as the band from the digested Kasal vector (~2350 base pairs). All three clones were correct.

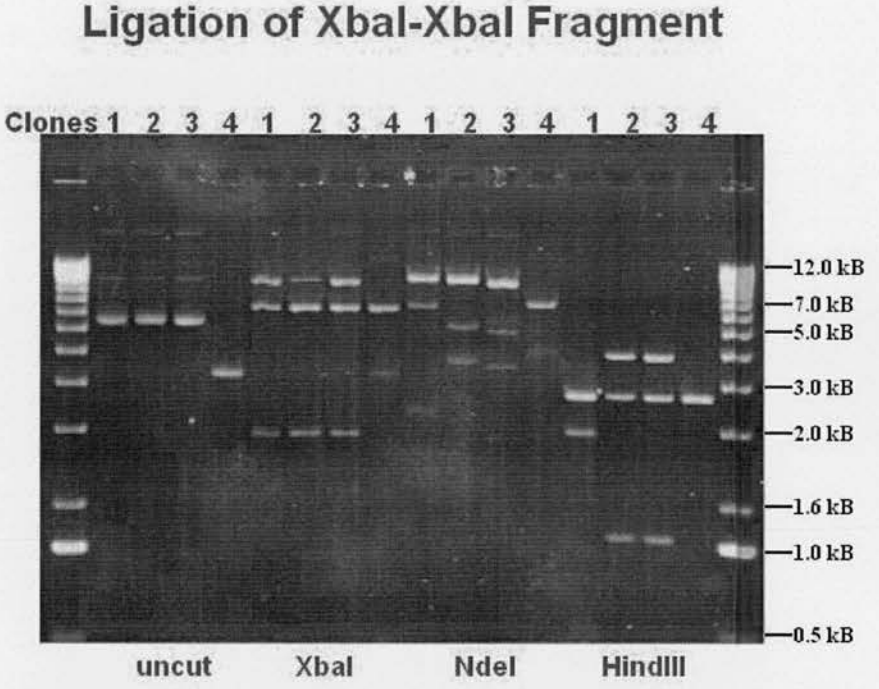

Figure 14. Ligation of XbaI-XbaI fragment.
The uncut DNA showed an apparent size difference between clones 1, 2 and 3 with the XbaI-XbaI fragment inserted and clone 4 without the insertion. The XbaI digest resulted in a 2993 base pair band and a backbone of 7601 base pairs in the case of the first 3 clones. In clone 4 I visualized the linearised vector DNA of 7601 base pairs. In all four clones there was residual undigested DNA that account for the extra bands.
The NdeI digest gave a 3295 base pair band (backbone 7299 base pairs) in clone 1 (correct orientation) and a 4584 base pair band (backbone 6010 base pairs) in clone 2 and 3 (incorrect orientation) and linearised clone 4. Undigested DNA could be seen too.
The HindIII digest resulted in a 3030 and a 3769 base pair HindIII-HindIII fragment in clone 1 (correct orientation). The backbone is 3795 base pairs therefore the gel photo showed a double band (top band). In clones 2 and 3 (incorrect orientation) a 1705 and a 3769 base pair HindIII-HindIII fragment and the 5120 base pair backbone was obtained.

The neo coding sequence flanked by two loxP sites was inserted at the XhoI site created by mutagenesis (Figure 7 Step 8, Figure 16a and b). Ten clones were screened using XhoI and XbaI digests. Clones 2, 6 and 9 were found positive with the neo-containing fragment inserted in the right orientation In the right orientation I visualized a 2993, a 4718 (containing the mutation site) and a 4231 base pair band (Figure 16a and b).

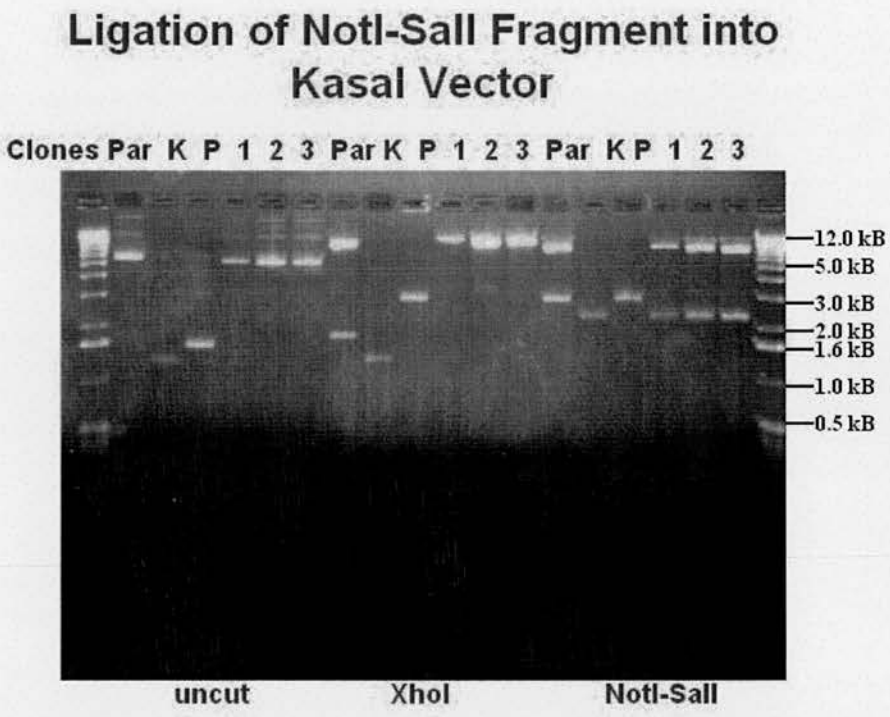

Figure 15. Ligation of NotI-SalI fragment.
The parental clone (Par), the Kasal vector (K), the pBlueIIKS (P) and the three clones are presented. The size difference between the uncut vectors is apparent.
In the parental clone the XhoI digest produced a 1725 base pair fragment and the backbone, Kasal vector was not affected and pBlueIIKS vector was linearised. In the correct clones (1, 2, 3) only one XhoI site remained resulting in one 9985 base pair band.
The NotI-SalI digest produced one visible band in the case of the Kasal and the pBlueIIKS vector. A 7633 base pair NotI-SalI band was dropped in the parental and the three positive clones while the smaller bands indicated the size difference between the two vectors (Kasal-2352 base pairs, pBlueIIKS-2961 base pairs).

The vector then was excised by NotI-SalI and inserted into DTA containing pBluescript vector, which was digested by NotI-XhoI (Figure 7 Step 9, Figure 17). This cloning step ablated the SalI site at the 3' end, but allowing linearization by NotI before ES cell targeting. Only one colony grew after transformation of the ligation mixture due to lower transformation efficiency resulting from the large plasmid size. The clone (pBlueDTA-DelValMut) proved to be positive.

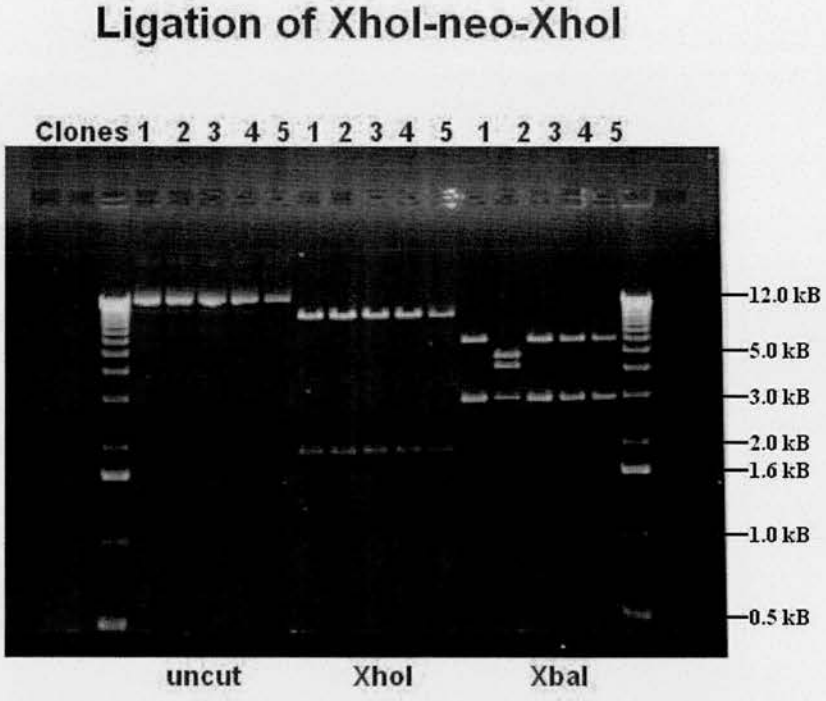

Figure 16a. Ligation of XhoI-neo-XhoI.
On the figure clones 1 to 5 are presented. If the neo-containing fragment was inserted, the XhoI digest resulted in a 1957 base pair band and the backbone (9985 base pairs) regardless of the orientation of the fragment. XbaI digest produced three bands in all clones. In the right orientation (clone 2) a 2993, a 4718 (containing the mutation site) and a 4231 base pair band was visualized. In clones where the fragment was inserted in the opposite orientation (1, 3, 4, 5) the three bands were of 2993, 2973 (containing the mutation site) and 5976 base pairs. In that case I saw only two bands, one of which was a double band.

The final vector (Figure 18) is 9590 base pairs (plus the 4 kB pBlue-DTA vector backbone) with a 3' homology arm of 2.3 kB and a 5' homology arm of 5.8 kB. It contains the DelValine mutation alongside with two sites created for further analysis (NheI, XhoI). The neo selection cassette is inserted at the XhoI site. The final clone pBlueDTA-DelValMut was further tested by SpeI, ClaI, NcoI, NheI and NdeI digests and was shown to be correct.

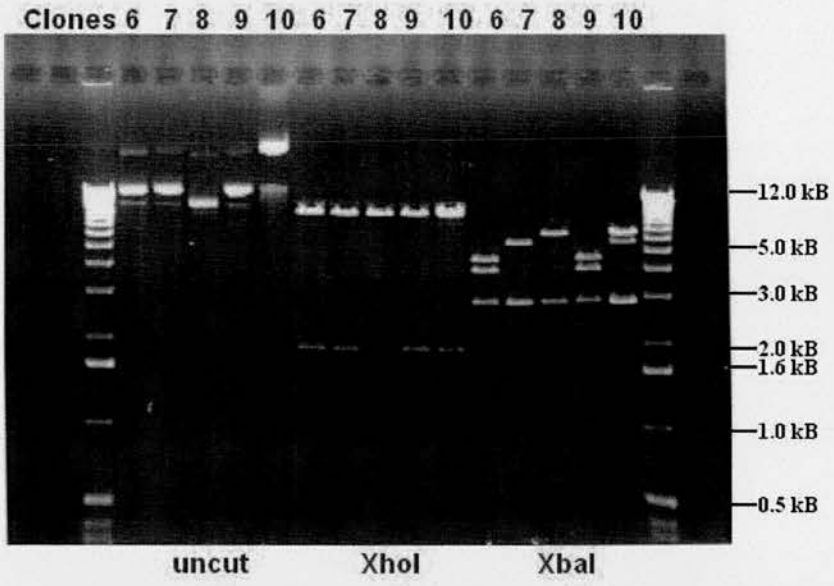

Figure 16b. Ligation of XhoI-neo-XhoI.
On the figure clones 6 to 10 are presented. The XhoI-neo-XhoI fragment wasn't inserted into clone 8 indicated by the presence of only one XhoI and only two XbaI sites. Digest patterns of clones 6 and 9 proved that the neo-containing fragment was inserted in the right orientation. Clone 7 contained the neo fragment in the opposite orientation. Clone 10 contained the desired fragment in the opposite orientation (double band in the case of XbaI digest was visualized), but the XbaI digest was incomplete resulting in an extra band.

The final vector was further screened by sequencing with primers DelVal 2, 3, 358, 3261, 6102, 6211, 6662, 7914, III and V to check whether the ligation junctions were correct and the mutation site was intact. The details of the sequencing reaction can be found in the materials and methods. Sequencing results revealed that the targeting vector was correct and ready for electroporation into embryonic stem cells.

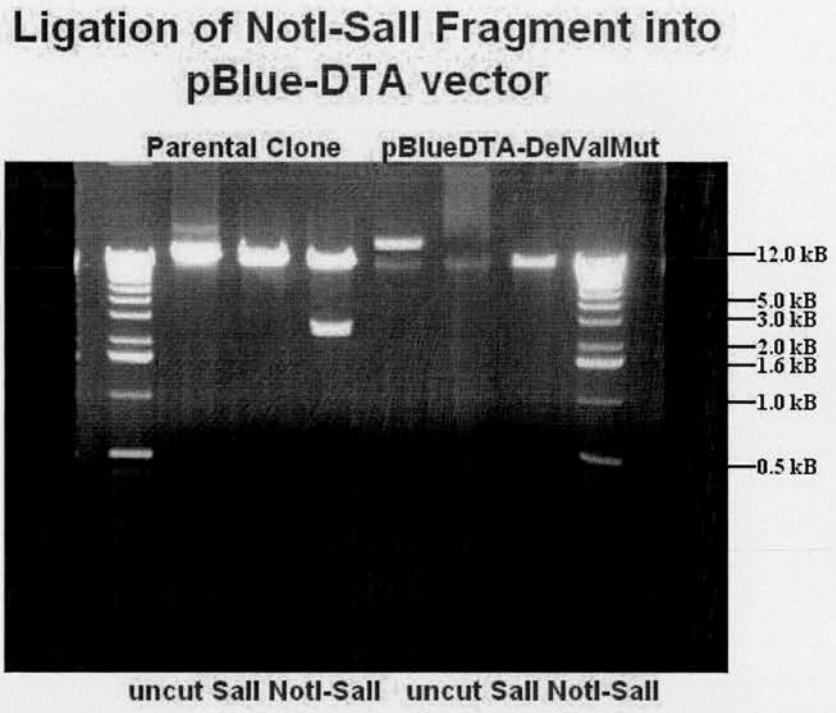

Figure 17. Insertion of the final targeting vector into DTA-containing pBluescript vector. The parental clone and clone pBlueDTA-DelValMut were digested by SalI and NotI-SalI. SalI digest only linearised the parental vector while NotI-SalI digest gave two bands in the parental clone, but only linearised the final vector, in which the SalI site was ablated.

ES cell targeting

The pBlueDTA-DelValine vector was electroporated into E14TG2a ES cells as described in detail in the materials and methods.

150μg of vector was linearised with NotI, precipitated, washed with 70% ethanol and resuspended in 100 μl PBS the night before electroporation. Passage number 10 E14TG2a cells (2.3×10^6) were grown up from frozen stock to yield about 5×10^7 cells, trypsinised and resuspended in a final volume of PBS that gave about $1X10^8$ cells/600 μl. The cells (passage 15, 5.4×10^7 in total) were electroporated at 0.8 kV, 3 μF (resulting in a time constant of 0.2 sec) in the gene pulsar and plated at a density of 5×10^6, 10^6, 5×10^5 and 10^5 cells per plate (21 plates in total).

G418 (200μg/ml) was added one day after electroporation and selection was continued for 10 days. About 200 neomycin-resistant colonies were picked and expanded. From the colonies 136 grew up and were transferred into 24 well plates for expansion. Duplicate plates were frozen for further expansion while the originals were used to obtain genomic DNA. Southern blotting with 3' and 5' external probes and an internal probe was used to screen the colonies.

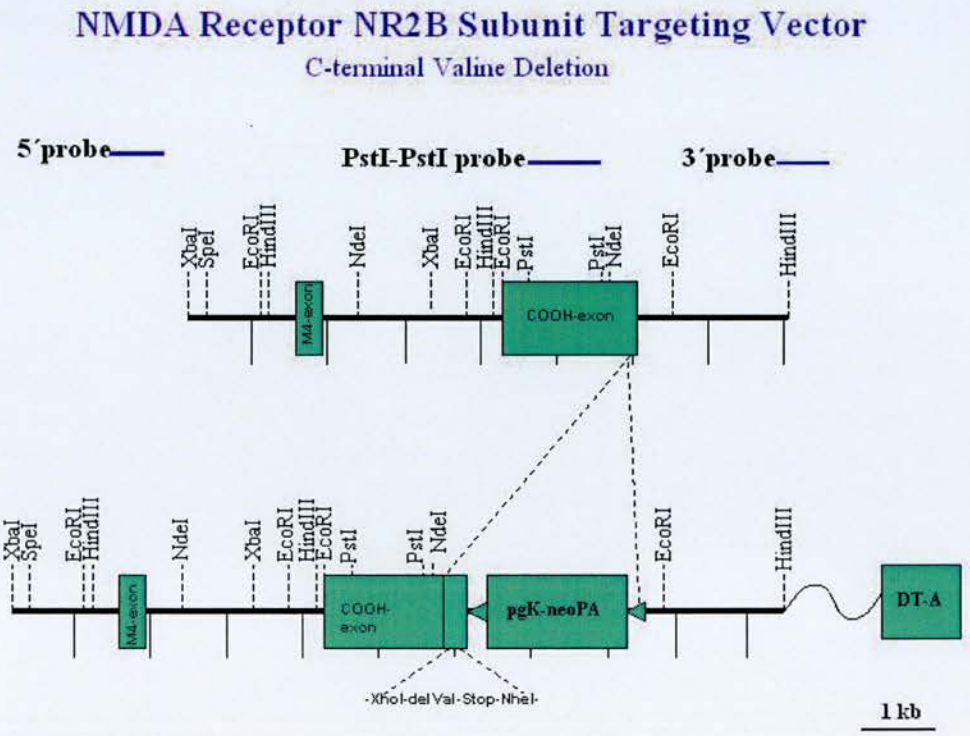

Figure 18. NR2B DelValine Targeting Vector.
In the final targeting vector the terminal valine was deleted and XhoI and NheI sites were created. PgK-neoPA selection cassette was inserted at the XhoI site. The 3' homology arm is 2.3 kB and the 5' homology arm is 5.8 kB. The targeting vector is ~10 kB.

Southern blots

The neo cassette contains XbaI and BglII sites, while the NheI site exists in the lines containing the mutation (created by mutagenesis). These restriction sites were used to screen the embryonic stem cell lines obtained after electroporation. First all ES

cell clones (136) were screened using the 3' flanking probe thereafter the positive ones were further checked using the internal and the 5' flanking probe.

The 3' probe was obtained by digesting subclone pNR2B-3' probe with HindIII-XbaI. The 569 base pair fragment was purified, labelled using Rediprime™ II random prime labelling system and used for probing the filter containing the genomic DNA samples as described in materials and methods. The 871 base pair PstI-PstI internal probe was obtained from subclone pNR2B-2.6 by digesting with PstI while the 5' flanking probe was amplified with Roche's Expand Long Template PCR system using 5' probe-1 and 2 primers (Find sequence information in the appendix.) and subclone pNR2B-13SacI as a template.

The wild type genomic DNA digested with XbaI and hybridised with the 3' probe gave a 5 kB band, while the mutant lines with correct homologous recombination yielded a 2.5 kB band (Figure 19).

In the first Southern Blots presented below 10 μg genomic DNA was digested with high concentration XbaI restriction enzyme and run on a 0.8% agarose gel. On each gel wild type genomic DNA was run alongside the ones to be screened. The samples were transferred onto nitrocellulose (Hybond™-N) and crosslinked to the filter using UV. The filter was prehybridized at 65 °C for 4 hours then probed at 65 °C overnight. After washing the filter it was wrapped in Sarah wrap, placed into a cassette with Kodak X-ray film over it and was left at –80 °C to expose.

A total of 39 ES cell clones were found positive using southern blotting with the 3' probe. This showed an initial 28.7% targeting efficiency. Clones 1-15, 3-3, 3-8, 3-10, 3-14, 5-18, 6-8, 7-1, 7-11, 7-14, 7-16, 8-4, 8-8, 9-17, 9-20 and 12-11 were chosen for further characterization. In the following figures those southern blots are demonstrated alongside with the gel photos, which contained the above clones.

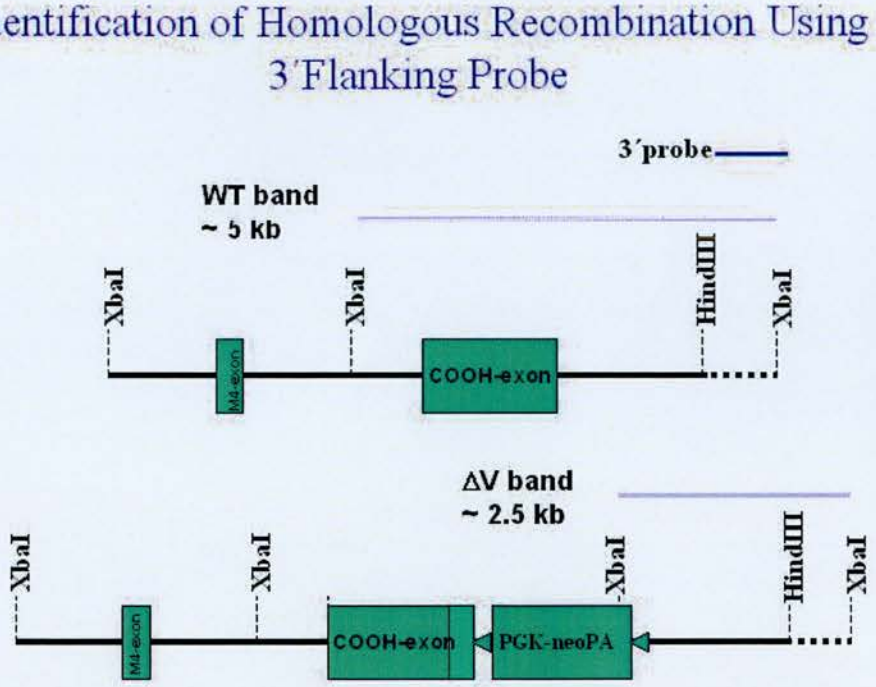

Figure 19. Southern Blot Using 3' Flanking Probe.
From all the clones picked 136 were screened to check correct homologous recombination using XbaI digest and the 3' flanking probe. The XhoI-neo-XhoI cassette inserted contains an XbaI site due to which a 2.5 kB band can be visualized in the positive clones alongside the 5 kB wild type band.

If the gDNA was digested with BglII and probed with internal probe or the 5' probe, I got a ~14 kB band for WT clones and ~8 kB band for mutants with correct homologous recombination (Figure 24 and 25). When I used NheI digest and the internal probe, I again obtained a ~14 kB band for WT clones and ~8 kB band for mutants.

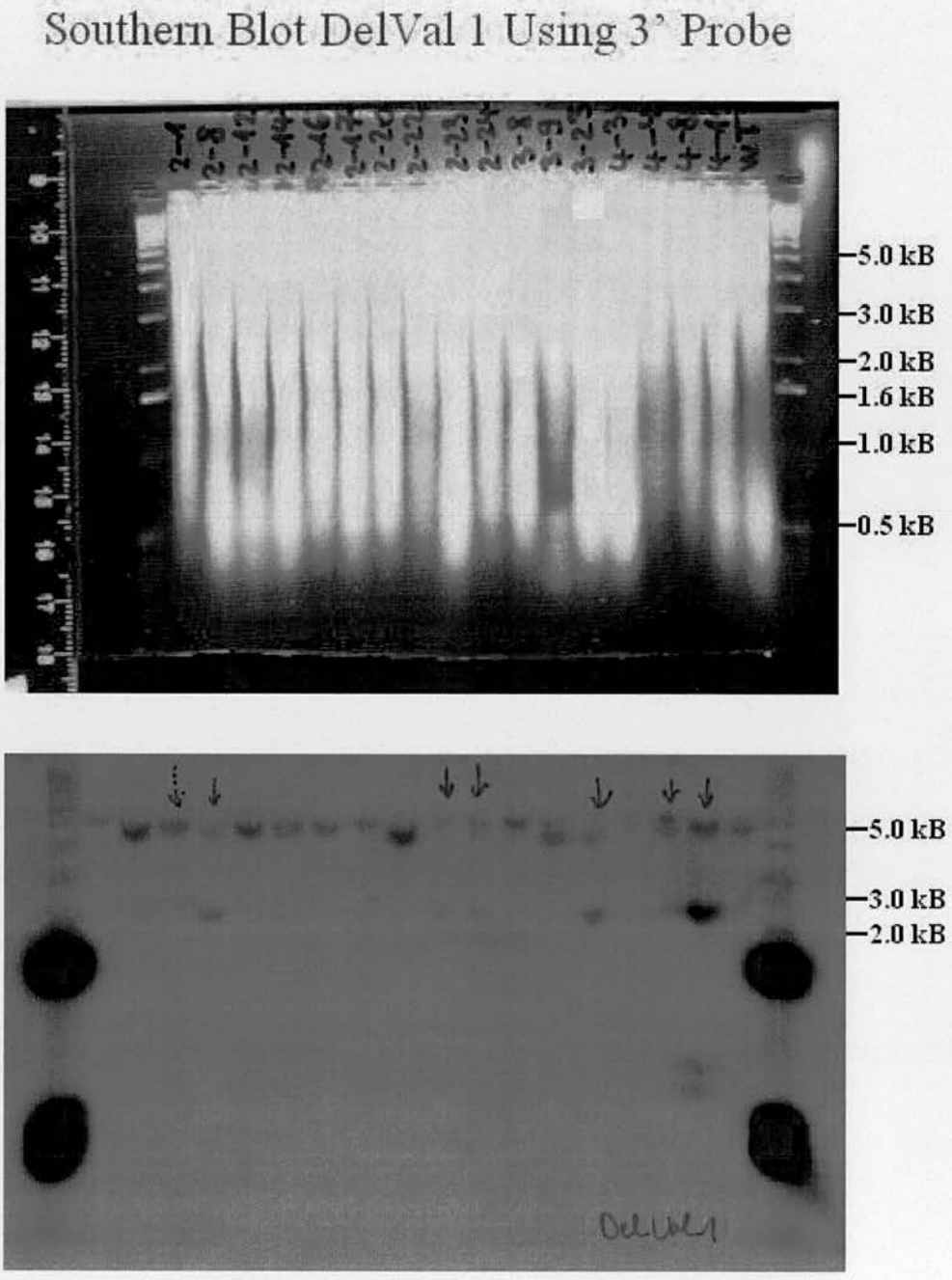

Figure 20. Southern Blot DelVal 1 using XbaI digest and the 3' probe.
The photo on the top is the gel picture, while the one at the bottom is the blot after exposure. The ES cell clones are indicated on the top.
After digesting with XbaI and probing with the 3' probe I obtained a 5 kB wild type and a 2.5 kB homozygous band in the correct clones. 3' positive clones are 2-12, 2-14, 2-24, 3-8, 4-3, 4-8 and 4-11.

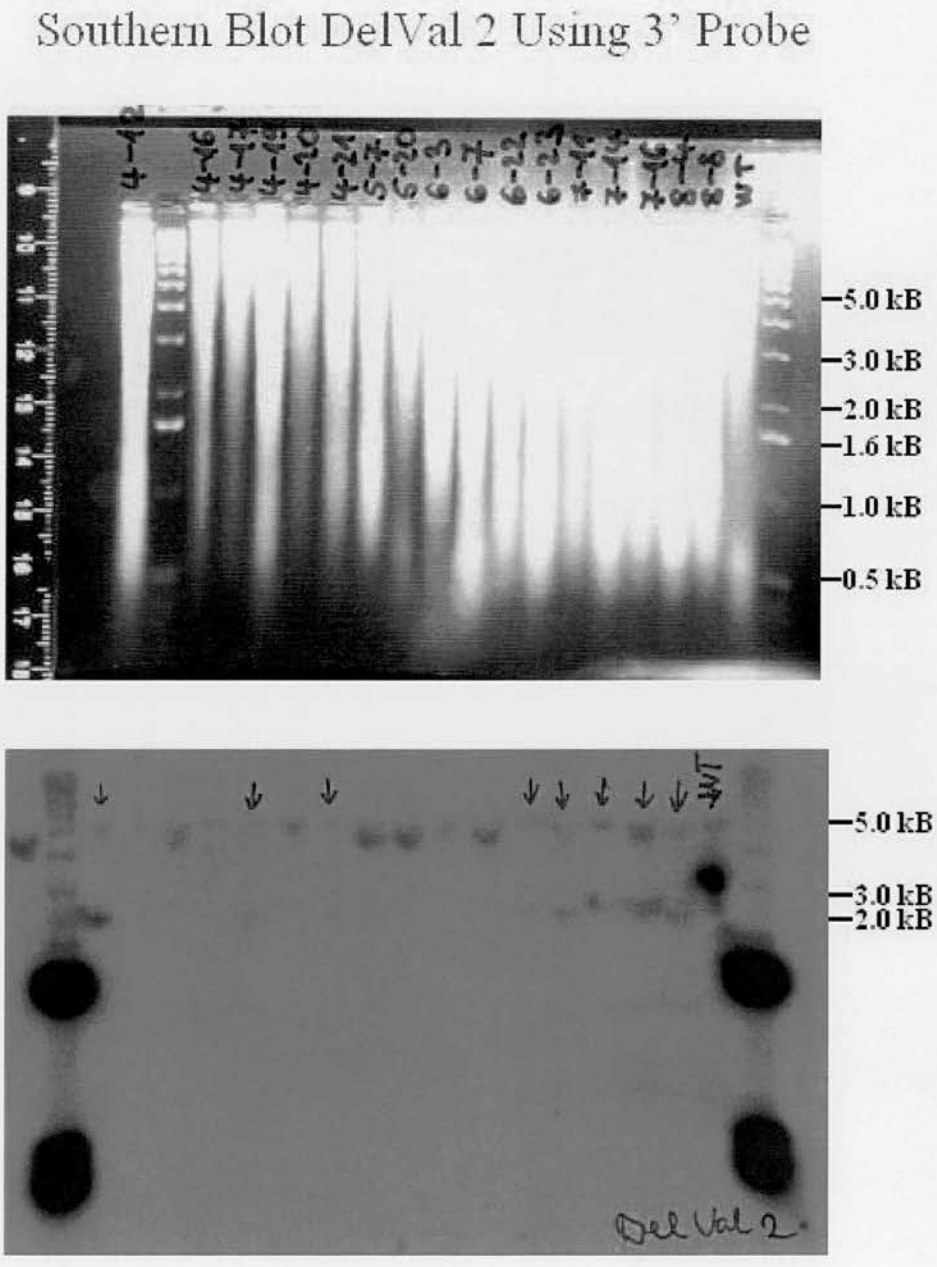

Figure 21. Southern Blot DelVal 2 using XbaI digest and the 3' probe.
The photo on the top is the gel picture, while the one at the bottom is the blot after exposure.
The ES cell clones are indicated on the top.
3' positive clones are 4-16, 4-21, 5-20, 7-11, 7-14, 7-16, 8-4 and 8-8.

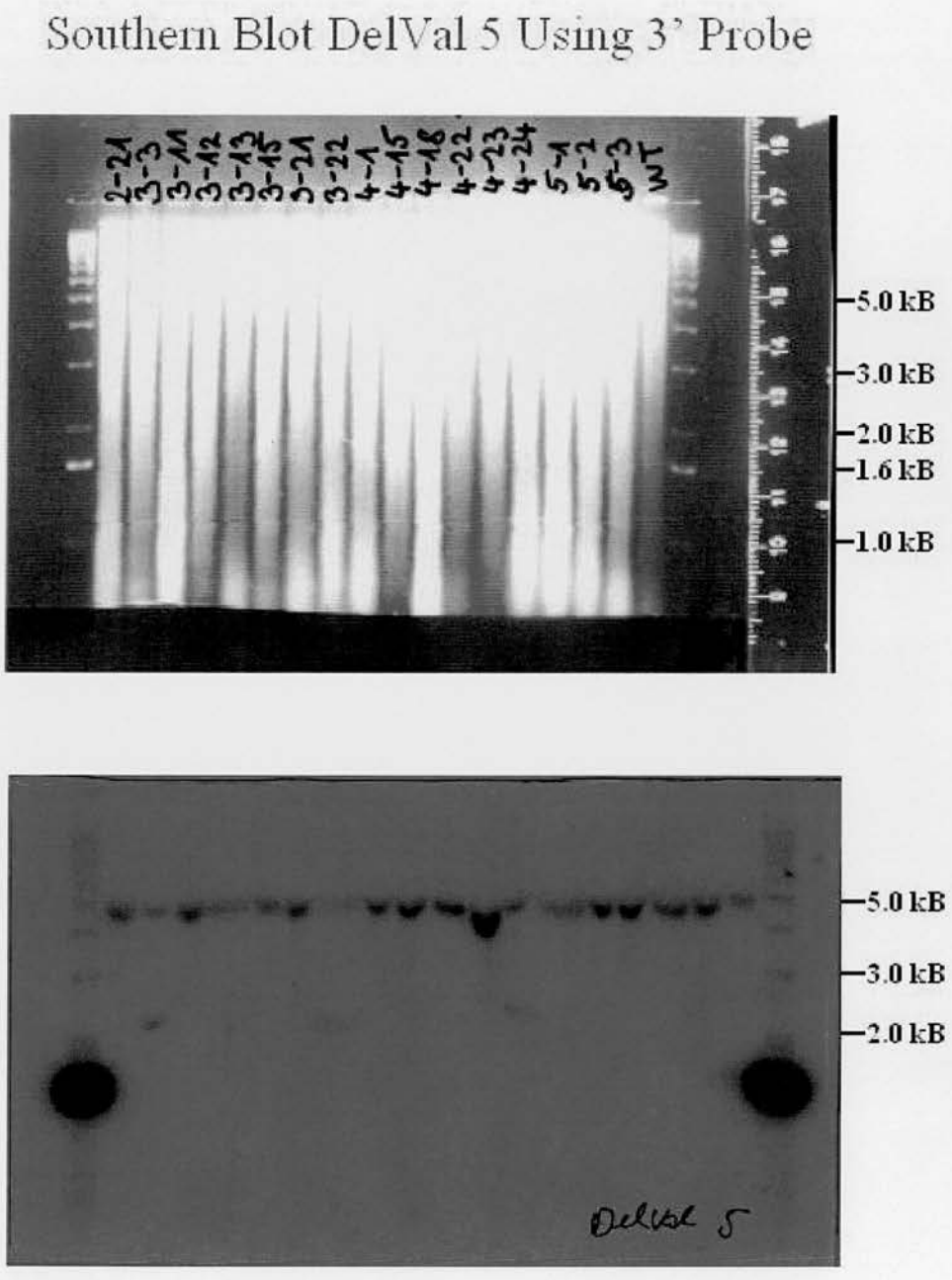

Figure 22. Southern Blot DelVal 5 using XbaI digest and the 3' probe.
The photo on the top is the gel picture, while the one at the bottom is the blot after exposure.
The ES cell clones are indicated on the top.
3' positive clones are 3-3 and 4-22.

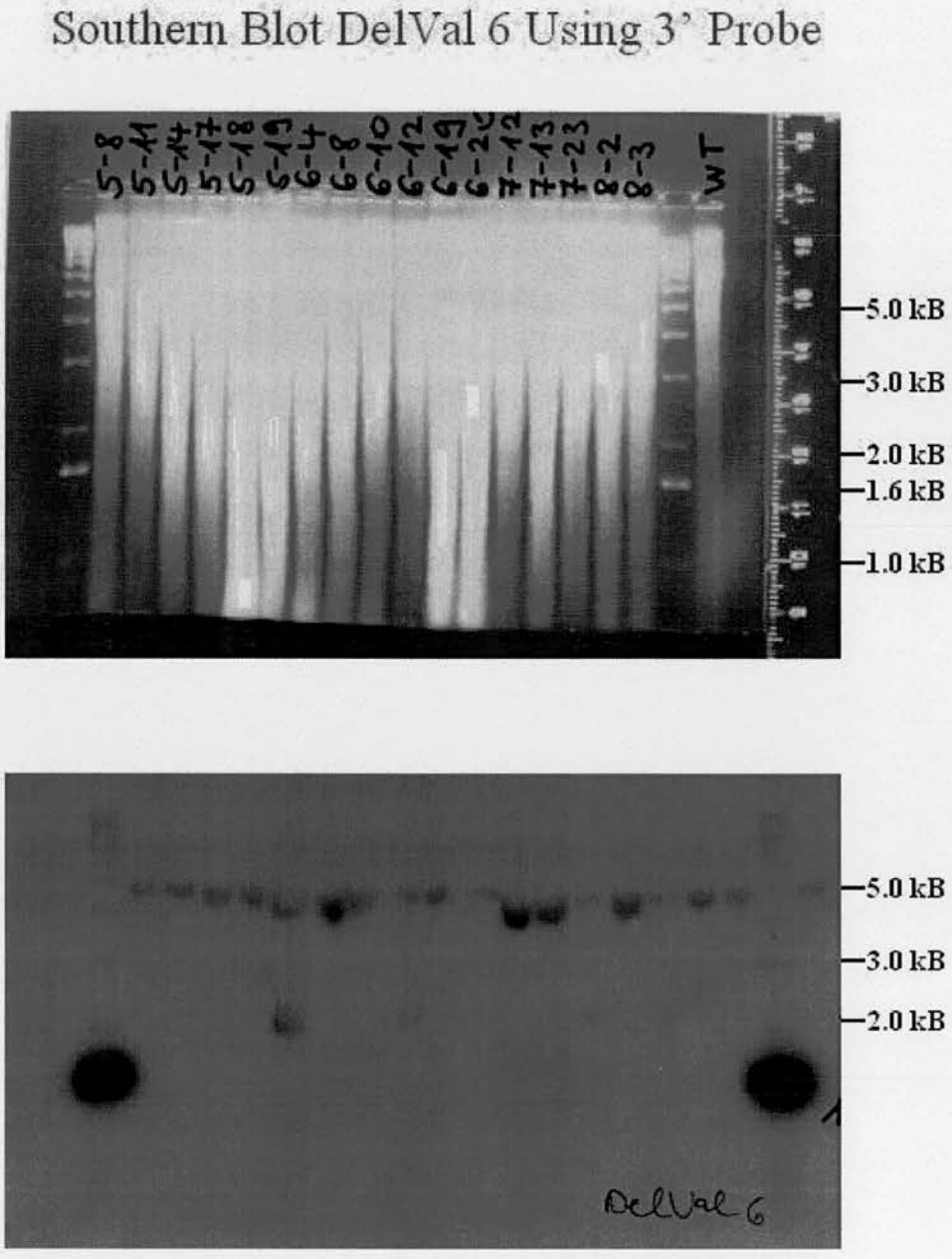

Figure 23. Southern Blot DelVal 6 using XbaI digest and the 3' probe.
The photo on the top is the gel picture, while the one at the bottom is the blot after exposure.
The ES cell clones are indicated on the top.
3' positive clones are 5-18, 6-8, 7-12, 7-23 and 8-2.

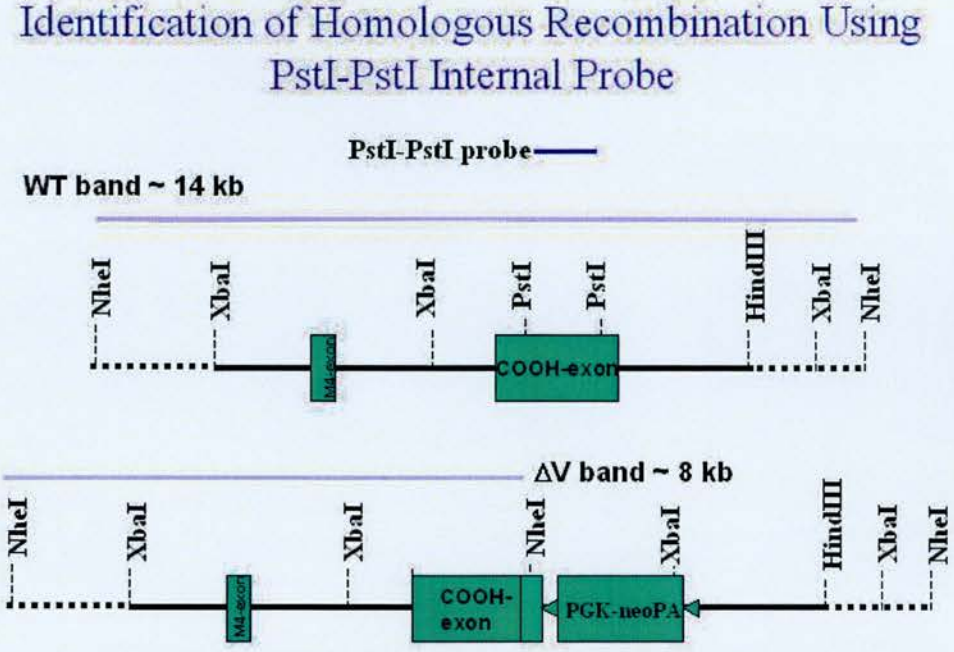

Figure 24. Southern Blot Using Internal Probe.
I used BglII digest when screening with the PstI-PstI internal probe. Due to the existence of the extra BglII sites in the neo cassette I could visualize an 8 kB mutant band alongside the 14 kB wild type band in the correct clones.

10 μg genomic DNA was digested with high concentration BglII or NheI restriction enzyme and run on a 0.75% agarose gel. On each gel wild type genomic DNA was run alongside the ones to be screened. The samples were transferred onto nitrocellulose (Hybond^{TM}-N), crosslinked to the filter using UV, prehybridized, probed, placed into a cassette with Kodak X-ray film and exposed in the same manner as in the case of the 3' probe. Cell lines DelVal 3-3, 5-18, 7-11, 7-14 and 8-8 were identified correctly targeted clones. The gel photos can be seen alongside the Southern Blots below. The cells were then expanded and used for producing chimaeric mice. In the following figures southern blots (of the positive clones) using the internal probe and the 5' probe are demonstrated alongside with the gel photos.

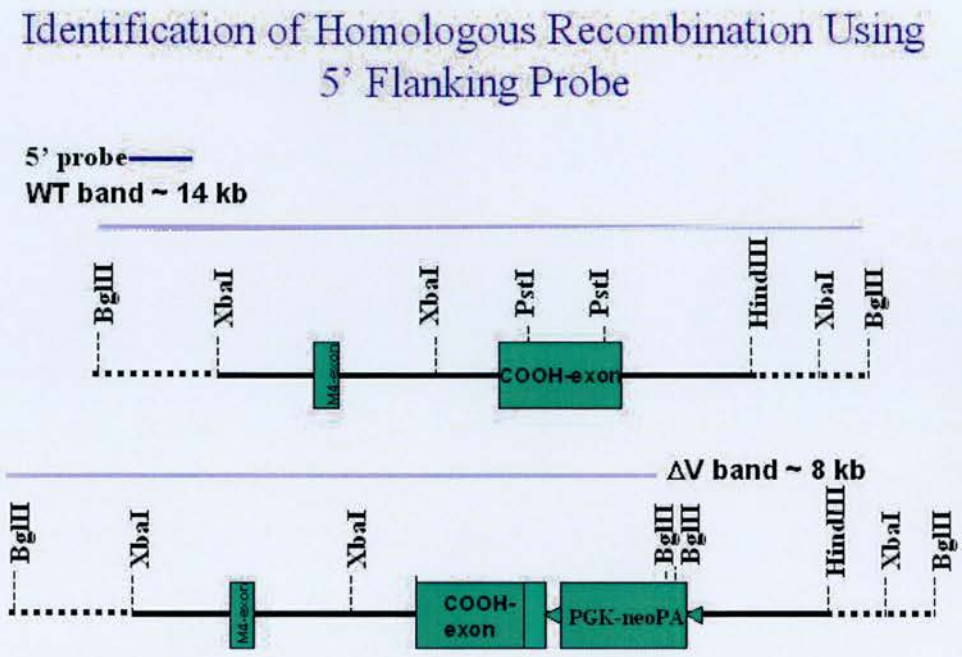

Figure 25. Southern Blot Using 5' Flanking Probe.
Clones 1-15, 3-3, 5-18, 7-11, 7-14, 7-16, 8-4 and 8-8 were screened using BglII digest and the 5' probe amplified by PCR reaction. Correct clones contained two BglII sites at the 3' end of the XhoI-neo-XhoI insert therefore I could visualize an 8 kB mutant band alongside the 14 kB wild type band.

The clones were further checked using BglII and NheI (Figure 32 and 33) restriction digests to confirm that the mutation site is correct and that the neo cassette is inserted. Genomic DNA obtained from the ES cells was used as a template for PCR reactions to amplify fragments containing either the NheI site created by mutagenesis or the BglII sites inserted with the neo cassette. Two sets of primers were used to amplify the two fragments, the first DelVal 5603 and pLox 91, the second pLox 1603 and DelVal 6215. The amplified fragments (650 and 430 base pairs respectively) were purified and digested with NheI and BglII respectively. If the mutation site was intact the NheI restriction digest yielded two bands (~560 and ~90 base pairs) and although the smaller band was not visible I could see the size difference between the uncut 650 base pair band and the NheI digested 560 base pair band (Figure 33). If the neo cassette was inserted correctly then due to the extra BglII sites I got two bands (~320 and ~110 base pairs) when running the samples on the agarose gel (Figure 32).

Southern Blot DelVal Internal Probe 3

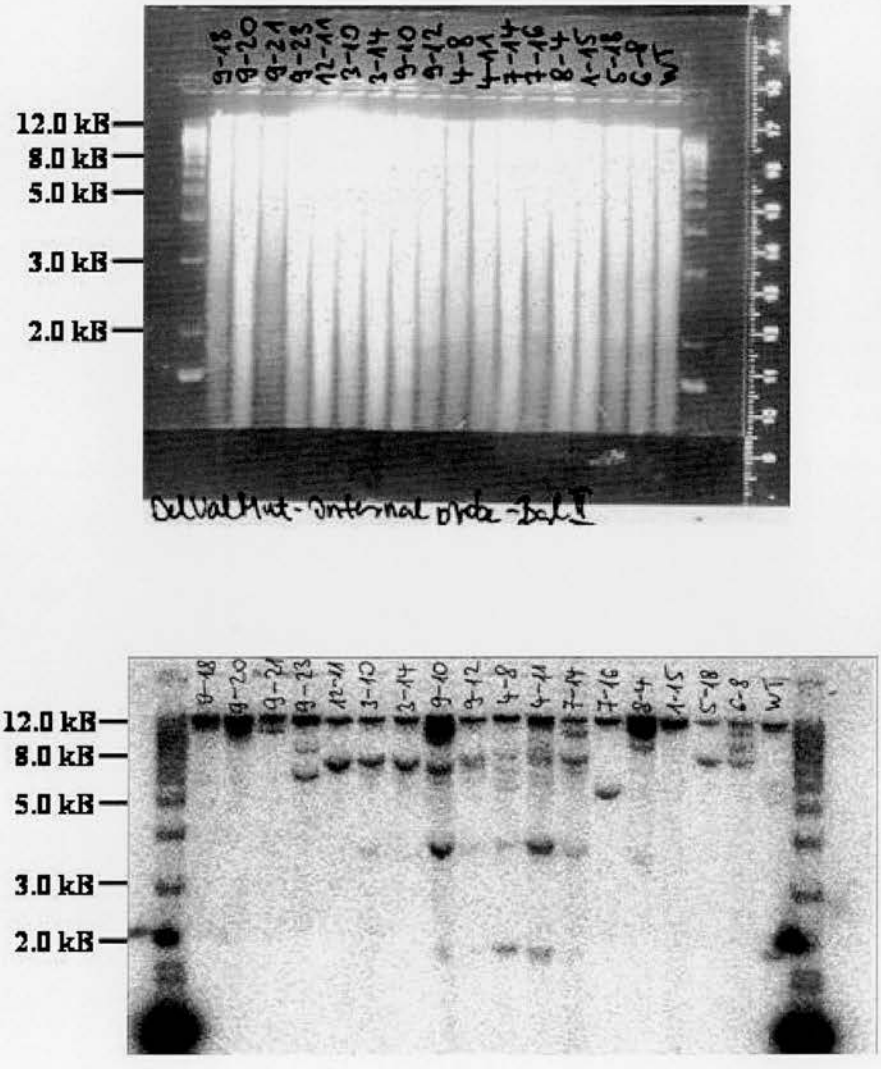

Figure 26. Southern Blot Internal Probe 3 using BglII digest and the PstI-PstI Probe.
The photo on the top is the gel picture, while the one at the bottom is the blot after exposure. The ES cell clones are indicated on the top.
Clones 7-14 and 5-18 are positive using the internal probe and tested positive in further experiments as well. In the case of the 3' probe positive clone 1-15 I only obtained a wild type band. 3' positive clones 7-16, 8-4, 6-8 didn't give a conclusive result due to the quality of the blot (possible degradation or contamination) and were tested again. Clone 9-20 was confirmed wild type and used in later experiments as additional control.

Southern Blot DelVal Internal Probe 5

Figure 27. Southern Blot Internal Probe 5 using BglII digest and the PstI-PstI Probe.
The photo on the top is the gel picture, while the one at the bottom is the blot after exposure. The ES cell clones are indicated on the top.
Clones 3-3 and 5-18 are positive using the internal probe. In the case of the 3' probe positive clone 1-15 I only obtained a wild type band.
Please note that the gel was "wavy" possibly due to uneven pressure when transferring the gDNA to the nitrocellulose membrane. Also the amount of gDNA transferred varied. However the mutant bands and the wild type bands are clearly visible and are the right size.

Southern Blot DelVal Internal Probe 17

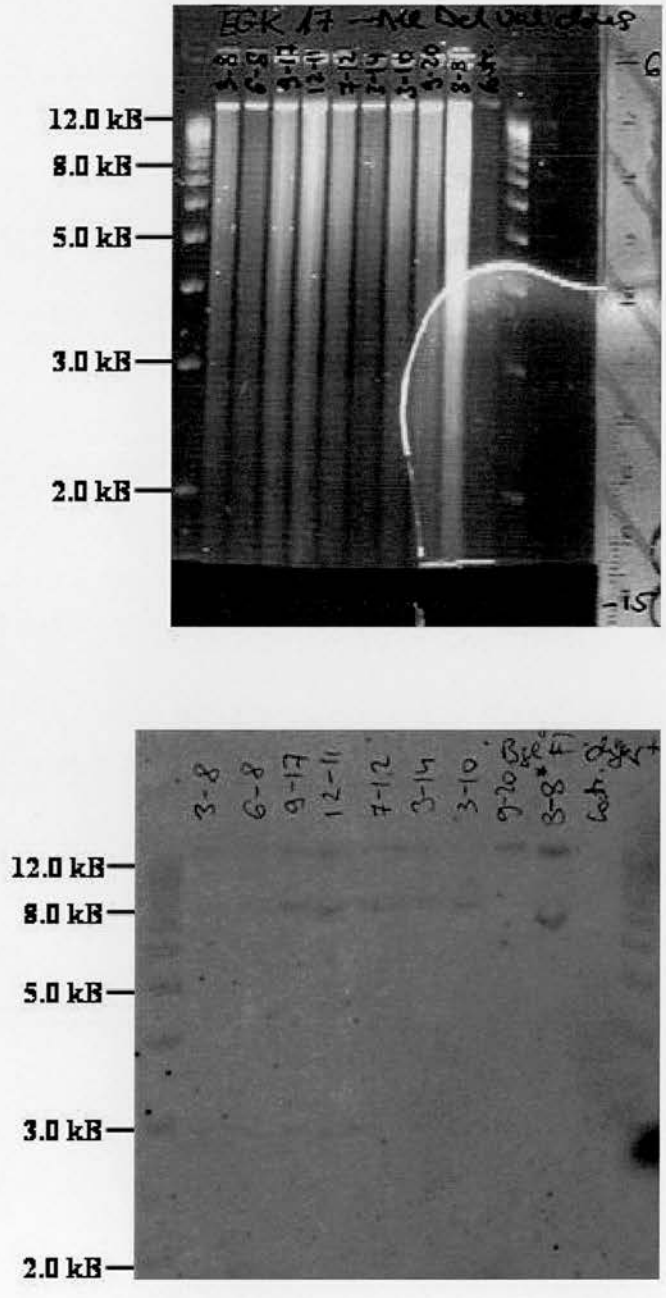

Figure 28. Southern Blot Internal Probe 17 using BglII digest and the PstI-PstI Probe.
The photo on the top is the gel picture, while the one at the bottom is the blot after exposure. The ES cell clones are indicated on the top.
Clones 3-8, 6-8, 9-17, 12-11, 7-1, 3-14, 3-10 and 8-8, which seemed correct in previous experiments but had to be retested to further confirm, showed positive using the internal probe. Clone 9-20 was confirmed wild type in previous experiments and was used here as an additional control.

Southern Blot DelVal 9 Using 5' Probe

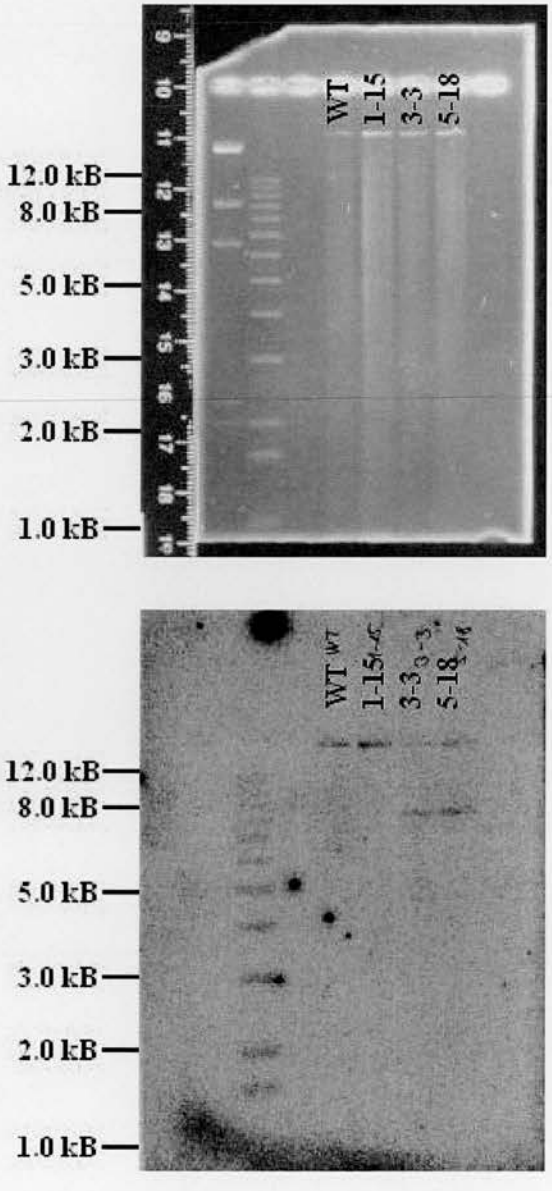

Figure 29. Southern Blot DelVal 9 using BglII digest and the 5' probe.
The photo on the top is the gel picture, while the one at the bottom is the blot after exposure.
The ES cell clones are indicated on the top.
5' positive clones are 3-3 and 5-18.

Southern Blot DelVal 11 Using 5' Probe

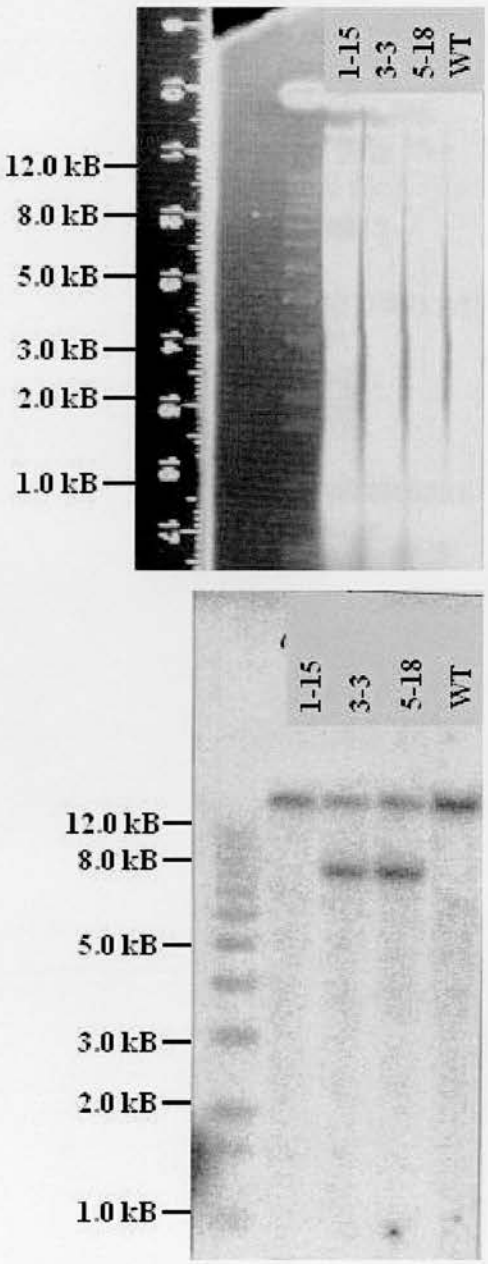

Figure 30. Southern Blot DelVal 11 using BglII digest and the 5' probe.
The previous blot was repeated to visualize the bands better.
5' positive clones are 3-3 and 5-18.

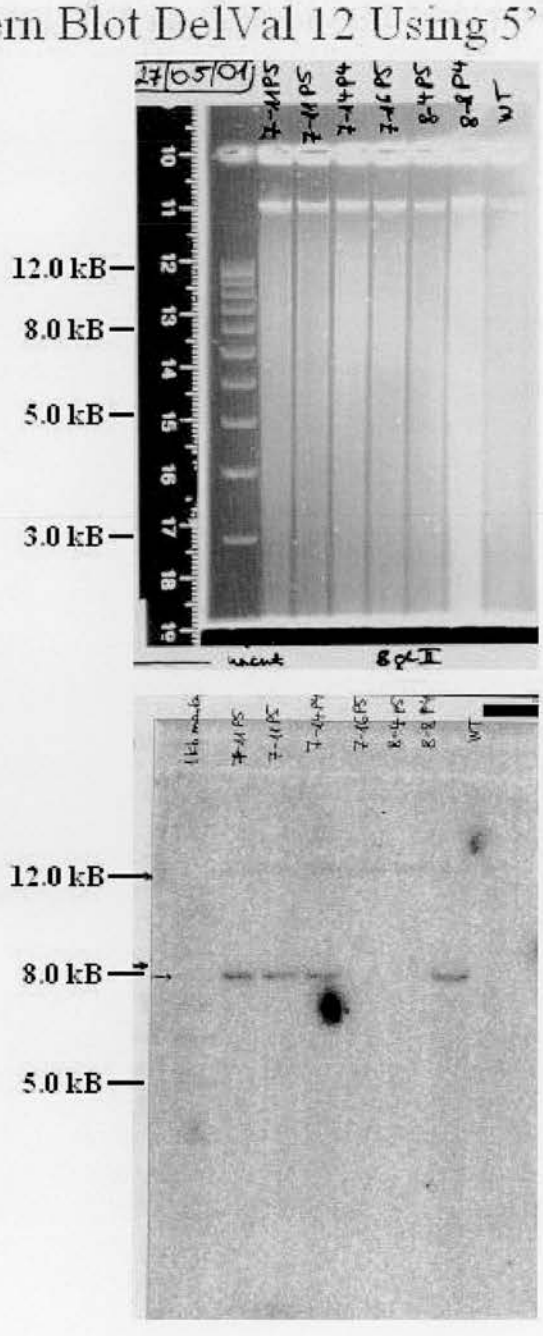

Figure 31. Southern Blot DelVal 9 using BglII digest and the 5' probe.
The photo on the top is the gel picture, while the one at the bottom is the blot after exposure. The ES cell clones are indicated on the top (Clone 7-11 is represented twice, the sample in the second lane was digested overnight and then further until the afternoon after adding extra 1µl BglII enzyme, the sample in the first lane was only digested from the morning until the afternoon.).
5' positive clones are 7-11, 7-14 and 8-8.

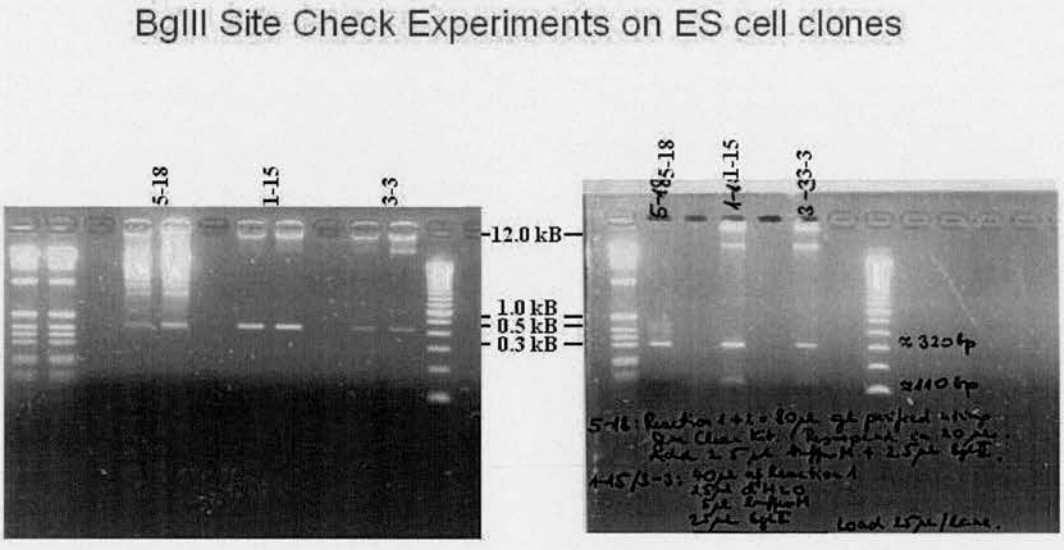

Figure 32. BglII site check experiment on ES cell clones 1-15, 3-3 and 5-18.
On the left the result of the PCR amplification is presented. Using primers pLox 1603 and DelVal 6215 a 431 base pair fragment is amplified.
If the neo cassette was inserted correctly then due to the two extra BglII sites (very close to each other) I got two bands (~320 base pairs and ~110 base pairs) when digesting the 431 base pair purified fragment with BglII restriction enzyme. This is represented on the gel photo to the right.

Generation of chimaeras

Clones DelVal 3-3, 5-18, 7-14 and 8-8 were injected into blastocysts to generate chimaeras (Table 4). The targeted embryonic stem cells (E14TG2a isolated from the light coloured 129 P2/Ola Hsd mouse strain) carrying the mutation in one chromosome were injected into blastocyst-stage embryos obtained from black mice (C57Bl/6). Upon survivor the cells assimilated into the inner cell mass of the embryos and participated in the formation of the chimaeric mice (mice containing cells from two different strains). The microinjections were carried out by Jane Robinson, our chief technician.

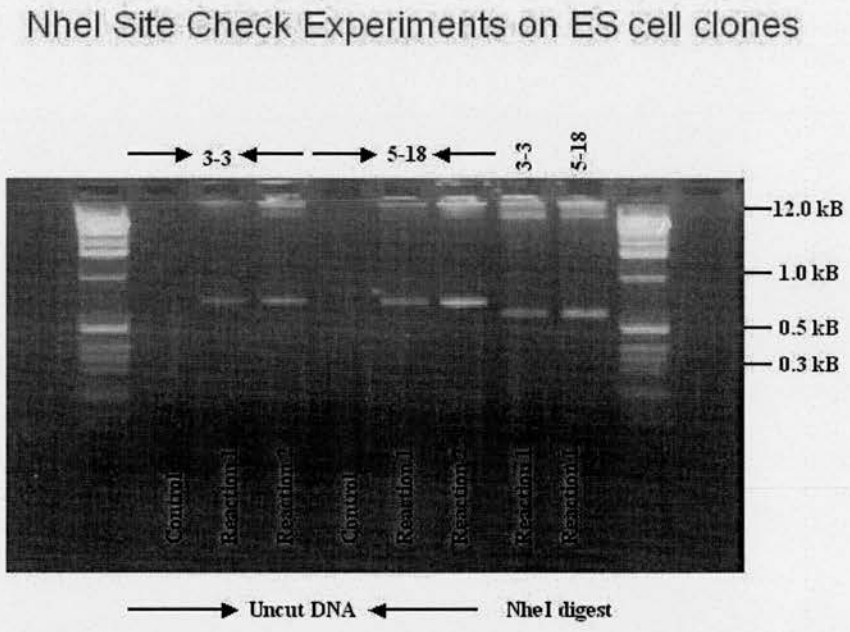

Figure 33. NheI site check experiment on ES cell clones 3-3 and 5-18.
On the figure the result of the PCR amplification and that of the NheI digest is presented. Using primers DelVal 5603 and pLox 91 a ~650 base pair fragment is amplified.
If the mutation site was intact an NheI site was present in the fragment. By digesting with NheI restriction enzyme I got two bands (~560 base pairs and ~90 base pairs) and although the smaller band was not visible I could see the size difference between the uncut 650 base pair band and the NheI digested 560 base pair band. This is represented on the gel photo to the right.

The first round of injections was done in September 2001 using clone DelVal 5-18 (Table 4). Four male and one female chimaeras were born from which three males survived. They were all mated with two females from the MF1 strain (Find in detail in section 2C.) each to check germline transmission. When cells that were injected contributed to the formation of the reproductive cells of the chimaeric mouse then germline transmission occurred. The event is indicated by the silver fur colour of the heterozygous offsprings. These mice from the test crosses were then intercrossed to produce homozygous mice containing the desired mutation in both chromosomes. The first three chimaeras didn't give germline transmission.

Date	Cell Line	Embryos Injected	Transfers	♀/♂ Chimaeras	Germline Transmission
25.06.01.	DelVal 5-18		1	None	
27.06.01.	DelVal 5-18	29	3	None	
03.07.01.	DelVal 5-18	14	1	None	
04.07.01.	DelVal 5-18	29	2	1 Male	
10.07.01.	DelVal 5-18	26	2	None	
11.07.01.	DelVal 5-18	29	3	1 Male 1 Female	
17.07.01.	DelVal 5-18	32	3	2 Male	
18.07.01.	DelVal 5-18	13	1	None	
18.10.02.	DelVal 3-3	4	1	None	
24.10.02.	DelVal 5-18	6	1	None	
08.11.02.	DelVal 8-8	16	2	1 Male 3 Female	25.02.03.
22.11.02.	DelVal 8-8	7	1	None	
28.11.02.	DelVal 5-18	14	1	None	
29.11.02.	DelVal 7-14	15	1	None	
23.01.03.	DelVal 7-14	21	2	None	
24.01.03.	DelVal 7-14	13	1	None	
29.01.03.	DelVal 8-8	12	1	None	
30.01.03.	DelVal 8-8	14	1	None	
05.02.03.	DelVal 8-8	24	2	None	
06.02.03.	DelVal 8-8	21	1	None	
17.07.03.	DelVal 7-14	12	1	2 Male	
17.07.03.	DelVal 5-18	11	1	2 Male	
18.07.03.	DelVal 5-18	13	1	None	

Table 4. Blastocyst injections of DelValine clones.
On the figure the date of injection, the cell line, the number of embryos injected, the number of recipients into which the embryos were injected and the sex of the resulting chimaeras is presented.
Three male and one female chimaeras were obtained from cell line DelVal 5-18, one male and three female chimaeras from cell line DelVal 8-8 and two male chimaeras from cell line DelVal 7-14. Germline transmission was achieved from cell line DelVal 8-8.

These injections were performed in the Centre for Genome Research, where the tissue culture and animal house facilities were well established. The second round of injections was postponed until the unproven facilities at the Department of Neuroscience were tried out and the animal house was set up. Unfortunately this took longer time than originally estimated and prevented any further injections from being performed for more than one year.

The second set of injections was done in April 2002, which produced no chimaeras. The third set of injections in October-November 2002 produced one male and three female chimaeras from the cell line DelVal 8-8 (Table 4). Further two male chimaeras were obtained from cell line DelVal 7-14 and another two from cell line 5-18 from injections done in July 2003. As a total 375 embryos were injected with cell lines DelVal 3-3, 5-18, 7-14 and 8-8 and used in 26 transfers from which only 13 chimaeras were obtained. This low efficiency was observed when injecting other clones produced in the laboratory as well.

Germline transmission

The male chimaera from the cell line DelVal 8-8 was set up with two MF1 female mice and germline transmission was achieved on 25th February 2003 which was indicated by the silver fur colour of the litter.

The offsprings were genotyped using three different combinations of primers NR2B 5910, pLox 413, pLox 1540 and NR2B 6456 with *Qiagen Hot Star Taq*. The different primer combination used amplified different sizes of bands or none (Figure 34) in wild type or heterozygous mice. These same reactions were later used to genotype the offsprings coming from the heterozygous-heterozygous intercrosses producing homozygous mice. Alternatively a reaction with *Long Range PCR* using primers NR2B 5910 and NR2B 6456 could be used (Figure 34).

After obtaining the initial information about the genotype of the mice, new primers were designed to get a larger band that is easier to visualize when using the AXB and CXD combination. Hence primers A' (SWAP NR2A 3924), B' (pLox 91), C' (pLox

1603) and D' (NR2B 8035) were used instead of A, B, C and D (Figure 34) when regenotyping mice W1-10 and R1-6 (Figure 35 and 36). These mice are the offsprings of chimaera DelVal 8-8 from the first two litters. In the next figures the gel photos of the genotyping reaction can be seen.

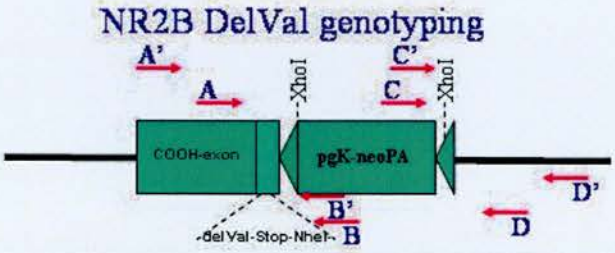

Genotype / Primers and PCR reaction	Wild Type	Heterozygous	Homozygous
A X B **Taq polymerase**	NO AMPLIFICATION	~ 0.5 KB BAND AMPLIFIED	~ 0.5 KB BAND AMPLIFIED
A' X B' **Taq polymerase**	NO AMPLIFICATION	~ 2.3 KB BAND AMPLIFIED	~ 2.3 KB BAND AMPLIFIED
C X D **Taq polymerase**	NO AMPLIFICATION	~ 0.5 KB BAND AMPLIFIED	~ 0.5 KB BAND AMPLIFIED
C' X D' **Taq polymerase**	NO AMPLIFICATION	~ 2.0 KB BAND AMPLIFIED	~ 2.0 KB BAND AMPLIFIED
A X D **Taq polymerase**	~ 0.5 KB wt BAND AMPLIFIED	~ 0.5 KB wt BAND AMPLIFIED	NO AMPLIFICATION
A X D **Long Template PCR**	~ 0.5 KB wt BAND AMPLIFIED	~ 0.5 KB wt AND 2.3 KB homo BAND AMPLIFIED	~ 2.3 KB homo BAND AMPLIFIED

Figure 34. NR2B DelValine Genotyping.
Primers A: NR2B 5910 B: pLox 413 C: pLox 1540 D: NR2B 6456.
In wild type mice AXB and CXD combination didn't result in amplification because of the lack of the neo cassette while the AXD combination gave a 546 base pair band (~0.5 kB). In the heterozygous offsprings a 642 base pair band was amplified in the AXB combination, a 546 base pair band in the AXD combination (~0.5 kB) and an extra 2346 base pair band using *Long Range PCR*. In homozygous mice (further described) I amplified a 642 base pair band in the AXB and a 734 base pair band in the CXD combination (~0.5 kB). The AXD combination produced a 2.3 kB homozygous band, but only using *Long Range PCR* since the Taq polymerase can't amplify that size fragment.
Primers A': Primer SWAP NR2A 3924 B': pLox 91 C': pLox 1603 D': NR2B 8035.
By using the *Qiagen Hot Star Taq* system and primer combination A'XB' I obtained a ~2.3 kB band in heterozygous and homozygous mice and no band in wild type mice while the primer combination C'XD' produced a ~2 kB band in heterozygous and homozygous mice and no band in wild type mice.

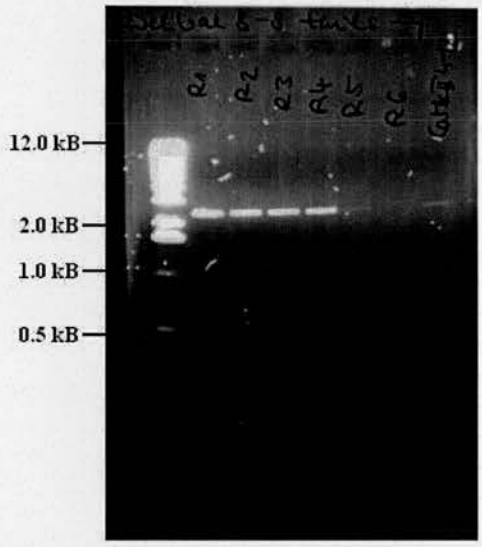

Figure 35. Genotyping of NR2B DelVal 8-8 tails coming from the chimaeraXMF1 test cross. Primers SWAP NR2A 3924 (A') and pLox 91 (B') were used in the PCR reaction. By using the *Qiagen Hot Star Taq* system I obtained a ~2.3 kB band in heterozygous mice and no band in wild type mice. Offsprings R1-5 were positive, heterozygous while R6 was negative, wild type.
The sample in the right side lane, CaMKII 4-12 is a positive control showing the ~2.3 kB band.

In the first litter of the DelVal 8-8 test cross two of the offsprings were heterozygous out of ten, in the second litter five out of six. Another thirteen heterozygous mice were obtained before the chimaera was found dead on the 12th September 2003 (Table 5.). None of the chimaeras from cell line DelVal 7-14 or 5-18 produced germline transmission and consequently were culled after producing several black litters.

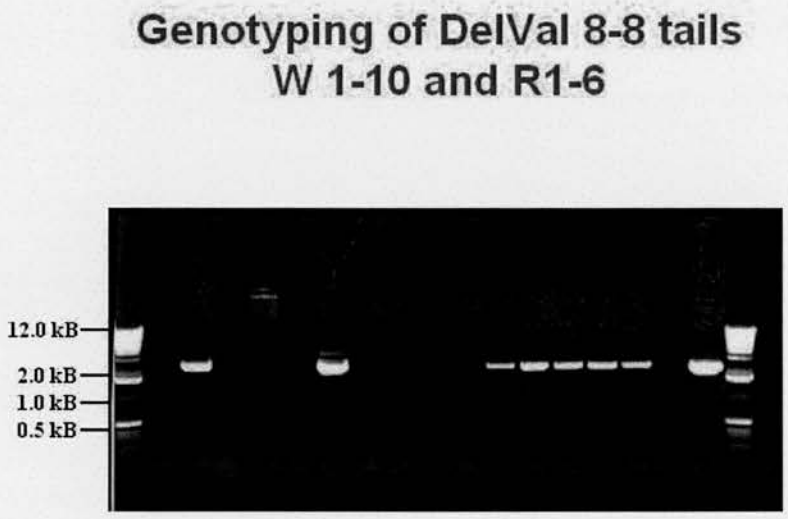

Figure 36. Genotyping of NR2B DelVal 8-8 tails coming from the chimaeraXMF1 test cross. Primers pLox 1603 (C') and DelVal 8035 (D') were used in the PCR reaction. By using the *Qiagen Hot Star Taq* system I obtained a ~2 kB band in heterozygous mice and no band in wild type mice. Offsprings W2 and 6, R1-5 were shown to be positive coinciding with previous genotyping results.
CaMKII 4-12 positive control is shown in the right side lane.

The first offsprings of the DelVal 8-8 chimaera were intercrossed to produce homozygous mice carrying the desired mutation in both chromosomes (Table 6). The genotyping was done using the same method as described before (Figure 34). On the next figure an example of the reactions using primers NR2B 5910 (A), pLox 413 (B), pLox 1540 (C) and NR2B 6456 (D) can be seen (Figure 37). Genomic DNA sample from mouse J9, which was tested homozygous in these reactions, was later used for screening with southern blot as well (Figure 38).

Date Set Up	Female	Date Litter Born	Litter	Heterozygous	Wild Type
09.01.03.	2XMF1	25.02.03.	10	1 Male 1 Female	3 Male 5 Female
		21.03.03.	6	2 Male 3 Female	1 Male
		30.04.03.	9	2 Male 2 Female	3 Male 2 Female
		10.06.03.	5	1 Male	4 Male
23.04.03.	2X129	19.05.03.	4	1 Male 2 Female	1 Female
26.05.03.	2XBl6	16.06.03.	12	2 Male 1 Female	4 Male 5 Female
		26.07.03.	3	None	3 Male
		01.08.03.	1	1 Female	None
		07.09.03.	9	1 Female	5 Male 3 Female

Table 5. Test cross of chimaera DelVal 8-8.
On the figure the date the crosses were set up, the strain of the female to which the chimaera was mated, the date the litters were born and their number, the number of heterozygous and wild type offsprings is presented.
Heterozygous offsprings were obtained by breeding the chimaera with all three female strains indicated. The males and females born from the first two litters (25.02.03. and 21.03.03. MF1 background) were mated to produce homozygous mice.

From cages 52, 53, 54, 70 and 71 25 homozygous, 73 heterozygous and 38 wild type offsprings were obtained. The homozygous mice were used for initial phenotypic characterization and further breeding. Another heterozygous female was set up with a Cre Deleter +/- male obtained from collaborator Dr Thomas J O'Dell to excise the neo selection cassette with further crosses. The male proved to be sterile and didn't produce any offsprings therefore the breeding was stopped. Due to a further relocation of the laboratory from the Centre for Neuroscience in Edinburgh to the Sanger Centre in Cambridge no further Cre Deleter mice were purchased and therefore no further breeding could be set up to excise the neo selection cassette. In table 6 the genotyping results of the various litters coming from the intercrosses are presented.

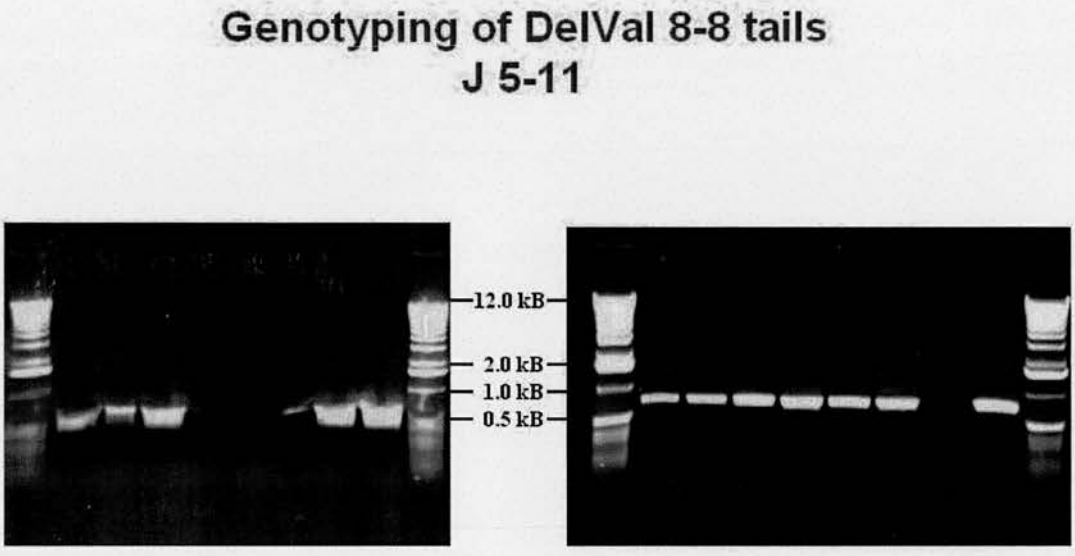

Figure 37. Genotyping of NR2B DelVal 8-8 tails coming from heterozygous intercross.
On the left results of the PCR reaction using primers NR2B 5910 (A) and NR2B 6456 (D), on the right using NR2B 5910 (A) and pLox 413 (B).
Using the AXD primer combination I got a 546 base pair band in wild type and heterozygous mice, while there is no amplification in homozygous mice (The *Qiagen Hot Star Taq* system cannot amplify the 2.3 kB homozygous band.). Using the AXB combination I didn't get amplification in wild type mice (lack of neo cassette) and obtained a 642 base pair band in heterozygous and homozygous mice. R1 heterozygous sample was presented for comparison.
By analysing the results I concluded that mice J5, 6 and 7 are heterozygous, mice J8, 9 and 10 are homozygous and mouse J11 is wild type.

Southern blot of DelValine homozygous mice

Genomic DNA from the tail and the liver of a homozygous mouse J9 was used to further check mutation by Southern Blot (Figure 38). The experiment was done in the same way as in the case of the embryonic stem cell lines (Find in detail in Section 2A.) Using the 3' probe for wild type genomic DNA I obtained the normal 5 kB band, using the ES cell genomic DNA of cell line DelVal 8-8 I obtain a 5kB wild type and a 2.5 KB homozygous band, while using the genomic DNA of the homozygous mouse obtained from tail or liver a single 2.5 kB band could be

visualised. This further proved the homozygosity of the particular mouse and that the genotyping reaction (by PCR) could be used in further mice.

Date	Male	Female	Litter Born	Litter	Homozygous	Heterozygous	Wild Type
26.05.03.	DelVal 8-8+/-	DelVal 8-8+/-	15.06.03.	5	1F	1M 2F	1M
cage 52			16.08.03.	9	2F	3M 3F	0
			10.12.03.	8 3 dead	0	4F	1F
			12.02.04.	2	0	1F	1F
26.05.03.	DelVal 8-8+/-	DelVal 8-8+/-	15.06.03.	5	1M 2F	1M	1M
cage 53			04.08.03.	8 1eaten	2M 1F	4F	1M
			25.08.03.	eaten			
			15.09.03.	13 1 dead	1F	4M 2F	2M 3F
			09.10.03.	10	1M 1F	4M 1F	2M 1F
			03.11.03.	9	1M 1F	3M 3F	1M
			29.11.03.	6	1F	2M 2F	1M
			18.12.03.	12	2F	2M 4F	2M 2F
			12.01.04.	7 2 dead	0	1M 1F	1M 2F
26.05.03.	DelVal 8-8+/-	DelVal 8-8+/-	07.07.03.	1 dead			
cage 54			07.10.03.	6	1F	1M 3F	1M
			17.11.03.	10	2M 1F	1M 2F	2M 2F
			31.12.03.	eaten			
27.05.03.	+/-Cre Deleter	DelVal 8-8+/-	None				
cage 55							
23.07.03.	DelVal 8-8+/-	DelVal 8-8+/-	15.08.03.	7	1M 2F	1F	2M 1F
cage 70			07.09.03.	6	0	3M 2F	1M
			01.12.03.	3	1M	2M	0
23.07.03.	DelVal 8-8+/-	DelVal 8-8+/-	15.08.03.	4 1eaten	0	1M	2F
cage 71			26.09.03.	1 dead			
			15.10.03.	2	0	1F	1F
			05.11.03.	10	0	3M 3F	2M 2F

Date	Male	Female	Litter Born	Litter	Homozygous	Heterozygous	Wild Type
			01.12.03.	4 2eaten	0	2F	0
			19.12.03.	3 1 dead	0	1M 1F	0
			09.01.04.	eaten			

Table 6. Intercross of DelVal 8-8 heterozygous mice.
On the figure the strain of the female and male mice mated, the date the litters were born and their number, the number of homozygous, heterozygous and wild type offsprings is presented. 25 homozygous, 73 heterozygous and 38 wild type mice were obtained.

Phenotype

The homozygous mice (Figure 39 and 40) appeared runted, smaller than the other littermates when born, in some cases only half the size. By about week 10 they more or less seemed to catch up in weight. The fur was ruffled and the right eye looked like it was half closed, smaller than in wild type and heterozygous animals. By week ten they generally developed dermatitis-type skin condition, started scratching and had inflamed eyes and sore ears. This was seen in 21 of the 25 homozygous animals. Many had to be culled due to animal house regulations.

Although plans have been made to monitor the body weight of the mice from birth to about 10 weeks old to quantify the differences and make conclusions based on statistical analysis, after the relocation of the laboratory there were no successful injections and no more homozygous mice were obtained so far. These tests will have to be done when the mice are available in sufficient number.

Southern Blot Using 3' Probe on DelVal 8-8 gDNA

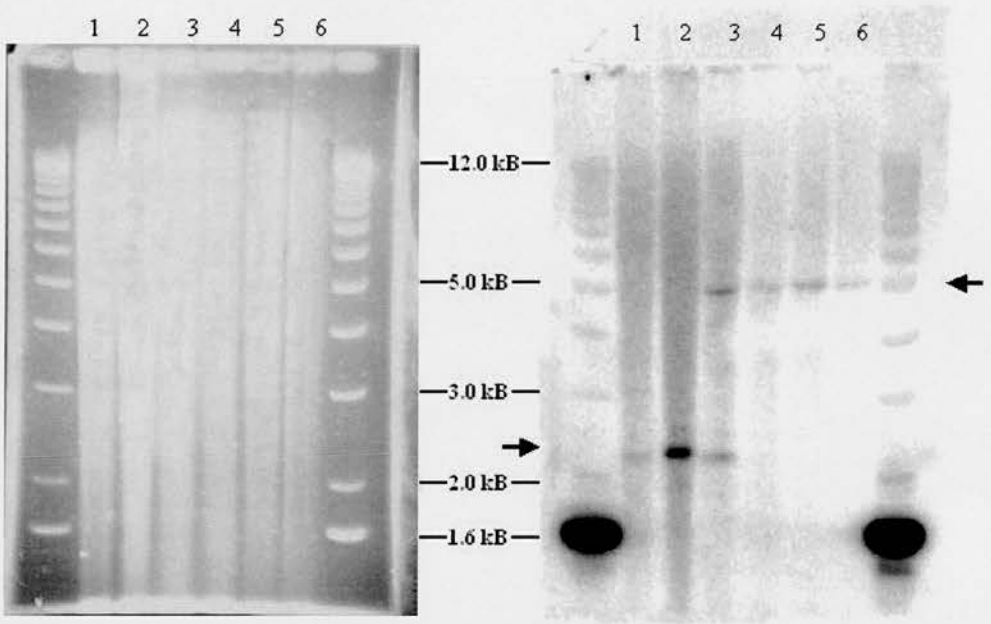

Figure 38. Southern Blot on DelVal 8-8 homozygous genomic DNA.
To the left is the gel photo, to the right is the blot after exposure. Lanes 1 to 6 on the figure are the following:
1. gDNA from tail of homozygous mouse J9 2. gDNA from liver of homozygous mouse J9
3. gDNA from ES cell clone DelVal 8-8 4. control gDNA from merged samples
5. control gDNA from clone NR2A 1-7, 6. control gDNA from SynGAP targeting.
Homozygous male mouse J9 came from the second litter (04.08.03) of cage 53 (Table 6).
In lanes 1 and 2 I could only visualize a 2.5 kb homozygous band (indicated by arrow) showing that the mutation was present in both chromosomes of mouse J9. In lane 3 I could see a 2.5 kB homozygous and a 5 kb (indicated by arrow) wild type band demonstrating the heterozygosity of the ES cell line DelVal 8-8. In lanes 4, 5 and 6 I only obtained a 5 kb wild type band when using various wild type genomic DNA.

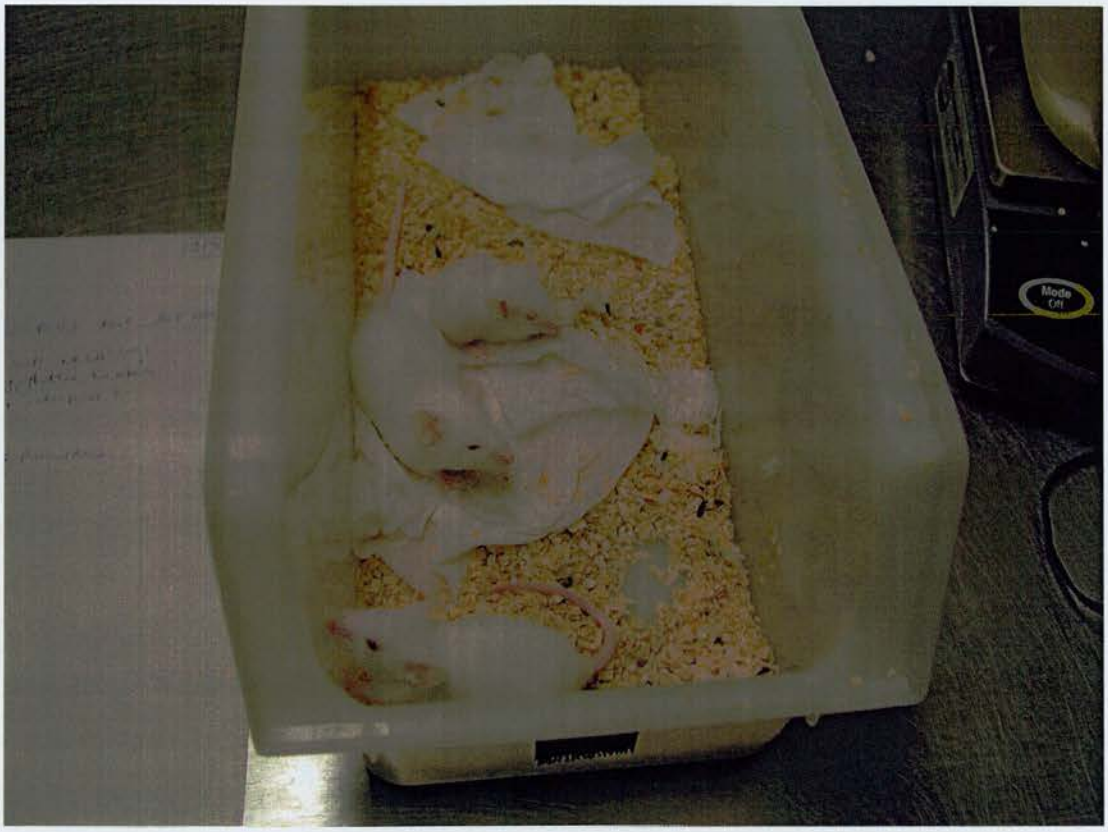

Figure 39. DelVal 8-8 homozygous mice.
On the photo three littermates are shown from the DelVal 8-8 heterozygous intercross. Two of the mice (J9, 10) are homozygous, one (J11) is wild type (See genotyping results in figure 37.). The wild type mouse is the one in the middle and its larger size is obvious. The mouse on the far end is runted and shows the strange looking right eye.

Fertility of DelVal 8-8 homozygous mice

The homozygous mice carrying the DelValine mutation were set up to breed to check their fertility and if possible to produce more homozygous offsprings for further experiments. One intercross was set up on 17th September 2003. The mice had to be culled on 15th December 2003 due to the dermatitis-like infection. During that time period no offsprings were born (Table 7).

Figure 40. DelVal 8-8 homozygous mice.
J11 wild type mouse is again the one in the middle. The other two J9 (on the right) and J10 (on the left) show the half closed right eye and the small size of J9 is very apparent.

Another male homozygous mouse was set up to breed with an $NR2A^{\Delta C}$ female. The aim of this cross apart from the fertility check was to obtain mice that have no C-terminal interactions of the NR2B subunit (because of the valine deletion) and of the NR2A subunit either (deletion of the C-terminus). Both male and female offsprings were obtained from this intercross (Table 7), which was set up to produce the mice explained. I can therefore conclude that the mice carrying the mutation DelValine are fertile and that DelVal 8-8/ $NR2A^{\Delta C}$ double heterozygous mice are viable.

Date	Male	Female	Litter Born	Litter	Male	Female
17.09.03.	DelVal8-8-/-	DelVal8-8-/-				
cage 90						
17.09.03	DelVal8-8-/-	NR2A$^{\Delta C}$-/-	10.10.03.	5	3	2
cage 91			17.11.03.	3	1	2

Table 7. Breeding of DelVal 8-8 homozygous mice.
On the figure the strain of the female and male mice mated, the date the litters were born and the number of the male and female is presented. 4 male and 4 female double heterozygous offsprings were obtained.

3C NR2B CaMKII Mutation

Introduction

One of the non-MAGUK proteins interacting with the C-terminus of the NMDA receptor is the Ca^{2+}-calmodulin-dependent protein kinase II (CaMKII). Postsynaptic calcium influx results in the autophosphorylation of Thr 286 residue of αCaMKII, which enables the molecule to remain activated even after dissociating from Ca^{2+}/CaM, its activator (Miller et al., 1988; Lou and Schulman, 1989). Thr 286 autophosphorylated αCaMKII is persistently active and it is necessary for NMDA dependent LTP induction at certain synapses (Giese et al., 1998; Cooke et al., 2006).

CaMKII has been suggested as a molecular switch for long-term memory storage based on its property to autophosphorylate and self-activate and its ability to bind to NMDA thereby anchoring AMPA receptors at the PSD (Lisman and Zhabotinsky, 2001). Inhibition of CaMKII blocks LTP in the hippocampal CA1 region (Malinow et al., 1998). The deletion of αCaMKII impairs E-LTP in the CA1 neurons of the hippocampus and also spatial learning (Silva et al., 1992a; Silva et al., 1992b). The mutation described in the following sections preventing the interaction of NR2B with the non-MAGUK protein, CaMKII can provide further insights into the function of

CaMKII and the importance of its interaction with the NMDA receptor in synaptic plasticity, learning and memory.

In the binding site of the NR2B C-terminus various amino acids were identified as key residues in mediating CaMKII interaction. Several mutations were generated to identify these critical amino acids in the CaMKII binding domain of NR2B described in the article "Mechanism and regulation of CaMKII targeting to the NR2B subunit of the NMDA Receptor." (Strack et al., 2000). On the bases of these findings three amino acids were mutated, a leucine to alanine, an arginine to glutamine and a serine to asparagine (Figure 41).

Figure 41. CaMKII site mutation.
Three amino acids (indicated in blue colour) were mutated in the CaMKII binding site (residues 1290-1309) of the NR2B C-terminus. The mutagenesis was done using Stratagene Quick Change™ Site-directed Mutagenesis Kit. Extra restriction sites BglII and BssHII were created at the same time by changing the NR2B sequence, but conserving the AS residues (indicated in pink colour).

Vector construction

From the plasmid pNR2B-19 the XbaI-NdeI fragment was subcloned into the artificial polylinker (-XbaI-NdeI-EcoRI) containing pBluescriptIIKS vector (Figure 42 Step 1). This new vector was used as a template for site directed mutagenesis to mutate a leucine (residue 1298) to alanine, an arginine (residue 1300) to glutamine and a serine (residue 1303) to asparagine in the CaMKII binding site (Find sequence information in the appendix.) of NR2B using Stratagene Quick Change™ Site-directed Mutagenesis Kit. At the same time a BssHII and a BglII site was created to use later for checking homologous recombination (Figure 41, Figure 42 Step 2).

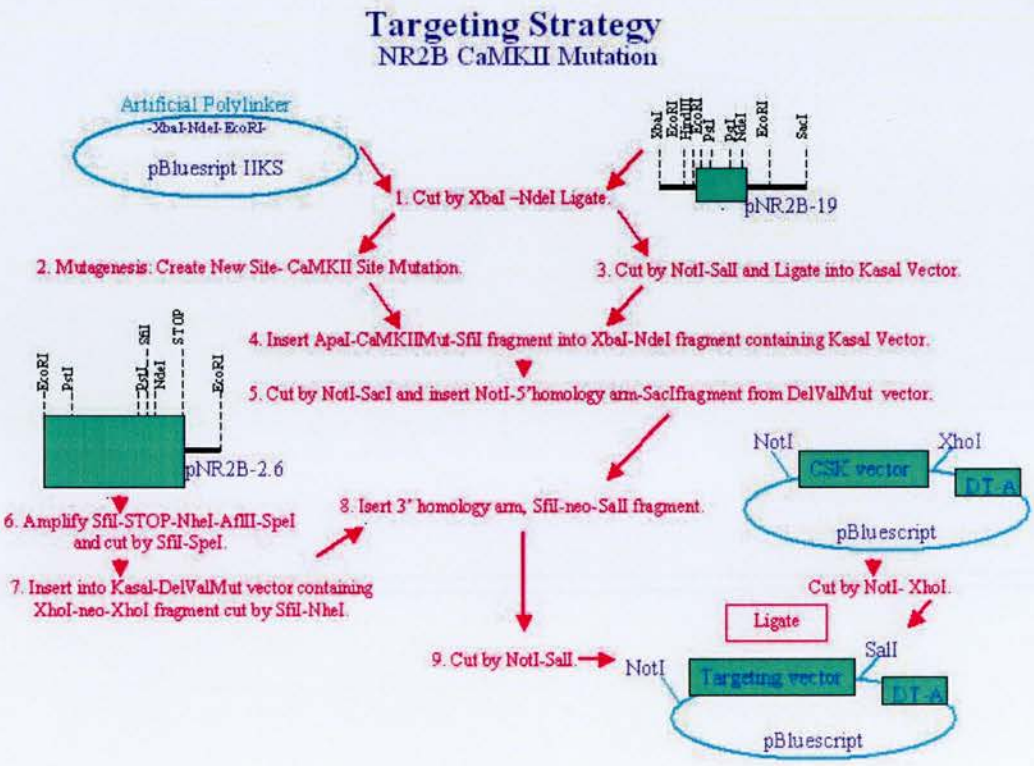

Figure 42. Targeting strategy of NR2B CaMKII site mutation.
The mutagenesis was done in the pBlueScriptKSII vector containing the XbaI-NdeI fragment from pNR2B-19. The 5' and 3' homology arms were obtained from the Kasal-DelValMut targeting subclones. The final targeting vector contains the neo sequence and is inserted into the DT-A containing pBluescript vector. The vectors and subclones used were provided by collaborator Dr Rolf Sprengel or produced during the DelValine mutation.

Twelve colonies were picked and checked by BglII and BssHII digests. Only the ones containing the mutation and the extra restriction sites created were linearised by these enzymes yielding a ~5.4 kB band. All clones were found positive. Clones CaMKIIMut 1 and 4 were then checked by further digestion with ApaI and SfiI (Figure 43) and sequenced using primers CaMKII 5148, 7130, 7214 and 7461. CaMKIIMut 4 was missing an A from position 5621 (NR2B sequence from Dr Rolf Sprengel 22/10/1999. Find sequence information in the appendix.). Clone CaMKII 1 was found correct and was used for later cloning steps.

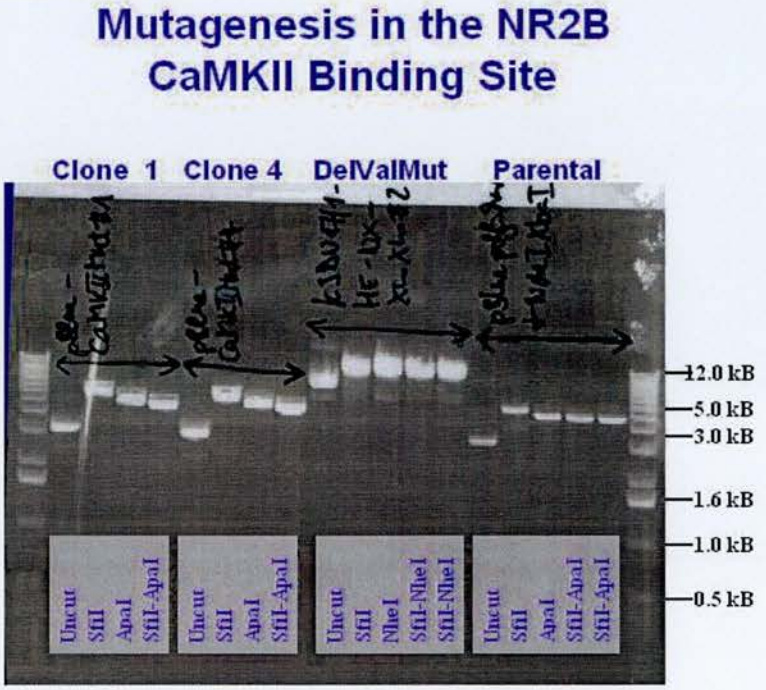

Figure 43. NR2B CaMKII mutation- Screening for correct mutagenesis.
On the figure clones 1 and 4, the parental subclone (Par.) the DelValMut targeting subclone described later is presented.
By digesting with SfiI I obtained correct bands of about 5400 bases in the cases of clones 1 and 4 and the parental subclone. When digesting with ApaI I could visualize a slightly smaller band since the pBluescriptIIKS backbone contains an extra ApaI site. Digesting with ApaI-SfiI drops the 431 base par band therefore the backbone was again was slightly smaller.
The DelValMut targeting subclone was analysed for the further cloning steps using the digests presented. The SfiI, NheI are unique sites therefore I obtained linearization however these digests were not complete on this occasion.

The XbaI-NdeI fragment containing pBluescriptIIKS vector (without the mutation) was then digested with NotI-SalI and this fragment was inserted into the Kasal vector (Described in section 3B.). This step was done to obtain a vector in which there is only one ApaI site. This vector was digested with ApaI-SfiI and the ApaI-CaMKIIMut-SfiI fragment obtained from step 2 (Figure 42) was inserted instead (Figure 42 Step 4). With this ligation step I ensured that apart from the ApaI-SfiI fragment the rest of the vector was obtained from an existing subclone. Therefore the only segment that had to be checked by sequencing was the 431 base pair long ApaI-CaMKIIMut-SfiI fragment.

For further cloning steps, such as inserting the 5' homology arm, I utilized an already existing subclone (Figure 7 Step 8, Figure 16a and b) from the DelValine targeting. This subclone contained the whole targeting vector DelValMut inclusive the XhoI-neo-XhoI fragment in the Kasal backbone. The vector was digested with NotI-SacI and this 5' homology arm was ligated into the mutated CaMKII site-containing vector (Figure 42 Step 5).

The same Kasal-DelValMut vector was digested with SfiI-NheI to ablate the mutation created by the previous targeting. By inserting the SfiI-STOP-NheI-AflII-SpeI fragment (amplified from pNR2B-2.6 in a way that extra sites NheI, AflII, SpeI were created) into the Kasal-DelValMut vector utilizing the compatible sticky ends of SpeI and NheI I produced a vector without the DelValine mutation, but with the various restriction sites usable for further targeting steps.

From this targeting subclone (Described in the previous paragraph.) I purified the SfiI-SalI fragment, which contained the Xho-neo-XhoI segment. It was then inserted into the vector containing the mutated CaMKII site and the 5' homology arm (Figure 42 Step 8).

The vector then was excised by NotI-SalI and inserted into DTA containing pBluescript vector, which was digested by NotI-XhoI (Figure 42 Step 9). This cloning step ablated the SalI site at the 3' end, but allowed linearization by NotI before ES cell targeting (Figure 44). Six colonies were picked from the bacterial plates and prescreened using restriction digest by BglII and BssHII. All were positive. Clone pBlueDTA-CaMKIIMut 1, 4, 5 and 6 were used for further testing by other digests and sequencing. On the next figure restriction digests of clone 1 are presented (Figure 44).

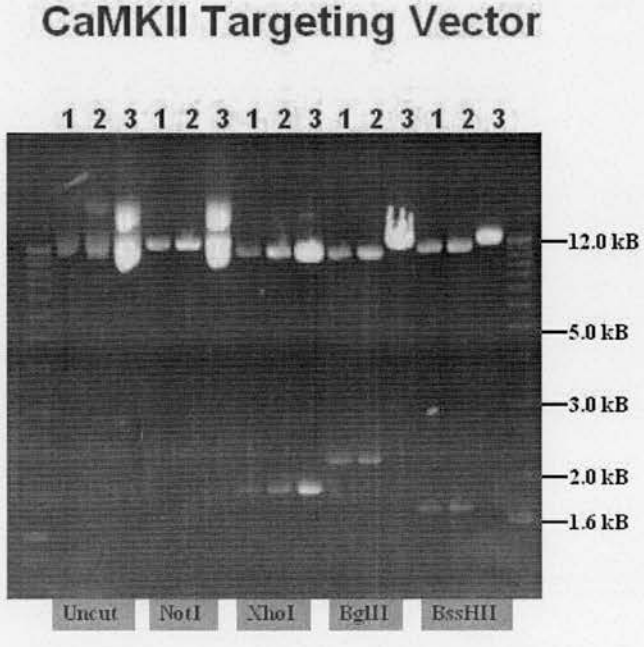

Figure 44. NR2B CaMKIIMut targeting vector.
On the figure clone 1 and 2 are different midipreps of the final targeting vector while clone 3 is the DelValMut targeting vector. These (in pBluescript-DTA vector) were compared using various restriction digests.
The NotI digest linearised both vectors since the site was preserved in the final ligation step while the SalI site was ablated. On the figure it can be seen that the DelValMut vector DNA was only partially digested.
The XhoI digest produced a ~1.9 kB band in all cases which corresponds to the XhoI-neo-XhoI fragment. In the case of the BglII digest I only saw a~2.2 kB band in the pBlueDTA-CaMKIIMut clones since in these there was a site created during mutagenesis while the two BglII sites in the neo cassette are very close to each other (the small band was not visualized). The BssHII digest similarly yielded a ~1.7 kB band in the pBlueDTA-CaMKIIMut clones and linearization in the pBlueDTA-DelValMut clone.

Clones pBlueDTA-CaMKIIMut 1, 4, 5 and 6 were further screened by sequencing with primers DelVal 358, CaMKII 3597, 5148, 5603, DelVal 6102, 7897 and 3261 (Find sequence information in the appendix.) to check whether the ligation junctions were correct and the mutation site was intact. The details of the sequencing reaction can be found in the materials and methods. Sequencing results revealed that the targeting vector pBlueDTA-CaMKIIMut 1 was correct and ready for electroporation into embryonic stem cells.

The final vector (Figure 45) is the same size as the DelValine targeting vector ~10 kB (plus the 4 kB pBlue-DTA vector backbone) with a 3' homology arm of 2.3 kB and a 5' homology arm of 5.8 kB. It contains three point mutations in the CaMKII binding site of NR2B alongside with two sites created for further analysis (BglII, BssHII). The neo selection cassette is inserted at the XhoI site. The final clone pBlueDTA-CaMKIIMut 1 was further tested by SpeI, ClaI, NcoI, NheI and NdeI digests and was shown to be correct and ready for electroporation into embryonic stem cells.

ES cell targeting

The pBlueDTA-CaMKIIMut vector was electroporated into E14TG2a ES cells as described in detail in the materials and methods.

150μg of vector was linearised with NotI, precipitated, washed with 70% ethanol and resuspended in 100 μl PBS the night before electroporation. Passage number 11 E14TG2a cells (4.5×10^5) were grown up from frozen stock to yield about 5×10^7 cells, trypsinized and resuspended in a final volume of PBS that will give about $1X10^8$ cells/600 μl. The cells (passage 17, 4×10^7 in total) were electroporated at 0.8 kV, 3 μF (time constant 0.1 sec) in the gene pulsar and plated at the density of 5×10^6, $2.5X10^6$, 10^6, $0.5X10^6$ and 2×10^5 cells per plate (20 plates in total).

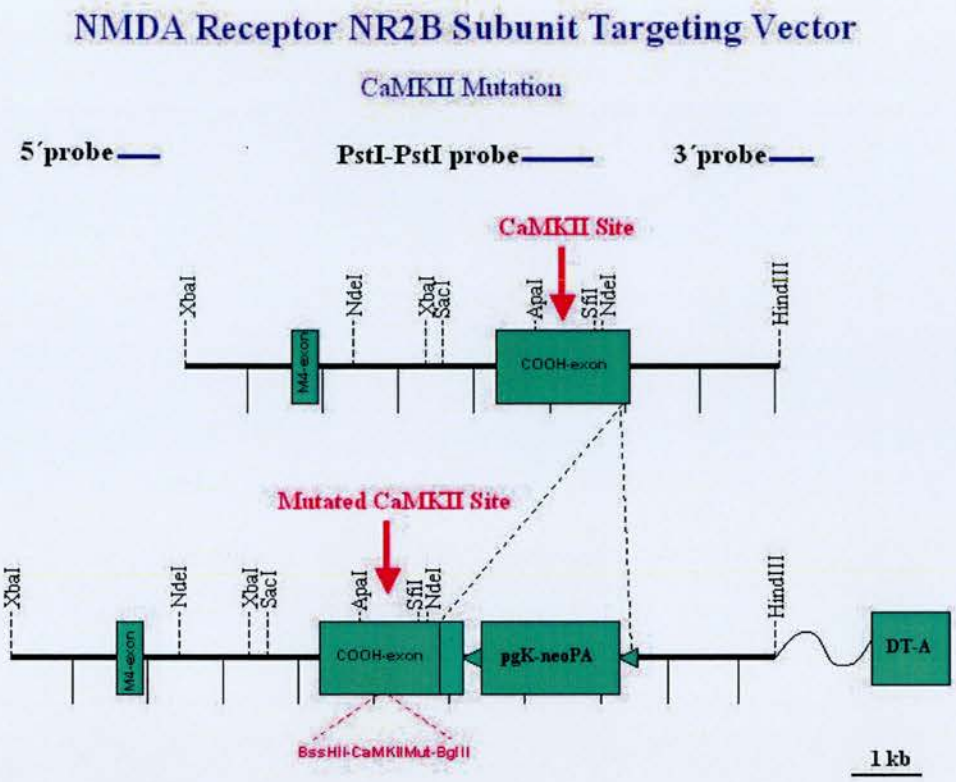

Figure 45. NR2B CaMKIIMut Targeting Vector.
In the final targeting vector three point mutations were created along with BglII and BssHII restriction sites. PgK-neoPA selection cassette was inserted at the XhoI site. The 3' homology arm is 2.3 kB and the 5' homology arm is 5.8 kB. The targeting vector is ~10 kB.

G418 (200μg/ml) was added one day after electroporation and selection was continued for 10 days. From the surviving neomycin-resistant colonies 148 were picked and grown up in 24 well plates. Duplicate plates containing 103 colonies were frozen for further expansion while the originals were used to obtain genomic DNA. Southern blotting with 3' and 5' external probes was used to screen the colonies.

Southern blots

The neo cassette contains XbaI and BglII sites, while the NheI, BsshII and another BglII site exists in the lines containing the mutation (created by mutagenesis). These restriction sites were used to screen the embryonic stem cell lines obtained after electroporation. First all ES cell clones (103) were screened using the 3' flanking probe thereafter the positive ones were further checked using the 5' flanking probe.

The HindIII-XbaI 3' probe and the PCR amplified (using 5' probe-1 and 2 primers) 5' probe was the same as in the case of the DelValine targeting vector. They were labelled using Rediprime™ II random prime labelling system and used for probing the filter containing the genomic DNA samples as described in materials and methods.

The wild type genomic DNA digested with XbaI and hybridised with the 3' probe gave a 5 kB band, while the mutant lines with correct homologous recombination yielded a 2.5 kB band as in the case of the previous, DelValine mutation (Figure 19). In the Southern Blots 10 μg wild type and targeted genomic DNA was digested with high concentration XbaI restriction enzyme and run on a 0.8% agarose gel. The samples were transferred onto nitrocellulose (Hybond™-N) and crosslinked to the filter using UV. The filter was prehybridized at 65 °C for 4 hours then probed at 65 °C overnight. After washing the filter it was wrapped in Sarah wrap, placed into a cassette with Kodak X-ray film over it and was left at –80 °C to expose. In the following figures southern blots (of the positive clones) using the 3' probe are demonstrated alongside with the gel photos (Figure 46).

The gDNA was then digested with BglII and probed with the 5' probe. I got a ~14 kB band for WT clones and a ~7 kB band (there is a BglII site created by mutagenesis next to the CaMKII binding site) for mutants with correct homologous recombination. 10 μg wild type and targeted genomic DNA was digested with high concentration BglII restriction enzyme and run on a 0.75% agarose gel. The samples were treated in the same manner as in the case of the 3' probe. Cell lines CaMKII 1-6 and 4-12 were identified as correctly targeted clones. The gel photos can be seen alongside the Southern Blots below. The cells were then expanded and used for producing chimaeric mice. In the following figures southern blots (of the positive clones) using the 5' probe are demonstrated alongside with the gel photos (Figure 47).

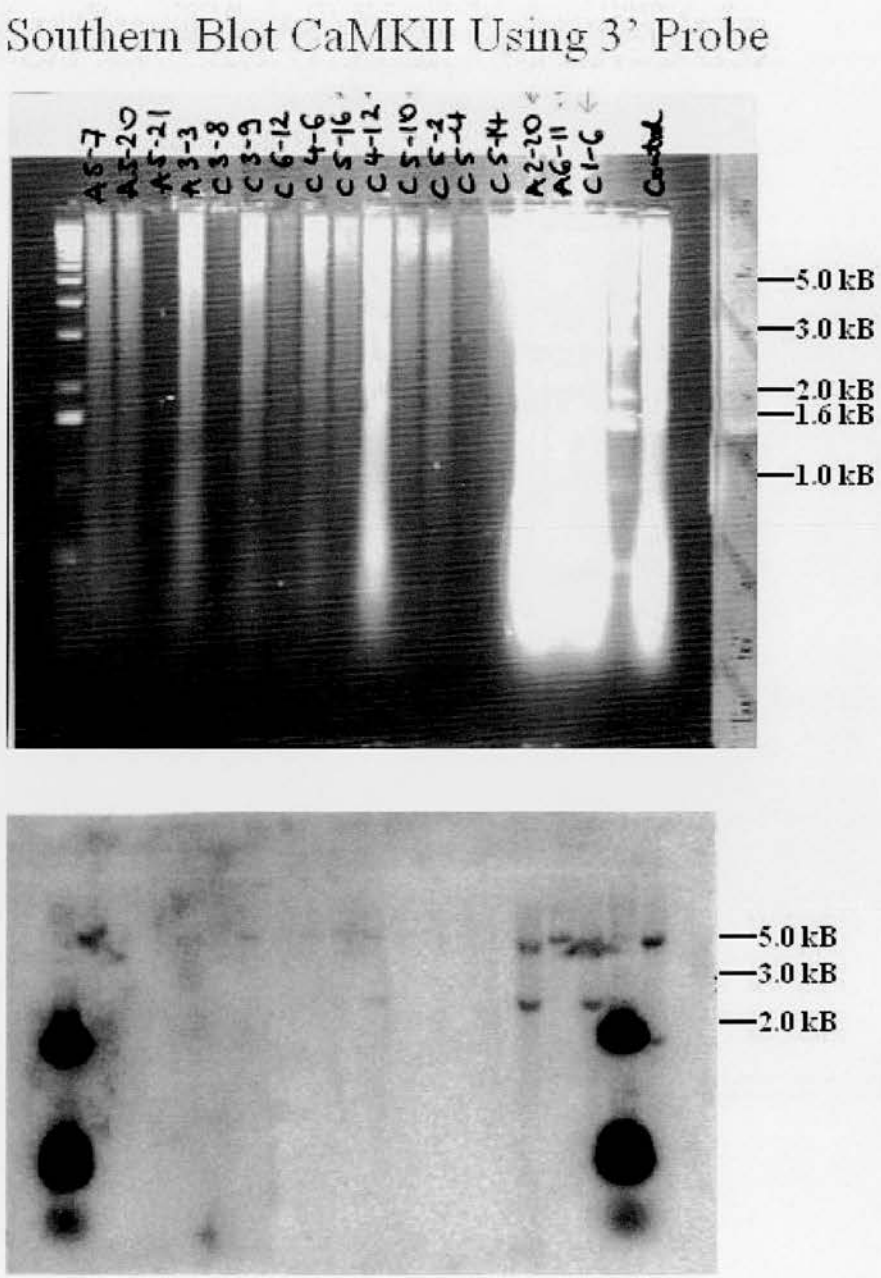

Figure 46. Southern Blot using XbaI digest and the 3' probe.
The photo on the top is the gel picture, while the one at the bottom is the blot after exposure. The ES cell clones are indicated on the top. C stands for CaMKII clones, A for NR2A clones (Find in detail in section 3D.).
After digesting with XbaI and probing with the 3' probe I obtained a 5 kB wild type and a 2.5 kB homozygous band in the correct clones. 3' positive clones were CaMKII 1-6, 4-12 NR2A 2-20 (band clearly seen) and possibly CaMKII 5-10 and 5-16 (band was not visible in the scanned image).

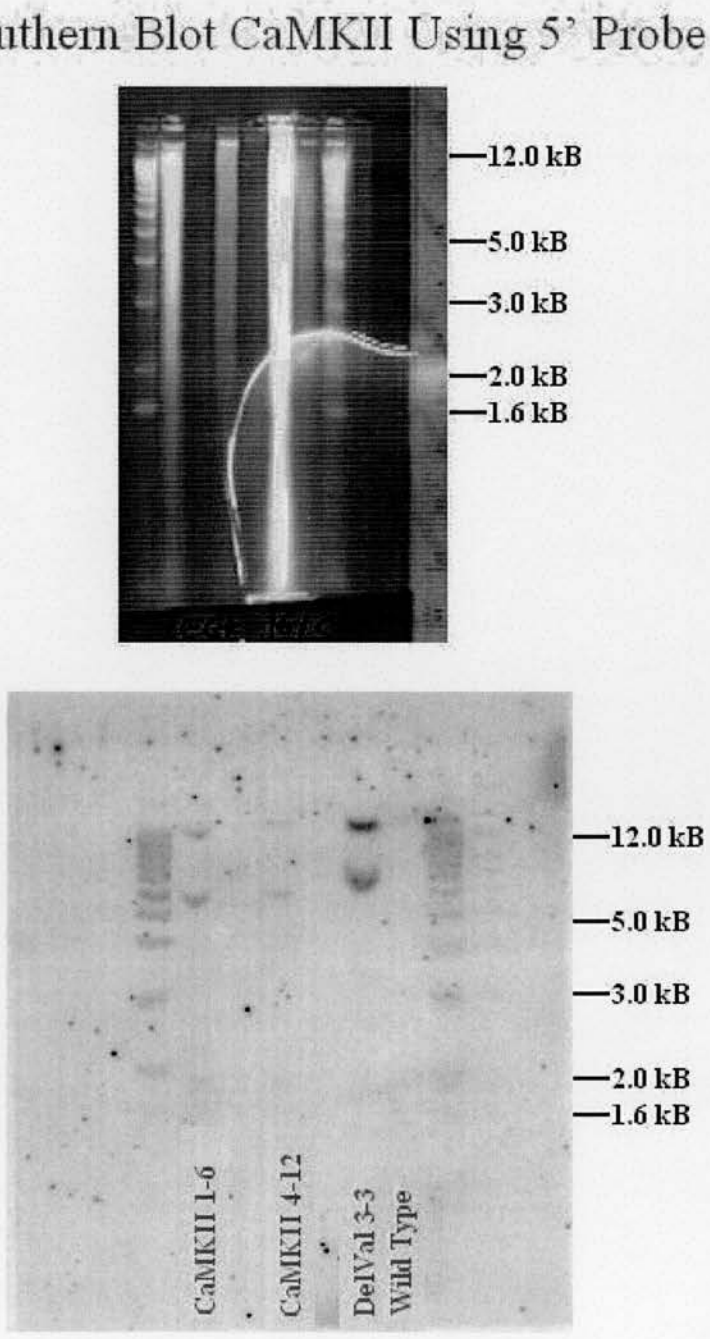

Figure 47. Southern Blot EGK 16C using BglII digest and the 5' probe.
The photo on the top is the gel picture, while the one at the bottom is the blot after exposure. The 5' positive ES cell clones are indicated. The size difference between the homozygous bands of the CaMKII clones (~7 kB) and the control DelValine clone (~8kB) could be seen. The wild type band was ~14 kB.

Generation of chimaeras

Clones CaMKII 1-6 and 4-12 were injected into blastocysts to generate chimaeras in February-April 2003. The microinjections were carried out by Jane Robinson, our chief technician. The details of the injections can be seen in table 8.

Date	Cell Line	Embryos Injected	Transfers	♀/♂ Chimaeras
13.02.03.	CaMKII 4-12	14	1	None
17.03.03.	CaMKII 4-12	13	1	None
08.04.03.	CaMKII 4-12	15	1	None
09.04.03.	CaMKII 1-6	18	2	1 Male
24.04.03.	CaMKII 4-12	17	2	None
24.04.03.	CaMKII 1-6	14	1	None
04.07.03.	CaMKII 4-12	18	1	None

Table 8. Blastocyst injections of CaMKII clones.
On the figure the date of injection, the cell line, the number of embryos injected, the number of recipients into which the embryos were injected and the sex of the resulting chimaeras is presented.

In total 109 embryos were injected and used for 9 transfers from which one chimaera was obtained from clone CaMKII 1-6. A test cross was set up with two MF1 females. The offsprings were all black. Germline transmission wasn't achieved. The test cross was terminated. No further injections were done to produce other chimaeras due to the relocation of the laboratory from the Centre for Neuroscience in Edinburgh to the Sanger Centre in Cambridge.

3D NR2A/NR2B COOH-Exon Swapping Mutation

Introduction

According to the time expression of the different subunits NR1 and NR2B play an important role in brain development and therefore it is not surprising that mice lacking these subunits die shortly after birth (Forrest et al., 1994; Li et al., 1994; Kutsuwada 1996). Mice without postnatally expressed NR2A and NR2C subunits are

viable (Sakimura et al., 1995; Ebralidze et al., 1996) nonetheless the equal importance of these subunits was also shown by numerous experiments.

In the hippocampus both NR2A and NR2B subunit-dependent signalling is implicated in long-term synaptic plasticity (McHugh et al., 1996; Kohr et al., 2003) (Find in detail in section 1F). The NR2A containing NMDA receptors were implicated in the induction of LTP while NR2B containing receptors were shown to be important for LTD in the hippocampus (Liu et al., 2004; Massey et al., 2004). Previous studies however using NR2B overexpressing mice with enhanced CA1 LTP and long-term memory suggested the contribution of NR2B subunits to hippocampal LTP and learning (Tang et al., 1999). Both NR2A and NR2B subunits were shown to be important for LTP induction in the ACC and the NR2B subunit was implicated in mediating contextual fear memory tested by assessing freezing behaviour (Zhao et al., 2005).

Since the NR2A and NR2B subunits of the NMDA receptor bind to different molecules (Table 2b and 2c), are involved in different mechanisms of synaptic plasticity and are implicated in different types of learning and memory (Find in detail in section 1E and 1F), I thought it to be interesting to delete the COOH-exon of the NR2B subunit and replace it by that of the NR2A. By doing so it can be seen what functional differences of the NR2A and NR2B containing NMDA receptors can be accounted for by the different cytoplasmic tails and the interactions mediated via them, which regions of the NR2B subunit are important for producing viable mutant mice and also to tell whether the interactions mediated by the NR2A C-terminus can rescue the lack of the NR2B subunit C-terminus. In the next section the key steps of the vector construction will be summarized.

Vector construction

The artificial polylinker (-NotI-SphI-XbaI-BamHI-NheI-SalI-) designed to provide restriction sites suitable for the cloning steps (Figure 48) was inserted into the Kasal vector (described in section 3B). For the next step I utilized an already existing subclone (Figure 7 Step 5) from the DelValine targeting. This subclone contained

the NR2B COOH-exon with the terminal valine deleted and the NheI site created by mutagenesis. The BamHI-NheI fragment from this subclone was inserted into the pKS vector, Kasal vector containing the artificial polylinker (Figure 48 Step 1).

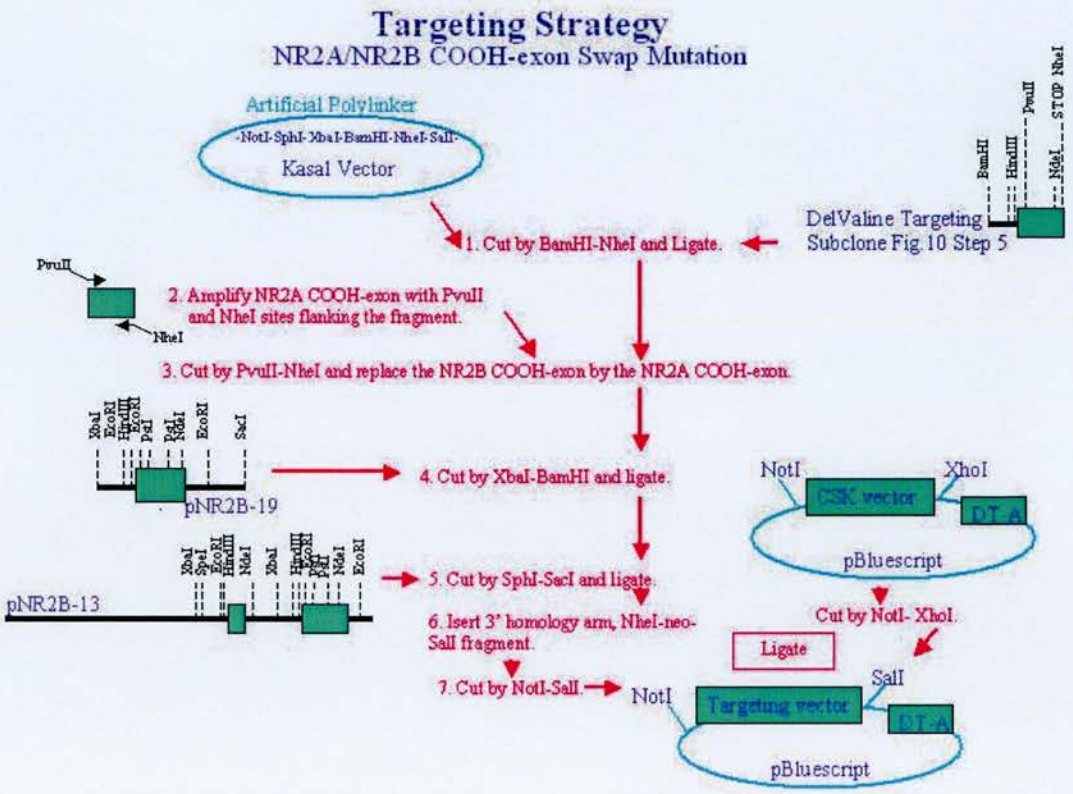

Figure 48. Targeting strategy of NR2A/NR2B COOH-exon swapping mutation.
The mutagenesis was done in the Kasal vector containing an artificial polylinker (-NotI-SphI-XbaI-BamHI-NheI-SalI-). The NR2A COOH-exon was amplified from genomic DNA and inserted to replace the COOH-exon of the NR2B. The 5' and 3' homology arms were obtained from existing subclones. The final targeting vector contains the neo sequence and is inserted into the DT-A containing pBluescript vector. The vectors and subclones indicated in figure 56 were provided by collaborator Dr Rolf Sprengel, the rest were produced during the DelValine mutation.

The NR2A COOH-exon was amplified (Figure 48 Step 2) from genomic DNA using primers NR2A-COOH 1 and 2 (Find sequence information in the appendix.). The ~1800 base pair fragment was purified as described in materials and methods, digested by BamHI-NheI and ligated into the vector described in the previous

paragraph (Figure 48 Step 3). Six colonies were picked from the bacterial plates and checked by restriction digestion using SacI and BglII. Clone pKS-NR2A 3 was further screened with other restriction digests, the results of which can be seen in figures 49 and 50. The clone was sequenced using primers SWAP 4277, SWAP-NR2A 170, 396, 609, 810, 1052, 1291 and 1515 (Find sequence information in the appendix.) to check correct amplification of the NR2A COOH-exon. It was confirmed positive and used for further cloning steps.

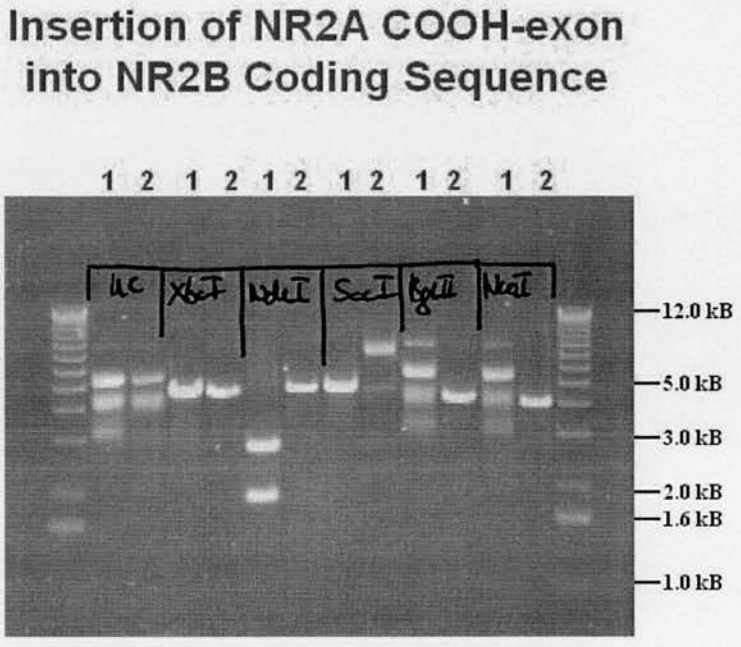

Figure 49. Restriction digests of clone pKS-NR2A 3.
On the figure the parental subclone (1) and clone pKS-NR2A 3 (2) is presented. XbaI digest linearised both parental and pKS-NR2A clones, because the restriction site was present in the artificial polylinker yielding an about 4.5 kB band. The NdeI site was present in the pKS vector and the NR2B COOH-exon, but not the NR2A COOH-exon. Therefore restriction digest linearised the pKS-NR2A clone and dropped a 1850 base pair band in the case of the parental clone. The SacI site was absent in the NR2A COOH-exon therefore I only saw linearization in the parental clone resulting in a 4.5 kB band. The BglII and NcoI sites on the other hand were only present in the NR2A COOH-exon (two each). Using these enzymes the parental subclone remained undigested and I got a 345 base pair BglII-BglII fragment and the backbone or a 438 base pair NcoI-NcoI fragment and the backbone. The PstI digest resulted in a 1229 base pair band in the case of the pKS-NR2A clone and in two bands (152 and 871 base pairs) in the parental subclone (apart from the backbone).

The 5' homology arm was inserted in two steps by ligating first the XbaI-BamHI fragment from subclone pNR2B-5.4 (Figure 48 Step 4) then the SphI-SacI fragment from subclone pNR2B-13 (Figure 48 Step 5). For the next cloning step, which was to insert the 3' homology arm, I utilized an already existing subclone (Figure 10 Step 8, Figure 16a and b) from the DelValine targeting, the same that was used for the CaMKII targeting as well. This subclone contained the whole targeting vector DelValMut inclusive the XhoI-neo-XhoI fragment in the Kasal backbone.

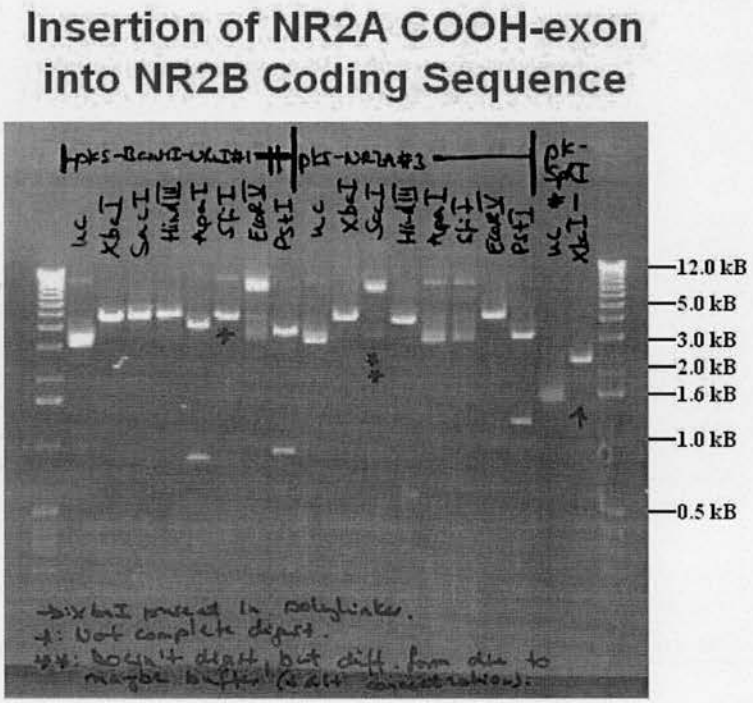

Figure 50. Restriction digests of clone pKS-NR2A 3.
On the figure results of further digests of the parental subclone and clone pKS-NR2A 3 is presented. HindIII linearised the parental clone and dropped a 247 base pair band in the case of the pkS-NR2A clone since there is an extra site in the NR2A COOH-exon. ApaI and SfiI were absent in the pKS-NR2A clone, but I saw digest in the parental clone (738 base pair band and linearization respective). EcoRV linearised the pKS-NR2A clone, but didn't digest the parental clone.
Based on the screening by restriction digests the clone was confirmed positive and used for further targeting steps.

The vector previously described was digested with NheI-SalI and this 3' homology arm containing the neo cassette was inserted into the NR2A-Swap vector (Figure 48

Step 6). Six colonies were picked from the bacterial plates and test digested with NcoI, SacI, EcoRI, EcoRV and ApaI digests (Figure 51). Clones 1 and 6 were used for the next step.

The vector then was excised by NotI-SalI and inserted into DTA containing pBluescript vector, which was digested by NotI-XhoI (Figure 48 Step 7). This cloning step ablated the SalI site at the 3' end, but allowed linearization by NotI before ES cell targeting. Six colonies were picked from the bacterial plates and prescreened using restriction digest by NotI and SalI. Clones 1, 2, 3 and 6 were found positive (Figure 52).

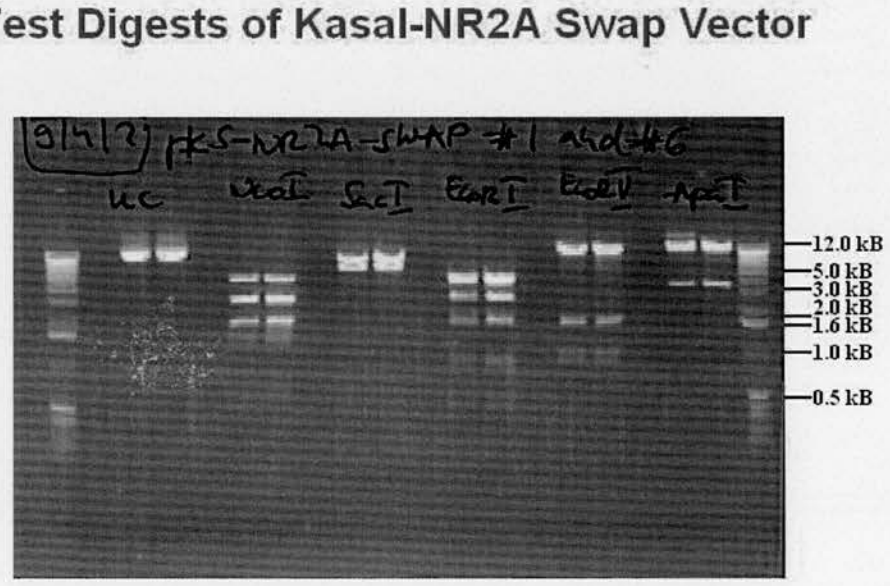

Figure 51. Restriction digests of clone pKS-NR2A 3.
On the figure clones pKS-NR2A-Swap 1 and 6 are presented. The same restriction digests (NcoI, SacI, EcoRI, EcoRV and ApaI) were used as in the previous cloning step. Both clones were confirmed positive and used for the next cloning step.

Clone pBlueDTA-NR2A-Swap 1 was further tested by NotI, SalI, XhoI, PvuII and ApaI digests and was sequenced using primers SWAP 4277, SWAP-NR2A 170, 396, 609, 810, 1052, 1291, 1515, CaMKII 3597, DelVal 3261, V and 7914 to check

whether the ligation junctions were correct and the amplified fragment was intact. The details of the sequencing reaction can be found in section 2A. The sequencing results revealed that the targeting vector pBlueDTA-NR2A-Swap was correct and ready for electroporation into embryonic stem cells.

The final vector is the same size as the DelValine targeting vector ~10 kB (plus the 4 kB pBlue-DTA vector backbone) with a 3' homology arm of 1.8 kB and a 5' homology arm of 6 kB. It contains the NR2A COOH-exon inserted instead of that of the NR2B, and an NheI site created by mutagenesis of the DelValine vector subclone. The neo selection cassette was inserted together with the 3' homology arm and was flanked by two XhoI sites.

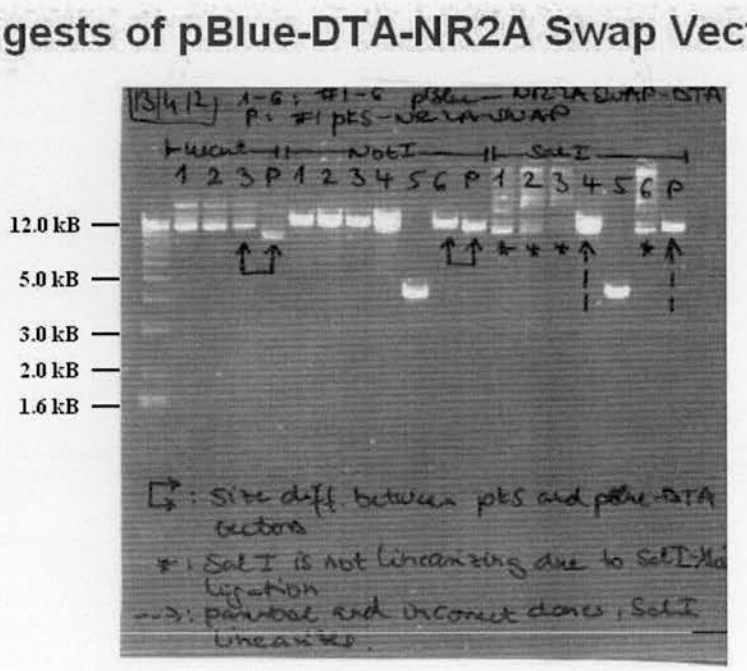

Figure 52. Restriction digests of the final targeting vector.
On the picture clones 1 to 6 and the parental clones (P) are presented. The correct clones were linearised by NotI digest, but remained undigested after SalI digest since the SalI restriction site was ablated by the SalI-XhoI ligation step. The size difference between the vectors could also be seen (indicated by the double arrows) since the Kasal vector was smaller (~2.3 kB) than the pBluescript-DTA vector (~4 kB). Clones 1, 2, 3 and 6 were confirmed correct by restriction digest.

ES cell targeting

The pBlueDTA-NR2A-SWAP vector was electroporated into E14TG2a ES cells as described in detail in the materials and methods in two separate rounds.

150μg of vector was linearised with NotI on both occasions, precipitated, washed with 70% ethanol and resuspended in 100 μl PBS the night before electroporation. Passage number 11 and 12 E14TG2a cells (4.5×10^5) were grown up from frozen stock to yield about 5×10^7 cells, trypsinized and resuspended in a final volume of PBS that will give about $1X10^8$ cells/600 μl. The cells were then electroporated at 0.8 kV, 3 μF (time constant 0.1 sec) in the gene pulsar and plated at densities ranging from 5×10^6 to 2×10^5 cells per plate (40 plates in total).

G418 (200μg/ml) was added one day after electroporation and selection was continued for 10 days. In total 238 neomycin-resistant colonies were picked and grown up in 24 well plates. 166 colonies were frozen for further expansion while the originals were used to obtain genomic DNA. Southern blotting with 3' and 5' external probes were used to screen the colonies.

Southern blots

The neo cassette contains XbaI and BglII sites, while the NheI, BsshII and another BglII site exists in the lines containing the mutation (created by mutagenesis). These restriction sites were used to screen the embryonic stem cell lines obtained after electroporation. First all ES cell clones (103) were screened using the 3' flanking probe thereafter the positive ones were further checked using the 5' flanking probe.

The HindIII-XbaI 3' probe was the same as in the case of the DelValine targeting vector. The 5' probe (~500 base pairs) was PCR amplified using primers Swap 5' probe 1 and 2 and subclone pNR2B-13/SacI as the template. The probes were labelled using Rediprime™ II random prime labelling system and used for probing the filter containing the genomic DNA samples as described in materials and methods.

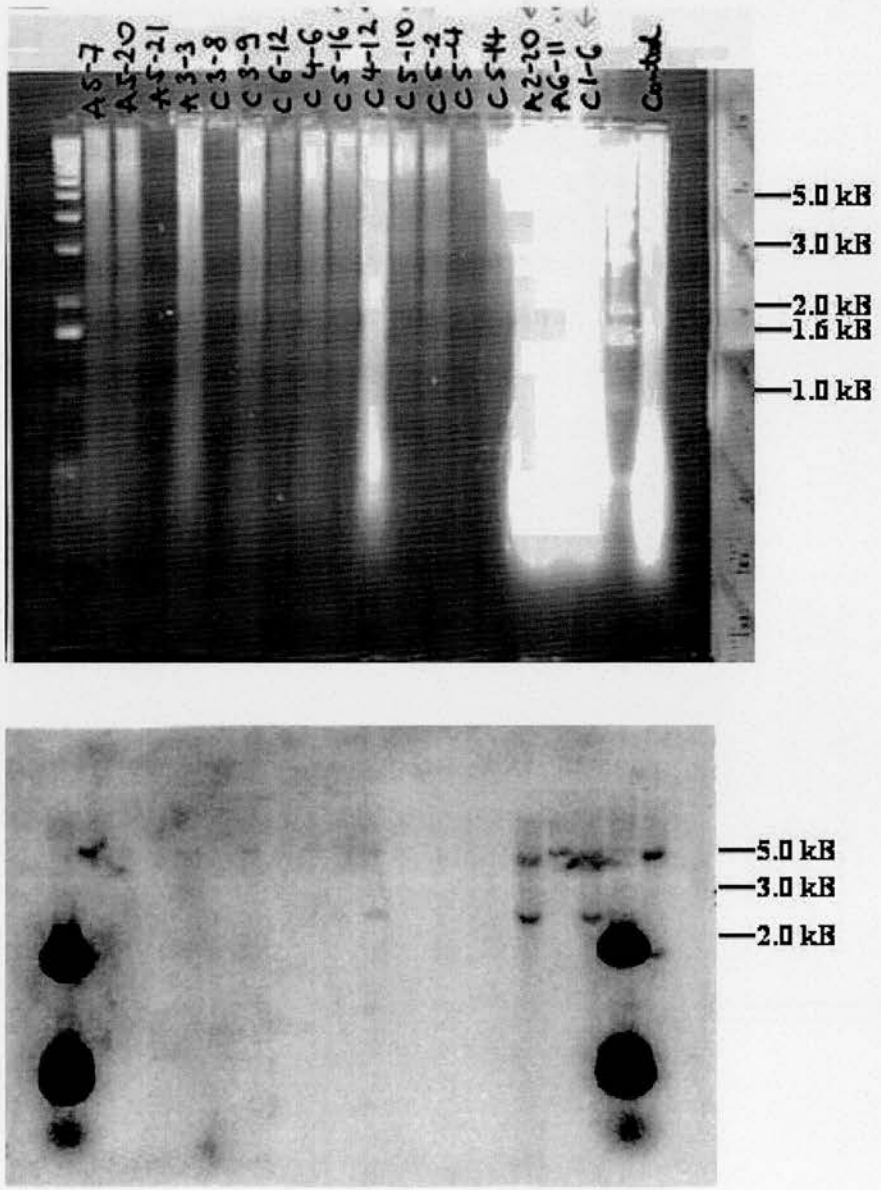

Figure 53. Southern Blot using XbaI digest and the 3' probe.
The photo on the top is the gel picture, while the one at the bottom is the blot after exposure. The ES cell clones are indicated on the top. C stands for CaMKII clones, A for NR2A clones. After digesting with XbaI and probing with the 3' probe I obtained a 5 kB wild type and a 2.5 kB homozygous band in the correct clones. 3' positive clone was NR2A 2-20.

Southern Blot NR2A Swap Using 5' Probe

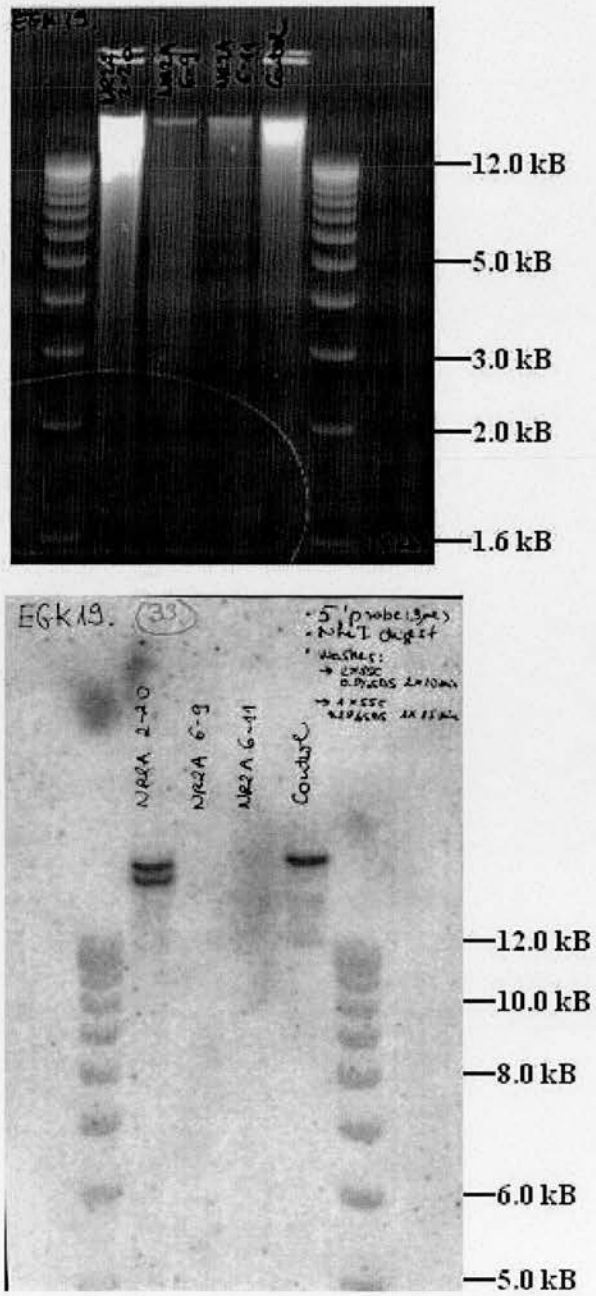

Figure 54. Southern Blot EGK 19 using BglII digest and the 5' probe.
The photo on the top is the gel picture, which was run further until the 5 kB marker ran right to the bottom so that I had better separation of the top bands. The photo at the bottom is the blot after exposure.
The 5' positive ES cell clone NR2A 2-20 clearly showed the wild type and the homozygous bands.

The wild type genomic DNA digested with XbaI and hybridised with the 3' probe gave a 5 kB band, while the mutant lines with correct homologous recombination yielded a 2.5 kB band as in the case of the previous, DelValine mutation (Figure 19). In the Southern Blots 10 μg wild type and targeted genomic DNA was digested with high concentration XbaI restriction enzyme and run on a 0.8% agarose gel. The samples were transferred onto nitrocellulose (Hybond^{TM}-N) and crosslinked to the filter using UV. The filter was prehybridized at 65 °C for 4 hours then probed at 65 °C overnight. After washing the filter it was wrapped in Sarah wrap, placed into a cassette with Kodak X-ray film over it and was left at –80 °C to expose. In the following figures southern blots (of the positive clones) using the 3' probe are demonstrated alongside with the gel photos (Figure 53).

The gDNA was then digested with NheI and probed with the 5' probe. I got a ~14-15 kB band for WT clones, which was previously approximated by doing a southern blot on wild type genomic DNA. The mutant band was smaller due to the extra NheI site created by mutagenesis for mutants with correct homologous recombination. 10 μg wild type and targeted genomic DNA was digested with high concentration BglII restriction enzyme and run on a 0.75% agarose gel. The samples were treated in the same manner as in the case of the 3' probe. Cell line NR2A 2-20 was identified correctly targeted. In the next figure the southern blot (of the positive clone) using the 5' probe is demonstrated alongside with the gel photo (Figure 54).

The only correctly targeted clone was NR2A 2-20. The 24-well plate containing the frozen clone was defrosted and treated as usual described in materials and methods. The cells however didn't start multiplying therefore I couldn't recover the clone. Another round of ES cell targeting is needed to be done to get more positive clones to be used for chimaera generation.

Chapter 4: Discussion

Scientists' attention and interest has always been drawn to subjects that are relevant to the health of the human being. With the development of various laboratory techniques such as gene manipulation, cloning or the possibility to duplicate *in vivo* processes *in vitro*, neuroscience and genetics now has a very important impact on medicine and consequently on the individual cases of millions of patients. To find out the underlying mechanisms of pain, the core processes in the development of cancer or, like in our research, to map the molecular interactions involved in learning and memory to help people suffering from neurodegenerative diseases, is an exciting challenge. Here we discuss our results obtained by generation of transgenic animals that have genetically manipulated NMDA receptors. The obvious question is why the NMDA receptor is so interesting. In many neurological and psychiatric conditions the contribution of the NMDA receptor, especially its NR2B subunit plays a very important role. Therefore, the use of various NMDA receptor mutations should generate useful data to then develop novel treatments.

The involvement of the NMDA receptor in Parkinson's disease seems more and more apparent. In animal studies where 6-hydroxydopamine lesion is used to imitate and produce the syndromes of Parkinson's, the NR1 and NR2B subunit expression is decreased (Dunah et al., 2000) and tyrosine phosphorylation of NR2B is decreased. Ifenprodil selectively blocks NR2B containing receptors and if rats with induced Parkinson's are treated then their locomotor activity significantly increases (Nash et al., 1999). Using levadopa, the decrease in the subunit expression and phosphorylation can be reversed (Oh et al., 1998). In another study the levadopa treatment induced hyperphosphorylation of NR1 on serine and of NR2A and NR2B on tyrosine residues (Dunah et al., 2000; Hallett et al., 2005). CP-101,606, a selective antagonist of the NR2B containing NMDA receptors had antiparkinsonian effects on levadopa-induced symptomes by decreasing locomotor disfunction (Steece-Collier et al., 2000). Amantidine, a non-competitive NMDA antagonist, also has anti-

parkinsonic properties providing further evidence for the involvement of the NMDA-connected synaptic plasticity in the development of the disease.

In Huntington's chorea there is also evidence for the involvement of the NMDA receptor. The NR1 and NR2B containing receptors show an increased current (Chen et al., 1999) and both NR1/NR2A and NR1/NR2B receptors produce an increased level of excitotoxic cell death upon glutamate stimulation when coexpressed with the mutant huntingtin protein (Zeron et al., 2001). Hypofunction of the NMDA receptor system produces schizophrenia-like psychotic state in healthy individuals (Olney et al., 1999). Specifically, upregulation of the NR2B subunit appears to mediate the disease (Grimwood et al., 1999). The NR2B subunit of the NMDA receptor is also involved in pain (Chizh et al., 2001). Overexpression of NR2B in forebrain increased the paw-licking behaviour in rats upon peripheral formaline injection (Wei et al., 2001). After producing hindpaw inflammation using complete Freund's adjuvant, NR1, NR2A and NR2B mRNA levels were upregulated (Miki et al., 2002). The NR2B subunit expression is also involved in chronic ethanol exposure suggesting a role in alcohol tolerance, dependence and withdrawal (Nagy, 2004).

In some previous NMDA receptor mutants complete analysis of the animals was not possible because the homozygous mice didn't survive (Forrest et al., 1994; Kutsuwada et al., 1996; Sprengel et al., 1998). The NR1 knockout mice died 8-15 hours after birth due to respiratory failure (Forrest et al., 1994). While the overall neuroanatomy in these animals was normal, the NR1 expression was abolished and the NR2B expression was reduced. The condition could be rescued by ectopic expression of NR1-1a suggesting that the viability is dependent on the level of expression (Forrest et al., 1994; Li et al., 1994; Iwasato et al., 1997). The NR2B knockout mice died perinatally as a result of an impairement in the suckling response (Kutsuwada et al., 1996). Their cardiovascular and respiratory systems were normal, the trigeminal neuronal pattern formation however was impaired (Kutsuwada et al., 1996). The NR2B C-terminal deletion mice also died perinatally. The cause of lethality was suggested to be the lack of protein-protein interactions (Sprengel et al., 1998). The NR2B protein level was decreased by about half, the intracellular

signalling was impaired due to the missing domain and the clustering and synaptic localization of the receptor was impaired (Sprengel et al., 1998; Mori et al., 1998). The various NR2A mutants are viable (Sakimura et al., 1995; Sprengel et al., 1998). Based on these findings, the NR1 and NR2B subunits are thought to play a major role in development, viability, neuronal pattern formation and synaptic plasticity. The aim of this project was to generate novel mutations in the NR2B subunit of the NMDA receptor, specifically in the C-terminal region, ones which disrupt crucial interactions with downstream molecules, but that conserve viability at the same time, to give us the possibility of a thorough analysis.

One of the important molecular interactions involves the E-S/T-X-V motif located at the extreme C-termini of the NR2 subunits. This sequence binds the PDZ domain containing MAGUK proteins such as PSD-95, chapsyn-110 or SAP 102. These further interact with nNOS (Holscher et al., 1997), fyn (Grant et al., 1992) or SynGAP (Chen et al., 1998). Deleting the terminal valine from the binding motif was a candidate for disrupting the interaction of NR2B with PDZ domains without affecting normal expression levels of the protein still producing viable mice. *In vitro* data generated in the laboratory by Dr Holger Husi showed that the valine deletion does in fact disrupt the interaction with PSD-95.

As we predicted the NR2B DelValine homozygous mice were in fact viable and although they had a severe phenotype, they survived to adulthood. The homozygous DelValine mice (J9 or 10 Figure 39 and 40) were runted, appeared smaller than the other littermates when born, their fur was ruffled and the right eye looked small, half closed. By about week 10 they more or less caught up in weight, but developed dermatitis-type skin condition, started scratching and had inflamed eyes and sore ears. This was seen in 21 of the 25 homozygous animals. The heterozygous offsprings showed no apparent phenotypic difference from the wild type littermates. Tests to monitor the body weight of the mice from birth to about 10 weeks old to quantify the differences and make conclusions based on statistical analysis have to be done after obtaining mice in sufficient number.

The homozygous offsprings were set up to breed to check their fertility. A male homozygous mouse was intercrossed with an NR2A$^{\Delta C}$ female. The aim of this cross apart from the fertility check was to obtain mice that have no C-terminal interactions of the NR2B subunit (because of the valine deletion) and of the NR2A subunit either (deletion of the C-terminus). We obtained both male and female offsprings from this intercross (Table 7), which were set up in an intercross to produce the mice explained. We can therefore conclude that the mice carrying the DelValine mutation are fertile and that DelVal 8-8/ NR2A$^{\Delta C}$ double heterozygous mice are viable. Since the NR2A$^{\Delta C}$ and the NR2B DelValine homozygotes are both viable and we hypothesized that the viability is connected to the non-MAGUK interactions of the NR2B C-terminus, we could expect the double homozygous offsprings to survive, too.

While the full analysis of this mutant needs to be carried out, preliminary electrophysiological data on the DelValine mice produced in collaboration with Dr Thomas J O'Dell at the University of California showed reduced LTP compared to wild type using two different induction protocols (Figure 55 and 56). The same reduction can be observed in the case of the NR2A$^{\Delta C}$ mice (Figure 5), but in a frequency-dependent manner (only in the 5Hz/3 min protocol). This suggests that NR2B was in fact prevented from binding to PSD-95, which in turn prevented coupling to SynGAP. The impaired CA1 LTP observed in SynGAP knockout mice (Komiyama et al., 2002) therefore might be dependent on that interaction. If that is so, we would expect that spatial learning will be impaired in our mutant as it was observed in the case of the SynGAP knockouts.

In the NR2B knockout mice the lack of CA1 LTD was reported (Kutsuwada et al., 1996). Since the NR2B C-terminal deletion mice were not viable and no such tests were done in the SynGAP mice either, the DelValine mutants could provide further evidence for the involvement of the particular subunit and the importance of the MAGUK or non-MAGUK interaction in the induction of LTD.

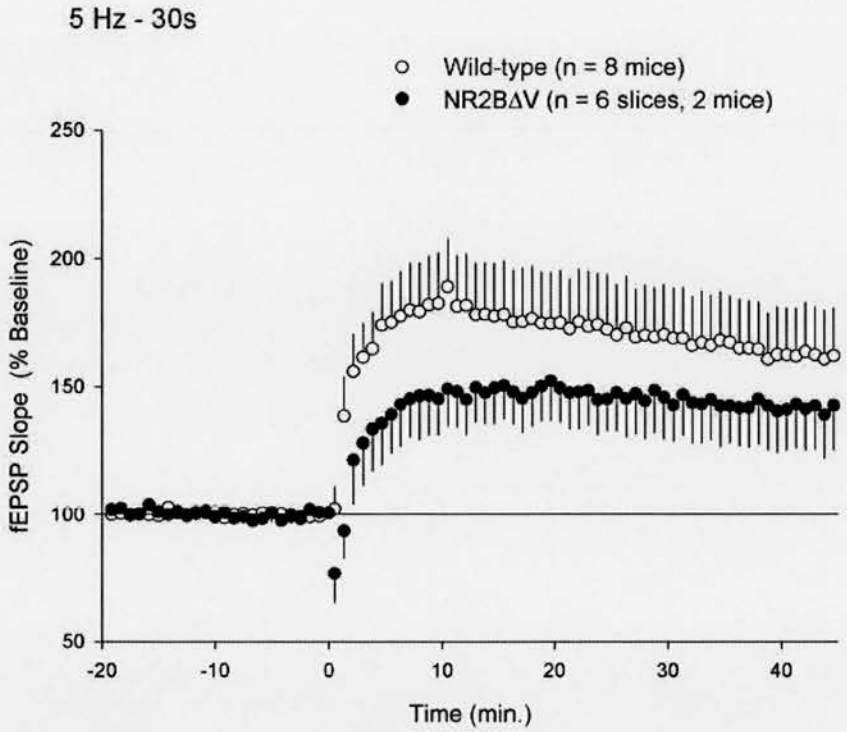

Figure 55. Electrophysiological data of NR2B DelValine mice using the 5Hz/3 min protocol. Hippocampal slices obtained from wild-type and NR2B DelValine mutant mice were prepared using standard techniques. Slices were maintained in interface-type chambers (Fine Science Tools Inc., Foster City, CA, USA) and continuously perfused (at 1 – 2 ml/min) with warm (30 °C), oxygenated ACSF for at least 1 hour prior to an experiment. All recordings were performed in interface-type cambers.
After obtaining a stable, 20 minute long period of baseline synaptic transmission LTP was induced (at time = 0) by a single 30 second long train of 5 Hz stimulation (150 pulses). The average of fEPSPs evoked 40 – 45 minutes post 5 Hz stimulation was used for statistical comparisons (Student t-tests) between wild type and NR2B DelValine mutant mice. The LTP of the mutant mice is significantly reduced compared to wild type. The data was produced by collaborator Dr Thomas J O'Dell.

In the barrel cortex of the NR1 knockouts and the NR2B C-terminal deletion mutants there are no barrel boundaries formed, the cells are distributed uniformly (Iwasato et al., 2000; Sprengel et al., 1998; Mohrmann et al., 2002). This shows that the NMDA receptor activity is required to form maps in the somatosensory cortex. If the barrel formation is dependent on the MAGUK protein interactions of the NR2B subunit then we'll observe similar features in the case of the NR2B DelValine homozygous mice.

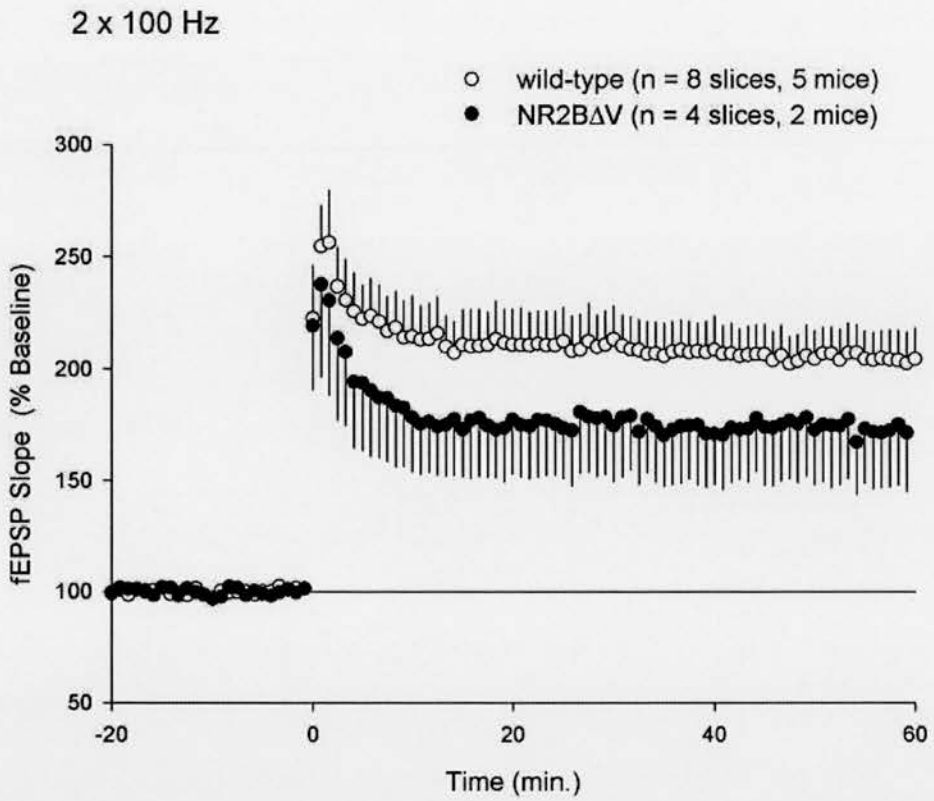

Figure 56. Electrophysiological data of NR2B DelValine mice using the 2X100 Hz protocol. Hippocampal slices were prepared, maintained and experiments were conducted as described before.
At time = 0 LTP was induced by two 1 second long trains of 100 Hz stimulation (inter-train interval = 10 seconds). The LTP of the mutant mice is reduced compared to wild type in this induction protocol as well. The data was produced by collaborator Dr Thomas J O'Dell.

The viability of this mutant suggests that the lethality seen in the NR2B C-terminal deletion mice (suggested to be due to the lack of protein-protein interactions) is not connected to the interaction with the MAGUK proteins via the NR2B C-terminus. It is more likely that interactions with the non-MAGUK proteins (such as CaMKII), binding to other sections of the C-terminus rather than the E-S/T-X-V motif, play an important role in determining viability. The disrupted clustering and synaptic localization of the receptors, observed in the NR2B C-terminal deletion mice (Mori et al., 1998), needs to be checked in the NR2B DelValine homozygous mutants as well. Since the PSD-95 mediated enhancement of NMDA receptor clustering and inhibition of NR2-mediated internalization (Kim et al., 1996; Roche et al., 2001) is blocked by the interruption between PSD-95 and the NR2B subunit of the NMDA

receptor in the NR2B DelValine mice, we can expect similar results that were described in the NR2B C-terminal deletion mutants. The disruption of the NR2B-PSD-95 interaction can be confirmed by immunoprecipitation and subsequent immunoblotting.

Although much is needed to be done to properly characterise this mutant, we made a very important step forward to understand how molecular interactions within the C-terminal domain of the NR2B subunit affect the function of the NMDA receptor by generating viable mutants.

The second mutation was aimed to prevent the binding between NR2B and another highly researched molecule, Ca^{2+}-calmodulin-dependent protein kinase II, a serine/threonine kinase that has been proposed as a molecular switch for memory storage (Lisman, 1985; Lisman et al., 2002). Previously it was shown that the induction of LTP was followed by an increased autonomous activity of CaMKII (Fukunaga et al., 1993) and an increase in autophosphorylation (Fukunaga et al., 1995; Barria et al., 1997; Lengyel et al., 2004). However a recent report indicates that there is only a transient increase in autonomous activity, but a persistent increase in autophosphorylation (Lengyel et al., 2004) suggesting that instead of maintained autonomous activity, molecular interactions might be important for the expression of LTP.

Postsynaptic calcium influx results in the binding of Ca^{2+}/CaM and the activation of CaMKIIα. In this active state neighbouring CaMKIIα subunits can phosphorylate the Thr 286 residue, which enables the molecule to remain activated even after dissociating from Ca^{2+}/CaM, its activator (Miller et al., 1988; Lou and Schulman, 1989). Further sites then become autophosphorylated in the Ca^{2+}/CaM binding domain of CaMKII blocking Ca^{2+}/CaM reassociation. Thr 286 autophosphorylated CaMKIIα is persistently active, translocates to the PSD, binds directly to the NMDA receptor (Strack and Colbran, 1998; Leonard et al., 1999; Bayer et al., 2001) and is necessary for NMDA dependent LTP induction but only at certain synapses such as Schaffer commissural synapses in CA1 region (Giese et al., 1998; Cooke et al.,

2006). AP-5 blocks the glutamate-induced translocation, which suggests that NR2B is necessary for normal function and targeting of CaMKII to the PSD (Shen and Meyer, 1999).

Various mutations have been analysed to test the effects of the disrupted CaMKII-NMDA interaction and CaMKII autophosphorylation, which gave further importance to the production of the proposed novel mutants. In CaMKIIα knockout mice deficient CA1 LTP was observed in the initial experiments (Silva et al., 1992a) however in a later study a significantly reduced LTP was shown which was suggested to be due to the compensatory action of CaMKIIβ (Hinds et al., 1998). In CaMKII T286A autophosphorylation deficient mutants no NMDA receptor dependent LTP was observed (after P9), while LTD was unaffected (Giese et al., 1998; Yasuda et al., 2003). In a recent study it was shown that switching NR2B-containing NMDA receptors, which have high affinity to CaMKII, to NR2A-containing receptors with low affinity to CaMKII reduces LTP in hippocampal slices (Barria and Malinow, 2005). In these transfection studies it was also shown that mutations in the NR2B subunit (NR2B RS/QD) that reduce the association with CaMKII prevent LTP (Barria and Malinow, 2005). To produce mice with similar modifications as in this particular study and obtain *in vivo* data is an exciting option to take these investigations one step further.

The viability of the NR2B DelValine mutant suggests that the lethality seen in the NR2B C-terminal deletion mice is not connected to the interaction with the MAGUK proteins via the C-terminus. The NR2B CaMKII mutants could provide evidence whether it is the interaction with the non-MAGUK protein CaMKII that determines viability. If they are however viable electrophysiological experiments could be conducted to produce further evidence for the involvement of the association between NR2B and CaMKII in some forms of synaptic plasticity.

Apart from testing the NR2B CaMKII mutants in the widely used Morris water maze, various other learning tasks (provided that the mice are viable), such as cued fear conditioning or contextual fear conditioning can be used. It can be potentially

interesting to intercross the NR2B CaMKII homozygous mutants with CaMKII T286A mutants in the view of some recent studies challenging the proposal that CaMKII autophosphorylation is essential in long term memory formation (Discussed in the next paragraphs.). This will result in achieving a prevention of binding via both the substrate binding site, which is proposed to be reversible and Ca^{2+}/CaM-dependent, and the T286-site as well, where a persistent interaction is suggested to be formed (Bayer et al., 2006).

When tested in the Morris water maze the T286A mutants showed impaired spatial long term memory formation (Giese et al., 1998), but this might have been due to their inability to learn the task as suggested by a recent study (Irvine et al., 2005). In these experiments CaMKII T286A mutant mice were tested in different hippocampus- and amygdala-dependent learning tasks, such as passive avoidance task, cued fear conditioning and contextual fear conditioning. After a single training trial the mutants didn't, but after massed training protocol they did form LTM (Irvine et al., 2005) suggesting a dissociation between LTP (T286A mutants are deficient in CA1 LTP.) and LTM in certain protocols. CaMKII autophosphorylation however is needed for LTM formation after a single trial (Irvine et al., 2005). By testing the NR2B CaMKII mutants and the double mutants in these tasks we could provide further insight into the bases of LTM formation. It could be interesting to see whether we observe any differences between the mutants in the massed training protocol induced long-term memory.

Binding of CaMKII to NR2B can occur in two distinct ways. One is the enzyme-substrate binding via the catalytic (active) site of CaMKII resulting in the phosphorylation of NR2B Serine 1303, the other via the non-catalytic site of CaMKII which results in the localization of CaMKII to the PSD (Leonard et al., 1999; Strack et al., 2000; Bayer et al., 2001; Bayer et al., 2006). In the substrate binding site residues 1290-1309 of the NR2B subunit are critical for binding to CaMKII (Leonard et al., 1999). In this region Lys 1292, Leu 1298, Arg 1299, Arg 1300, Glu 1301 and Ser 1303 have been identified essential for binding by site directed mutagenesis (Strack et al., 2000). Phosphorylation of Ser 1303 inhibits binding to CaMKII. Based

on these data we mutated three amino acids, the leucine 1298 to alanine, the arginine 1300 to glutamine and the serine 1303 to asparagine in the CaMKII binding region of the NR2B subunit by which we aimed to prevent the interaction between the two molecules. Blastocyst injections were done using two clones, CaMKII 1-6 and CaMKII 4-12 and we obtained one chimaera from cell line CaMKII 1-6. Further injections are needed to achieve germline transmission.

The third mutation, the NR2A/NR2B COOH exon swapping mutation, was designed based on the observations that the NR2A and NR2B subunits of the NMDA receptor have distinct binding partners, are differentially phosphorylated on their tyrosine and serine residues and through these, they are involved in distinct signalling and physiological processes. The following are a few examples. NR2A-containing NMDA receptors promote, while NR2B-containing receptors inhibit the surface expression of GluR1 (Kim et al., 2005). Developmental replacement of the NR2B subunits by NR2A in the cerebellum during granule cell maturation is crucial for normal motor coordination (Schlett et al., 2004). NR2B subunit expression is increased in cultured hippocampal and cortical neurones after chronic ethanol exposure suggesting a role in alcohol tolerance, dependence and withdrawal (Nagy, 2004). Another example is the possible involvement of these subunits in governing the direction of synaptic strength (Discussed in the next paragraphs.). Deleting the COOH-exon of the NR2B subunit and replacing it by that of the NR2A can highlight the importance of the NR2B subunit in development, viability, neuronal pattern formation and synaptic plasticity and can also to tell whether the interactions mediated by the NR2A C-terminus can rescue the lack of the NR2B subunit C-terminus. The mutation can show the importance of the interactions mediated via the NR2B cytoplasmic tail.

Two hypotheses have been proposed to explain what is governing the direction of synaptic strength, whether it is LTP or LTD elicited. One is that the magnitude and time course of the postsynaptic calcium entry is crucial, with LTP being triggered after a brief increase in intracellular Ca^{2+} concentration with a high magnitude, while LTD expressed after a prolonged low rise in intracellular Ca^{2+} concentration (Bear

and Malenka, 1994; Cummings et al., 1996; Yang et al., 1999). In the other explanation it is proposed that the induction of LTP or LTD is connected to the subunit composition of the NMDA receptor (Liu et al., 2004; Massey et al., 2004). In the hippocampus both NR2A and NR2B subunit-dependent signalling is implicated in long-term synaptic plasticity (McHugh et al., 1996; Kohr et al., 2003). It has been suggested that the NR2A containing NMDA receptors are important in the induction of LTP while NR2B containing receptors are important for LTD in the hippocampus (Liu et al., 2004; Massey et al., 2004). These results were based on pharmacological experiments using selective blockade of the particular subunits. Previous studies however using NR2B overexpressing mice with enhanced CA1 LTP and long-term memory suggested the contribution of NR2B subunits to hippocampal LTP and learning (Tang et al., 1999). The contribution of the NR2B subunit to the induction of LTP was also shown in NR2A knockout mutants, in mice lacking the C-terminus of the NR2A subunit and in pharmacological experiments using NR2A blockers (Kohr et al., 2003; Berberich et al., 2005; Weitlauf et al., 2005). In recent studies it was also shown that NR2B is not involved in LTD induction (Bartlett et al., 2006; Morishita et al., 2006) and it was suggested that it is more likely the mode of how the intracellular Ca^{2+} concentration is increased to be responsible in governing the direction of synaptic strength rather than the subunit composition of the NMDA receptor.

The anterior cingulate cortex (ACC) has been suggested to play a role in remote fear and spatial memory (Maviel et al., 2004; Frankland et al., 2004). Both NR2A and NR2B subunits were shown to be important for LTP induction in the ACC and the NR2B subunit was implicated in mediating contextual fear memory (Zhao et al., 2005). The NR2A/NR2B COOH exon swapping mutation could supply invaluable data to the importance of the particular subunits in the induction of LTP and LTD in the hippocampus and other brain regions as well provided that the mice are viable.

The targeting vector for this interesting mutation is ready for electroporation and further ES cell targeting is essential for obtaining positive clones. Once homozygous

mice are produced a series of experiments (as described before) are possible to conduct, if they are viable.

Additionally to obtain more insight into the process of how the particular NMDA receptor subunits are involved in analgesia, pain, dependence and tolerance, we could chronically treat the three types of mutant mice with morphine to achieve dependence or tolerance and to screen for any alterations in the NR1/NR2 protein levels. Differences in the response to pain after treatment (analysed by hot-plate or tail-flick tests) can also be checked. By developing drugs, that act on the NMDA receptor in a subunit and region specific manner in certain pain-related areas of the brain, a new way of decreasing chronic pain can be developed other than with morphine, which is known to be addictive.

Chapter 5: Appendix

5A Protocols

Techniques related to manipulation of DNA

Preparation of miniprep DNA using Promega's Wizard Plus Minipreps DNA Purification System

1. Inoculate one colony into a 3 ml LB media.
2. Incubate overnight at 37 °C providing appropriate aeration by shaking at 225 rpm.
3. Pellet 1.5 ml saturated culture in an eppendorf tube by spinning in picofuge for 2 minutes (10000 g).
4. Decant supernatant.
5. Add the rest of the culture and spin again.
6. Take off supernatant using Gilson pipette.
7. Resuspend pellet in 200 µl Cell Resuspension Solution (50 mM Tris-HCl pH 7.5, 10 mM EDTA, 100 µg/ml RNase A) by vortexing.
8. Add 200 µl Cell Lysis Solution (0.2 M NaOH, 1% SDS) and invert 4 times to mix.
9. Add 200 µl Neutralization Solution (1.32 M potassium acetate pH 4.8) and invert 4 times to mix.
10. Spin at 14000 rpm for 5 minutes.
11. Transfer the plasmid DNA containing supernatant into an eppendorf tube containing 1 ml of DNA Purification Resin.
12. Invert 4 times to mix.
13. Insert a 2 ml syringe barrel into a Minicolumn and place it into an eppendorf tube. Pour the DNA Resin mixture into the syringe. Insert the plunger and press the solution through the Minicolumn.

14. Remove the plunger and add 2 ml Column Wash Solution (80 mM potassium acetate, 8.3 mM Tris-HCl pH 7.5, 40 μM EDTA, 55% ethanol). Insert the plunger again and press the solution through the Minicolumn.
15. Remove the syringe and spin column at 14000 rpm for two minutes to get rid of residual Column Wash Solution.
16. Transfer Minicolumn into a new eppendorf tube. Add 50 μl TE (10 mM Tris-Cl pH 8.0, 1 mM EDTA) buffer and wait 1 minute.
17. Spin at 14000 rpm for 30 seconds.
18. Store plasmid DNA at –20 °C.

Preparation of midiprep DNA using Qiagen's Plasmid Midi Kit

1. Inoculate a few colonies into 50 ml LB media.
2. Incubate overnight at 37 °C providing appropriate aeration by shaking at 225 rpm.
3. Pellet the saturated culture in a Falcon tube by spinning at 3000 rpm for 15 minutes at 4 °C.
4. Decant supernatant.
5. Spin again for 2 minutes.
6. Take off supernatant using Gilson pipette.
7. Resuspend pellet in 4 ml buffer P1 (50 mM Tris-HCl pH 8.0, 10 mM EDTA, 100 μg/ml Rnase A) by vortexing.
8. Transfer into Falcon 2059 tube.
9. Add 4 ml buffer P2 (0.2 M NaOH, 1% SDS) and invert 4 times to mix.
10. Incubate at room temperature for 5 minutes meanwhile prepare QIA filter cartridge.
11. Add 4 ml buffer P3 (3.0 M potassium acetate pH 5.5) and invert 4 times to mix.
12. Pour mixture into the equilibrated cartridge and incubate for 10 minutes.
13. Prepare column by equilibrating it with 10 ml buffer QBT (750 mM NaCl, 50 mM MOPS pH 7.0, 15% isopropanol, 0.15% triton X-100).

14. Press mixture through the cartridge into the column and allow the column to empty by gravity flow.
15. Wash the column with 10 ml buffer QC (1 M NaCl, 50 mM MOPS pH 7.0, 15% isopropanol) twice.
16. Elute DNA with 5 ml buffer QF (1.25 M NaCl, 50 mM Tris-HCl pH 8.5, 15% isopropanol).
17. Add 3.5 ml isopropanol and invert 4 times to mix.
18. Spin at 8000 rpm for 30 minutes at 4 °C.
19. Take off supernatant carefully.
20. Add 2 ml 70% ethanol.
21. Spin at 8000 rpm for 10 minutes at 4 °C.
22. Take off supernatant and air dry pellet.
23. Resuspend pellet in appropriate amount of TE (10mM Tris-Cl pH 8.0, 1 mM EDTA) buffer.
24. Store plasmid DNA at –20 °C.

Restriction digestion of DNA

1. Perform digests at 1 unit restriction enzyme per μg DNA, in reactions of 50-100 μg/ml DNA.
2. Perform digests in 1x restriction enzyme buffer for 1-2 hours at the recommended temperature.
3. **For vector linearization**: Run approx 200 ng digest alongside uncut DNA on a gel to check digestion. Optional: when digested, inactivate the enzyme by heating to 70 °C 5 minutes in the water bath. If using for ligations with phosphorylated insert, the vector must be dephosphorylated to prevent self-ligation. Do this prior to purification. Otherwise, the linearised vector may be purified by phenol: chloroform extraction and ethanol precipitation.
4. **Otherwise**: Purify DNA fragment of interest by electrophoresis on a 0.8 - 2% agarose gel until the bands are sufficiently separated, and recover the relevant DNA fragment from the gel.

Dephosphorylation of vector DNA

Dephosphorylation of the vector 5' end must be performed to prevent self-ligation of vector digested with only one restriction enzyme.

1. Directly following vector restriction digestion, add 3 units of calf intestinal alkaline phosphatase (CIAP, Boehringer Mannheim) per μg vector DNA.
2. Incubate at 37 °C for 1 hour.
3. Then add 0.5 units CIAP per μg vector DNA.
4. Incubate for 15 minutes at 55°C.
5. Run the entire reaction on a 1% agarose gel to separate vector backbone from stuffer fragment.
6. Recover the dephosphorylated vector from the gel, using phenol: chloroform extraction method. CIAP-treated DNA requires 2x phenol: chloroform extractions (Stratagene Catalogue) to separate the CIAP as it binds strongly to the DNA.

Phenol: chloroform: isoamyl alcohol extraction of DNA

1. Estimate the volume of the DNA solution.
2. Add an equal volume of phenol: chloroform: isoamyl alcohol solution (25:24:1).
3. Vortex (unless purifying genomic DNA, if so invert tube 6 times to minimize shearing).
4. Spin at 14000 *g* for 3 minutes.
5. Remove aqueous top phase to a new tube.
6. Add an equivalent volume of TE (0.1 mM EDTA, 10 mM Tris-HCl pH 8) to the phenol phase, vortex and spin again.
7. Remove the aqueous layer to a new tube to ensure maximum DNA recovery.
8. Ethanol precipitate the DNA.

Ethanol precipitation of DNA

1. Estimate the volume of the DNA solution.
2. Add 3 M potassium acetate (pH 5.2) to a final concentration of 0.3 M.
3. Mix well.
4. Add 2 volumes -20 °C ethanol and mix the solution well. Store the solution in the -70 °C freezer to allow DNA precipitation for 15-20 min or snap freeze in liquid nitrogen.
5. Mix well.
6. Recover the DNA by spinning at 4 °C for 10 min at 14000g (10,500rpm SS-35).
7. Carefully remove the supernatant
8. Fill the tube half way up with ice cold 70% ethanol and spin at 14000*g* for 2 minutes at 4°C (10 500rpm SS-35).
9. Carefully remove the supernatant.
10. Air-dry the pellet at room temperature.
11. Dissolve DNA pellet in the desired volume of TE.
12. After phenol: chloroform: IAA DNA extraction and ethanol precipitation, DNA recovery should be above 80%.

Recovery of DNA from agarose gels (phenol method)

1. Excise DNA bands from the gel using a sterile blade.
2. Estimate volume and double with TE buffer. Melt at 65°C for 5-10 minutes.
3. Add 1 volume of Tris-buffered phenol at room temperature and mix by inversion.
4. Centrifuge for 3 minutes at 10-12000 rpm.
5. Transfer aqueous phase to a new tube. Repeat phenol extraction step.
6. Centrifuge for 3 minutes at 10-12000 rpm.

7. Transfer aqueous phase to new tube containing 0.1 volume of 4M lithium chloride solution.
8. Mix by inversion; a white precipitate forms immediately.
9. Place tube on ice for 2 minutes.
10. Centrifuge for 3 minutes at 10-12000 rpm.
11. Transfer aqueous phase to new tube leaving behind a transparent pellet.
12. Add 1µl of carrier (glycogen) and precipitate with 2.5 volumes of cold ethanol.
13. Mix, leave at -70°C 5-10 minutes or snap freeze in liquid nitrogen and spin as previously (10-12000 rpm) for 10 minutes.
14. Wash the pellet with 1ml 70% ethanol then dry under vacuum or air-dry.
15. Resuspend in 10-20µl of deionised water or TE buffer.
16. Check DNA recovery using the GeneQuant.

Recovery of DNA from agarose gels using BIO101 Geneclean Spin Kit

1. Excise DNA bands from the gel using a sterile blade and place it into a Geneclean Spin Filter.
2. Add 400 µl Geneclean Spin Glassmilk. Melt at 65°C for 5-10 minutes. Invert every minute.
3. Centrifuge for 2 minutes at 10-12000 rpm.
4. Empty tube and add 500 µl Geneclean Spin New Wash to the filter.
5. Centrifuge for 30 seconds at 10-12000 rpm then empty the tube.
6. Spin for 2 minutes to get rid of residual wash solution.
7. Place the Spin Filter into an empty Catch Tube and add 11 µl TE buffer. Incubate for 1 minute and spin for 30 seconds at 10-12000 rpm.
8. Add an additional 11 µl TE buffer. Incubate for 1 minute and spin for 30 seconds at 10-12000 rpm.
9. Check DNA recovery using the GeneQuant.
10. Store the DNA at –20 °C.

Ligation of insert and vector

1. Ligate vector and insert in reactions containing 50ng or 100ng vector. Vary insert: vector ratios from 1:1 to 5:1.
2. Perform control reactions for each ligation:
    - No insert DNA control - to assay for re-ligation of the digested vector.
    - No DNA control – to monitor ligation reagents for contaminants.
    - Competent cells only - check for contaminating plasmids.
    - Without ligase - to monitor for background level.
3. Set up ligation reactions containing 3 units T4 DNA ligase (Promega) in 1x ligase buffer.
4. Incubate on ice, allowing ice to melt to room temperature overnight (or at 10°C overnight).
5. Transform competent *E. coli* cells with ligation mixture.

Preparation of chemical competent cells

1. Spread DH5α cells onto a bacterial plate from glycerol stock-solution kept at –20 °C.
2. Incubate overnight at 37°C.
3. Inoculate a few colonies into a 50 ml LB media-containing beaker.
4. Incubate overnight at 37 °C providing appropriate aeration by shaking at 225 rpm.
5. Dilute the saturated culture 100X in to 10 ml of fresh LB media.
6. Incubate at 37 °C while shaking at 225 rpm until the optical density reaches 0.6-0.7.
7. Put on ice for 5 minutes.
8. Spin at 3000 rpm for 15 minutes in cold room.
9. Decant supernatant.
10. Spin at 3000 rpm for 5 minutes in cold room.

11. Take off the rest of the supernatant using Gilson pipette.
12. Dissolve the pellet in 1 ml 10 mM $CaCl_2$ solution by shaking then add up to 10 ml.
13. Put on ice for 1 hour.
14. Spin at 3000 rpm for 15 minutes in cold room.
15. Decant supernatant.
16. Resuspend pellet in 1 ml 10 mM $CaCl_2$ solution.
17. Use 100 µl cell suspension per transformation.

Transformation of chemical competent cells

1. Add 5µl of DNA ligation mix to a 100µl aliquot of competent cells or use 30ng DNA if growing up stock plasmid.
2. Incubate on ice for 20 minutes.
3. Heat shock the cells at 42°C for 1 minute to allow DNA uptake by the cells.
4. Incubate on ice for 5 minutes.
5. Add 900µl of SOC medium (1.5mL SOB base; 7.5µl 2M $MgCl_2$; 30µl 1M glucose) to the cells.
6. Shake tubes at 225rpm for 45 minutes at 37°C to allow expression of the ampicillin resistance gene.
7. **For vector stock transformations**: spread 50-100µl of the culture onto L-agar plates containing appropriate antibiotics.
8. **For ligation reactions**: pellet cells by spinning at 3000rpm for 2 minutes; resuspend cells in 100-200µl of the supernatant and plate out using 100µl stock.

Preparation of electro competent cells

1. Spread DH5α cells onto a bacterial plate from glycerol stock-solution kept at –20 °C.
2. Incubate overnight at 37°C.

3. Inoculate a few colonies into a 50 ml LB media-containing beaker.
4. Incubate overnight at 37 °C providing appropriate aeration by shaking at 225 rpm.
5. Dilute the saturated culture 100X by adding 2,5 ml solution to 250 ml of fresh LB media.
6. Incubate at 37 °C while shaking at 225 rpm until the optical density reaches 0.6-0.7.
7. Put on ice for 30 minutes.
8. Pour solution into 4 Falcon tubes, each containing 45 ml.
9. Spin at 3000 rpm for 15 minutes in cold room.
10. Decant supernatant and add the rest of the culture solution.
11. Spin at 3000 rpm for 15 minutes in cold room.
12. Decant supernatant.
13. Spin at 3000 rpm for 5 minutes in cold room.
14. Take off the rest of the supernatant using Gilson pipette.
15. Dissolve the pellet in 5 ml 10% glycerol solution by shaking then add glycerol up to 45 ml (per tube).
16. Spin at 3000 rpm for 5 minutes in cold room.
17. Decant supernatant.
18. Repeat step 15-17 once more.
19. Resuspend pellet into 150 µl of 10% glycerol solution/tube.
20. Merge the contents of the four tubes.
21. Aliquot solution into 0.5 µl eppendorf tubes, 40 µl each.
22. Snap freeze tubes in liquid nitrogen.
23. Store at –80 °C.

Transformation of electro competent cells

1. Thaw an aliquot of electro competent cells on ice.
2. Add 5µl of DNA ligation mix to a 40µl aliquot of competent cells or use 30ng DNA if growing up stock plasmid.

3. Put cell-DNA mixture into prechilled Gene Pulser (BioRad) cuvettes.
4. Electroporate at 25 μF, 200 Ω, 2,5 kV.
5. Add 900μl of SOC medium (1.5mL SOB base [2% tryptone, 0.5% yeast extract, 10mM NaCl]; 7.5μl 2M $MgCl_2$; 30μl 1M glucose) to the cells.
6. Shake tubes at 225rpm for 45 minutes at 37°C to allow expression of the ampicillin resistance gene.
7. **For vector stock transformations**: spread 50-100μl of the culture onto L-agar plates containing appropriate antibiotics.
8. **For ligation reactions**: pellet cells by spinning at 3000rpm for 2 minutes; resuspend cells in 100-200μl of the supernatant and plate out using 100μl stock.

Sequencing reaction for automated sequencer

1. Prepare the reaction mixture in total of 10 μl.
    - 0.5 μg DNA template
    - 1 μl of 3.2 pmol/μl primer
    - 4 μl Big Dye Terminator Ready Reaction Mix
    - dH_2O up to 10 μl
2. Add a drop of mineral oil to tube.
3. Run sequencing reaction.
    - 96 °C, 30 seconds
    - 50 °C, 15 seconds
    - 60 °C, 4 minutes
    - Repeat 25 times.
4. Add 10 μl dH_20 to reaction mixture and remove from under the mineral oil.
5. Add 2 μl 3 M sodium acetate pH 4.6 and 50 μl 95% ethanol.
6. Mix and incubate on ice for 15 minutes.
7. Spin at 14000 rpm for 20 minutes increasing the speed gradually.
8. Remove the supernatant using Gilson pipette.

9. Add 120 µl 70% ethanol.
10. Spin at 14000 rpm for 5 minutes.
11. Remove supernatant.
12. Air dry pellet.
13. Resuspend pellet in 4 µl ABI loading buffer (deionised formamide and 25 mM EDTA pH 8.0 containing 50 mg/ml Blue dextran in a ratio of 5:1 formamide to EDTA/Blue dextran).
14. Sequence in ABI PRISM 310 Genetic Analyzer.

Southern Blot

Preparation of filter

1. Digest genomic DNA with the appropriate high concentration enzyme overnight.
2. Add a small amount of extra enzyme and further incubate for 6-8 hours to ensure complete digestion.
3. Run samples on an agarose gel containing no ethidium bromide at 12-18V overnight.
4. Stain and photograph the gel as normal; do not forget to put a ruler by the side of it.
5. Cut off one corner of the gel as an orientation marker.
6. Immerse the gel in 0.2N HCl for 10 minutes then rinse with dH_2O.
7. Immerse the gel in 0.5M NaOH; 1.5M NaCl for 45min. A change of buffer is useful. Rinse with dH_2O.
8. Immerse the gel in 1M Tris-Cl pH 7.4; 1.5M NaCl for 30min. A change of buffer is useful. Rinse with dH_2O.
9. Place the gel on a gel tank turned upside down, which was previously covered with a layer of dH_2O and Saran wrap in a way that no air bubbles are present.
10. Cut a piece of nitrocellulose (Hybond^{TM}-N) to the same dimensions as the gel and give it an orientation marker.

11. Place the nitrocellulose carefully onto the gel making sure that no air bubbles are trapped between the two.
12. Cut a piece of 3mm Whatman filter paper to the same dimensions as the gel and place it on top.
13. Cut a stack of Kleenex paper to the same dimensions as the gel so that it stands at 10-15cm high.
14. Place a gel tray on top of the stack and put a small weight on he top. Leave overnight at room temperature.
15. Remove the sheets of paper with forceps, remove the filter crosslink the DNA to the filter using UV.

Prehybridization

1. Prewarm the hybridization tube to 65 °C.
2. Prepare the prehybridization solution and put it into the tube.
    - 27 ml of 6X SSC and 0.5% SDS
    - 3 ml of 50X Denhardts (BSA, Ficoll, PVP)
    - 300 µl of Salmon Testes DNA previously fragmented by boiling at 100 °C for 5 minutes and placing it on ice for 2 minutes.
3. Soak the filter in 20X SSC and place it into the hybridization tube with the DNA facing to the inside of the tube. Ensure that no air bubbles are present between the tube and the filter.
4. Rotate at 65 °C for 4 hours.

Probing the filter

1. Dilute the DNA probe to be labelled to a concentration of 2.5-25 ng/45 µl in TE buffer.
2. Denature the DNA by heating to 95-100 °C for 5 minutes in water bath.
3. Place the tube on ice for 5 minutes.

4. Add the DNA to the reaction tube of Rediprime™ II, random prime labelling system (Amersham Pharmacia).
5. Add 5 µl Redivue [^{32}P] dCTP and mix.
6. Incubate at 37 °C for 10 minutes.
7. Add 5 µl 0.2 M EDTA to stop the reaction.
8. Add the reaction mixture to a ProbeQuant G-50 Microcolumn, which has been previously prepepared (snap off bottom of column and spin at 3000 rpm for 1 minute.)
9. Spin column at 3000 rpm for 1 minute.
10. Denature the labelled DNA by heating to 95-100 °C for 5 minutes in water bath.
11. Place the tube on ice for 5 minutes.
12. Add probe to hybridization solution.
13. Rotate at 65 °C overnight.

Washing the filter

1. Leave the filter in the tube and discard the hybridization solution.
2. Rinse the filter with 65 °C wash buffer 1 (2X SSC, 0.5% SDS). Add 30 ml wash buffer 1 and rotate at 65 °C for 10 minutes.
3. Repeat step 2.
4. Add 30 ml wash buffer 2 (1X SSC, 0.25% SDS) and rotate at 65 °C for 15 minutes.
5. Discard wash buffer two and wash with buffer 3 (0.5X SSC, 0.1% SDS) if background is still high.
6. Wrap filter in Saran wrap while still damp.
7. Place into a cassette and put Kodak X-ray film over it in the dark room.
8. Leave at –80 °C to expose.
9. Develop the film.

Preparation of high molecular weight (HMW) DNA from mouse tails

1. Earmark mouse at three weeks of age.
2. Cut half an inch of tail into 750 µl of tail buffer (50 mM Tris pH 8.0, 1 mM EDTA, 1 mM NaCl, 1% SDS).
3. Add 30 µl of 10 mg/ml Proteinase K.
4. Mix and incubate in rotator at 55 °C overnight.
5. Add 20 µl of 30 mg/ml RNAse A and incubate in water bath at 37 °C for 1 hour.
6. Add 500 µl of phenol, mix and rotate overnight at 4 °C.
7. Spin in microfuge at 14000 rpm for 5 minutes.
8. Transfer aqueous top layer and interphase into new tube.
9. Add 500 µl of phenol: chloroform: isoamyl alcohol solution (25:24:1).
10. Rotate for 4 hours at 4 °C.
11. Spin in microfuge at 14000 rpm for 5 minutes.
12. Transfer aqueous top layer into new tube.
13. Add 500 µl of chloroform: isoamyl alcohol solution (24:1).
14. Rotate for 4 hours at 4 °C.
15. Spin in microfuge at 14000 rpm for 5 minutes.
16. Transfer aqueous top layer into new tube.
17. Add 1 ml of isopropanyl alcohol and invert to mix. Precipitation of fibrous HMW DNA can be observed.
18. Spool DNA with a yellow tip and dip briefly into 70% ethanol.
19. Place DNA into 100 µl of TE pH 7.4.
20. Allow the DNA to resuspend overnight at 4 °C.
21. Store at 4 °C.

NR2A$^{\Delta C}$ genotyping

1. Prepare the mastermix and dispense 48 µl per tube.
    - 5 µl 10X buffer

- 5 µl DMSO
- 1 µl 10mM dNTP's
- 1 µl 40 µM primer Rsp10
- 1 µl 40 µM primer Rsp 26
- 34.75 µl dH_2O
- 0.25 µl Qiagen Hot Star Taq added last after 2.5 minute UV zap of mastermix.

2. To precipitate out SDS put tails on dry ice for 1 minute.
3. Spin at 14000 rpm for 15 minutes in cold room.
4. Place tubes on ice and take 2 µl from the top layer of each sample and add to PCR reaction.
5. Run samples on Hybaid PCR machine.
    - 15 minutes at 95 °C then
    - 30 seconds at 94 °C
    - 1 minute at 57 °C
    - 3 minutes at 72 °C X 40 cycles.

NR2B$^{\Delta C}$ genotyping

1. Prepare the mastermix and dispense 48 µl per tube.
    - 5 µl 10X buffer
    - 1 µl 10mM dNTP's
    - 1 µl 40 µM primer NR2B-1
    - 1 µl 40 µM primer NR2B-3
    - 39.75 µl dH_2O
    - 0.25 µl Qiagen Hot Star Taq added last after 2.5 minute UV zap of mastermix.
2. To precipitate out SDS put tails on dry ice for 1 minute.
3. Spin at 14000 rpm for 15 minutes in cold room.

4. Place tubes on ice and take 2 µl from the top layer of each sample and add to PCR reaction.
5. Run samples on Hybaid PCR machine.
    - 15 minutes at 95 °C then
    - 20 seconds at 94 °C
    - 30 seconds at 55 °C
    - 1 minutes at 72 °C X 35 cycles then
    - 10 minutes at 72 °C.
6. The homozygous band is 1311 bp, the WT band is 136 bp.

NR2B DelValine genotyping

Reaction using Qiagen Hot Star Taq

1. Prepare the mastermix and dispense 48 µl per tube.
    - 5 µl 10X buffer
    - 1 µl 10mM dNTP's
    - 1 µl 40 µM primer 1
    - 1 µl 40 µM primer 2
    - 39.75 µl dH_2O
    - 0.25 µl Qiagen Hot Star Taq added last after 2.5 minute UV zap of mastermix.
2. To precipitate out SDS put tails on dry ice for 1 minute.
3. Spin at 14000 rpm for 15 minutes in cold room.
4. Place tubes on ice and take 2 µl from the top layer of each sample and add to PCR reaction.
5. Run samples on Hybaid PCR machine.
    - 15 minutes at 95 °C then
    - 20 seconds at 94 °C
    - 30 seconds at 65 °C
    - 2 minutes at 72 °C X 35 cycles then

- 10 minutes at 72 °C.

Long Range PCR

1. Prepare mastermix A.
    - 20 µl dH_2O
    - 0.6 µl 25mM dNTP's
    - 2 µl 20 µM primer 1
    - 2 µl 20 µM primer 2
2. Prepare mastermix B.
    - 16 µl dH_2O
    - 5 µl buffer 1
    - 1 µl expand enzyme (Roche) was added after hot start of reaction.
3. To precipitate out SDS put tails on dry ice for 1 minute.
4. Spin at 14000 rpm for 15 minutes in cold room.
5. Place tubes on ice and take 2 µl from the top layer of each sample to 2 µl of dH_2O.
6. Add 25 µl of mastermix A, 20 µl of mastermix B, mix and start reaction.
7. Run samples on Eppendorf PCR machine.
8. 30 seconds at 93 °C then pause and incubate at 93 °C for 15 minutes. Add 1 µl expand enzyme per sample. Restart reaction.
    - 10 seconds at 93 °C
    - 30 seconds at 60 °C
    - 2 minutes at 65 °C X 10 cycles then
    - 10 seconds at 93 °C
    - 30 seconds at 60 °C
    - 2 minutes at 65 °C with 20 seconds of increment X 20 cycles then
    - 7 minutes at 68 °C.

Primers

A: NR2B 5910 A': SWAP NR2A 3924

B: pLox 413 B': pLox 91

C: pLox 1540 C': pLox 1603

D: NR2B 6456 D': NR2B 8035

Analysis of results

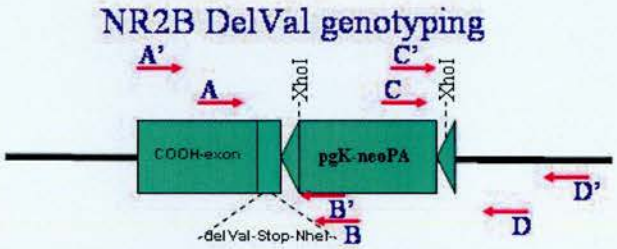

Genotype / Primers and PCR reaction	Wild Type	Heterozygous	Homozygous
A X B **Taq polymerase**	NO AMPLIFICATION	~ 0.5 KB BAND AMPLIFIED	~ 0.5 KB BAND AMPLIFIED
A' X B' **Taq polymerase**	NO AMPLIFICATION	~ 2.3 KB BAND AMPLIFIED	~ 2.3 KB BAND AMPLIFIED
C X D **Taq polymerase**	NO AMPLIFICATION	~ 0.5 KB BAND AMPLIFIED	~ 0.5 KB BAND AMPLIFIED
C' X D' **Taq polymerase**	NO AMPLIFICATION	~ 2.0 KB BAND AMPLIFIED	~ 2.0 KB BAND AMPLIFIED
A X D **Taq polymerase**	~ 0.5 KB wt BAND AMPLIFIED	~ 0.5 KB wt BAND AMPLIFIED	NO AMPLIFICATION
A X D **Long Template PCR**	~ 0.5 KB wt BAND AMPLIFIED	~ 0.5 KB wt AND 2.3 KB homo BAND AMPLIFIED	~ 2.3 KB homo BAND AMPLIFIED

Tissue culture of embryonic stem cells

Stock Solutions

1X GMEM

PBS

Glutamine/Pyruvate

Non-essential Amino Acids

ß-Mercaptoethanol

Testers

Leishmans Stain

Mitomycin 'C'

LIF	HAT (50X)
Foetal Calf Serum	G418
1% Gelatin	
Trypsin	

Plastics

The main supplier of tissue culture is Iwaki from Bibby Sterilin. Other suppliers used are Falcon, Corning and Nunc.

150 cm^2 Flasks	IWAKI	1 ml Cryotubes	NUNC
75 cm^2 Flasks	IWAKI	150 ml Tubes	CORNING
25 cm^2 Flasks	IWAKI	15 ml Tubes	CORNING
96 Well Plates	IWAKI	30 ml Universals	BIBBY STERILIN
48 Well Plates	NUNC	150 mm Dishes	IWAKI
24 Well Plates	IWAKI	100 mm Petri Dish	BIBBY STERILIN
12 Well Plates	IWAKI	60 mm Petri Dish	BIBBY STERILIN
6 Well Plates	IWAKI	30 mm Petri Dish	BIBBY STERILIN
4 Well Plates	NUNC	1 Well IVF Dish	FALCON
100 mm Dishes	IWAKI	Electroporation Cuvette	BIORAD
100 mm Dishes	NUNC	Micro-pipett Tips	ALPH
60 mm Dishes	CORNING	12.5 cm^2 Flasks	FALCON

Media preparation

1X GMEM	380 ml
Non-essential Amino Acids	4 ml
Glutamine+Sodium Pyruvate	8 ml
ß-Mercaptoethanol	400 µl
Foetal Calf Serum	40 ml

All media should be prepared in the Class II cabinets using sterile technique. Once the media has been prepared a TESTER should be set up (5ml of media should be added to the 5ml tester) and incubated overnight to ensure sterility. Do not use media if more than one month old.

Thawing embryonic stem cells

1. Place 9.5 ml of prewarmed media in a universal.
2. Retrieve cells from the liquid nitrogen. It is important that cells are thawed as quickly as possible, this is done by placing them in the 37°C water bath.
3. Once they are thawed transfer cells to the warm media to dilute out the DMSO in which the cells are frozen. The cells are transferred to the universal using a plugged pasteur pipette.
4. Spin cells down in the bench centrifuge, at 1000rpm for 5 minutes.
5. The media is then aspirated off very carefully to avoid disturbing the cell pellet.
6. Resuspend cell pellet in 10 ml (or other adequate amount) of prewarmed media gently, as they are very fragile at this stage.
7. Transfer to appropriate flask followed by gassing with a CO_2/air mixture (5%/95%).
8. The cells are checked under the microscope and then placed in the incubator.
9. Cells should be thawed first thing in the morning and then the media should be changed at the end of the day. This removes any dead cells and dilutes out the rest of the DMSO.

Passaging embryonic stem cells

1. Draw off media using aspirator.
2. Add 5 ml of PBS down opposite side of the flask from the cells.
3. Wash cells then draw off PBS using aspirator.
4. REPEAT steps 2 + 3.

5. Add 1ml of trypsin down opposite side of the flask (Use 0.5 ml trypsin for 1 well of a 6 well plate or 4 drops of trypsin for 1 well of a 24 well plate.). Ensure trypsin covers cell monolayer. Recap flask and place in the incubator for approx. 30 seconds*.
6. Tap flask to dissociate the cells.
7. Check under microscope to ensure cells have dissociated..
8. Add 4 ml of media for 1ml of trypsin. The media will stop the action of the trypsin.
9. Transfer cells to a universal and spin down in the bench centrifuge. 5 minutes at 1200rpm.
10. Resuspend cells in 5 ml of media, pipetting up and down 2 or 3 times to ensure a single cell suspesion. Count cells using haemocytometer.
11. Add 10^6 cells to a $25cm^2$ gelatinised flask. The number of cells added to larger flasks should be adjusted accordingly.

A guide for quantity of media to the size of flask is as follows:

- 10 ml/$25cm^2$ flask
- 30 ml/$75cm^2$ flask
- 50 ml/$150cm^2$ flask

1. For fibroblast cell lines use half the stated quantity of media.
2. For ES cells add 1 ul of LIF / ml of media in the flask to get a final concentration of 1000 unit LIF/ ml media. Gas flask with 5%CO_2/95% air mixture and close lid tightly. Return to incubator.

Freezing embryonic stem cells

1. Prepare freezing solution: 10% DMSO in culture media. (Add 2 ml of DMSO to 18 ml of media to provide a stock solution.)
2. Trypsinise as for normal cultures.

3. Once cells have dissociated resuspend in 8.5 ml culture media and place in a universal.
4. Spin cells in bench centrifuge at 1200rpm for 5 minutes.
5. Aspirate off supernatant carefully to prevent disturbing the cell pellet.
6. Resuspend in appropriate volume of freezing solution. Mix gently.
7. Place 0.5ml cell suspension in cryotube, labelled with cell line name, passage number, date, and your initials. The number of vials per flask is dependent on the size of the flask:
    - $25cm^2$ flask gives 2 vials
    - $75cm^2$ flask gives 4-5 vials
    - $150cm^2$ flask gives 8-10 vials
8. Place the cryotubes in the $-80^{o}C$ freezer overnight and then transfer to cellbank the following day.

Embryonic stem cell electroporation

1. 150μg of vector was linearised with NotI, precipitated, washed with 70% ethanol and resuspended in 100 μl PBS the night before electroporation.
2. E14TG2a cells were grown up from frozen stock to yield ~ 5×10^7 cells (4-6 large- 150 cm^2 tissue culture flasks).
3. Trypsinise cells as usual and resuspend in 5 ml PBS per universal.
4. Combine cells and spin once more at 1200 rpm for 5 minutes.
5. Resuspend final pellet in a volume of PBS that will give about $1X10^8$ cells/600 μl.
6. Using plugged pipette add cells to electroporation cuvette.
7. Add the 100 μl DNA solution and mix gently.
8. Place the cuvette in the gene pulsar and electroporate at 0.8 kV, 3μF. Time constant should be 0.1 second.
9. Incubate mixture in cuvette at room temperature for 10 minutes.
10. Add 20 ml media and plate cells in 10cm tissue culture dishes at densities of 5×10^6, 10^6, 5×10^5 and 10^5 cells per plate.

11. G418 selection (200 μg/ml) was added one day after electroporation and selection was continued for 10 days.
12. Pick a large number of colonies 10-12 days after electroporation and grow them up in 24 well plates.
13. Split the confluent wells to generate one plate to freeze for later expansion of cell line and a duplicate plate from which DNA was extracted for analysis by Southern blotting.

Picking colonies

1. Add 2 drops of trypsin or media from plugged Pasteur into alternate rows of 96 well plates.
2. Choose well separated colonies and circle each on the underside of the plate.
3. Wash plate with PBS twice.
4. Add 5 ml PBS.
5. Use a p200 Gilson pipette set to 50 μl and pick up the colony by scraping it off the plate and drawing it into the pipette tip.
6. Place the colony into the prepared 96 well plate and dissociate.
7. Transfer it into 1 well of a 24 well plate and add 1.5 ml media.

Extraction of genomic DNA from embryonic stem cells in culture

Extraction Buffer:
0.1M EDTA
0.2M NaCl
0.05M Tris-HCl pH 8
0.5% SDS
50μg/ml DNase-free RNase
Never vortex HMW DNA!

Large scale extraction:

1. Grow up 10^8 cells as a monolayer or in suspension as required. Yield from 10^8 cells should be approximately 300μg.
2. For monolayer culture: decant the medium and rinse the cells twice in PBS. Recover the cells by trypsinisation for ES cells. Quench trypsin with media and transfer cells to 50ml Falcon tube.
3. For suspension culture: transfer cells to 50ml Falcon tube.
4. Centrifuge at 500 g for 10 minutes.
5. Resuspend cell pellet in 10ml PBS by gentle pipetting.
6. Centrifuge at 500 g for 10 minutes.
7. Resuspend cell pellet in 20 ml Extraction Buffer.
8. Add Proteinase K to 100 μg/ml and gently swirl the tube to mix the components. Incubate the tube in the water bath for 3 hours, gently inverting the tube every 20 minutes. Then put the tube on a roller or a wheel overnight at RT (or 37 °C if possible). The solution should be reasonably clear and viscous at the end of the incubation. More Proteinase K may be added to achieve this (add more Proteinase K to 200 μg/ml and incubate again).
9. Transfer to a large beaker. Add 20 ml of pre-equilibrated phenol: chloroform: IAA (first check pH = 8) and seal with parafilm. Gently swirl by hand 10-15 min to mix the two phases. The larger the surface area available, the easier this will be. Ideally you should achieve an emulsion at this stage.
10. Transfer the mixture to a 50 ml disposable plastic tube and centrifuge at 1500 g for 10 min at RT to separate the phases.
11. Remove the aqueous phase into a new tube using a cut-off (to widen the bore) 5 ml disposable pipette tip. Care must be taken not to disturb the interface and when DNA is very viscous this is hard to achieve
12. Steps 8-10 should be repeated to accomplish at least three extractions. The aqueous phase should be clear at this point.
13. Dialyse the aqueous phase against 1000 volume of TE. This should be performed for 30 min at RT to prevent SDS precipitation in the sample followed by overnight at 4°C. Allow room for expansion in dialysis bag.

14. The absorbance of DNA at 260nm and 280nm should be measured using quartz cuvettes. The $^{260}/_{280}$ ratio should be >1.8. If this is not the case, repeat steps 4-9 adding additional SDS to 1%. An A_{260} of 1.0 in a 1cm light path is equivalent of a DNA concentration of 50 µg/ml. Store the DNA at 4 °C.
15. An aliquot of the DNA should be analysed by electrophoresis through a 0.3% gel agarose gel. Multimers of bacteriophage lambda or commercially available DNAs can serve as mol wt markers. The prepared DNA is normally at least 100 kb and preferably exceeds 200 kb.

Extraction from 24 well plate:

1. Use 500 µl of extraction buffer/well.
2. Extract overnight at 37 °C as normal.
3. Use 500 µl phenol then 500 µl phenol: chloroform: IAA for cleaning of DNA.
4. Proceed as before and resuspend DNA in 100 µl TE buffer.

5B Primer Sequences

Name	Sequence (5' to 3')	Nucleotides	Melting Temperature °C
DelValMut 1	CTTTCTAGTATTGAGTCTGATTAGCTAGC	53	78.5
	TCGAGTGAGGGAAGAGAGAGAGAG		
DelValMut 2	CTCTCTCTCTCTTCCCTCACTCGAGCTAG	53	78.5
	CTAATCAGACTCAATACTAGAAAG		
DelVal 1	GGAGACCACAACGGTTTCCCTCTA	24	69.9
DelVal 2	GGCAGGGGCGTCGAAAACAAGG	22	75.9
DelVal 3	CCCCCGACTCTTTCCGTGACAT	22	72.1
DelVal 4	CTTTGTTAGCAGCCGGATCG	20	66.7
DelVal I	TCCCGCGAAATTAATACGATACA	23	66.2
DelVal II	AACAAGTCCTCAGTGACCACTGCC	24	69.6
DelVal III	GGCAGTGGTCACTGAGGACTTGTT	24	69.6

Name	Sequence (5' to 3')	Nucleotides	Melting Temperature °C
DelVal IV	GGACAGACGCGGGAAGAAGAGAAC	24	71.8
DelVal V	GTTCTCTTCTTCCCGCGTCTGTCG	24	72.7
DelVal VI	CAAGACCCGTTTAGAGGCCCAAG	23	72.7
DelVal 358	GACCTAGTTGACAGACCCACGT	22	64.2
DelVal 3261	TTTCCCTCTGACCTTTTCTGCT	22	65.1
DelVal 6102	CAACAAAAACCCCAGGGC	18	65.2
DelVal 6211	CCCTCCCGCACCCACCTT	18	71.8
DelVal 6662	CCCCTCAGCAGATGCCAACC	20	71.2
DelVal 7914	TCACACAGGGTGGCGTCCAAAG	22	73.4
Polylinker DelVal 1	CTAGATGCGTCGCCATATGTGCGTCGCG	28	81.2
Polylinker DelVal 2	AATTCGCGACGCACATATGGCGACGCAT	28	81.5
Polylinker Del XhoI-1	ACATCTGACG	10	22.1
Polylinker Del XhoI-2	TCGACGTCAGATGTGTAC	18	55.0
NR2B 5'-1	CCTGGAATAGAAAGAGCACTGCCC	24	69.6
NR2B 5'-2	GGACCTAGTTGACAGACCCACGT	23	67.3
5 PGEX	GGGCTGGCAAGCCACGTTTGGTG	23	78.5
3 PGEX	CCGGGAGCTGCATGTGTCAGAGG	23	75.9
BAMC	GGGCCCGGATCCCGGTATCTACAGCTG	42	86.0
	TATCCACGGAGTAGC		
CECO	CCCGGGGAATTCTCAGACATCAGACTC	43	78.4
	AATACTAGAAAGTTTC		
DelVal 7897	GCTGCCCTGCCCTCCCCTCACACA	24	81.1
DelVal 7898	CTGCCCTGCCCTCCCCTCACAC	22	76.9
BAMC 1	GGGCCCGGATCCCCGGTATCTACAGCT	43	87.0
	GTATCCACGGAGTAGC		
BAMC 2	GGGCCCGGATCCCCAAGGACAGCTAA	45	92.9
	AGAAGCGGCCAGCCTCGGC		
CECO 2	CCCGGGGAATTCTCAGACATCAGACTC	43	76.6
	AATACTAGAAAGTTTC		

Name	Sequence (5' to 3')	Nucleotides	Melting Temperature °C
5' PROBE-1	CCTACCTGGAATGAATGTCTTT	22	60.7
5' PROBE-2	CCTTGCCCTCCACCTCTTCAAC	22	69.9
CELERA 5 SEQ	CAAACACCAAGCATCCGGTATAA	23	66.4
FLOXED 3' PROBE 1	CCCAACATACTGCATTTTCTCCC	23	69.8
FLOXED 3' PROBE 2	ACCCATCCAACCCACTTCCGCAG	23	77.7
DelVal 6121	TTTCAATGGCTCCAGCAATG	20	65.9
DelVal 6215	CAGCCCTATCCCTCCCGCACCCAC	24	78.9
pLOX 91	AAGCGCCTCCCCTACCCGGT	20	73.6
pLOX 1603	TGAAGGCTCTTTACTATTGCTTTATG	26	62.4
DelVal 8035	AGGATGTGACGTGAAGAGACAT	22	68.4
DelVal 5603	GCCCAGAAGAAGAATCGGAACAAA	24	69.8
CaMKII Mut-1	AAGGCCCAGAAGAAGAATCGGAACAAAG	84	95.0
	CGCGCCAGCAGCACGACTACGACACCTT		
	CGTAGATCTTCAGAAGGAGGAGGCCTTG		
CaMKII Mut-2	CAAGGCCTCCTCCTTCTGAAGATCTACGA	84	95.0
	AGGTGTCGTAGTCGTGCTGCTGGCGCGC		
	TTTGTTCCGATTCTTCTTCTGGGCCTT		
CaMKII-1	AGGCCCGGCCGCCTTGGCCCCAGGCA	30	93.5
	GCGT		
CaMKII-2	TCCGGGACTAGTCTAGTTCTTAAGTAGG	60	80.7
	CAGCTAGCTCAGACATCAGACTCAATA		
	CTAGA		
CaMKII-3597	GAAAGCAAAAGTTAAAGGGTGAAT	24	62.2
CaMKII-5148	AACAAAGGAGAACTCGCCTCAC	22	65.6
NR2A-COOH 1	CCCGGGCAGCTGCATCCATGGAGTGC	35	87.8
	ACATTGAAG		
NR2A-COOH 2	CCCGGGGCTAGCTTAGACATCAGATTC	43	79.6
	AATACTAGGCATTTTC		
SWAP 5'PROBE-1	AGCGATTTGGGCACACTTGTCCTT	24	72.2

Name	Sequence (5' to 3')	Nucleotides	Melting Temperature °C
SWAP 5'PROBE-2	CCACACCGAAAGGCTGAGGGAG	22	72.9
PK-SPH 1	GGCCGCTAAAGCATGCATGTCTAGACT	50	88.9
	AGAGTGGATCCGCGTGGGCTAGCTAG		
	GTTG		
PK-SPH 2	TCGACAACCTAGCTAGCCCACGCGGAT	57	87.4
	CCACTCTAGTCTAGACATGCATGCTTTA		
	GC		
SWAP 4277	TTTATGGTGTGTTTGGGTTTCTCTGA	26	67.9
SWAP-NR2A 170	CTGACTTCATCCAAAGAGGCTCAC	24	67.1
SWAP-NR2A 396	GGTGGCTGTCAGCACTGAATCCAA	24	73.2
SWAP-NR2A 609	CACATGCCACAGGGAGCCAGATAA	24	72.7
SWAP-NR2A 810	CATTGAAAACATAGTCTTGCCTGA	24	63.9
SWAP-NR2A 1052	GCTGCCTCTCAAACCTGCCCACCT	24	75.7
SWAP-NR2A 1291	CTCGACAAACCCAGGGAGATAGA	23	67.8
SWAP-NR2A 1515	GTACGGGGATGACCAACGCTTAGT	23	69.6
SWAP-NR2A 3924	CTATGGTGCTTCCAATATTCTGC	23	64.0
SWAP-NR2A 1737	CTCACTTCATGCCTGTGTCACTT	23	63.2
SWAP 1929	AGCATTCAGAAGGACCAAGGAC	22	65.5
CECOA	CCCGGGGAATTCTTAGACATCAGATTC	43	78.5
	AATACTAGGCATTTTC		
BAMCA-1	GGGCCCGGATCCCCGGCATCTACAGT	44	92.5
	TGCATCCATGGAGTGCAC		
BAMCA-2	GGGCCCGGATCCCCGCCACATGCCAC	48	90.0
	AGGGGAGCCAGATAATAATAAG		
NR2B-1NEW	CATTGCTTCATGGGTGTCTGTTC	23	67.6
pLOX 91FW	ACCGGGTAGGGGAGGCGCTT	20	73.6
pLOX 1603 REV	CATAAAGCAATAGTAAAGAGCCTTCA	26	62.4
NR2B 5910	TCAGTGCTTGCTTCACGGCAGC	22	73.9

Name	Sequence (5' to 3')	Nucleotides	Melting Temperature °C
pLOX 413	CCCAGAAAGCGAAGGAGCAAAG	22	69.9
pLOX 1540	TGGAAGGATTGGAGCTACGGG	21	69.2
pLOX 6456	CTCCTCTCCAGCCTCCCACACT	22	70.1

5C Genomic Sequences

NR2B sequenced area

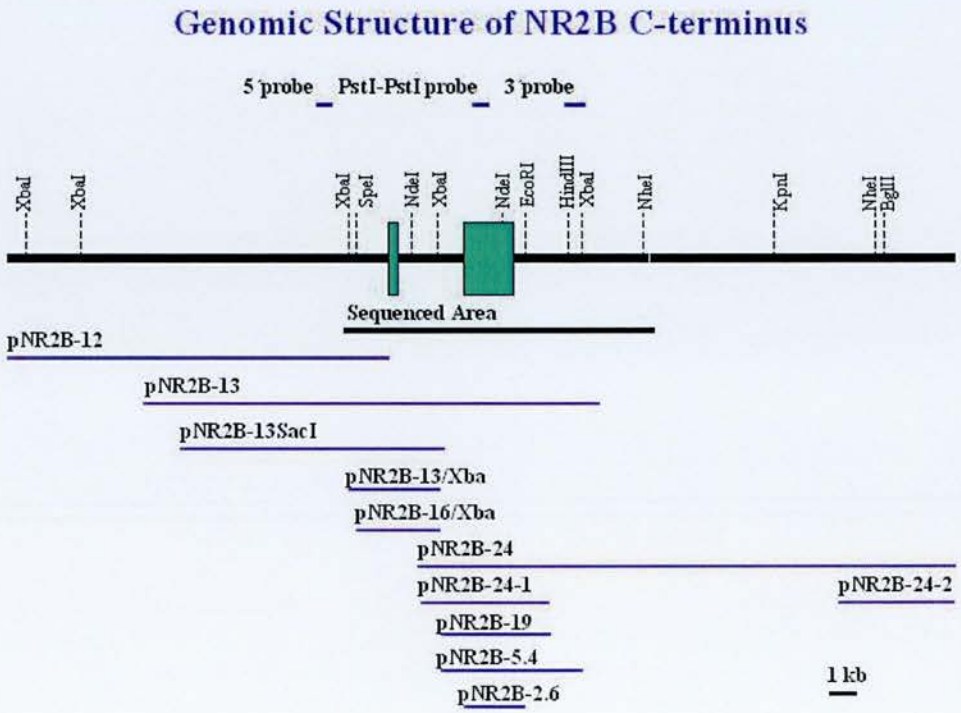

Figure 57. Genomic structure of the NR2B C-terminus.
On the figure the M4 and the COOH exon of the NR2B subunit is indicated by green rectangles. The various subclones are demonstrated by blue continuous lines. The sequenced area is shown by a black continuous line. The most important restriction sites are indicated.

In the following NR2B sequence (Figure 57 Sequenced area.) the M4 exon is highlighted in yellow, the COOH exon is highlighted in light blue. The CaMKII

binding site (corresponding to residues 1290-1309) is shown in dark blue while the stop codon in red.

TAGATGTCACCCTACATGTGGCACAACACCAGACAGATGTAGGGCAGTGCTCTTTCT
ATTCCAGGAGGGAGGGAAGTGAAACAAATGTTTGTCTGTTTCTACATCCTTCATTCT
TCCCTTCCACGGTCTTCTGGTTGAAGAGGTGGAGGGCAAGGATCCTCAGATGTAGAT
ACCAGAAGGCATTTCCTGTGTCTTTCTGGTCATGGGCTGGACACTGAGAAATGTATC
TCACCGGACTACTATCTTCTGCATTTCTCTTCATGTCCTTGCCCCAAACAGTCTACC
CATAATCCTCACACACAAACTAATCTAGATAGAGATGATCTTCACTCTGCATGGTTC
CGAAGTCCACCAGACACGTGGGTCTGTCAACTAGGTCCATGGGACATTTTTTATTGG
GGAAGACATCAGAGACACAAGGCCAGGGTCAGGTTTCCAGGTTCCACCTGAATCTGG
CTTCTACACTAGTTAGAAAAAGCATTGTTGAATCAAAGAAGAGAAGAAACGTGAGTG
GATTTCTATAAGAACGAGTAGGGGTTTGTAGCTGGAATGCTGATAAGCCATGCTGGT
ATAACCAGTAGTCACAGCCAAATGGATCCAGACTCTATTACCAAGTAGATCAGTAGA
AAGGATTTTGGGATTCATTGTGCTATGCAAATGCAAAATTTTAGCAAACTAGACTTT
CATTTGTATGAATTAGTGACATCCTGGAGTAGGTACTTGTTTTCTTTGTCTTTTGCT
TGTTTGGTTGGTTTTGGTTTTTGGTTTTGGGGTTTTGGGTTTTGGGTTTTGGGTTTT
GGGGGGTGTTGTTTGAGATGTTTACATTTCTACTGATTAGTGTCTAGTGATAGTAGG
TCAGAGTCTGACACAACTGGAGAAGTCCTTGTCCCTTTAAGCAGAGTTGAGAGGAGG
CAAGTTTAGGTGATCATGTTTCATTCCAGCTTCCTCCTCATTTGGGTTTCATATTTT
CCTCTAAAAGACTTCTGAAATTCTGAGAGAGCATAATGATTCAACCTCTTTCAATCT
CTGTCTACCTCTCCTTCCTCAACCTAATGTGCTCTGTATAATTCCAAGTTTTTACTT
GTTTGGTTATGTTATCCCCACTGTCTATAAAACAGAGGTCAGAGAGTTTAACTTCAG
AATTCTTTTACTAAGCTTTCTTTGCTGAGTTCTGCTTGAACTGGTTTTCTTGTCTCT
CTGTAAATGAGCATCTATTTTTCTACTTCTTCCTTGGTGATAATTCTACACCTGCTG
CCTGCAATGCCTTTAAATATAATATAAATTAAAATCCATCCCCAGTCTCAAGTTTCT
CTCTCTCCTCTCTCTCTCTCTCTCTCTCTCTCTCTCTCTCTCTCTCTCTCTCTCTCT
CTCTCTCTCTCTCCCTCCCTCCCTCTCTCTCCCTCCCTCTCAAACCCATTGACTGCT
TTTCTCACAAACTGTTCTCACTAATTTGAACTCTTGTTCCTTGCATGGCATATTGTA
TATAATACCAAGCATTGAGCTGCAATTTGCACTGGCTAGAGCAGAGTCACAAGGAAG
TCCCATGTCCTTGAGTTACCTGTGTTCCATTCATTACATTTCCACTAAATACTTGGA
ATGTATTGATGAGTTAAGATATAATGGCATTAATAAAATGTATTCTTTTTCTCTTTT
TGTGTTTGTCCCTTTCTGTCTATTCTCTTCTTCAATGTCCTTCCTTCTTTCTCACCT

TTCTCCTCCCTCCCTCCTCTATCTGTCTCCTTCTTGTCCTCGTTCTAGGGGAGATGG
AAGAACTGGAAGCTCTCTGGCTCACTGGCATTTGCCACAATGAGAAGAATGAGGTTA
TGAGCAGCCAGCTGGACATTGACAACATGGCGGGCGTCTTCTATATGTTGGGGGCAG
CCATGGCTCTCAGCCTCATCACCTTCATCTGTGAACATCTCTTCTATTGGCAGTTCC
GACATTGCTTCATGGGTGTCTGTTCTGGCAAGCCTGGCATGGTCTTCTCCATCAGCA
GAGTAAGTGTTTTGATTGAGATACTCAGAGCTTGCTAAGGACAGTTCAGCCTTGCTC
AGCAAAGAGACCAAGAAGGTGCTTGTTCCAGCCTTATGTGGCTAAATCATAAAGCCA
GATCACGGGCACTTCCCCAAGGGTCTGTGTGAGAGAATTTCAAATGCTTCTAAGATG
GGTGGTGCTATGTTTCTTTCCTTCCATTTTAGACTCAGACATTTGATTTTTCTATCA
AATTTGGCTTTTCCCCATTTGCCTCTTACACCACCACTAATTGATTCTGTATAGGCT
GCATTAATCAATTGATCCTTTGAGGTAGGAATCATAACATTTTCTTAAATAGCATAG
TGTCACATAGCTTATTCTAACACACAAAGACATATTATTGGTGTTTTTACTGTTCCT
ATATTTTAACCACATGTGAAGTAAGGGAAATTAAAGAGCCTAAAGGGTGGACACAGT
GACATATGCCCACAATAAATACCAACACTGGAAGACTACAGCAGGAGGATCACGTGT
GGGCATGTGTATGTGCCTGGGTCTGTGGAGTACAGATATAAATACCATTTGAAAGAG
CCTAAAGAACCCAAGTCTTGATTAATTTAAAAAAAAAAAAGTATATTACAAAAACTT
ACTTAAAAGGAACAAGACTCCAGGCCATTCTTTGTTTAGATCACCTTCATTTCTGAT
TCAAATTGAGGTATTAGGAAAGCAGTTAGATATATGAAACTCGGGTCACAGATGGGG
AGTTTTTAAAGAGTAGGATTCTTCTGATTTTGTTGATATAGTTGTGGGGACTCACAC
ATGGAGTGGTGAACTCAAATATCCTTTTAGGATTGAAGATCGTGTTGCAGATATGAC
TCAAATAGAGTTATGAAAGAAAATGGATTTCTCATCAAACTGTTTCATTTTCTGGAC
ATTTTCCTGTAGTGTTTTAGGGGACAGGGGAACAATTTCTCCATTTCCTCTCTAGCT
GTCAGTGTGCCCAGGTCATTCAGTCACATAAGAACAGGAGAAAGGAGCTTGTGGGGC
TCCTGGTCCCTGGGCCCCGTTATTCAGCACTTCCTAGAGGCCAGAGAGGTGGGAGAA
AAGAGAAATTTAAGTTGTGGCCCTCTGACATGGGCACTGTCTTCACAGAAGAGGACA
CTTGGCATTTCTTCCTGACGACTGTCAAGAGGTCAGAAGTAAGAAGCAGAAAGGGAG
TAGAGTGCCCTCCAGGAAGACCTTGTGTCTCACAAGGCCTGACACTTCTTGGCCACA
TAGCTACCATTTTTCCCTCTGACCTTTTCTGCTCTTGTCCCTGACCGCTCAGATAAT
CTTCTTTTCTAGACTAACCTTCTTGTGTGTAAAGACACCGTTTAAAGCCACTTCTTC
ATCTGCCTCACCTTGCTAGGGAAGTTTGTTTGCCTTTCAAGCAGCACATGAGAGATG
AATAGTAGCTGACCTGACTTGAGATGTGGGGACACTGTCTGCCCAGGCAAGCAACCC
AGCCTTCCTCACAGATGCTGTTTTTCAGTGCCCCGAACAAGTAGCTGTTTGCCCGGC
GTTCTTCATCAATACTAATTTGATAGAACATTAATTATTTATGATAATATTGACTAT

AAAAAAGAAAGCAAAAGTTAAAGGGTGAATAAAGGAGAGACCTCAACAAGGGAGTTA
TTCATTCACATTGAGCTCTTGATATTTGTCCCACTTTTTCCCTCCCACAGTGTAGGC
CACAGCAGTAGAAAATCCTTCTTTGACCCCAGGGCTTTCCAACTCTCTGTGTGAATT
CAGTTCATGCTTAGCTACAGAACAACATTGCTCCCTTGGTATTTGCTGATCAAAATT
CTAATAAAAAATAACTGGTCAAAATCGGTCAGAGCCAGAACAAGAAGCCACTGTGAG
CAGCATCAGCCAGGCTTGGGCCGACCAGAGCTAAGTGGCTCTAGTGTCTATGGTGCT
TCCAATATTCTGCTCCTGCTTTTTGCTATATGTCTACAGCCTGGATCCCTTTATAAA
ATGTAAGACTCTGCGTCCTAAATAGGAGGGAAACCCAAGATAGATCGCGGGTTTAGT
TGAGGCACATAAGCCATGTCCTCTGTTTATTTGAGTCCTCTGGTATGATCACTCCCC
TCCCTGATGGCAGATTGTGATCGTTAGCTCATGAAATGAAGTTGGCTGAATTCAAGG
GGCTACATCAACCAAGCTTCTAGTCACGTTTTCTGTGAATTCAGCAAACTGCCTGCC
TCATGATTCTCCTATCTTTATCTTACCTCATTAAATCATCAGTGGTAGGGCACTGTT
GTTTATGGTGTGTTTGGGTTTCTCTGAATTCAATGTGTACCATCCTATGTCCCTTCA
GGGTATCTACAGCTGTATCCACGGAGTAGCTATAGAGGAGCGCCAATCCGTGATGAA
CTCCCCCACTGCCACCATGAACAACACACTCCAATATCCTACGCTTGCTCCGAAC
GGCCAAAAACATGGCCAACCTGTCTGGAGTCAACGGCTCCCCCCAGAGTGCCCTGGA
CTTCATCCGCCGTGAGTCCTCTGTCTATGACATCTCTGAGCATCGCCGCAGCTTCAC
GCATTCAGACTGCAAGTCGTACAATAACCCACCCTGTGAGGAAAACCTGTTCAGTGA
CTACATTAGTGAGGTAGAGAGAACATTTGGCAACCTGCAGCTGAAGGACAGCAATGT
GTACCAAGACCACTATCACCATCACCACCGGCCCCACAGCATCGGCAGCACCAGCTC
CATTGATGGGCTCTATGACTGTGACAACCCACCCTTTACCACCCAGCCCAGGTCAAT
CAGCAAGAAACCCCTGGACATTGGCCTGCCCTCTTCCAAACACAGCCAGCTCAGCGA
CCTGTACGGCAAGTTCTCTTTCAAGAGTGACCGTACAGTGGCCATGATGACTTGATT
CGATCGGATGTCTCAGACATCTTCACGCATACTGTCACCTATGGCAACATCGAGGGC
AACGCAGCCAAGAGGAGGAAGCAGCAATATAAGGACAGTCTAAAGAAGCGGCCAGCC
TCGGCCAAATCTAGGAGGGAGTTTGATGAAATCGAGCTGGCCTACCGTCGCCGACCA
CCCCGCTCCCCAGACCACAAGCGCTACTTCAGGGACAAAGAAGGGCTCCGAGACTTC
TACCTGGACCAGTTCCGAACAAAGGAGAACTCGCCTCACTGGGAGCACGTGGACTTA
ACTGACATTTACAAAGAACGTACATGTGACTTCAAGCGAGATTCGGTCAGTGGAGGC
GGGCCCTGTACCAACAGGTCTCACCTTAAACACGGAACAGGCGATAAGCACGGAGTG
GTAGGCGGGGTGCCTGCTCCTTGGGAGAAGAACCTGACCAATGTGGATTGGGAGGAT
AGGTCTGGGGGCAACTTCTGCCGCAGCTGTCCCTCCAAGCTGCACAATTACTCCTCT
ACGGTGGCAGGGCAAAACTCGGGCCGGCAGGCCTGCATCAGGTGTGAGGCCTGCAAG

AAGGCTGGCAACCTGTATGACATCAGCGAGGACAACTCCCTGCAGGAACTGGACCAG
CCGGCTGCCCCTGTGGCTGTGTCATCCAACGCCTCCACCACCAAGTACCCTCAAAGC
CCGACTAATTCCAAGCCCCAGAAGAAGAATCGGAACAAACTGCGCCGGCAGCACTCC
TACGACACCTTCGTGGACCTGCAGAAGGAGGAGGCCGCCTTGGCCCCACGCAGCGTG
AGCCTGAAAGACAAGGGCCGATTCATGGATGGGAGCCCCTACGCCCATATGTTTGAG
ATGCCAGCTGGTGAGAGCTCCTTTGCCAACAAGTCCTCAGTGACCACTGCCGGACAC
CATCACAACAATCCCGGCAGCGGCTACATGCTCAGCAAGTCGCTCTACCCTGACCGG
GTCACGCAAAACCCTTTCATCCCCACTTTTGGGGATGATCAGTGCTTGCTTCACGGC
AGCAAATCCTACTTCTTCAGGCAGCCCACGGTGGCAGGGGCGTCGAAAACAAGGCCG
GACTTCCGGGCCCTTGTCACCAATAAGCCAGTGGTGTCGGCCCTTCATGGGGCTGTG
CCAGGTCGTTTCCAGAAGGACATTTGTATAGGGAACCAGTCCAACCCCTGTGTGCCT
AACAACAAAAACCCCAGGGCTTTCAATGGCTCCAGCAATGGACATGTTTATGAGAAA
CTTTCTAGTATTGAGTCTGATGTCTGAGTGAGGGAAGAGAGAGAGAGAGATTAAG
GTGGGTGCGGGAGGGATAGGGCTGTGGGCCGCGTGGTGCGCATGTCACGGAAAGAGT
CGGGGGTGAACTTGGCTCCCATTCGCTTTTTCTTCTTCTTTTAATTTCTCTATGGGA
TCCTGGAGTTCTGGTTCCTTACTGAAGGCAACCCTCGTGGCCAGCACCCTTTCTCCT
CCCTTGCGCAGTTCTCTTCTTCCCGCGTCTGTCCACCATTCCTGTTCCCATAAGAGG
ATAGAACGGGCCTCAGTGTGGGAGGCTGGAGAGGAGACCAGAAGCGCTGCCTGTGTG
CTTCTTCCTAGCGCAGAAGGGCTCTGAGCGATTCACTTTGAGCGAGGCTTTCCTGAT
ACTGCTCTTTTTGTTCAGGCAAGGAAGCGAAGGTGTTTATCTAAGGAAGGCCATTGA
ACCTCCTGCTCCTAAGAGAGAAGAGGCTTTCTCTGAATTCTTGCTGCATGGTTGGCA
TCTGCTGAGGGGCCATGTGCCAAGCAGAGGGCAGGAAGTCGTTGTATATATATAAGC
CAAAAAGATAATAATAATAATAAAAACTTTCTTCAGCTTCAGAAGCCTCAGGGGTGG
TGAACCAAGGGAGAAGCCATTGGTAGAAGAGAGATTCCTGAACGAAGTGGGTAGTTC
ACTGCTACAGTGTCCCATGGTGCATTGGAAGCAAGAGTATGGGACTGTGTATGCACA
TATACATGTACACCTGCACTCACACGTAGTCAGGTGCCTCTGAATACAGAGAACGAA
ACCTCGACTGGCTGCTTCCTCCCACATACGAAAGCAATGCGCTTTTTTTTTTTTTTT
TTTTTTGGCTTATATATAAACTGATGTCAAAGGTTACCCCAATTTGGGCTATCTCTC
CATTTTTTCCTTCTTGAGTGAAGGTATAGAGATTCTTGATGAAGACGAATCCGTATT
GCAGAAAAGACAACAGAAAGAAATGAGTGGAACTGAGTCAACCCTACAGAATACTTT
GCCAGTAGCTGCTAATGCTTTCCACCAGCTTGGGCAGAGAGAGCTTTTCAGTAAGGC
TGAAGGGAAATGGAAATAGTGTGAGTCCTTTACTCATACTTAGAATCTAGGCATTCA
GCCCCTTAGCTGGATGAGGTTTTGGGGAAAGCTCTTCGTATAAGGCTTTGTGAAAGA

GAGCCATTACAGTAGGGTGAGAGAGGGGGATGTTTTTAGTCATTAATGGTAGGGTTA
GTGAGAAAGGGGGATGTTTTCAATGCTTTGATCCCTTCTTACTTAACCTAGAACTGA
AAGGGCAAGCAAATTCCCCCTGAATTGGTGATGTATCAAGGGGACACGTGGGGGAGA
GAAATGAGCTCATCGCCAAGGGTACATCCCTGGAAAGCCAGAGAGCATGAAGGATTG
AGAAGTGGGAGCCTGGGTCCCTAGGCATGTGACTTGAAATAGTGCAAGCGCTTCGGC
AAGCCCCAGTTCCCTCTCAGATTGTACCACTCGACAGTGAATGTGCTTGCGTGCCTG
CGTGTACGTGTGTGTGTGTGCGTGTGCGTGTGCGTGTGCGTGTGTGTGTGTGTGT
GTGTGTGTGTGTAAAACTACAGGGATGGGGGTGCTGGCAGGTGTGATGCCCCCTCAC
TTAAAGTTGGAAAATTAAGAAGGGAAATGAATATTTGTCACTGCCCGACCTGAAACT
TGGGGTAGGGGTGTTCCATGGGTCAGTTCTGCTGCCCTGCCCTCCCCTCACACAGGG
TGGCGTCCAAAGAGCCCTGGGTCTATGTGGAAGCTTGACTGCAGGATCGCCGTGTGG
CACACAGGACACATAAACCAGAAAGGTGCTTATTCTTCTCTGGAACGAAGCTGCCAT
GTCTCTTCACGTCACATCCTCCTGGCCTGCTTCTTGCCTTCCTGGTCGCCCCGCCTC
ATGGCCTCCCCTCATCCCCATACTCGACTGCTGTCTCCCACCTTCCTCCTTGATTTC
TTTTTAATTTTTTTTTTACCTCAGTATCTCTCATTTAAATGCCAACTGAAGGCCTTG
TTTTCTTTCTAAAATGAACGTGGGGGCAAGGGGCTGAACCTCTCAACACCCTGGAGA
GAGGAGCGCGGAGTGCTTTATTTTAGGTTCCAGGAAAGACTCTGAGAGAGGACAGAG
GGCGTGAGGCGTCTCCCAGAGGAAGAAGGAGAAGGGCCATAGAAACATTGCTTCACT
CTGGCTCTGTCCAAGGGCCAGAGGCTCATCCCCCACTCTTCCTCTTACCTCACCCTT
TAAAATTTTAAAAAGAAAAAAAAAAAAAGGAAAAAAAAAAAAAGAAAAAACCAAACC
AACTAACCTAGCGAACAGCAATCTAGAGC

NR2A COOH exon

In the following NR2BA sequence the COOH exon is represented with some 5' flanking sequence (containing the primer sequences) The COOH exon is highlighted in light blue while the stop codon is indicated by red.

GGCATCTACAGTTGCATCCATGGAGTGCACATTGAAGAAAAGAAGAAGTCTCCAGAC
TTCAATCTGACTGGGTCACAGAGCAACATGCTAAAGCTTCTCCGCTCAGCTAAAAAC
ATCTCCAACATGTCCAACATGAACTCCTCGCGAATGGACTCACCCAAAAGAGCTGCT
GACTTCATCCAAAGAGGCTCACTTATTGTGGACATGGTTTCAGACAAGGGAAATTTG

ATATACTCAGATAACAGGTCCTTTCAAGGGAAGGACAGTATATTTGGAGAAAACATG

AATGAACTGCAAACATTTGTGGCCAACAGGCACAAGGATAGTCTCAGTAACTATGTG

TTTCAGGGACAGCATCCTCTCACTCTCAATGAGTCCAACCCCAACACAGTGGAGGTG

GCTGTCAGCACTGAATCCAAAGGGAACTCCCGACCCCGGCAGCTTTGGAAGAAATCC

ATGGAGTCTCTACGCCAGGATTCTCTAAACCAGAACCCAGTCTCCCAGAGGGATGAG

AAGACTGCAGAGAATAGGACCCACTCCCTAAAGAGTCCTAGGTATCTTCCAGAAGAG

GTAGCCCATTCTGACATTTCTGAAACCTCAAGCCGGGCCACATGCCACAGGGAGCCA

GATAATAATAAGAACCACAAGACCAAGGATAACTTCAAAAGGTCAATGGCCTCTAAA

TACCCCAAGGACTGTAGTGAGGTTGAACGTACCTACGTGAAAACCAAAGCAAGTTCT

CCCAGGGATAAGATCTACACCATCGATGGTGAGAAGGAGCCCAGCTTCCACTTAGAT

CCTCCACAGTTCATTGAAAACATAGTCTTGCCTGAGAATGTGGACTTCCCAGATACC

TACCAAGATCACAATGAGAATTTCCGCAAGGGGGACTCCACACTGCCCATGAACAGG

AACCCACTACACAATGAAGATGGGCTTCCCAACAATGACCAGTATAAACTCTATGCC

AAGCACTTTACCTTGAAAGACAAGGGTTCCCCACATAGTGAGGGCAGTGATCGATAT

CGGCAGAACTCCACGCATTGCAGAAGCTGCCTCTCAAACCTGCCCACCTACTCAGGC

CACTTTACCATGAGATCTCCTTTCAAGTGTGATGCCTGTCTGCGGATGGGGAACCTC

TATGACATTGATGAAGACCAGATGCTTCAGGAGACAGGCAACCCAGCTACTCGTGAG

GAGGCCTACCAGCAGGACTGGTCACAGAACAACGCCCTCCAGTTCCAGAAGAACAAG

CTAAAGATTAATCGACAGCACTCCTATGATAACATTCTCGACAAACCCAGGGAGATA

GACCTTAGCAGGCCCTCTCGTAGCATAAGCCTCAAGGACAGGGAAAGGCTACTGGAG

GGCAACTTATACGGGAGCCTGTTCAGTGTCCCCTCAAGCAAACTCTTGGGGAACAAA

AGCTCCCTTTTCCCCCAAGGTCTGGAGGACAGCAAGAGGAGCAAATCTCTCTTGCCA

GACCATACCTCTGATAATCCTTTCCTCCACACGTACGGGGATGACCAACGCTTAGTT

ATTGGGAGATGTCCCTCGGACCCTTACAAACACTCATTGCCATCACAGGCAGTAAAT

GACAGCTATCTTCGGTCATCCTTGAGGTCAACAGCATCATATTGCTCCAGGGACAGT

CGGGGCCACAGTGATGTGTATATTTCAGAGCATGTTATGCCTTATGCTGCAAATAAG

AATAACATGTACTCTACCCCCAGGGTTTTAAATTCCTGCAGCAATAGACGTGTGTAC

AAGAAAATGCCTAGTATTGAATCTGATGTCTAA

Chapter 6: References

Abel T, Nguyen PV, Barad M, Deuel TA, Kandel ER, Bourtchouladze R. Genetic demonstration of a role for PKA in the late phase of LTP and in hippocampus-based long-term memory. Cell. 1997 Mar 7; 88(5): 615-26.

Abeliovich A, Chen C, Goda Y, Silva AJ, Stevens CF, Tonegawa S. Modified hippocampal long-term potentiation in PKC gamma-mutant mice. Cell. 1993 Dec 31; 75(7): 1253-62.

Abeliovich A, Paylor R, Chen C, Kim JJ, Wehner JM, Tonegawa S. PKC gamma mutant mice exhibit mild deficits in spatial and contextual learning. Cell. 1993 Dec 31; 75(7): 1263-71.

Adolphs R, Cahill L, Schul R, Babinsky R. Impaired declarative memory for emotional material following bilateral amygdala damage in humans. Learn Mem. 1997 Sep-Oct; 4(3):291-300.

Aiba A, Kano M, Chen C, Stanton ME, Fox GD, Herrup K, Zwingman TA, Tonegawa S.Deficient cerebellar long-term depression and impaired motor learning in mGluR1 mutant mice. Cell. 1994 Oct 21; 79(2): 377-88.

Aiba A, Chen C, Herrup K, Rosenmund C, Stevens CF, Tonegawa S.Reduced hippocampal long-term potentiation and context-specific deficit in associative learning in mGluR1 mutant mice. Cell. 1994 Oct 21; 79(2): 365-75.

Akagi K, Sandig V, Vooijs M, Van der Valk M, Giovannini M, Strauss M, Berns A. Cre-mediated somatic site-specific recombination in mice. Nucleic Acids Res. 1997 May 1; 25(9): 1766-73.

Alger BE and Teyler TJ. Long-term and short-term plasticity in the CA1, CA3, and dentate regions of the rat hippocampal slice. Brain Res. 1976 Jul 16; 110(3): 63-80.

Alkon DL. Membrane depolarization accumulates during acquisition of an associative behavioral change. Science. 1980 Dec 19; 210(4476):1375-6.

Allison DW, Gelfand VI, Spector I, Craig AM. Role of actin in anchoring postsynaptic receptors in cultured hippocampal neurons: differential attachment of NMDA versus AMPA receptors. J Neurosci. 1998 Apr 1; 18(7):2423-36.

Anagnostaras SG, Gale GD, Fanselow MS. Hippocampus and contextual fear conditioning: recent controversies and advances. Hippocampus. 2001; 11(1):8-17.

Andersson O, Stenqvist A, Attersand A, von Euler G. Nucleotide sequence, genomic organization, and chromosomal localization of genes encoding the human NMDA receptor subunits NR3A and NR3B. Genomics. 2001 Dec; 78(3): 178-84.

Anwyl R.Metabotropic glutamate receptors: electrophysiological properties and role in plasticity. Brain Res Brain Res Rev. 1999 Jan; 29(1): 83-120.

Armstrong N, Sun Y, Chen GQ, Gouaux E. Structure of a glutamate-receptor ligand-binding core in complex with kainate. Nature. 1998 Oct 29; 395(6705):913-7.

Ascher P, Nowak L. The role of divalent cations in the N-methyl-D-aspartate responses of mouse central neurones in culture. J Physiol. 1988 May; 399: 247-66.

Atkins CM, Selcher JC, Petraitis JJ, Trzaskos JM, Sweatt JD. The MAPK cascade is required for mammalian associative learning. Nat Neurosci. 1998 Nov; 1(7): 602-9.

Bach ME, Hawkins RD, Osman M, Kandel ER, Mayford M. Impairment of spatial but not contextual memory in CaMKII mutant mice with a selective loss of hippocampal LTP in the range of the theta frequency. Cell. 1995 Jun 16; 81(6): 905-15.

Bailey CH, Chen M. Long-term sensitization in Aplysia increases the number of presynaptic contacts onto the identified gill motor neuron L7. Proc Natl Acad Sci U S A. 1988 Dec; 85(23):9356-9.

Bailey CH, Chen M. Structural plasticity at identified synapses during long-term memory in Aplysia. J Neurobiol. 1989 Jul; 20(5):356-72.

Baranano DE, Ferris CD, Snyder SH. Atypical neural messengers. Trends Neurosci. 2001 Feb; 24(2):99-106.

Bardoni R, Torsney C, Tong CK, Prandini M, MacDermott AB. Presynaptic NMDA receptors modulate glutamate release from primary sensory neurons in rat spinal cord dorsal horn. J Neurosci. 2004 Mar 17; 24(11): 2774-81.

Barria A, Muller D, Derkach V, Griffith LC, Soderling TR. Regulatory phosphorylation of AMPA-type glutamate receptors by CaM-KII during long-term potentiation. Science. 1997 Jun 27; 276(5321):2042-5.

Barria A, Malinow R. NMDA receptor subunit composition controls synaptic plasticity by regulating binding to CaMKII. Neuron. 2005 Oct 20; 48(2):289-301.

Bartha L, Brenneis C, Schocke M, Trinka E, Koylu B, Trieb T, Kremser C, Jaschke W, Bauer G, Poewe W, Benke T. Medial temporal lobe activation during semantic language processing: fMRI findings in healthy left- and right-handers. Brain Res Cogn Brain Res. 2003 Jul; 17(2):339-46.

Bartlett TE, Bannister NJ, Collett VJ, Dargan SL, Massey PV, Bortolotto ZA, Fitzjohn SM, Bashir ZI, Collingridge GL, Lodge D. Differential roles of NR2A and NR2B-containing NMDA receptors in LTP and LTD in the CA1 region of two-week old rat hippocampus. Neuropharmacology. 2006 Aug 9.

Bartsch D, Ghirardi M, Skehel PA, Karl KA, Herder SP, Chen M, Bailey CH, Kandel ER. Aplysia CREB2 represses long-term facilitation: relief of repression converts transient facilitation into long-term functional and structural change. Cell. 1995 Dec 15; 83(6):979-92.

Bashir ZI, Jane DE, Sunter DC, Watkins JC, Collingridge GL. Metabotropic glutamate receptors contribute to the induction of long-term depression in the CA1 region of the hippocampus. Eur J Pharmacol. 1993 Aug 3; 239(1-3):265-6.

Bassand P, Bernard A, Rafiki A, Gayet D, Khrestchatisky M. Differential interaction of the tSXV motifs of the NR1 and NR2A NMDA receptor subunits with PSD-95 and SAP97. Eur J Neurosci. 1999 Jun; 11(6): 2031-43.

Bayer KU, De Koninck P, Leonard AS, Hell JW, Schulman H. Interaction with the NMDA receptor locks CaMKII in an active conformation. Nature. 2001 Jun 14; 411(6839):801-5.

Bayer KU, LeBel E, McDonald GL, O'Leary H, Schulman H, De Koninck P. Transition from reversible to persistent binding of CaMKII to postsynaptic sites and NR2B. J Neurosci. 2006 Jan 25; 26(4):1164-74.

Bear MF, Malenka RC. Synaptic plasticity: LTP and LTD. Curr Opin Neurobiol. 1994 Jun; 4(3):389-99.

Bear MF, Abraham WC. Long-term depression in hippocampus. Annu Rev Neurosci. 1996; 19: 437-62. Review.

Beaver CJ, Ji Q, Fischer QS, Daw NW. Cyclic AMP-dependent protein kinase mediates ocular dominance shifts in cat visual cortex. Nat Neurosci. 2001 Feb; 4(2): 159-63.

Bendel O, Meijer B, Hurd Y, von Euler G. Cloning and expression of the human NMDA receptor subunit NR3B in the adult human hippocampus. Neurosci Lett. 2005 Mar 22; 377(1): 31-6. Epub 2004 Dec 15.

Bengzon J, Okabe S, Lindvall O, McKay RD. Suppression of epileptogenesis by modification of N-methyl-D-aspartate receptor subunit composition. Eur J Neurosci. 1999 Mar; 11(3): 916-22.

Berberich S, Punnakkal P, Jensen V, Pawlak V, Seeburg PH, Hvalby O, Kohr G. Lack of NMDA receptor subtype selectivity for hippocampal long-term potentiation. J Neurosci. 2005 Jul 20; 25(29):6907-10.

Bleakman D. Kainate receptor pharmacology and physiology. Cell Mol Life Sci. 1999 Nov 15; 56(7-8):558-66.

Bliss TV and Lømo T. Long-lasting potentiation of synaptic transmission in the dentate area of the anaesthetized rabbit following stimulation of the perforant path. J Physiol. 1973 Jul; 232(2): 331-56.

Bliss TV, Collingridge GL. A synaptic model of memory: long-term potentiation in the hippocampus. Nature. 1993 Jan 7; 361(6407):31-9.

Bliss TV, Richter-Levin G. Spatial learning and the saturation of long-term potentiation. Hippocampus. 1993 Apr; 3(2): 123-5.

Bliss T, Errington M, Fransen E, Godfraind JM, Kauer JA, Kooy RF, Maness PF, Furley AJ. Long-term potentiation in mice lacking the neural cell adhesion molecule L1. Curr Biol. 2000 Dec 14-28; 10(24): 1607-10.

Boglari G, Erhardt P, Cooper GM, Szeberenyi J. Intact Ras function is required for sustained activation and nuclear translocation of extracellular signal-regulated kinases in nerve growth factor-stimulated PC12 cells. Eur J Cell Biol. 1998 Jan; 75(1): 54-8.

Bortolotto ZA, Clarke VR, Delany CM, Parry MC, Smolders I, Vignes M, Ho KH, Miu P, Brinton BT, Fantaske R, Ogden A, Gates M, Ornstein PL, Lodge D, Bleakman D, Collingridge GL. Kainate receptors are involved in synaptic plasticity. Nature. 1999 Nov 18; 402(6759):297-301.

Bortolotto ZA, Nistico R, More JC, Jane DE, Collingridge GL. Kainate receptors and mossy fiber LTP. Neurotoxicology. 2005 Oct; 26(5):769-77. Epub 2005 Jun 6.

Bourtchuladze R, Frenguelli B, Blendy J, Cioffi D, Schutz G, Silva AJ. Deficient long-term memory in mice with a targeted mutation of the cAMP-responsive element-binding protein. Cell. 1994 Oct 7; 79(1):59-68.

Bozon B, Kelly A, Josselyn SA, Silva AJ, Davis S, Laroche S. MAPK, CREB and zif268 are all required for the consolidation of recognition memory. Philos Trans R Soc Lond B Biol Sci. 2003 Apr 29; 358(1432):805-14.

Bradley A, Evans M, Kaufman MH, Robertson E. Formation of germ-line chimaeras from embryo-derived teratocarcinoma cell lines. Nature. 1984 May 17-23; 309(5965): 255-6.

Brandon EP, Zhuo M, Huang YY, Qi M, Gerhold KA, Burton KA, Kandel ER, McKnight GS, Idzerda RL. Hippocampal long-term depression and depotentiation are defective in mice carrying a targeted disruption of the gene encoding the RI beta subunit of cAMP-dependent protein kinase. Proc Natl Acad Sci U S A. 1995 Sep 12; 92(19): 8851-5.

Brenman JE, Christopherson KS, Craven SE, McGee AW, Bredt DS. Cloning and characterization of postsynaptic density 93, a nitric oxide synthase interacting protein. J Neurosci. 1996 Dec 1; 16(23):7407-15.

Brorson JR, Li D, Suzuki T. Selective expression of heteromeric AMPA receptors driven by flip-flop differences. J Neurosci. 2004 Apr 7; 24(14):3461-70.

Brose N, Gasic GP, Vetter DE, Sullivan JM, Heinemann SF. Protein chemical characterization and immunocytochemical localization of the NMDA receptor subunit NMDA R1. J Biol Chem. 1993 Oct 25; 268(30): 22663-71.

Burnashev N, Schoepfer R, Monyer H, Ruppersberg JP, Gunther W, Seeburg PH, Sakmann B. Control by asparagine residues of calcium permeability and magnesium blockade in the NMDA receptor. Science. 1992 Sep 4; 257(5075): 1415-9.

Cahill L, Prins B, Weber M, McGaugh JL. Beta-adrenergic activation and memory for emotional events. Nature. 1994 Oct 20; 371(6499):702-4.

Caputi A, Gardoni F, Cimino M, Pastorino L, Cattabeni F, Di Luca M. CaMKII-dependent phosphorylation of NR2A and NR2B is decreased in animals characterized by hippocampal damage and impaired LTP. Eur J Neurosci. 1999 Jan; 11(1):141-8.

Carroll RC, Beattie EC, von Zastrow M, Malenka RC. Role of AMPA receptor endocytosis in synaptic plasticity. Nat Rev Neurosci. 2001 May; 2(5):315-24.

Casadio A, Martin KC, Giustetto M, Zhu H, Chen M, Bartsch D, Bailey CH, Kandel ER. A transient, neuron-wide form of CREB-mediated long-term facilitation can be stabilized at specific synapses by local protein synthesis. Cell. 1999 Oct 15; 99(2):221-37.

Castellucci VF, Blumenfeld H, Goelet P, Kandel ER. Inhibitor of protein synthesis blocks long-term behavioral sensitization in the isolated gill-withdrawal reflex of Aplysia. J Neurobiol. 1989 Jan; 20(1):1-9.

Castellucci VF, Kandel ER. A quantal analysis of the synaptic depression underlying habituation of the gill-withdrawal reflex in Aplysia. Proc Natl Acad Sci U S A. 1974 Dec; 71(12):5004-8.

Castillo PE, Weisskopf MG, Nicoll RA. The role of Ca2+ channels in hippocampal mossy fiber synaptic transmission and long-term potentiation. Neuron. 1994 Feb; 12(2):261-9.

Castro CA, Silbert LH, McNaughton BL, Barnes CA. Recovery of spatial learning deficits after decay of electrically induced synaptic enhancement in the hippocampus. Nature. 1989 Nov 30; 342(6249): 545-8.

Chapman PF, Kairiss EW, Keenan CL, Brown TH. Long-term synaptic potentiation in the amygdala. Synapse. 1990; 6(3):271-8.

Chazot PL, Stephenson FA. Molecular dissection of native mammalian forebrain NMDA receptors containing the NR1 C2 exon: direct demonstration of NMDA receptors comprising NR1, NR2A, and NR2B subunits within the same complex. J Neurochem. 1997 Nov; 69(5): 2138-44.

Cheffings CM, Colquhoun D. Single channel analysis of a novel NMDA channel from Xenopus oocytes expressing recombinant NR1a, NR2A and NR2D subunits. J Physiol. 2000 Aug 1; 526 Pt 3: 481-91.

Chen A, Muzzio IA, Malleret G, Bartsch D, Verbitsky M, Pavlidis P, Yonan AL, Vronskaya S, Grody MB, Cepeda I, Gilliam TC, Kandel ER. Inducible enhancement of memory storage and synaptic plasticity in transgenic mice expressing an inhibitor of ATF4 (CREB-2) and C/EBP proteins. Neuron. 2003 Aug 14; 39(4):655-69.

Chen HJ, Rojas-Soto M, Oguni A, Kennedy MB. A synaptic Ras-GTPase activating protein (p135 SynGAP) inhibited by CaM kinase II. Neuron. 1998 May;20(5):895-904. Erratum in: Neuron 2002 Jan 3; 33(1): 151.

Chen N, Luo T, Wellington C, Metzler M, McCutcheon K, Hayden MR, Raymond LA. Subtype-specific enhancement of NMDA receptor currents by mutant huntingtin. J Neurochem. 1999 May; 72(5): 1890-8.

Cheung HH, Gurd JW. Tyrosine phosphorylation of the N-methyl-D-aspartate receptor by exogenous and postsynaptic density-associated Src-family kinases. J Neurochem. 2001 Aug; 78(3): 524-34.

Chizh BA, Headley PM, Tzschentke TM. NMDA receptor antagonists as analgesics: focus on the NR2B subtype. Trends Pharmacol Sci. 2001 Dec; 22(12): 636-42.

Cho KO, Hunt CA, Kennedy MB. The rat brain postsynaptic density fraction contains a homolog of the Drosophila discs-large tumor suppressor protein. Neuron. 1992 Nov; 9(5):929-42.

Choi DW. Glutamate neurotoxicity and diseases of the nervous system. Neuron. 1988 Oct; 1(8):623-34.

Christian KM, Thompson RF. Neural substrates of eyeblink conditioning: acquisition and retention. Learn Mem. 2003 Nov-Dec; 10(6):427-55.

Christian KM, Thompson RF. Long-term storage of an associative memory trace in the cerebellum. Behav Neurosci. 2005 Apr; 119(2):526-37.

Chung HJ, Huang YH, Lau LF, Huganir RL.Regulation of the NMDA receptor complex and trafficking by activity-dependent phosphorylation of the NR2B subunit PDZ ligand. J Neurosci. 2004 Nov 10; 24(45): 10248-59.

Coan EJ, Saywood W, Collingridge GL. MK-801 blocks NMDA receptor-mediated synaptic transmission and long term potentiation in rat hippocampal slices. Neurosci Lett. 1987 Sep 11; 80(1): 111-4.

Collingridge GL, Kehl SJ, McLennan H. Excitatory amino acids in synaptic transmission in the Schaffer collateral-commissural pathway of the rat hippocampus. J Physiol. 1983 Jan; 334: 33-46.

Contractor A, Swanson G, Heinemann SF. Kainate receptors are involved in short- and long-term plasticity at mossy fiber synapses in the hippocampus. Neuron. 2001 Jan; 29(1):209-16.

Cooke SF, Wu J, Plattner F, Errington M, Rowan M, Peters M, Hirano A, Bradshaw KD, Anwyl R, Bliss TV, Giese KP. Autophosphorylation of alphaCaMKII is not a general requirement for NMDA receptor-dependent LTP in the adult mouse. J Physiol. 2006 Aug 1; 574(Pt 3):805-18. Epub 2006 May 25.

Cooke SF, Bliss TV. Plasticity in the human central nervous system. Brain. 2006 Jul; 129(Pt 7):1659-73. Epub 2006 May 3.

Cummings JA, Mulkey RM, Nicoll RA, Malenka RC. Ca2+ signaling requirements for long-term depression in the hippocampus. Neuron. 1996 Apr; 16(4):825-33.

Curtis DR, Phillis JW, Watkins JC. Chemical excitation of spinal neurones. Nature. 1959 Feb 28; 183(4661): 611-2.

Divecha N, Irvine RF. Phospholipid signaling. Cell. 1995 Jan 27; 80(2): 269-78.

Dong H, Zhang P, Song I, Petralia RS, Liao D, Huganir RL. Characterization of the glutamate receptor-interacting proteins GRIP1 and GRIP2. J Neurosci. 1999 Aug 15; 19(16):6930-41.

Dudek SM, Bear MF. Homosynaptic long-term depression in area CA1 of hippocampus and effects of N-methyl-D-aspartate receptor blockade. Proc Natl Acad Sci U S A. 1992 May 15; 89(10): 4363-7.

Dunah AW, Luo J, Wang YH, Yasuda RP, Wolfe BB. Subunit composition of N-methyl-D-aspartate receptors in the central nervous system that contain the NR2D subunit. Mol Pharmacol. 1998 Mar; 53(3): 429-37.

Dunah AW, Wang Y, Yasuda RP, Kameyama K, Huganir RL, Wolfe BB, Standaert DG. Alterations in subunit expression, composition, and phosphorylation of striatal N-methyl-D-aspartate glutamate receptors in a rat 6-hydroxydopamine model of Parkinson's disease. Mol Pharmacol. 2000 Feb; 57(2): 342-52.

Dunah AW, Standaert DG. Subcellular segregation of distinct heteromeric NMDA glutamate receptors in the striatum. J Neurochem. 2003 May; 85(4):935-43.

Durand GM, Bennett MV, Zukin RS. Splice variants of the N-methyl-D-aspartate receptor NR1 identify domains involved in regulation by polyamines and protein kinase C. Proc Natl Acad Sci U S A. 1993 Jul 15;90(14):6731-5. Erratum in: Proc Natl Acad Sci U S A 1993 Oct 15; 90(20):9739.

Dutar P, Vaillend C, Viollet C, Billard JM, Potier B, Carlo AS, Ungerer A, Epelbaum J. Spatial learning and synaptic hippocampal plasticity in type 2 somatostatin receptor knock-out mice. Neuroscience. 2002; 112(2): 455-66.

Ebralidze AK, Rossi DJ, Tonegawa S, Slater NT. Modification of NMDA receptor channels and synaptic transmission by targeted disruption of the NR2C gene. J Neurosci. 1996 Aug 15; 16(16): 5014-25.

El-Husseini AE, Topinka JR, Lehrer-Graiwer JE, Firestein BL, Craven SE, Aoki C, Bredt DS. Ion channel clustering by membrane-associated guanylate kinases. Differential regulation by N-terminal lipid and metal binding motifs. J Biol Chem. 2000 Aug 4; 275(31):23904-10.

English JD, Sweatt JD. Activation of p42 mitogen-activated protein kinase in hippocampal long term potentiation. J Biol Chem. 1996 Oct 4; 271(40): 24329-32.

English JD, Sweatt JD. A requirement for the mitogen-activated protein kinase cascade in hippocampal long term potentiation. J Biol Chem. 1997 Aug 1; 272(31): 19103-6.

Eriksson M, Nilsson A, Froelich-Fabre S, Akesson E, Dunker J, Sieger A, Folkesson R, Benedikz E, Sundstrom E. Cloning and expression of the human N-methyl-D-aspartate receptor subunit NR3A. Neurosci Lett. 2002 Mar 22; 321(3): 177-81. Erratum in: Neurosci Lett 2002 Oct 4; 331(1): 69-70.

Fagni L, Olivier M, Lafon-Cazal M, Bockaert J. Involvement of divalent ions in the nitric oxide-induced blockade of N-methyl-D-aspartate receptors in cerebellar granule cells. Mol Pharmacol. 1995 Jun; 47(6):1239-47.

Ferrer-Montiel AV, Sun W, Montal M. Molecular design of the N-methyl-D-aspartate receptor binding site for phencyclidine and dizolcipine. Proc Natl Acad Sci U S A. 1995 Aug 15; 92(17):8021-5.

Fink CC, Meyer T. Molecular mechanisms of CaMKII activation in neuronal plasticity. Curr Opin Neurobiol. 2002 Jun; 12(3): 293-9.

Fletcher EL, Hack I, Brandstatter JH, Wassle H. Synaptic localization of NMDA receptor subunits in the rat retina. J Comp Neurol. 2000 Apr 24; 420(1):98-112.

Forrest D, Yuzaki M, Soares HD, Ng L, Luk DC, Sheng M, Stewart CL, Morgan JI, Connor JA, Curran T. Targeted disruption of NMDA receptor 1 gene abolishes NMDA response and results in neonatal death. Neuron. 1994 Aug; 13(2): 325-38.

Frankland PW, Bontempi B, Talton LE, Kaczmarek L, Silva AJ. The involvement of the anterior cingulate cortex in remote contextual fear memory. Science. 2004 May 7; 304(5672):881-3.

Frey U, Huang YY, Kandel ER. Effects of cAMP simulate a late stage of LTP in hippocampal CA1 neurons. Science. 1993 Jun 11; 260(5114):1661-4.

Frost WN, Castellucci VF, Hawkins RD, Kandel ER. Monosynaptic connections made by the sensory neurons of the gill- and siphon-withdrawal reflex in Aplysia participate in the storage of long-term memory for sensitization. Proc Natl Acad Sci U S A. 1985 Dec; 82(23):8266-8269.

Fukunaga K, Stoppini L, Miyamoto E, Muller D. Long-term potentiation is associated with an increased activity of Ca2+/calmodulin-dependent protein kinase II. J Biol Chem. 1993 Apr 15; 268(11):7863-7.

Fukunaga K, Muller D, Miyamoto E. Increased phosphorylation of Ca2+/calmodulin-dependent protein kinase II and its endogenous substrates in the induction of long-term potentiation. J Biol Chem. 1995 Mar 17; 270(11):6119-24.

Fürst K. Introduction to the pharmacology of positive psychotropic compounds. Pharmacology. 2001: 323-325.

Gaertner TR, Kolodziej SJ, Wang D, Kobayashi R, Koomen JM, Stoops JK, Waxham MN. Comparative analyses of the three-dimensional structures and enzymatic properties of alpha, beta, gamma and delta isoforms of Ca2+-calmodulin-dependent protein kinase II. J Biol Chem. 2004 Mar 26; 279(13):12484-94. Epub 2004 Jan 12.

Garcia EP, Mehta S, Blair LA, Wells DG, Shang J, Fukushima T, Fallon JR, Garner CC, Marshall J. SAP90 binds and clusters kainate receptors causing incomplete desensitization. Neuron. 1998 Oct; 21(4):727-39.

Gardoni F, Caputi A, Cimino M, Pastorino L, Cattabeni F, Di Luca M. Calcium/calmodulin-dependent protein kinase II is associated with NR2A/B subunits of NMDA receptor in postsynaptic densities. J Neurochem. 1998 Oct; 71(4): 1733-41.

Gardoni F, Schrama LH, van Dalen JJ, Gispen WH, Cattabeni F, Di Luca M. AlphaCaMKII binding to the C-terminal tail of NMDA receptor subunit NR2A and its modulation by autophosphorylation. FEBS Lett. 1999 Aug 13; 456(3): 394-8.

Gardoni F, Bellone C, Cattabeni F, Di Luca M. Protein kinase C activation modulates alpha-calmodulin kinase II binding to NR2A subunit of N-methyl-D-aspartate receptor complex. J Biol Chem. 2001 Mar 9; 276(10): 7609-13. Epub 2000 Dec 04.

Garner CC, Nash J, Huganir RL. PDZ domains in synapse assembly and signalling. Trends Cell Biol. 2000 Jul; 10(7):274-80.

Gerlai R, Henderson JT, Roder JC, Jia Z. Multiple behavioral anomalies in GluR2 mutant mice exhibiting enhanced LTP. Behav Brain Res. 1998 Sep; 95(1):37-45.

Giese KP, Fedorov NB, Filipkowski RK, Silva AJ. Autophosphorylation at Thr286 of the alpha calcium-calmodulin kinase II in LTP and learning. Science. 1998 Feb 6; 279(5352):870-3.

Glanzman DL, Mackey SL, Hawkins RD, Dyke AM, Lloyd PE, Kandel ER. Depletion of serotonin in the nervous system of Aplysia reduces the behavioral enhancement of gill withdrawal as well as the heterosynaptic facilitation produced by tail shock. J Neurosci. 1989 Dec; 9(12):4200-13.

Gormezano I, Schneiderman N, Deaux E, Fuentes I. Nictitating membrane: classical conditioning and extinction in the albino rabbit. Science. 1962 Oct 5; 138:33-4.

Gooney M, Shaw K, Kelly A, O'Mara SM, Lynch MA. Long-term potentiation and spatial learning are associated with increased phosphorylation of TrkB and extracellular signal-regulated kinase (ERK) in the dentate gyrus: evidence for a role for brain-derived neurotrophic factor. Behav Neurosci. 2002 Jun; 116(3): 455-63.

Gossen M, Freundlieb S, Bender G, Muller G, Hillen W, Bujard H. Transcriptional activation by tetracyclines in mammalian cells. Science. 1995 Jun 23; 268(5218): 1766-9.

Gossler A, Doetschman T, Korn R, Serfling E, Kemler R.Transgenesis by means of blastocyst-derived embryonic stem cell lines. Proc Natl Acad Sci U S A. 1986 Dec; 83(23): 9065-9.

Grant SG, O'Dell TJ, Karl KA, Stein PL, Soriano P, Kandel ER. Impaired long-term potentiation, spatial learning, and hippocampal development in fyn mutant mice. Science. 1992 Dec 18; 258(5090): 1903-10.

Grimwood S, Slater P, Deakin JF, Hutson PH. NR2B-containing NMDA receptors are up-regulated in temporal cortex in schizophrenia. Neuroreport. 1999 Feb 25; 10(3): 461-5.

Grosshans DR, Browning MD. Protein kinase C activation induces tyrosine phosphorylation of the NR2A and NR2B subunits of the NMDA receptor. J Neurochem. 2001 Feb; 76(3): 737-44.

Gu JG, Albuquerque C, Lee CJ, MacDermott AB. Synaptic strengthening through activation of Ca2+-permeable AMPA receptors. Nature. 1996 Jun 27; 381(6585):793-6.

Gurd JW, Bissoon N. The N-methyl-D-aspartate receptor subunits NR2A and NR2B bind to the SH2 domains of phospholipase C-gamma. J Neurochem. 1997 Aug; 69(2): 623-30.

Hall RA, Soderling TR. Differential surface expression and phosphorylation of the N-methyl-D-aspartate receptor subunits NR1 and NR2 in cultured hippocampal neurons. J Biol Chem. 1997 Feb 14; 272(7): 4135-40.

Hallett PJ, Dunah AW, Ravenscroft P, Zhou S, Bezard E, Crossman AR, Brotchie JM, Standaert DG. Alterations of striatal NMDA receptor subunits associated with the development of dyskinesia in the MPTP-lesioned primate model of Parkinson's disease. Neuropharmacology. 2005 Mar; 48(4): 503-16.

Harding TC, Geddes BJ, Murphy D, Knight D, Uney JB. Switching transgene expression in the brain using an adenoviral tetracycline-regulatable system. Nat Biotechnol. 1998 Jun; 16(6): 553-5.

Harris EW, Cotman CW. Long-term potentiation of guinea pig mossy fiber responses is not blocked by N-methyl D-aspartate antagonists. Neurosci Lett. 1986 Sep 25; 70(1):132-7.

Haskins J, Gu L, Wittchen ES, Hibbard J, Stevenson BR. ZO-3, a novel member of the MAGUK protein family found at the tight junction, interacts with ZO-1 and occludin. J Cell Biol. 1998 Apr 6; 141(1):199-208.

Hawkins RD, Castellucci VF, Kandel ER. Interneurons involved in mediation and modulation of gill-withdrawal reflex in Aplysia. I. Identification and characterization. J Neurophysiol. 1981 Feb; 45(2):304-14.

Hawkins LM, Chazot PL, Stephenson FA. Biochemical evidence for the co-association of three N-methyl-D-aspartate (NMDA) R2 subunits in recombinant NMDA receptors. J Biol Chem. 1999 Sep 17; 274(38): 27211-8.

Hayashi T. A physiological study of epileptic seizures following cortical stimulation in animals and its application to human clinics. Jpn. J Physiol. 1952(3): 46-64.

Hayashi T. Keio J. Med. 1954 3: 183-192.

Hebb DO. The organisation of behaviour: A neuro- psychological theory. New York: John Wiley.

Heisler LK, Tecott LH. Knockout Corner: Neurobehavioural consequences of a serotonin 5-HT(2C) receptor gene mutation. Int J Neuropsychopharmacol. 1999 Mar; 2(1): 67-69.

Herb A, Burnashev N, Werner P, Sakmann B, Wisden W, Seeburg PH. The KA-2 subunit of excitatory amino acid receptors shows widespread expression in brain and forms ion channels with distantly related subunits. Neuron. 1992 Apr; 8(4):775-85.

Higuchi M, Single FN, Kohler M, Sommer B, Sprengel R, Seeburg PH. RNA editing of AMPA receptor subunit GluR-B: a base-paired intron-exon structure determines position and efficiency. Cell. 1993 Dec 31; 75(7):1361-70.

Higuchi M, Maas S, Single FN, Hartner J, Rozov A, Burnashev N, Feldmeyer D, Sprengel R, Seeburg PH. Point mutation in an AMPA receptor gene rescues lethality in mice deficient in the RNA-editing enzyme ADAR2. Nature. 2000 Jul 6; 406(6791): 78-81.

Hinds HL, Tonegawa S, Malinow R. CA1 long-term potentiation is diminished but present in hippocampal slices from alpha-CaMKII mutant mice. Learn Mem. 1998 Sep-Oct; 5(4-5): 344-54.

Hirao K, Hata Y, Ide N, Takeuchi M, Irie M, Yao I, Deguchi M, Toyoda A, Sudhof TC, Takai Y. A novel multiple PDZ domain-containing molecule interacting with N-methyl-D-aspartate receptors and neuronal cell adhesion proteins. J Biol Chem. 1998 Aug 14; 273(33):21105-10.

Hirao K, Hata Y, Yao I, Deguchi M, Kawabe H, Mizoguchi A, Takai Y. Three isoforms of synaptic scaffolding molecule and their characterization. Multimerization between the isoforms and their interaction with N-methyl-D-aspartate receptors and SAP90/PSD-95-associated protein. J Biol Chem. 2000 Jan 28; 275(4): 2966-72.

Hisatsune C, Umemori H, Inoue T, Michikawa T, Kohda K, Mikoshiba K, Yamamoto T. Phosphorylation-dependent regulation of N-methyl-D-aspartate receptors by calmodulin. J Biol Chem. 1997 Aug 15; 272(33):20805-10.

Hisatsune C, Umemori H, Mishina M, Yamamoto T. Phosphorylation-dependent interaction of the N-methyl-D-aspartate receptor epsilon 2 subunit with phosphatidylinositol 3-kinase. Genes Cells. 1999 Nov; 4(11): 657-66.

Hollmann M, Boulter J, Maron C, Beasley L, Sullivan J, Pecht G, Heinemann S. Zinc potentiates agonist-induced currents at certain splice variants of the NMDA receptor. Neuron. 1993 May; 10(5): 943-54.

Hollmann M, Maron C, Heinemann S. N-glycosylation site tagging suggests a three transmembrane domain topology for the glutamate receptor GluR1. Neuron. 1994 Dec; 13(6): 1331-43.

Hollmann M, Heinemann S. Cloned glutamate receptors. Annu Rev Neurosci. 1994; 17: 31-108.

Holscher C, Anwyl R, Rowan MJ. Block of theta-burst-induced long-term potentiation by (1S,3S)-1-aminocyclopentane-1,3-dicarboxylic acid: further evidence against long-term potentiation as a model for learning. Neuroscience. 1997 Nov; 81(1): 17-22.

Honer M, Benke D, Laube B, Kuhse J, Heckendorn R, Allgeier H, Angst C, Monyer H, Seeburg PH, Betz H, Mohler H. Differentiation of glycine antagonist sites of N-methyl-D-aspartate receptor subtypes. Preferential interaction of CGP 61594 with NR1/2B receptors. J Biol Chem. 1998 May 1; 273(18):11158-63.

Huang YY, Kandel ER. Recruitment of long-lasting and protein kinase A-dependent long-term potentiation in the CA1 region of hippocampus requires repeated tetanization. Learn Mem. 1994 May-Jun; 1(1): 74-82.

Huang YY, Kandel ER, Varshavsky L, Brandon EP, Qi M, Idzerda RL, McKnight GS, Bourtchouladze R. A genetic test of the effects of mutations in PKA on mossy fiber LTP and its relation to spatial and contextual learning. Cell. 1995 Dec 29; 83(7): 1211-22.

Huang YY, Kandel ER. Postsynaptic induction and PKA-dependent expression of LTP in the lateral amygdala. Neuron. 1998 Jul; 21(1):169-78.

Huang CC, Hsu KS. Sustained activation of metabotropic glutamate receptor 5 and protein tyrosine phosphatases mediate the expression of (S)-3,5-dihydroxyphenylglycine-induced long-term depression in the hippocampal CA1 region. J Neurochem. 2006 Jan; 96(1):179-94. Epub 2005 Nov 8.

Husi H, Ward MA, Choudhary JS, Blackstock WP, Grant SG. Proteomic analysis of NMDA receptor-adhesion protein signaling complexes. Nat Neurosci. 2000 Jul; 3(7): 661-9.

Husi H and Grant SG. Proteomics of the nervous system. Trends in Neurosciences. 2001 May; 24(5): 259-66.

Hynd MR, Scott HL, Dodd PR. Differential expression of N-methyl-D-aspartate receptor NR2 isoforms in Alzheimer's disease. J Neurochem. 2004 Aug; 90(4): 913-9.

Ikeda K, Nagasawa M, Mori H, Araki K, Sakimura K, Watanabe M, Inoue Y, Mishina M. Cloning and expression of the epsilon 4 subunit of the NMDA receptor channel. FEBS Lett. 1992 Nov 16; 313(1): 34-8.

Ikeda K, Araki K, Takayama C, Inoue Y, Yagi T, Aizawa S, Mishina M. Reduced spontaneous activity of mice defective in the epsilon 4 subunit of the NMDA receptor channel. Brain Res Mol Brain Res. 1995 Oct; 33(1): 61-71.

Impey S, Obrietan K, Wong ST, Poser S, Yano S, Wayman G, Deloulme JC, Chan G, Storm DR. Cross talk between ERK and PKA is required for Ca2+ stimulation of CREB-dependent transcription and ERK nuclear translocation. Neuron. 1998 Oct; 21(4): 869-83.

Irie M, Hata Y, Takeuchi M, Ichtchenko K, Toyoda A, Hirao K, Takai Y, Rosahl TW, Sudhof TC. Binding of neuroligins to PSD-95. Science. 1997 Sep 5; 277(5331):1511-5.

Irvine EE, Vernon J, Giese KP. AlphaCaMKII autophosphorylation contributes to rapid learning but is not necessary for memory. Nat Neurosci. 2005 Apr; 8(4):411-2. Epub 2005 Mar 20.

Isaac JT, Nicoll RA, Malenka RC. Evidence for silent synapses: implications for the expression of LTP. Neuron. 1995 Aug; 15(2): 427-34.

Ishii T, Moriyoshi K, Sugihara H, Sakurada K, Kadotani H, Yokoi M, Akazawa C, Shigemoto R, Mizuno N, Masu M, et al. Molecular characterization of the family of the N-methyl-D-aspartate receptor subunits. J Biol Chem. 1993 Feb 5; 268(4): 2836-43.

Itzstein C, Cheynel H, Burt-Pichat B, Merle B, Espinosa L, Delmas PD, Chenu C. Molecular identification of NMDA glutamate receptors expressed in bone cells. J Cell Biochem. 2001 Apr 2-27; 82 (1): 134-44.

Iwasato T, Erzurumlu RS, Huerta PT, Chen DF, Sasaoka T, Ulupinar E, Tonegawa S. NMDA receptor-dependent refinement of somatotopic maps. Neuron. 1997 Dec; 19(6): 1201-10.

Iwasato T, Datwani A, Wolf AM, Nishiyama H, Taguchi Y, Tonegawa S, Knopfel T, Erzurumlu RS, Itohara S. Cortex-restricted disruption of NMDAR1 impairs neuronal patterns in the barrel cortex. Nature. 2000 Aug 17; 406(6797): 726-31.

Jaskolski F, Coussen F, Mulle C. Subcellular localization and trafficking of kainate receptors. Trends Pharmacol Sci. 2005 Jan; 26(1):20-6.

Jesaitis LA, Goodenough DA. Molecular characterization and tissue distribution of ZO-2, a tight junction protein homologous to ZO-1 and the Drosophila discs-large tumor suppressor protein. J Cell Biol. 1994 Mar; 124(6):949-61.

Jia CY, Nie J, Wu C, Li C, Li SS. Novel Src homology 3 domain-binding motifs identified from proteomic screen of a Pro-rich region. Mol Cell Proteomics. 2005 Aug; 4(8):1155-66. Epub 2005 May 31.

Jia Z, Agopyan N, Miu P, Xiong Z, Henderson J, Gerlai R, Taverna FA, Velumian A, MacDonald J, Carlen P, Abramow-Newerly W, Roder J. Enhanced LTP in mice deficient in the AMPA receptor GluR2. Neuron. 1996 Nov; 17(5): 945-56.

Jia Z, Lu YM, Agopyan N, Roder J.Gene targeting reveals a role for the glutamate receptors mGluR5 and GluR2 in learning and memory. Physiol Behav. 2001 Aug; 73(5): 793-802.

Jo K, Derin R, Li M, Bredt DS. Characterization of MALS/Velis-1, -2, and -3: a family of mammalian LIN-7 homologs enriched at brain synapses in association with the postsynaptic density-95/NMDA receptor postsynaptic complex. J Neurosci. 1999 Jun 1; 19(11): 4189-99.

Johnson JW, Ascher P. Glycine potentiates the NMDA response in cultured mouse brain neurons. Nature. 1987 Feb 5-11; 325(6104): 529-31.

Kadotani H, Hirano T, Masugi M, Nakamura K, Nakao K, Katsuki M, Nakanishi S. Motor discoordination results from combined gene disruption of the NMDA receptor NR2A and NR2C subunits, but not from single disruption of the NR2A or NR2C subunit. J Neurosci. 1996 Dec 15; 16(24): 7859-67.

Kakegawa W, Tsuzuki K, Yoshida Y, Kameyama K, Ozawa S. Input- and subunit-specific AMPA receptor trafficking underlying long-term potentiation at hippocampal CA3 synapses. Eur J Neurosci. 2004 Jul; 20(1):101-10.

Kakegawa W, Yuzaki M. A mechanism underlying AMPA receptor trafficking during cerebellar long-term potentiation. Proc Natl Acad Sci U S A. 2005 Dec 6; 102(49):17846-51. Epub 2005 Nov 22.

Kandel ER, Schwartz JH, Jessel TM. Principles of neural science. Third edition. Elsevier, New York. 1991.

Kang H, Sun LD, Atkins CM, Soderling TR, Wilson MA, Tonegawa S. An important role of neural activity-dependent CaMKIV signaling in the consolidation of long-term memory. Cell. 2001 Sep 21; 106(6):771-83.

Kellendonk C, Tronche F, Casanova E, Anlag K, Opherk C, Schutz G. Inducible site-specific recombination in the brain. J Mol Biol. 1999 Jan 8; 285(1): 175-82.

Kelly A, Lynch MA. Long-term potentiation in dentate gyrus of the rat is inhibited by the phosphoinositide 3-kinase inhibitor, wortmannin. Neuropharmacology. 2000 Feb 14; 39(4): 643-51.

Kemp N, McQueen J, Faulkes S, Bashir ZI. Different forms of LTD in the CA1 region of the hippocampus: role of age and stimulus protocol. Eur J Neurosci. 2000 Jan; 12(1):360-6.

Kim E, Niethammer M, Rothschild A, Jan YN, Sheng M. Clustering of Shaker-type K+ channels by interaction with a family of membrane-associated guanylate kinases. Nature. 1995 Nov 2; 378(6552):85-8.

Kim E, Cho KO, Rothschild A, Sheng M. Heteromultimerization and NMDA receptor-clustering activity of Chapsyn-110, a member of the PSD-95 family of proteins. Neuron. 1996 Jul; 17(1):103-13.

Kim E, Naisbitt S, Hsueh YP, Rao A, Rothschild A, Craig AM, Sheng M. GKAP, a novel synaptic protein that interacts with the guanylate kinase-like domain of the PSD-95/SAP90 family of channel clustering molecules. J Cell Biol. 1997 Feb 10; 136(3):669-78.

Kim MJ, Dunah AW, Wang YT, Sheng M. Differential roles of NR2A- and NR2B-containing NMDA receptors in Ras-ERK signalling and AMPA receptor trafficking. Neuron. 2005 Jun 2; 46(5): 745-60.

Kim WT, Kuo MF, Mishra OP, Delivoria-Papadopoulos M. Distribution and expression of the subunits of N-methyl-D-aspartate (NMDA) receptors; NR1, NR2A and NR2B in hypoxic newborn piglet brains. Brain Res. 1998 Jul 13; 799(1): 49-54.

Kirwan CB, Stark CE. Medial temporal lobe activation during encoding and retrieval of novel face-name pairs. Hippocampus. 2004; 14(7):919-30.

Kobayashi K, Manabe T, Takahashi T. Presynaptic long-term depression at the hippocampal mossy fiber-CA3 synapse. Science. 1996 Aug 2; 273(5275):648-50.

Kohler M, Burnashev N, Sakmann B, Seeburg PH. Determinants of Ca2+ permeability in both TM1 and TM2 of high affinity kainate receptor channels: diversity by RNA editing. Neuron. 1993 Mar; 10(3):491-500.

Kohr G, Eckardt S, Luddens H, Monyer H, Seeburg PH. NMDA receptor channels: subunit-specific potentiation by reducing agents. Neuron. 1994 May; 12(5):1031-40.

Kohr G, Jensen V, Koester HJ, Mihaljevic AL, Utvik JK, Kvello A, Ottersen OP, Seeburg PH, Sprengel R, Hvalby O. Intracellular domains of NMDA receptor subtypes are determinants for long-term potentiation induction. J Neurosci. 2003 Nov 26; 23(34):10791-9.

Kojima N, Wang J, Mansuy IM, Grant SG, Mayford M, Kandel ER. Rescuing impairment of long-term potentiation in fyn-deficient mice by introducing Fyn transgene. Proc Natl Acad Sci U S A. 1997 Apr 29; 94(9): 4761-5.

Kolb B, Buhrmann K, McDonald R, Sutherland RJ. Dissociation of the medial prefrontal, posterior parietal, and posterior temporal cortex for spatial navigation and recognition memory in the rat. Cereb Cortex. 1994 Nov-Dec; 4(6):664-80.

Komiyama NH, Watabe AM, Carlisle HJ, Porter K, Charlesworth P, Monti J, Strathdee DJ, O'Carroll CM, Martin SJ, Morris RG, O'Dell TJ, Grant SG. SynGAP regulates ERK/MAPK signaling, synaptic plasticity, and learning in the complex with postsynaptic density 95 and NMDA receptor. J Neurosci. 2002 Nov 15; 22(22): 9721-32.

Koponen E, Voikar V, Riekki R, Saarelainen T, Rauramaa T, Rauvala H, Taira T, Castren E. Transgenic mice overexpressing the full-length neurotrophin receptor

trkB exhibit increased activation of the trkB-PLCgamma pathway, reduced anxiety, and facilitated learning. Mol Cell Neurosci. 2004 May; 26(1): 166-81.

Krupp JJ, Vissel B, Thomas CG, Heinemann SF, Westbrook GL. Interactions of calmodulin and alpha-actinin with the NR1 subunit modulate Ca2+-dependent inactivation of NMDA receptors. J Neurosci. 1999 Feb 15; 19(4):1165-78.

Kuner T, Schoepfer R. Multiple structural elements determine subunit specificity of Mg2+ block in NMDA receptor channels. J Neurosci. 1996 Jun 1; 16(11):3549-58.

Kurschner C, Mermelstein PG, Holden WT, Surmeier DJ. CIPP, a novel multivalent PDZ domain protein, selectively interacts with Kir4.0 family members, NMDA receptor subunits, neurexins, and neuroligins. Mol Cell Neurosci. 1998 Jun; 11(3): 161-72.

Kuryatov A, Laube B, Betz H, Kuhse J.Mutational analysis of the glycine-binding site of the NMDA receptor: structural similarity with bacterial amino acid-binding proteins. Neuron. 1994 Jun;12(6): 1291-300.

Kutsuwada T, Kashiwabuchi N, Mori H, Sakimura K, Kushiya E, Araki K, Meguro H, Masaki H, Kumanishi T, Arakawa M, et al. Molecular diversity of the NMDA receptor channel. Nature. 1992 Jul 2; 358(6381): 36-41.

Kutsuwada T, Sakimura K, Manabe T, Takayama C, Katakura N, Kushiya E, Natsume R, Watanabe M, Inoue Y, Yagi T, Aizawa S, Arakawa M, Takahashi T, Nakamura Y, Mori H, Mishina M. Impairment of suckling response, trigeminal neuronal pattern formation, and hippocampal LTD in NMDA receptor epsilon 2 subunit mutant mice. Neuron. 1996 Feb; 16(2): 333-44.

Laezza F, Doherty JJ, Dingledine R. Long-term depression in hippocampal interneurons: joint requirement for pre- and postsynaptic events. Science. 1999 Aug 27; 285(5432):1411-4.

Laube B, Kuhse J, Betz H. Evidence for a tetrameric structure of recombinant NMDA receptors. J Neurosci. 1998 Apr 15; 18(8): 2954-61.

Laurie DJ, Seeburg PH. Ligand affinities at recombinant N-methyl-D-aspartate receptors depend on subunit composition. Eur J Pharmacol. 1994 Aug 16; 268(3):335-45.

Lengyel I, Voss K, Cammarota M, Bradshaw K, Brent V, Murphy KP, Giese KP, Rostas JA, Bliss TV. Autonomous activity of CaMKII is only transiently increased following the induction of long-term potentiation in the rat hippocampus. Eur J Neurosci. 2004 Dec; 20(11):3063-72.

Leonard AS, Hell JW. Cyclic AMP-dependent protein kinase and protein kinase C phosphorylate N-methyl-D-aspartate receptors at different sites. J Biol Chem. 1997 May 2; 272(18): 12107-15.

Leonard AS, Lim IA, Hemsworth DE, Horne MC, Hell JW. Calcium/calmodulin-dependent protein kinase II is associated with the N-methyl-D-aspartate receptor. Proc Natl Acad Sci U S A. 1999 Mar 16; 96(6): 3239-44.

Levenes C, Daniel H, Crepel F. Long-term depression of synaptic transmission in the cerebellum: cellular and molecular mechanisms revisited. Prog Neurobiol. 1998 May; 55(1):79-91.

Li Y, Erzurumlu RS, Chen C, Jhaveri S, Tonegawa S. Whisker-related neuronal patterns fail to develop in the trigeminal brainstem nuclei of NMDAR1 knockout mice. Cell. 1994 Feb 11; 76(3): 427-37.

Li BS, Sun MK, Zhang L, Takahashi S, Ma W, Vinade L, Kulkarni AB, Brady RO, Pant HC. Regulation of NMDA receptors by cyclin-dependent kinase-5. Proc Natl Acad Sci U S A. 2001 Oct 23; 98(22): 12742-7. Epub 2001 Oct 02.

Liao D, Scannevin RH, Huganir R. Activation of silent synapses by rapid activity-dependent synaptic recruitment of AMPA receptors. J Neurosci. 2001 Aug 15; 21(16): 6008-17.

Liao F, Shin HS, Rhee SG. Tyrosine phosphorylation of phospholipase C-gamma 1 induced by cross-linking of the high-affinity or low-affinity Fc receptor for IgG in U937 cells. Proc Natl Acad Sci U S A. 1992 Apr 15; 89(8):3659-63.

Liao GY, Wagner DA, Hsu MH, Leonard JP. Evidence for direct protein kinase-C mediated modulation of N-methyl-D-aspartate receptor current. Mol Pharmacol. 2001 May; 59(5): 960-4.

Lin CH, Yeh SH, Lin CH, Lu KT, Leu TH, Chang WC, Gean PW. A role for the PI-3 kinase signaling pathway in fear conditioning and synaptic plasticity in the amygdala. Neuron. 2001 Sep 13; 31(5): 841-51.

Lin JW, Wyszynski M, Madhavan R, Sealock R, Kim JU, Sheng M. Yotiao, a novel protein of neuromuscular junction and brain that interacts with specific splice variants of NMDA receptor subunit NR1. J Neurosci. 1998 Mar 15; 18(6): 2017-27.

Lin SY, Wu K, Len GW, Xu JL, Levine ES, Suen PC, Mount HT, Black IB. Brain-derived neurotrophic factor enhances association of protein tyrosine phosphatase PTP1D with the NMDA receptor subunit NR2B in the cortical postsynaptic density. Brain Res Mol Brain Res. 1999 Jun 18; 70(1): 18-25.

Lin Y, Skeberdis VA, Francesconi A, Bennett MV, Zukin RS. Postsynaptic density protein-95 regulates NMDA channel gating and surface expression. J Neurosci. 2004 Nov 10; 24(45):10138-48.

Lipton SA, Kim WK, Choi YB, Kumar S, D'Emilia DM, Rayudu PV, Arnelle DR, Stamler JS. Neurotoxicity associated with dual actions of homocysteine at the N-

methyl-D-aspartate receptor. Proc Natl Acad Sci U S A. 1997 May 27; 94(11):5923-8.

Lisman JE. A mechanism for memory storage insensitive to molecular turnover: a bistable autophosphorylating kinase. Proc Natl Acad Sci U S A. 1985 May; 82(9):3055-7.

Lisman JE, Zhabotinsky AM. A model of synaptic memory: a CaMKII/PP1 switch that potentiates transmission by organizing an AMPA receptor anchoring assembly. Neuron. 2001 Aug 2; 31(2):191-201.

Lisman J, Schulman H, Cline H. The molecular basis of CaMKII function in synaptic and behavioural memory. Nat Rev Neurosci. 2002 Mar; 3(3):175-90.

Liu H, Wang H, Sheng M, Jan L, Jan YN, Basbaum AI. Evidence for presynaptic N-methyl-D-aspartate autoreceptors in the spinal cord dorsal horn. Proc Natl Acad Sci U S A. 1994 Aug 30; 91(18): 8383-7.

Liu L, Wong TP, Pozza MF, Lingenhoehl K, Wang Y, Sheng M, Auberson YP, Wang YT. Role of NMDA receptor subtypes in governing the direction of hippocampal synaptic plasticity. Science. 2004 May 14; 304(5673): 1021-4.

Liu Y, Zhang G, Gao C, Hou X. NMDA receptor activation results in tyrosine phosphorylation of NMDA receptor subunit 2A(NR2A) and interaction of Pyk2 and Src with NR2A after transient cerebral ischemia and reperfusion. Brain Res. 2001 Aug 3; 909(1-2): 51-8.

Lomeli H, Mosbacher J, Melcher T, Hoger T, Geiger JR, Kuner T, Monyer H, Higuchi M, Bach A, Seeburg PH. Control of kinetic properties of AMPA receptor channels by nuclear RNA editing. Science. 1994 Dec 9; 266(5191):1709-13.

Losi G, Prybylowski K, Fu Z, Luo J, Wenthold RJ, Vicini S. PSD-95 regulates NMDA receptors in developing cerebellar granule neurons of the rat. J Physiol. 2003 Apr 1; 548(Pt 1):21-9. Epub 2003 Feb 7.

Lou LL, Schulman H. Distinct autophosphorylation sites sequentially produce autonomy and inhibition of the multifunctional Ca2+/calmodulin-dependent protein kinase. J Neurosci. 1989 Jun; 9(6):2020-32.

Lovinger DM, Wong KL, Murakami K, Routtenberg A. Protein kinase C inhibitors eliminate hippocampal long-term potentiation. Brain Res. 1987 Dec 8; 436(1): 177-83.

Lu YM, Jia Z, Janus C, Henderson JT, Gerlai R, Wojtowicz JM, Roder JC.Mice lacking metabotropic glutamate receptor 5 show impaired learning and reduced CA1 long-term potentiation (LTP) but normal CA3 LTP. J Neurosci. 1997 Jul 1; 17(13): 5196-205.

Lu YM, Roder JC, Davidow J, Salter MW. Src activation in the induction of long-term potentiation in CA1 hippocampal neurons. Science. 1998 Feb 27; 279(5355):1363-7.

Luo JH, Fu ZY, Losi G, Kim BG, Prybylowski K, Vissel B, Vicini S. Functional expression of distinct NMDA channel subunits tagged with green fluorescent protein in hippocampal neurons in culture. Neuropharmacology. 2002 Mar; 42(3): 306-18.

Lynch G, Larson J, Kelso S, Barrionuevo G, Schottler F. Intracellular injections of EGTA block induction of hippocampal long-term potentiation. Nature. 1983 Oct 20-26; 305(5936):719-21.

Lynch MA.Long-term potentiation and memory. Physiol Rev. 2004 Jan; 84(1): 87-136.

Mahanty NK, Sah P. Calcium-permeable AMPA receptors mediate long-term potentiation in interneurons in the amygdala. Nature. 1998 Aug 13; 394(6694):683-7.

Malenka RC, Kauer JA, Perkel DJ, Mauk MD, Kelly PT, Nicoll RA, Waxham MN. An essential role for postsynaptic calmodulin and protein kinase activity in long-term potentiation. Nature. 1989a Aug 17; 340(6234):554-7.

Malenka RC, Kauer JA, Perkel DJ, Nicoll RA. The impact of postsynaptic calcium on synaptic transmission--its role in long-term potentiation. Trends Neurosci. 1989b Nov; 12(11): 444-50.

Malinow R, Schulman H, Tsien RW. Inhibition of postsynaptic PKC or CaMKII blocks induction but not expression of LTP. Science. 1989 Aug 25; 245(4920): 862-6.

Malinow R, Malenka RC. AMPA receptor trafficking and synaptic plasticity. Annu Rev Neurosci. 2002; 25:103-26. Epub 2002 Mar 4.

Malleret G, Haditsch U, Genoux D, Jones MW, Bliss TV, Vanhoose AM, Weitlauf C, Kandel ER, Winder DG, Mansuy IM. Inducible and reversible enhancement of learning, memory, and long-term potentiation by genetic inhibition of calcineurin. Cell. 2001 Mar 9; 104(5): 675-86.

Manabe T, Aiba A, Yamada A, Ichise T, Sakagami H, Kondo H, Katsuki M. Regulation of long-term potentiation by H-Ras through NMDA receptor phosphorylation. J Neurosci. 2000 Apr 1; 20(7):2504-11.

Mansour M, Nagarajan N, Nehring RB, Clements JD, Rosenmund C. Heteromeric AMPA receptors assemble with a preferred subunit stoichiometry and spatial arrangement. Neuron. 2001 Dec 6; 32(5):841-53.

Maragos WF, Chu DC, Young AB, D'Amato CJ, Penney JB Jr. Loss of hippocampal [3H]TCP binding in Alzheimer's disease. Neurosci Lett. 1987 Mar 9; 74(3): 371-6.

Margolis B, Li N, Koch A, Mohammadi M, Hurwitz DR, Zilberstein A, Ullrich A, Pawson T, Schlessinger J. The tyrosine phosphorylated carboxyterminus of the EGF receptor is a binding site for GAP and PLC-gamma. EMBO J. 1990 Dec; 9(13):4375-80.

Markram H, Lubke J, Frotscher M, Sakmann B. Regulation of synaptic efficacy by coincidence of postsynaptic APs and EPSPs. Science. 1997 Jan 10; 275(5297):213-5.

Martin KC, Michael D, Rose JC, Barad M, Casadio A, Zhu H, Kandel ER. MAP kinase translocates into the nucleus of the presynaptic cell and is required for long-term facilitation in Aplysia. Neuron. 1997 Jun; 18(6): 899-912.

Massey PV, Johnson BE, Moult PR, Auberson YP, Brown MW, Molnar E, Collinridge GL, Bashir ZI. Differential roles of NR2A and NR2B-containing NMDA receptors in cortical long-term potentiation and long-term depression. J Neurosci. 2004 Sep 8; 24(36): 7821-8.

Matthies H, Schroeder H, Becker A, Loh H, Hollt V, Krug M. Lack of expression of long-term potentiation in the dentate gyrus but not in the CA1 region of the hippocampus of mu-opioid receptor-deficient mice. Neuropharmacology. 2000 Apr 3; 39(6): 952-60.

Maviel T, Durkin TP, Menzaghi F, Bontempi B. Sites of neocortical reorganization critical for remote spatial memory. Science. 2004 Jul 2; 305(5680):96-9. Erratum in: Science. 2004 Aug 13; 305(5686):946.

Mayford M, Bach ME, Huang YY, Wang L, Hawkins RD, Kandel ER. Control of memory formation through regulated expression of a CaMKII transgene. Science. 1996 Dec 6; 274(5293): 1678-83.

Mazzucchelli C, Vantaggiato C, Ciamei A, Fasano S, Pakhotin P, Krezel W, Welzl H, Wolfer DP, Pages G, Valverde O, Marowsky A, Porrazzo A, Orban PC, Maldonado R, Ehrengruber MU, Cestari V, Lipp HP, Chapman PF, Pouyssegur J, Brambilla R. Knockout of ERK1 MAP kinase enhances synaptic plasticity in the striatum and facilitates striatal-mediated learning and memory. Neuron. 2002 May 30; 34(5): 807-20.

McHugh TJ, Blum KI, Tsien JZ, Tonegawa S, Wilson MA. Impaired hippocampal representation of space in CA1-specific NMDAR1 knockout mice. Cell. 1996 Dec 27; 87(7):1339-49.

McGahon BM, Murray CA, Horrobin DF, Lynch. Age-related changes in oxidative mechanisms and LTP are reversed by dietary manipulation. Neurobiol Aging. 1999 Nov-Dec; 20(6): 643-53.

McGuinness N, Anwyl R, Rowan M.The effects of external calcium on the N-methyl-D-aspartate induced short-term potentiation in the rat hippocampal slice. Neurosci Lett. 1991 Sep 30; 131(1): 13-6.

McHugh TJ, Blum KI, Tsien JZ, Tonegawa S, Wilson MA. Impaired hippocampal representation of space in CA1-specific NMDAR1 knockout mice. Cell. 1996 Dec 27; 87(7): 1339-49.

Meguro H, Mori H, Araki K, Kushiya E, Kutsuwada T, Yamazaki M, Kumanishi T, Arakawa M, Sakimura K, Mishina M. Functional characterization of a heteromeric NMDA receptor channel expressed from cloned cDNAs. Nature. 1992 May 7; 357(6373): 70-4.

Miki K, Zhou QQ, Guo W, Guan Y, Terayama R, Dubner R, Ren K. Changes in gene expression and neuronal phenotype in brain stem pain modulatory circuitry after inflammation. J Neurophysiol. 2002 Feb; 87(2): 750-60.

Miller SG, Patton BL, Kennedy MB. Sequences of autophosphorylation sites in neuronal type II CaM kinase that control Ca2(+)-independent activity. Neuron. 1988 Sep; 1(7):593-604.

Milner B. Disorders of learning and memory after temporal lobe lesions in man. Clin Neurosurg. 1972; 19:421-46.

Milner B, Squire LR, Kandel ER. Cognitive neuroscience and the study of memory. Neuron. 1998 Mar; 20(3):445-68.

Milner PM and Glickman S. In cognitive processes and the brain. Princeton, NU: Van nostrand. 1965. 97-111. (Original: Milner B. Les troubles de la memoire accompagnant les lesions hippocampiques bilaterales. Physiologie de l'Hippocampe, Colloques Internationaux 1962. 107: 257-272.)

Minichiello L, Korte M, Wolfer D, Kuhn R, Unsicker K, Cestari V, Rossi-Arnaud C, Lipp HP, Bonhoeffer T, Klein R. Essential role for TrkB receptors in hippocampus-mediated learning. Neuron. 1999 Oct; 24(2): 401-14.

Miyamoto Y, Yamada K, Noda Y, Mori H, Mishina M, Nabeshima T. Lower sensitivity to stress and altered monoaminergic neuronal function in mice lacking the NMDA receptor epsilon 4 subunit. J Neurosci. 2002 Mar 15; 22(6): 2335-42.

Miyashiro K, Dichter M, Eberwine J. On the nature and differential distribution of mRNAs in hippocampal neurites: implications for neuronal functioning. Proc Natl Acad Sci U S A. 1994 Nov 8; 91(23): 10800-4.

Mizuno K, Giese KP. Hippocampus-dependent memory formation: do memory type-specific mechanisms exist? J Pharmacol Sci. 2005 Jul; 98(3):191-7. Epub 2005 Jun 19.

Mohn AR, Gainetdinov RR, Caron MG, Koller BH. Mice with reduced NMDA receptor expression display behaviors related to schizophrenia. Cell. 1999 Aug 20; 98(4): 427-36.

Mohrmann R, Kohr G, Hatt H, Sprengel R, Gottmann K. Deletion of the C-terminal domain of the NR2B subunit alters channel properties and synaptic targeting of N-methyl-D-aspartate receptors in nascent neocortical synapses. J Neurosci Res. 2002 May 1; 68(3): 265-75.

Montarolo PG, Goelet P, Castellucci VF, Morgan J, Kandel ER, Schacher S. A critical period for macromolecular synthesis in long-term heterosynaptic facilitation in Aplysia. Science. 1986 Dec 5; 234(4781):1249-54.

Monyer H, Sprengel R, Schoepfer R, Herb A, Higuchi M, Lomeli H, Burnashev N, Sakmann B, Seeburg PH. Heteromeric NMDA receptors: molecular and functional distinction of subtypes. Science. 1992 May 22; 256(5060): 1217-21.

Monyer H, Burnashev N, Laurie DJ, Sakmann B, Seeburg PH. Developmental and regional expression in the rat brain and functional properties of four NMDA receptors. Neuron. 1994 Mar; 12(3): 529-40.

Mori H, Manabe T, Watanabe M, Satoh Y, Suzuki N, Toki S, Nakamura K, Yagi T, Kushiya E, Takahashi T, Inoue Y, Sakimura K, Mishina M. Role of the carboxy-terminal region of the GluR epsilon2 subunit in synaptic localization of the NMDA receptor channel. Neuron. 1998 Sep; 21(3): 571-80.

Morishita W, Lu W, Smith GB, Nicoll RA, Bear MF, Malenka RC. Activation of NR2B-containing NMDA receptors is not required for NMDA receptor-dependent long-term depression. Neuropharmacology. 2006 Aug 7.

Moriyoshi K, Masu M, Ishii T, Shigemoto R, Mizuno N, Nakanishi S. Molecular cloning and characterization of the rat NMDA receptor. Nature. 1991 Nov 7; 354(6348): 31-7.

Morris JS, Frith CD, Perrett DI, Rowland D, Young AW, Calder AJ, Dolan RJ. A differential neural response in the human amygdala to fearful and happy facial expressions. Nature. 1996 Oct 31; 383(6603):812-5.

Morris RG, Garrud P, Rawlins JN, O'Keefe J. Place navigation impaired in rats with hippocampal lesions. Nature. 1982 Jun 24; 297(5868):681-3.

Morris RG, Anderson E, Lynch GS, Baudry M. Selective impairment of learning and blockade of long-term potentiation by an N-methyl-D-aspartate receptor antagonist, AP5. Nature. 1986 Feb 27-Mar 5; 319(6056): 774-6.

Morris RG. Synaptic plasticity and learning: selective impairment of learning rats and blockade of long-term potentiation in vivo by the N-methyl-D-aspartate receptor antagonist AP5. J Neurosci. 1989 Sep; 9(9): 3040-57.

Morris RG, Davis S, Butcher SP. Hippocampal synaptic plasticity and NMDA receptors: a role in information storage? Philos Trans R Soc Lond B Biol Sci. 1990 Aug 29; 329(1253): 187-204.

Moult PR, Gladding CM, Sanderson TM, Fitzjohn SM, Bashir ZI, Molnar E, Collingridge GL. Tyrosine phosphatases regulate AMPA receptor trafficking during metabotropic glutamate receptor-mediated long-term depression. J Neurosci. 2006 Mar 1; 26(9):2544-54.

Mulkey RM, Malenka RC. Mechanisms underlying induction of homosynaptic long-term depression in area CA1 of the hippocampus. Neuron. 1992 Nov; 9(5): 967-75.

Mulkey RM, Endo S, Shenolikar S, Malenka RC. Involvement of a calcineurin/inhibitor-1 phosphatase cascade in hippocampal long-term depression. Nature. 1994 Jun 9; 369(6480):486-8.

Muller BM, Kistner U, Veh RW, Cases-Langhoff C, Becker B, Gundelfinger ED, Garner CC. Molecular characterization and spatial distribution of SAP97, a novel presynaptic protein homologous to SAP90 and the Drosophila discs-large tumor suppressor protein. J Neurosci. 1995 Mar; 15(3 Pt 2):2354-66.

Muller BM, Kistner U, Kindler S, Chung WJ, Kuhlendahl S, Fenster SD, Lau LF, Veh RW, Huganir RL, Gundelfinger ED, Garner CC. SAP102, a novel postsynaptic protein that interacts with NMDA receptor complexes in vivo. Neuron. 1996 Aug; 17(2):255-65.

Munoz A, Woods TM, Jones EG. Laminar and cellular distribution of AMPA, kainate, and NMDA receptor subunits in monkey sensory-motor cortex. J Comp Neurol. 1999 May 17; 407 (4): 472-90.

Murphy DD, Segal M. Morphological plasticity of dendritic spines in central neurons is mediated by activation of cAMP response element binding protein. Proc Natl Acad Sci U S A. 1997 Feb 18; 94(4): 1482-7.

Nagy J. The NR2B subtype of NMDA receptor: a potential target for the treatment of alcohol dependence. Curr Drug Targets CNS Neurol Disord. 2004 Jun; 3(3): 169-79.

Nakazawa K, Quirk MC, Chitwood RA, Watanabe M, Yeckel MF, Sun LD, Kato A, Carr CA, Johnston D, Wilson MA, Tonegawa S. Requirement for hippocampal CA3 NMDA receptors in associative memory recall. Science. 2002 Jul 12; 297(5579): 211-8. Epub 2002 May 30.

Nakazawa T, Komai S, Tezuka T, Hisatsune C, Umemori H, Semba K, Mishina M, Manabe T, Yamamoto T. Characterization of Fyn-mediated tyrosine phosphorylation sites on GluR epsilon 2 (NR2B) subunit of the N-methyl-D-aspartate receptor. J Biol Chem. 2001 Jan 5; 276(1): 693-9.

Nakazawa T, Komai S, Watabe AM, Kiyama Y, Fukaya M, Arima-Yoshida F, Horai R, Sudo K, Ebine K, Delawary M, Goto J, Umemori H, Tezuka T, Iwakura Y, Watanabe M, Yamamoto T, Manabe T. NR2B tyrosine phosphorylation modulates fear learning as well as amygdaloid synaptic plasticity. EMBO J. 2006 Jun 21; 25(12):2867-77. Epub 2006 May 18.

Nash JE, Hill MP, Brotchie JM. Antiparkinsonian actions of blockade of NR2B-containing NMDA receptors in the reserpine-treated rat. Exp Neurol. 1999 Jan; 155(1): 42-8.

Nguyen PV, Kandel ER. Brief theta-burst stimulation induces a transcription-dependent late phase of LTP requiring cAMP in area CA1 of the mouse hippocampus. Learn Mem. 1997 Jul-Aug; 4(2):230-43.

Nishi M, Hinds H, Lu HP, Kawata M, Hayashi Y. Motoneuron-specific expression of NR3B, a novel NMDA-type glutamate receptor subunit that works in a dominant-negative manner. J Neurosci. 2001 Dec 1; 21(23): RC185.

Noda Y, Mamiya T, Manabe T, Nishi M, Takeshima H, Nabeshima T. Role of nociceptin systems in learning and memory. Peptides. 2000 Jul; 21(7): 1063-9.

Nosten-Bertrand M, Errington ML, Murphy KP, Tokugawa Y, Barboni E, Kozlova E, Michalovich D, Morris RG, Silver J, Stewart CL, Bliss TV, Morris RJ.Normal spatial learning despite regional inhibition of LTP in mice lacking Thy-1. Nature. 1996 Feb 29; 379(6568): 826-9.

Nowak L, Bregestovski P, Ascher P, Herbet A, Prochiantz A. Magnesium gates glutamate-activated channels in mouse central neurones. Nature. 1984 Feb 2-8; 307(5950):462-5.

O'Dell TJ, Grant SG, Karl K, Soriano PM, Kandel ER. Pharmacological and genetic approaches to the analysis of tyrosine kinase function in long-term potentiation. Cold Spring Harb Symp Quant Biol. 1992; 57: 517-26.

Oh JD, Russell DS, Vaughan CL, Chase TN, Russell D. Enhanced tyrosine phosphorylation of striatal NMDA receptor subunits: effect of dopaminergic denervation and L-DOPA administration. Brain Res. 1998 Nov 30;813(1):150-9. Erratum in: Brain Res 1999 Feb 27; 820(1-2): 117.

Okabe S, Collin C, Auerbach JM, Meiri N, Bengzon J, Kennedy MB, Segal M, McKay RD. Hippocampal synaptic plasticity in mice overexpressing an embryonic subunit of the NMDA receptor. J Neurosci. 1998 Jun 1; 18(11): 4177-88.

Okabe S, Miwa A, Okado H. Alternative splicing of the C-terminal domain regulates cell surface expression of the NMDA receptor NR1 subunit. J Neurosci. 1999 Sep 15; 19(18):7781-92.

Olney JW, Newcomer JW, Farber NB. NMDA receptor hypofunction model of schizophrenia. J Psychiatr Res. 1999 Nov-Dec; 33(6): 523-33. Review.

O'Mara SM, Rowan MJ, Anwyl R. Metabotropic glutamate receptor-induced homosynaptic long-term depression and depotentiation in the dentate gyrus of the rat hippocampus in vitro. Neuropharmacology. 1995 Aug; 34(8):983-9.

Omkumar RV, Kiely MJ, Rosenstein AJ, Min KT, Kennedy MB. Identification of a phosphorylation site for calcium/calmodulindependent protein kinase II in the NR2B subunit of the N-methyl-D-aspartate receptor. J Biol Chem. 1996 Dec 6; 271(49): 31670-8.

Paoletti P, Ascher P, Neyton J. High-affinity zinc inhibition of NMDA NR1-NR2A receptors. J Neurosci. 1997 Aug 1; 17(15):5711-25. Erratum in: J Neurosci 1997 Oct 15;17(20).

Park M, Penick EC, Edwards JG, Kauer JA, Ehlers MD. Recycling endosomes supply AMPA receptors for LTP. Science. 2004 Sep 24; 305(5692):1972-5.

Park Y, Jo J, Isaac JT, Cho K. Long-term depression of kainate receptor-mediated synaptic transmission. Neuron. 2006 Jan 5; 49(1):95-106.

Patterson SL, Pittenger C, Morozov A, Martin KC, Scanlin H, Drake C, Kandel ER. Some forms of cAMP-mediated long-lasting potentiation are associated with release of BDNF and nuclear translocation of phospho-MAP kinase. Neuron. 2001 Oct 11; 32(1):123-40.

Penfield W, Milner B. Memory deficit produced by bilateral lesions in the hippocampal zone. AMA Arch Neurol Psychiatry. 1958 May; 79(5):475-97.

Perkel DJ, Hestrin S, Sah P, Nicoll RA.Excitatory synaptic currents in Purkinje cells. Proc Biol Sci. 1990 Aug 22; 241(1301): 116-21.

Plant T, Schirra C, Garaschuk O, Rossier J, Konnerth A. Molecular determinants of NMDA receptor function in GABAergic neurones of rat forebrain. J Physiol. 1997 Feb 15; 499 (Pt 1): 47-63.

Pourcho RG, Qin P, Goebel DJ. Cellular and subcellular distribution of NMDA receptor subunit NR2B in the retina. J Comp Neurol. 2001 Apr 23; 433(1):75-85.

Premkumar LS, Auerbach A. Stoichiometry of recombinant N-methyl-D-aspartate receptor channels inferred from single-channel current patterns. J Gen Physiol. 1997 Nov; 110(5): 485-502.

Puchalski RB, Louis JC, Brose N, Traynelis SF, Egebjerg J, Kukekov V, Wenthold RJ, Rogers SW, Lin F, Moran T, et al. Selective RNA editing and subunit assembly of native glutamate receptors. Neuron. 1994 Jul; 13(1):131-47.

Quinlan JE, Davies J.Excitatory and inhibitory responses of Purkinje cells, in the rat cerebellum in vivo, induced by excitatory amino acids. Neurosci Lett. 1985 Sep 16; 60(1): 39-46.

Rao A, Kim E, Sheng M, Craig AM. Heterogeneity in the molecular composition of excitatory postsynaptic sites during development of hippocampal neurons in culture. J Neurosci. 1998 Feb 15; 18(4):1217-29.

Raditsch M, Ruppersberg JP, Kuner T, Gunther W, Schoepfer R, Seeburg PH, Jahn W, Witzemann V. Subunit-specific block of cloned NMDA receptors by argiotoxin636. FEBS Lett. 1993 Jun 7; 324(1):63-6.

Rapp PR, Rosenberg RA, Gallagher M. An evaluation of spatial information processing in aged rats. Behav Neurosci. 1987 Feb; 101(1): 3-12.

Reymann KG, Brodemann R, Kase H, Matthies H. Inhibitors of calmodulin and protein kinase C block different phases of hippocampal long-term potentiation. Brain Res. 1988 Oct 4; 461(2): 388-92.

Robertson E, Bradley A, Kuehn M, Evans M. Germ-line transmission of genes introduced into cultured pluripotential cells by retroviral vector. Nature. 1986 Oct 2-8; 323(6087): 445-8.

Roche KW, Standley S, McCallum J, Dune Ly C, Ehlers MD, Wenthold RJ. Molecular determinants of NMDA receptor internalization. Nat Neurosci. 2001 Aug; 4(8):794-802.

Rock DM, MacDonald RL. Spermine and related polyamines produce a voltage-dependent reduction of N-methyl-D-aspartate receptor single-channel conductance. Mol Pharmacol. 1992 Jul; 42(1):157-64.

Rosenbaum RS, Ziegler M, Winocur G, Grady CL, Moscovitch M. "I have often walked down this street before": fMRI studies on the hippocampus and other structures during mental navigation of an old environment. Hippocampus. 2004; 14(7):826-35.

Rosenblum K, Dudai Y, Richter-Levin G. Long-term potentiation increases tyrosine phosphorylation of the N-methyl-D-aspartate receptor subunit 2B in rat dentate gyrus in vivo. Proc Natl Acad Sci U S A. 1996 Sep 17; 93(19):10457-60.

van Rossum D, Kuhse J, Betz H. Dynamic interaction between soluble tubulin and C-terminal domains of N-methyl-D-aspartate receptor subunits. J Neurochem. 1999 Mar; 72(3): 962-73.

Routtenberg A, Cantallops I, Zaffuto S, Serrano P, Namgung U.Enhanced learning after genetic overexpression of a brain growth protein. Proc Natl Acad Sci U S A. 2000 Jun 20; 97(13): 7657-62.

Ruscheweyh R, Sandkuhler J. Role of kainate receptors in nociception. Brain Res Brain Res Rev. 2002 Oct; 40(1-3):215-22.

Sakimura K, Kutsuwada T, Ito I, Manabe T, Takayama C, Kushiya E, Yagi T, Aizawa S, Inoue Y, Sugiyama H, et al. Reduced hippocampal LTP and spatial learning in mice lacking NMDA receptor epsilon 1 subunit. Nature. 1995 Jan 12; 373(6510): 151-5.

Sanchez-Perez AM, Felipo V. Serines 890 and 896 of the NMDA receptor subunit NR1 are differentially phosphorylated by protein kinase C isoforms. Neurochem Int. 2005 Jun 2.

Sanna PP, Cammalleri M, Berton F, Simpson C, Lutjens R, Bloom FE, Francesconi W. Phosphatidylinositol 3-kinase is required for the expression but not for the induction or the maintenance of long-term potentiation in the hippocampal CA1 region. J Neurosci. 2002 May 1; 22(9): 3359-65. Erratum in: J Neurosci 2002 Dec 1;22(23):10507.

Sarnyai Z, Sibille EL, Pavlides C, Fenster RJ, McEwen BS, Toth M.Impaired hippocampal-dependent learning and functional abnormalities in the hippocampus in mice lacking serotonin(1A) receptors. Proc Natl Acad Sci U S A. 2000 Dec 19; 97(26): 14731-6.

Schafe GE, Nadel NV, Sullivan GM, Harris A, LeDoux JE. Memory consolidation for contextual and auditory fear conditioning is dependent on protein synthesis, PKA, and MAP kinase. Learn Mem. 1999 Mar-Apr; 6(2):97-110.

Schlett K, Pieri I, Metzger F, Marchetti L, Steigerwald F, Dere E, Kirilly D, Tarnok K, Barabas B, Varga AK, Gerspach J, Huston J, Pfizenmaier K, Kohr G, Eisel UL. Long-term NR2B expression in the cerebellum alters granule cell develoment and leads to NR2A-downregulation and motor deficits. Mol Cell Neurosci. 2004 Nov; 27(3): 215-26.

Schorge S, Colquhoun D. Studies of NMDA receptor function and stoichiometry with truncated and tandem subunits. J Neurosci. 2003 Feb 15; 23(4): 1151-8.

Schwartzkroin PA and Wester K. Long-lasting facilitation of a synaptic potential following tetanization in the in vitro hippocampal slice. Brain Res. 1975 May 16; 89(1): 107-19.

Scott DB, Blanpied TA, Swanson GT, Zhang C, Ehlers MD. An NMDA receptor ER retention signal regulated by phosphorylation and alternative splicing. J Neurosci. 2001 May 1; 21(9):3063-72.

Scoville WB, Milner B. Loss of recent memory after bilateral hippocampal lesions. J Neurol Neurosurg Psychiatry. 1957 Feb; 20(1):11-21.

Scoville WB, Milner B. Loss of recent memory after bilateral hippocampal lesions. 1957. J Neuropsychiatry Clin Neurosci. 2000 Winter; 12(1):103-13. (Re-edition of the above article.)

Seeber S, Becker K, Rau T, Eschenhagen T, Becker CM, Herkert M. Transient expression of NMDA receptor subunit NR2B in the developing rat heart. J Neurochem. 2000 Dec; 75(6): 2472-7.

Shen K, Meyer T. Dynamic control of CaMKII translocation and localization in hippocampal neurons by NMDA receptor stimulation. Science. 1999 Apr 2; 284(5411): 162-6.

Sheng M, Cummings J, Roldan LA, Jan YN, Jan LY. Changing subunit composition of heteromeric NMDA receptors during development of rat cortex. Nature. 1994 Mar 10; 368(6467): 144-7.

Shimizu E, Tang YP, Rampon C, Tsien JZ. NMDA receptor-dependent synaptic reinforcement as a crucial process for memory consolidation. Science. 2000 Nov 10; 290(5494): 1170-4. Erratum in: Science 2001 Mar 9; 291(5510): 1902.

Shin JH, Linden DJ. An NMDA receptor/nitric oxide cascade is involved in cerebellar LTD but is not localized to the parallel fiber terminal. J Neurophysiol. 2005 Dec; 94(6):4281-9. Epub 2005 Aug 24.

Silva AJ, Stevens CF, Tonegawa S, Wang Y. Deficient hippocampal long-term potentiation in alpha-calcium-calmodulin kinase II mutant mice. Science. 1992a Jul 10; 257(5067):201-6.

Silva AJ, Paylor R, Wehner JM, Tonegawa S. Impaired spatial learning in alpha-calcium-calmodulin kinase II mutant mice. Science. 1992b Jul 10; 257(5067):206-11.

Silva AJ, Kogan JH, Frankland PW, Kida S. CREB and memory. Annu Rev Neurosci. 1998; 21: 127-48.

Sommer B, Keinanen K, Verdoorn TA, Wisden W, Burnashev N, Herb A, Kohler M, Takagi T, Sakmann B, Seeburg PH. Flip and flop: a cell-specific functional switch in glutamate-operated channels of the CNS. Science. 1990 Sep 28; 249(4976):1580-5.

Sommer B, Kohler M, Sprengel R, Seeburg PH. RNA editing in brain controls a determinant of ion flow in glutamate-gated channels. Cell. 1991 Oct 4; 67(1):11-9.

Sprengel R, Suchanek B, Amico C, Brusa R, Burnashev N, Rozov A, Hvalby O, Jensen V, Paulsen O, Andersen P, Kim JJ, Thompson RF, Sun W, Webster LC, Grant SG, Eilers J, Konnerth A, Li J, McNamara JO, Seeburg PH. Importance of the intracellular domain of NR2 subunits for NMDA receptor function in vivo. Cell. 1998 Jan 23; 92(2): 279-89.

Standaert DG, Landwehrmeyer GB, Kerner JA, Penney JB Jr, Young AB. Expression of NMDAR2D glutamate receptor subunit mRNA in neurochemically identified interneurons in the rat neostriatum, neocortex and hippocampus. Brain Res Mol Brain Res. 1996 Nov; 42(1):89-102.

Steece-Collier K, Chambers LK, Jaw-Tsai SS, Menniti FS, Greenamyre JT. Antiparkinsonian actions of CP-101,606, an antagonist of NR2B subunit-containing N-methyl-d-aspartate receptors. Exp Neurol. 2000 May; 163(1): 239-43.

Steinberg JP, Huganir RL, Linden DJ. N-ethylmaleimide-sensitive factor is required for the synaptic incorporation and removal of AMPA receptors during cerebellar long-term depression. Proc Natl Acad Sci U S A. 2004 Dec 28; 101(52):18212-6. Epub 2004 Dec 17.

Steiner JP, Walke HT Jr, Bennett V. Calcium/calmodulin inhibits direct binding of spectrin to synaptosomal membranes. J Biol Chem. 1989 Feb 15; 264(5):2783-91.

Stevenson BR, Siliciano JD, Mooseker MS, Goodenough DA. Identification of ZO-1: a high molecular weight polypeptide associated with the tight junction (zonula occludens) in a variety of epithelia. J Cell Biol. 1986 Sep; 103(3):755-66.

St-Onge L, Furth PA, Gruss P. Temporal control of the Cre recombinase in transgenic mice by a tetracycline responsive promoter. Nucleic Acids Res. 1996 Oct 1; 24(19): 3875-7.

Strack S, Colbran RJ. Autophosphorylation-dependent targeting of calcium/ calmodulin-dependent protein kinase II by the NR2B subunit of the N-methyl- D-aspartate receptor. J Biol Chem. 1998 Aug 14; 273(33): 20689-92.

Strack S, McNeill RB, Colbran RJ. Mechanism and regulation of calcium/calmodulin-dependent protein kinase II targeting to the NR2B subunit of the N-methyl-D-aspartate receptor. J Biol Chem. 2000 Aug 4; 275(31): 23798-806.

Sucher NJ, Akbarian S, Chi CL, Leclerc CL, Awobuluyi M, Deitcher DL, Wu MK, Yuan JP, Jones EG, Lipton SA. Developmental and regional expression pattern of a novel NMDA receptor-like subunit (NMDAR-L) in the rodent brain. J Neurosci. 1995 Oct; 15(10): 6509-20.

Sullivan JM, Traynelis SF, Chen HS, Escobar W, Heinemann SF, Lipton SA. Identification of two cysteine residues that are required for redox modulation of the NMDA subtype of glutamate receptor. Neuron. 1994 Oct; 13(4): 929-36.

Sun P, Lou L, Maurer RA. Regulation of activating transcription factor-1 and the cAMP response element-binding protein by Ca2+/calmodulin-dependent protein kinases type I, II, and IV. J Biol Chem. 1996 Feb 9; 271(6):3066-73.

Suzuki K. MAP kinase cascades in elicitor signal transduction. J Plant Res. 2002 Jun; 115(3): 237-44.

Sze C, Bi H, Kleinschmidt-DeMasters BK, Filley CM, Martin LJ. N-Methyl-D-aspartate receptor subunit proteins and their phosphorylation status are altered selectively in Alzheimer's disease. J Neurol Sci. 2001 Jan 1; 182(2): 151-9.

Takagi N, Cheung HH, Bissoon N, Teves L, Wallace MC, Gurd JW. The effect of transient global ischemia on the interaction of Src and Fyn with the N-methyl-D-aspartate receptor and postsynaptic densities: possible involvement of Src homology 2 domains. J Cereb Blood Flow Metab. 1999 Aug; 19(8): 880-8.

Takagi N, Logan R, Teves L, Wallace MC, Gurd JW. Altered interaction between PSD-95 and the NMDA receptor following transient global ischemia. J Neurochem. 2000 Jan; 74(1): 169-78.

Tang YP, Shimizu E, Dube GR, Rampon C, Kerchner GA, Zhuo M, Liu G, Tsien JZ. Genetic enhancement of learning and memory in mice. Nature. 1999 Sep 2; 401(6748): 63-9.

Thach WT, Goodkin HP, Keating JG. The cerebellum and the adaptive coordination of movement. Annu Rev Neurosci. 1992; 15:403-42.

Thomas U, Ebitsch S, Gorczyca M, Koh YH, Hough CD, Woods D, Gundelfinger ED, Budnik V. Synaptic targeting and localization of discs-large is a stepwise process controlled by different domains of the protein. Curr Biol. 2000 Sep 21; 10(18):1108-17.

Thomson S, Mahadevan LC, Clayton AL. MAP kinase-mediated signalling to nucleosomes and immediate-early gene induction. Semin Cell Dev Biol. 1999 Apr; 10(2): 205-14.

Thompson RF. Neural mechanisms of classical conditioning in mammals. Philos Trans R Soc Lond B Biol Sci. 1990 Aug 29; 329(1253):161-70.

Thompson RF, Thompson JK, Kim JJ, Krupa DJ, Shinkman PG. The nature of reinforcement in cerebellar learning. Neurobiol Learn Mem. 1998 Jul-Sep; 70(1-2):150-76.

Thompson RF, Krupa DJ. Organization of memory traces in the mammalian brain. Annu Rev Neurosci. 1994; 17:519-49.

Tingley WG, Roche KW, Thompson AK, Huganir RL. Regulation of NMDA receptor phosphorylation by alternative splicing of the C-terminal domain. Nature. 1993 Jul 1; 364(6432): 70-3.

Tingley WG, Ehlers MD, Kameyama K, Doherty C, Ptak JB, Riley CT, Huganir RL. Characterization of protein kinase A and protein kinase C phosphorylation of the N-methyl-D-aspartate receptor NR1 subunit using phosphorylation site-specific antibodies. J Biol Chem. 1997 Feb 21; 272(8): 5157-66.

Topinka JR, Bredt DS. N-terminal palmitoylation of PSD-95 regulates association with cell membranes and interaction with K+ channel Kv1.4. Neuron. 1998 Jan; 20(1):125-34.

Toyoda H, Zhao MG, Zhuo M. Roles of NMDA receptor NR2A and NR2B subtypes for long-term depression in the anterior cingulate cortex. Eur J Neurosci. 2005 Jul; 22(2):485-94.

Traynelis SF, Burgess MF, Zheng F, Lyuboslavsky P, Powers JL. Control of voltage-independent zinc inhibition of NMDA receptors by the NR1 subunit. J Neurosci. 1998 Aug 15; 18(16):6163-75.

Tsien JZ, Chen DF, Gerber D, Tom C, Mercer EH, Anderson DJ, Mayford M, Kandel ER, Tonegawa S. Subregion- and cell type-restricted gene knockout in mouse brain. Cell. 1996a Dec 27; 87(7):1317-26.

Tsien JZ, Huerta PT, Tonegawa S. The essential role of hippocampal CA1 NMDA receptor-dependent synaptic plasticity in spatial memory. Cell. 1996b Dec 27; 87(7):1327-38.

Tulving E, Schacter DL. Priming and human memory systems. Science. 1990 Jan 19; 247(4940):301-6.

Vetter ML, Martin-Zanca D, Parada LF, Bishop JM, Kaplan DR. Nerve growth factor rapidly stimulates tyrosine phosphorylation of phospholipase C-gamma 1 by a kinase activity associated with the product of the trk protooncogene. Proc Natl Acad Sci U S A. 1991 Jul 1; 88(13):5650-4.

Vyklicky L Jr. Calcium-mediated modulation of N-methyl-D-aspartate (NMDA) responses in cultured rat hippocampal neurones. J Physiol. 1993 Oct; 470:575-600.

Wang Y, TesFaye E, Yasuda RP, Mash DC, Armstrong DM, Wolfe BB. Effects of post-mortem delay on subunits of ionotropic glutamate receptors in human brain. Brain Res Mol Brain Res. 2000 Sep 15; 80(2): 123-31.

Warrington EK, Weiskrantz L. New method of testing long-term retention with special reference to amnesic patients. Nature. 1968 Mar 9; 217(132):972-4.

Wechsler A, Teichberg VI. Brain spectrin binding to the NMDA receptor is regulated by phosphorylation, calcium and calmodulin. EMBO J. 1998 Jul 15; 17(14): 3931-9.

Wenzel A, Fritschy JM, Mohler H, Benke D. NMDA receptor heterogeneity during postnatal development of the rat brain: differential expression of the NR2A, NR2B, and NR2C subunit proteins. J Neurochem. 1997 Feb; 68(2): 469-78.

Wei F, Wang GD, Kerchner GA, Kim SJ, Xu HM, Chen ZF, Zhuo M. Genetic enhancement of inflammatory pain by forebrain NR2B overexpression. Nat Neurosci. 2001 Feb; 4(2): 164-9.

Weiss SW, Albers DS, Iadarola MJ, Dawson TM, Dawson VL, Standaert DG. NMDAR1 glutamate receptor subunit isoforms in neostriatal, neocortical, and hippocampal nitric oxide synthase neurons. J Neurosci. 1998 Mar 1; 18(5):1725-34.

Weisskopf MG, Castillo PE, Zalutsky RA, Nicoll RA. Mediation of hippocampal mossy fiber long-term potentiation by cyclic AMP. Science. 1994 Sep 23; 265(5180):1878-82.

Weitlauf C, Honse Y, Auberson YP, Mishina M, Lovinger DM, Winder DG. Activation of NR2A-containing NMDA receptors is not obligatory for NMDA receptor-dependent long-term potentiation. J Neurosci. 2005 Sep 14; 25(37):8386-90.

Williams K. Pharmacological properties of recombinant N-methyl-D-aspartate (NMDA) receptors containing the epsilon 4 (NR2D) subunit. Neurosci Lett. 1995 Jan 30; 184(3):181-4.

Williams K, Pahk AJ, Kashiwagi K, Masuko T, Nguyen ND, Igarashi K. The selectivity filter of the N-methyl-D-aspartate receptor: a tryptophan residue controls block and permeation of Mg2+. Mol Pharmacol. 1998 May; 53(5): 933-41.

Wisden W, Seeburg PH. Mammalian ionotropic glutamate receptors. Curr Opin Neurobiol. 1993 Jun; 3(3): 291-8. Review.

Woods DF, Bryant PJ. The discs-large tumor suppressor gene of Drosophila encodes a guanylate kinase homolog localized at septate junctions. Cell. 1991 Aug 9; 66(3):451-64.

Woodward JJ. Prostacyclin-induced rundown of N-methyl-D-aspartate receptor currents in HEK293 cells is protein kinase A-dependent and NR2 subunit-selective. J Neurochem. 2002 Feb; 80(4): 598-604.

Wyszynski M, Lin J, Rao A, Nigh E, Beggs AH, Craig AM, Sheng M. Competitive binding of alpha-actinin and calmodulin to the NMDA receptor. Nature. 1997 Jan 30; 385(6615):439-42.

Yamazaki M, Mori H, Araki K, Mori KJ, Mishina M.Cloning, expression and modulation of a mouse NMDA receptor subunit. FEBS Lett. 1992 Mar 23; 300(1): 39-45.

Yang M, Leonard JP. Identification of mouse NMDA receptor subunit NR2A C-terminal tyrosine sites phosphorylated by coexpression with v-Src. J Neurochem. 2001 Apr; 77(2): 580-8.

Yang SN, Tang YG, Zucker RS. Selective induction of LTP and LTD by postsynaptic [Ca2+]i elevation. J Neurophysiol. 1999 Feb; 81(2):781-7.

Yasuda H, Barth AL, Stellwagen D, Malenka RC. A developmental switch in the signaling cascades for LTP induction. Nat Neurosci. 2003 Jan; 6(1):15-6.

Yeckel MF, Kapur A, Johnston D. Multiple forms of LTP in hippocampal CA3 neurons use a common postsynaptic mechanism. Nat Neurosci. 1999 Jul; 2(7):625-33.

Yin JC, Wallach JS, Del Vecchio M, Wilder EL, Zhou H, Quinn WG, Tully T. Induction of a dominant negative CREB transgene specifically blocks long-term memory in Drosophila. Cell. 1994 Oct 7; 79(1):49-58.

Yokoi M, Kobayashi K, Manabe T, Takahashi T, Sakaguchi I, Katsuura G, Shigemoto R, Ohishi H, Nomura S, Nakamura K, Nakao K, Katsuki M, Nakanishi S.Impairment of hippocampal mossy fiber LTD in mice lacking mGluR2. Science. 1996 Aug 2; 273(5275): 645-7.

Zeron MM, Chen N, Moshaver A, Lee AT, Wellington CL, Hayden MR, Raymond LA. Mutant huntingtin enhances excitotoxic cell death. Mol Cell Neurosci. 2001 Jan; 17(1): 41-53.

Zhang L, Hsu JC, Takagi N, Gurd JW, Wallace MC, Eubanks JH. Transient global ischemia alters NMDA receptor expression in rat hippocampus: correlation with decreased immunoreactive protein levels of the NR2A/2B subunits, and an altered NMDA receptor functionality. J Neurochem. 1997 Nov; 69(5): 1983-94.

Zhang W, Linden DJ. Long-term depression at the mossy fiber-deep cerebellar nucleus synapse. J Neurosci. 2006 Jun 28; 26(26):6935-44.

Zhao MG, Toyoda H, Lee YS, Wu LJ, Ko SW, Zhang XH, Jia Y, Shum F, Xu H, Li BM, Kaang BK, Zhuo M. Roles of NMDA NR2B subtype receptor in prefrontal long-term potentiation and contextual fear memory. Neuron. 2005 Sep 15; 47(6):859-72.

Zhong J, Russell SL, Pritchett DB, Molinoff PB, Williams K. Expression of mRNAs encoding subunits of the N-methyl-D-aspartate receptor in cultured cortical neurons. Mol Pharmacol. 1994 May; 45(5): 846-53.